Increased removal of protein bound uremic toxins through reversible modification of the ionic strength during hemodiafiltration

Erhöhte Elimination proteingebundener Urämietoxine durch reversible Modifikation der Ionenstärke während der Hämodiafiltration

Source: http://www.heart-watch-blog.com (Jan. 29th, 2012)

Dissertation towards a Doctoral Degree at the Graduate School of Biology Julius-Maximilians-University Würzburg.

Submitted by **Eric DEVINE**

from Yerres (FRANCE)

Würzburg, 2013

Submitted on: June, 10th 2013 ....

Members of the thesis committee:

    Chairperson: Prof. Dr. W. Rössler ....

    Primary supervisor: PD Dr. Detlef H. Krieter ....

    Secondary supervisor: Prof. Dr. Markus Sauer ....

Date of public defense: July, 29th 2013 ....

Date of receipt of certificates: ....

1

AFFIDAVIT

I hereby declare that my thesis entitled "Increased removal of protein bound uremic toxins through reversible modification of the ionic strength during hemodiafiltration" is the result of my own work. I did not receive help or support from commercial consultants. All sources and/or materials applied are listed and specified in the thesis.

Furthermore, I verify that this thesis has not been submitted as part of another examination process neither in identical nor in similar form.

_____   _____
Place, date   Signature

ACKNOWLEDGEMENTS

TABLE OF CONTENTS

LIST OF FIGURES

LIST OF TABLES

LIST OF EQUATIONS

SUMMARY

A large number of metabolic waste products accumulate in the blood of patients with renal failure. Since these solutes have deleterious effects on the biological functions, they are called uremic toxins and have been classified in three groups: 1) small water soluble solutes (MW < 500 Da), 2) small solutes with known protein binding (MW < 500 Da), and 3) middle molecules (500 Da < MW < 60 kDa). Protein bound uremic toxins are poorly removed by conventional hemodialysis treatments because of their high protein binding and high distribution volume. The prototypical protein bound uremic toxins indoxyl sulfate (IS) and *p*-cresyl sulfate (*p*CS) are associated with the progression of chronic kidney disease, cardiovascular outcomes, and mortality of patients on maintenance hemodialysis. Furthermore, these two compounds are bound to albumin, the main plasma protein, via electrostatic and/or Van-der-Waals forces. The aim of the present thesis was to develop a dialysis strategy, based on the reversible modification of the ionic strength in the blood stream by increasing the sodium chloride (NaCl) concentration, in order to enhance the removal of protein bound substances, such as IS and *p*CS, with the ultimate goal to improve clinical patient outcomes.

Enhancing the NaCl concentration ([NaCl]) in both human normal and uremic plasma was efficient to reduce the protein bound fraction of both IS and *p*CS by reducing their binding affinity to albumin. Increasing the ionic strength was feasible during modified pre-dilution hemodiafiltration (HDF) by increasing the [NaCl] in the substitution fluid. The NaCl excess was adequately removed within the hemodialyzer. This method was effective to increase the removal rate of both protein bound uremic toxins. Its *ex vivo* hemocompatibility, however, was limited by the osmotic shock induced by the high [NaCl] in the substituate. Therefore, modified pre-dilution HDF was further iterated by introducing a second serial cartridge, named the serial dialyzers (SDial) setup. This setting was validated for feasibility, hemocompatibility, and toxin removal efficiency. A better hemocompatibility at similar efficacy was obtained with the SDial setup compared with the modified pre-dilution HDF. Both methods were finally tested in an animal sheep model of dialysis to verify biocompatibility. Low hemolysis and no activation of both the complement and the coagulation systems were observed when increasing the [NaCl] in blood up to 0.45 and 0.60 M with the modified pre-dilution HDF and the SDial setup, respectively.

In conclusion, the two dialysis methods developed to transitory enhance the ionic strength in blood demonstrated adequate biocompatibility and improved the removal of protein bound uremic toxins by decreasing their protein bound fraction. The concepts require follow-on clinical trials to assess their *in vivo* efficacy and their impact on long-term clinical outcomes.

ZUSAMMENFASSUNG

Eine große Zahl von Stoffwechselprodukten akkumuliert im Blut urämischer Patienten mit Nierenversagen. Da diese Moleküle schädliche Wirkungen auf die biologischen Funktionen haben, werden sie als Urämietoxine bezeichnet. Man teilt sie in drei Gruppen ein: 1) kleine wasserlösliche Substanzen (MG < 500 Da), 2) kleine, proteingebundene Substanzen (MG < 500 Da), 3) Mittelmoleküle (500 Da < MG < 60 kDa). Proteingebundene Urämietoxine werden wegen ihrer starken Proteinbindung und ihres Verteilungsvolumen durch klassische Hämodialyseverfahrens nur schlecht entfernt. Die prototypischen proteingebundenen Urämietoxine Indoxylsulfat (IS) und *p*-Cresylsulfat (*p*CS) sind bei chronischen niereninsuffizienten Patienten mit dem Fortschreiten der Niereninsuffizienz, Herz-Kreislauf-Erkrankungen und der Mortalität verbunden. Außerdem sind diese beiden Toxine an Albumin, dem wichtigsten Plasmaprotein, durch elektrostatische und/oder Van-der-Waals-Kräfte gebunden. Das Ziel der vorliegenden Arbeit war es, ein Dialyseverfahren basierend auf einer reversiblen Modifikation der Ionenstärke im Blut durch Erhöhung der Natriumchlorid (NaCl)-Konzentration zu entwickeln, um die Entfernung von proteingebundenen Molekülen wie IS und *p*CS zu erhöhen und dadurch eine Verbesserung des klinischen Verlauf der Patienten zu erreichen.

Die Erhöhung der NaCl-Konzentration ([NaCl]) sowohl in normalem als auch in urämischem menschlichem Plasma war geeignet, um den proteingebundenen Anteil von IS und *p*CS durch Schwächung ihrer Bindungsaffinität zu Albumin zu verringern. Die Erhöhung der Ionenstärke während einer modifizierten Prädilutions-Hämodiafiltration (HDF) konnte durch eine Erhöhung der [NaCl] in der Substitutionslösung umgesetzt werden; dabei wurde der NaCl-Überschuss innerhalb des Dialysators vollständig entfernt. Dieses Verfahren war effektiv, um die Entfernungsrate beider proteingebundenen Urämietoxine zu steigern; seine *Ex-vivo*-Hämokompatibilität war allerdings aufgrund des osmotischen Schocks infolge der hohen [NaCl] im Substituat begrenzt. Deshalb wurde eine Iteration der modifizierten Prädilutions-HDF durch Einbau eines zweiten, seriellen Dialysators vorgenommen, bezeichnet als serielles Dialysator System (SDial). Diese letzte Methode wurde dann bezüglich der Durchführbarkeit, der Hämokompatibilität und Toxinentfernung validiert. Durch das SDial-System konnte, verglichen mit der modifizierten Prädilutions-HDF, eine bessere Hämokompatibilität bei ähnlicher Wirksamkeit erzielt werden. Beide Methoden, modifizierte Prädilutions-HDF und SDial System, wurden abschließend in ein Tierdialysemodell mit Schafen transferiert, wobei eine zufriedenstellende Biokompatibilität demonstriert werden konnte.

Beide, zur vorübergehenden Erhöhung der Ionenstärke im Blut entwickelten Dialyseverfahren zeigten bei zufriedenstellender Biokompatibilität eine verbesserte Entfernung proteingebundener Urämietoxine durch Reduktion ihrer proteingebundenen Fraktion. In einem nächsten Schritt sind klinische Studien erforderlich, die diese Konzepte bezüglich ihrer *In-vivo*-Wirksamkeit und ihrer langfristigen Wirkung auf den Krankheitsverlauf untersuchen.

ABBREVIATIONS

$\beta_2 m$ β_2-microglobulin

γ removal rate

λ wavelength

[NaCl]   sodium chloride concentration

$[NaCl]_{ART}$ sodium chloride concentration in the arterial line

$[NaCl]_{blood}$ sodium chloride concentration in blood

$[NaCl]_{BM}$ sodium chloride concentration in blood downstream the first dialyzer / upstream the second one

$[NaCl]_{IN}$ sodium chloride concentration in the first dialyzer dialysate inlet

$[NaCl]_{OUT}$ sodium chloride concentration in the first dialyzer dialysate outlet

$[NaCl]_{SUB}$ sodium chloride concentration in the substitution fluid

$[NaCl]_{VEN}$ sodium chloride concentration in the venous line

AGE   advanced glycation end-products

ART   arterial (septum)

BGA   blood gas analysis

B_m number of binding sites

BM   between modules (septum)

BR   blood reservoir (septum)

C5a   complement component 5a

Ca^{2+} calcium ion

CH_3COOH acetic acid

CH_3COONa sodium acetate

CH_3COONH_4 ammonium acetate

CKD   chronic kidney disease

Cl^- chloride ion

CMPF   3-carboxy-4-methyl-5-propyl-2-furanpropionic acid

COHb   carboxyhemoglobin

CVD   cardiovascular disease

D123   Dihydrorhodamine 123

DMSO   Dimethyl sulfoxide

EDTA   Titriplex® III

ERA-EDTA   european renal association - european dialysis and transplant association

ESRD   end-stage renal disease

EtOH   ethanol

GFR   glomerular filtration rate

Hb   hemoglobin

HCO_3^- hydrogenocarbonate ion

Hct   hematocrit

HD   hemodialysis

HDF   hemodiafiltration

HEPES   4-(2-Hydroxyethyl) piperazine-1-ethanesulfonic acid N-(2-hydroxyethyl) piperazine-N'-(2-ethanesulfonic acid)

Hexapeptide   N-Formyl-Nle-Leu-Phe-Nle-Tyr-Lys

HF   hemofiltration

HHb   deoxyhemoglobin

HSA   human serum albumin

IS   indoxyl sulfate

K^+ potassium ion

K_0A mass transfer area coefficient

K$_2$HPO$_4$	di-potassium hydrogen phosphate	**Q$_{NaCl}$**	sodium chloride solution infusion flow rate
K$_A$	association constant	**Q$_{UF}$**	ultrafiltration flow rate (also weight-loss)
KCl	potassium chloride		
K$_D$	dissociation constant	**RBC**	red blood cell (erythrocyte)
LDH	lactate dehydrogenase	**RP-HPLC**	reversed-phase high pressure liquid chromatography
LPS	lipopolysaccharide		
MgCl$_2$	magnesium chloride		
MetHb	methemoglobin	**RR**	removal ratio
MW	molecular weight	**RRT**	renal replacement therapies
Na$^+$	sodium ion		
NaCitrate	sodium citrate	**SDial**	serial dialyzers
NaCl	sodium chloride	**SDial pre-HDF**	serial dialyzers pre-dilution hemodiafiltration
NaOH	sodium hydroxide		
NKF KDOQI	kidney disease outcomes quality initiative guidelines of the national kidney foundation	**SDial-TM pre-HDF**	serial dialyzers with transmembrane pre-dilution hemodiafiltration
NH$_4$COOH	ammonium formate	**TAT**	thrombin-antithrombin III
O$_2$Hb	oxyhemoglobin	**TBA**	tetrabutylammonium hydrogensulfate
OD	optical density		
PAA	phenyl acetic acid	**tHb**	total hemoglobin concentration
PBF	protein bound fraction		
PBS	phosphate buffered saline	**TMP**	transmembrane pressure
pCO$_2$	carbon dioxide partial pressure	**TP**	total protein concentration
		USRDS	united states renal data system
pCS	*para*-cresyl sulfate	**VEN**	venous (septum)
PD	peritoneal dialysis	**WBC**	white blood cell (leucocyte)
Phe	phenylalanine		
PLT	platelet (thrombocyte)		
Pmp	per million population		
pO$_2$	dioxygen partial pressure		
PTH	parathyroid hormone		
pre-HDF	pre-dilution hemodiafiltration		
Q$_B$	blood flow rate		
Q$_D$	dialysate flow rate		
Q$_{ex}$	first dialyzer dialysate flow rate (serial dialysers setup only)		
Q$_{inf}$	substituate flow rate		

INTRODUCTION

I.   Renal failure

Kidneys are key organs responsible for the removal of metabolism waste products, regulation of the water and acid-base balance. Through their hormone secretion, they are also involved in the regulation of blood pressure, erythropoiesis and bone mass. Progressive renal failure leads to the deterioration of biochemical and physiologic functions and, finally, to the uremic syndrome characterized by multiple symptoms, such as nausea, changes in mental status, heart problems, etc., and *in fine* death (1) . The retention of substances that are normally cleared by healthy kidneys and the derangement of renal hormonal and enzymatic homeostasis affect several functional systems, most of all the cardiovascular (e.g. hypertension, atherosclerosis), neurological, hematological (e.g. anemia) and immunological systems (e.g. susceptibility to infections). Coagulation disturbances are also observed in uremic patients leading to bleeding tendency (1).
Kidney failure may consist of either an acute and potentially temporary loss of function (acute kidney injury) or of a progressive loss of the renal function (chronic kidney disease, CKD).

1) CKD stages

A classification of CKD stages is proposed by the Kidney Disease Outcomes Quality Initiative guidelines of the National Kidney Foundation (NKF KDOQI) according to the kidney damage and function as estimated by the glomerular filtration rate (GFR) (2):

Stage	Description	GFR (mL/min/1.73m²)
1	Kidney damage with normal or increased GFR	≥ 90
2	Kidney damage with mild decreased GFR	60 to 89
3	Moderate decreased GFR	30 to 59
4	Severe decreased GFR	15 to 29
5	Kidney failure	< 15 (or dialysis)

Tab. 1: Stages of chronic kidney disease.
CKD stage 3 has been divided in two: 3a with GFR between 45 and 59 mL/min/1.73m², and 3b with GFR between 30 and 44 mL/min/1.73m²; thus with different rankings of adjusted relative risk with albuminuria (3). Patients on maintenance hemodialysis are classified as CKD stage 5D (4).

The renal function declines with time until being completely lost (CKD stage 5). This is called end-stage renal disease (ESRD) and requires treatment with any form of chronic dialysis or transplantation (1; 5).

2) <u>Epidemiology of chronic renal failure</u>

Data on the incidence[1] and prevalence[2] of chronic renal failure are collected around the world by various registries, such as the United States Renal Data System (USRDS) and the European Renal Association - European Dialysis and Transplant Association (ERA-EDTA).

The overall adjusted incident rate in Europe for the year 2010 (6) of the different countries ranged between 77 and 194 per million population (pmp) with diabetes mellitus, glomerulonephritis/-sclerosis, and hypertension being the main causes of renal failure. The incident rate per established therapy ranged from 55 to 153 pmp for hemodialysis, from 7.3 to 34 pmp for peritoneal dialysis, and from 0.3 to 14.5 pmp for transplantation. Prevalent patients for all treatments on December 31st, 2010 in Europe ranged from 574 to 1262 pmp (adjusted values) (6). Thus, about 220 000 patients were treated by hemodialysis, about 23 000 patients were treated by peritoneal dialysis, and 16 000 had been transplanted in Europe[3] in 2010 (6).

II.   <u>Uremic toxins</u>

1) <u>Uremic toxin classification</u>

Uremic toxins are biological agents accumulating in renal failure. Their interactions with biological systems may produce biological responses deleterious to the human body (7). Other compounds have no proven direct toxicity, but may be useful markers of uremic retention (1). The European Uremic Toxin Working Group proposed in 2003 a classification of the uremic toxins and stratified them into three groups (8):

- Small solutes (< 500 Da) with no protein binding,
- Solutes with known or likely protein binding,
- Middle molecules (≥ 500 Da).

Molecules with a molecular weight (MW) exceeding 60 kDa (cutoff of the glomerular basement membrane) are excluded from the middle molecule group. Thus, this group should be understood as molecules with a MW between 500 Da and 60 kDa (8). The proposed classification has been updated in 2008 (9) and in 2012 (10).

---

[1] Definition: number of new cases of a condition during a specific period of time.
[2] Definition: number of people in a given population with a particular disease at a given time.
[3] Countries included are: Austria, Belgium, Bosnia and Herzegovina, Croatia, Czech Republic, Denmark, Estonia, Finland, France (23 of 26 regions), former Yugoslav Republic of Macedonia, Greece, Iceland, Italy (14 of 20 regions), Latvia, Montenegro, Norway, Poland, Portugal, Romania, Russia, Serbia, Slovakia, Spain (18 of 19 regions), Sweden, The Netherlands, the United Kingdom, and Ukraine.

a. Free water-soluble small solutes

Solute		C_N	C_U	C_{max}	MW	Group
1-methyladenosine	µg/L	17.1 ± 5.1 / 10	104.0 ± 56.2 / 17	216.4	281	Ribonucleosides
8-OH-2'Deoxyguanosine	µg/L	0.64 ± 0.23		0.82	283	Purine
1-methylguanosine	µg/L	13.7 ± 16.9 / 10	41.6 ± 23.8 / 17	89.2	297	Ribonucleosides
1-methylnosine	µg/L	13.5 ± 3.9 / 10	620.4 ± 203.4 / 14	1027.2	282	Ribonucleosides
ADMA	mg/L	0.2 ± 0.06 / 6	1.6 ± 1.2 / 10	7.3	202	Guanidines
α-keto-δ-guanidinovaleric acid	µg/L	< 30.2 / 66	-	140.4	151	Guanidines
α-N-acetylarginine	µg/L	18.1 ± 24.8 / 16	328.3 ± 142.6 / 13	4580.0	216	Guanidines
Arab(in)itol	mg/L	< 0.6 / 33	15.0 ± 9.0 / 12	33.0	152	Polyols
Argininic acid	µg/L	< 77.0 / 66	80.5 ± 56.0 / 11	197.8	175	Guanidines
Benzylalcohol	mg/L	-	27.0 ± 50.7 / 17	187.9	108	
β-guanidinopropionic acid	µg/L	< 3.3 / 24	28.8 ± 18.3 / 29	65.4	131	Guanidines
β-lipoprotein	ng/L	< 55.3 / 10	62.7 / 22	108.8	461	Peptides
Creatine	mg/L	9.7 ± 3.3 / 24	134.0 ± 30.3 / 29	235.8	131	Guanidines
Creatinine	mg/L	< 12.0 / 23	136.0 ± 46.0 / 19746	240.0	113	Guanidines
Cytidine	µg/L	< 468.0	683.3 ± 287.8 / 7	1263.6	234	Purines
Dimethylglycine	µg/L	< 381.1 / 33	576.8 / 18	1040.3	103	
Dimethylguanosine						
Erythritol	mg/L	< 0.7 / 33	9.8 ± 14.0 / 12	37.0	122	Polyols
γ-guanidinobutyric acid	µg/L	< 3.6 / 24	33.3 ± 16.0 / 30	1750.0	145	Guanidines
Guanidine	µg/L	< 11.8 / 16	176.9 ± 83.8 / 13	800.0	59	Guanidines
Guanidinoacetic acid	µg/L	222.3 ± 79.6 / 24	383.8 ± 143.9 / 29	693.8	117	Guanidines
Guanidonosuccinic acid	mg/L	0.03 ± 0.01 / 16	6.5 ± 3.4 / 13	47.0	175	Guanidines
Guanilin						
Hypowanthine	mg/L	1.5 ± 0.5 / 145	2.0 ± 1.6 / 65	5.3	136	Purines
Inosine						
Malondialdehydes	µg/L	257.7 ± 81.7 / 30	428.8 ± 170.4 / 16	796.6	71	
Mannitol	mg/L	< 1.3 / 33	26.0 ± 25.0 / 12	76.0	182	Polyols
Methylguanidine	µg/L	< 7.3 / 24	773.8 ± 508.8 / 5	1820.0	73	Guanidines
Myoinositol	mg/L	< 10.0 / 8	94.0 ± 69.0 / 12	232.0	180	Polyols
N^2,N^2-dimethylguanosine	µg/L	9.0 ± 4.7 / 10	236.4 ± 89.7 / 14	415.8	311	Ribonucleosides
N^4 –acetylcytidine	µg/L	57.0 ± 17.1 / 10	159.6 ± 30.8 / 14	221.2	285	Ribonucleosides
N^6 –methyladenosine	µg/L	18.5 ± 8.4 / 10	70.3 ± 53.3 / 17	176.9	281	Ribonucleosides
N^6 –threonylcarbamoyladenosine	µg/L	35.5 ± 27.2 / 10	378.0 ± 151.2 / 17	680.4	378	Ribonucleosides
N-methyl-2-pyridone-5-carboxamide	mg/L	1.37 ± 0.68	4.02 ± 3.28	7.80	152	Nicotinamide
Nitrosodimethylamine						
Nitrosomethylamine						
Orotic acid	mg/L	0.5 ± 1.4 / 30	6.7 ± 16.0 / 22	38.7	174	Pyrimidines
Orotidine	mg/L	1.2 ± 1.6 / 30	20.2 ± 13.5 / 22	47.2	288	Pyrimidines
Oxalate	mg/L	0.3 ± 0.1 / 8	4.9 ± 1.4 / 8	7.6	90	
Phenylacetylglutamine	mg/L	< 4.7	53.3 ± 44.7 / 6	120.6	264	
Phenylethylamine						
Pseudouridine	mg/L	0.5 ± 5.8 / 30	13.1 ± 21.4 / 7	86.6	244	Ribonucleosides
SDMA	µg/L	76.1 ± 21.0 / 66	640.3 ± 212.1 / 38	1232.2	202	Guanidines
Sorbitol	mg/L	< 0.4 / 33	3.1 ± 2.1 / 12	7.3	182	Polyols
Taurocyamine	µg/L	< 52.2 / 24	-	121.8	174	Guanidines
Thiocyanate						
Threitol	µg/L	< 319.6 / 33	990.0 ± 920.0 / 12	5697.4	122	Polyols
Thymine	mg/L	-	2.8 ± 4.2 / 22	11.2	126	Pyrimidines
Trimethylamine	µg/L	24.7 ± 7.3		82.0	59	Amine
Uracil	µg/L	< 224.0	252.0 ± 154.6 / 7	448.0	112	Purines
Urea	g/L	< 0.4 / 23	2.3 ± 1.1 / 16	4.6	60	
Uric acid	mg/L	< 67.2	83.4 ± 44.5 / 7	146.7	168	Purines
Uridine	mg/L	1.5 ± 1.3 / 30	9.8 ± 11.4 / 22	32.6	244	Pyrimidines
Xanthine	mg/L	0.5 ± 1.4 / 180	1.5 ± 0.8 / 65	3.0	152	Purines
Xanthosine	µg/L	23.9 ± 12.8 / 10	96.6 ± 62.9 / 11	222.4	284	Ribonucleosides

Tab. 2: Free water-soluble low-molecular-weight solute concentrations.
The table was adapted from (8). Abbreviations are: C_N, normal concentration; C_U, mean/median uremic concentration; C_{max}, maximal uremic concentration; MW, molecular weight; ADMA, asymmetrical dimethylarginine; SDMA, symmetrical dimethylarginine. The underlined numbers behind the slash point to the number of data on which the means or medians have been obtained. No underlined number indicates that no data about the number of samples were available. Normal values are reported as means ± SD, or in the case of a single value as a maximum; uremic values are reported as mean ± SD or as a median.

Urea and creatinine are highly soluble in water and are the most abundant solutes to accumulate in blood as a consequence of renal failure. Thus, they are used as marker molecules to quantify and compare dialysis treatment efficacy and hemodialyzer properties (11).

b. **Protein bound solutes**

Since the various hemodialysis strategies focused for a long time on the removal of small water soluble molecules, protein-bound uremic toxins were qualified in 2001 as the "forgotten toxins" (12). In spite of their small MW, they behave like larger molecules since the carrier proteins are unable to pass dialysis membranes and, therefore, are retained in blood. Only the free, unbound fraction is dialyzed. Consequently, they are poorly removed by standard hemodialysis treatments (5; 7). However, only the free fraction of these toxins has an effect on biological system (8).

Solute		C_N	C_U	C_{max}	MW	Group
2-methoxyresorcinol	µg/L	-	19.6 ± 81.2 / 17	322.0	140	Phenols
3-deoxyglucosone	mg/L	0.3 ± 0.1 / 30	1.7 ± 1.0 / 27	3.5	162	AGE
CMPF	mg/L	7.7 ± 3.3 / 7	61.0 ± 16.5 / 15	94.0	240	
Fructoselysine	mg/L	-	58.1 ± 10.8 / 10	79.7	308	AGE
Glyoxal	µg/L	67.0 ± 20.0 / 7	221.0 ± 28.0 / 20	277.0	58	AGE
Hippuric acid	mg/L	< 5.0	247.0 ± 112.0 / 7	471.0	179	Hippurates
Homocysteine	mg/L	< 1.7 / 24	8.1 ± 1.6 / 7	26.4	135	
Hydroquinone	µg/L	-	50.6 ± 84.7 / 17	286.0	110	Phenols
Indole-3-acetic acid	µg/L	17.5 ± 17.5 / 7	875.0 ± 560.0 / 42	9076.9	175	Indoles
Indoxyl sulfate	mg/L	0.6 ± 5.4 / 40	53.0 ± 91.5 / 20	236.0	213	Indoles
Kinurenine	µg/L	< 391 / 7	686.4 ± 178.9 / 21	952.6	208	Indoles
Kynurenic acid	mg/L	< 1.0	-	9.5	189	Indoles
Leptin	µg/L	8.4 ± 6.7 / 56	72.0 ± 60.6 / 8	490.0	16000	Peptides
Melatonin	ng/L	26.5 ± 7.1 / 35	175.8 ± 130.2 / 13	436.2	126	Indoles
Methylglyoxal	µg/L	47.0 ± 12.0 / 15	110.0 ± 18.0 / 20	146.0	72	AGE
N^ε-(carboxymethyl)lysine	mg/L	1.1 ± 0.3 / 24	4.3 ± 1.3 / 44	6.9	204	AGE
p-cresol	mg/L	0.6 ± 1.0 / 12	20.1 ± 10.3 / 20	40.7	108	Phenols
Pentosidine	µg/L	51.6 ± 18.8 / 19	896.0 ± 448.0 / 24	2964.0	342	AGE
Phenyl acetic acid	mg/L	< 1.4	467.2 ± 10.6	474.6	136	
Phenols	mg/L	0.6 ± 0.2 / 12	2.7 ± 3.9 / 10	10.5	94	Phenols
P-OH-hippuric acid	mg/L		18.3 ± 6.6 / 13	31.5	195	Hippurates
Putrescine	µg/L	21.1 ± 7.9 / 10	77.4 ± 27.3 / 25	132.0	88	Polyamines
Quinolinic acid	mg/L	0.1 ± 0.05 / 10	1.5 ± 0.9 / 54	3.3	167	Indoles
Retinol-binding protein	mg/L	< 80	192.0 ± 78.0 / 112	369.2	21200	Peptides
Spermidine	µg/L	-	97.2 ± 45.0 / 25	187.2	145	Polyamines
Spermine	µg/L	-	18.2 ± 16.2 / 25	66.7	202	Polyamines

Tab. 3: Protein bound solute concentrations.
The table was adapted from (8). Abbreviations are: C_N, normal concentration; C_U, mean/median uremic concentration; C_{max}, maximal uremic concentration; MW, molecular weight; CMPF, 3-carboxy-4-methyl-5-propyl-2-furanpropionic acid; AGE, advanced glycation end products; RCC, reactive carbonyl compound. The underlined numbers behind the slash point to the number of data on which the means or medians have been obtained. No underlined number indicates that no data about the number of samples were available. Normal values are reported as means ± SD, or in the case of a single value as a maximum; uremic values are reported as mean ± SD or as a median.

Advanced glycation end-products (AGE) were classified among the protein-bound molecules; their binding to proteins is, however, different from that of other classical protein-bound solutes, such as indoxyl sulfate and p-cresol (8). AGE modifications are actually irreversible

modifications of proteins (covalent binding). Proteins form AGEs by different chemical steps (Schiff reaction, generation of Amadori products, carboxymethyllysin, pentosidine, pyrraline) when exposed to glucose or other carbohydrates (13).

c. __Middle molecules__

Solute		C_N	C_U	C_{max}	MW	Group
Adiponectin	*mg/L*	< 11.1		16.6	30000	Peptides
Adrenomedullin	*ng/L*	13.2 ± 4.6 / 17	41.8 ± 19.7 / 29	81.2	5729	Peptides
Atrial natriuretic peptide	*ng/L*	28.0 ± 12.2 / 23	202.0 ± 117.3 / 27	436.6	3080	Peptides
β_2-microglobulin	*mg/L*	< 2.0	55.0 ± 7.9 / 10	100.0	11818	Peptides
β-endorphin	*ng/L*	< 173.3 / 10	301.5 / 22	492.0	3465	Peptides
Basic FGF						
Calcitonin-gene related peptide	*ng/L*	< 20.0		21.8	3450	Peptides
Cholecystokinin	*ng/L*	< 20.0	45.9 ± 32.3 / 38	131.5	3866	Peptides
Clara cell protein	*mg/L*	< 0.1	3.3 ± 2.0 / 112	12.5	15800	Peptides
Complement factor D	*mg/L*	1.9 ± 0.5 / 5	19.8 ± 4.1 / 5	26.0	23750	
Cystatine C	*mg/L*	< 1.6	11.8 ± 3.0 / 112	20.0	13300	Peptides
Degranulation inhibiting protein I	*µg/L*	321.7 ± 59.7 / 23	713.7 ± 390.0 / 125	1631.4	14100	Peptides
Delta-sleep inducing peptide	*µg/L*	-	1.5 ± 0.9 / 7	3.3	848	Peptides
Desacylghrelin						
Dinucleoside polyphosphates						
Endothelin	*ng/L*	20.8 ± 3.8 / 23	63.0 ± 33.2 / 12	129.4	4283	Peptides
Ghrelin						
Hepcidin						
Hyaluronic acid	*µg/L*	< 124.0 / 86	215.0 ± 257.0 / 184	1843.0	25000	Peptides
Interleukin-1β	*ng/L*	< 160.0 / 15	428.0 ± 134.0 / 29	1700.0	32000	Cytokines
Interleukin-6	*ng/L*	13.3 ± 3.1 / 28	92.3 ± 117.9 / 230	328.1	24500	Cytokines
Interleukin-18						
κ-Ig light chain	*mg/L*	34.0 ± 15.0 / 15	70.0 ± 60.9 / 104	287.0	25000	Peptides
λ-Ig light chain	*mg/L*	31.0 ± 11.2 / 15	87.0 ± 60.9 / 104	328.0	25000	Peptides
Leptin	*µg/L*	8.4 ± 6.7 / 56	72.0 ± 60.6 / 8	490.0	16000	Peptides
Methionine-enkephalin	*ng/L*	< 18.3 / 10	32.2 / 22	75.5	555	Peptides
Motiline						
Neuropeptide	*ng/L*	< 80.0	64.9 ± 25.5 / 19	115.9	4272	Peptides
Octopamine						
Orexin A						
Parathyroid hormone	*µg/L*	< 0.06	1.2 ± 0.6 / 10	2.4	9225	Peptides
Retinol-binding protein	*mg/L*	< 80	192.0 ± 78.0 / 112	369.2	21200	Peptides
Substance P						
Tumor necrosis factor-α	*ng/L*	13.3 ± 3.0 / 28	114.0 ± 147.0 / 230	408.0	26000	Cytokines
Up$_4$A						
Uroguanylin						
Vasoactive intestinal peptide						

Tab. 4: Middle molecule concentrations.
The table was adapted from (8). Abbreviations are: C_N, normal concentration; C_U, mean/median uremic concentration; C_{max}, maximal uremic concentration; MW, molecular weight; FGF, fibroblast growth factor. The underlined numbers behind the slash point to the number of data on which the means or medians have been obtained. No underlined number indicates that no data about the number of samples were available. Normal values are reported as means ± SD, or in the case of a single value as a maximum; uremic values are reported as means ± SD or as a median.

The prototype of the middle molecule group is β_2-microglobulin (β_2m). Historically, concerns on the retention of β_2m rose when this protein was detected in a specific amyloid developing after several years of renal replacement therapy (14). As reviewed by Miyata and Drüeke (15; 16), β_2m and AGE-modified β_2m are implicated in dialysis-related amyloidosis, a disease recognized few decades ago characterized by carpal tunnel syndrome, arthropathy and the formation of bone cysts (13; 15; 16). β_2m is a constituent of the major

histocompatibilty complex class I antigen and it accumulates with progression of renal disease (15; 16; 17). This protein has been also related to cardiovascular disease (CVD), cardiovascular complications, and overall and cardiovascular mortality in hemodialysis patients (17; 18; 19; 20).

2) Uremic toxicity

CKD progression leads to the accumulation of metabolism waste products, which have a negative effect on health. Since the present thesis was focused on protein bound uremic toxins, the relevance of the studied compounds is presented in this part according to their adverse effects *in vivo* and *in vitro*.

a. Indoxyl sulfate

Indoxyl sulfate (IS) results from the degradation of dietary protein in the large intestine. More precisely, the amino acid tryptophan is metabolized into indole by tryptophanase in intestinal bacteria, such as *Escherichia coli*. After entering the blood stream, indole is metabolized into IS in the liver (21).
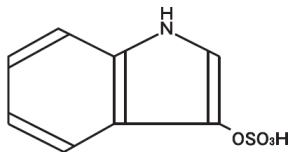
Fig. 1: Chemical structure of indoxyl sulfate.
MW: 213 Da.

With a protein binding of about 90% (22), this solute accumulates with progression of CKD (23) maybe due to a defect of organic anion transport and, thus, inducing renal cytotoxicity (24). In rats, IS is related to the progression of glomerular sclerosis (25). *In vitro* experiments have shown its implication in bone disorders observed in uremic patients: IS inhibits osteoclast differentiation and function (26) and induces also resistance to parathyroid hormone (PTH) in osteoblasts (27). IS is also associated with all-cause and cardiovascular mortality, CVD, and CKD progression (23; 28). *In vivo* observations have confirmed the vascular toxicity of IS by inducing aortic calcification and aortic wall thickening in rats (29); *in vitro* experiments also have demonstrated that IS inhibits endothelial proliferation and wound repair (30) by inducing oxidative stress in endothelial cells (31).

b. *p*-Cresol and *p*-cresyl sulfate

p-Cresol results from the degradation of the amino acid tyrosine by intestinal bacteria (32). Initial research has focused on *p*-cresol itself; however, it has been shown that this

compound circulates mainly as *p*-cresyl sulfate (*p*CS) in the blood stream (33; 34). *p*CS is about 95% bound to plasma proteins (33; 35).
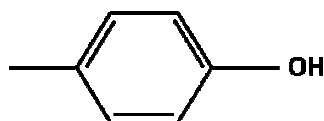
Fig. 2: Chemical structure of *p*-cresol.
MW: 108 Da.
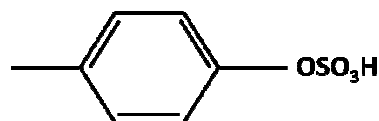
Fig. 3: Chemical structure of *p*-cresyl sulfate
MW: 187 Da.

In vivo, both *p*-cresol and *p*CS accumulate with decreasing renal function (36; 37) possibly due to reduced uptake by organic anion transporters (38). *p*CS is a predictor of CKD progression (28). The free concentration of both toxins is related to all-cause and cardiovascular mortality in hemodialysis patients (37; 39; 40). Furthermore, patients with high free serum *p*-cresol concentrations have a higher prevalence of hospitalization because of infections. This may be explained by an impaired leukocyte response (production of reactive oxygen species) to bacteria (41), reduced expression of endothelial adhesion molecules and impaired monocyte adhesion to endothelial cells (42). Unlike *p*-cresol, *p*CS activates leukocyte free radical production (pro-inflammatory effect) which may be involved in vascular disease of the uremic population (43). Meijers et al. demonstrated that the free serum concentration of *p*-cresol was associated with the number of circulating endothelial microparticles in hemodialysis patients (44). This is in accordance with *in vitro* experiments showing disruption of endothelial progenitor cell function (45), induction of endothelial microparticles shedding (44) and decrease of endothelial proliferation and wound repair (30) by *p*CS.

c. Phenyl acetic acid

Phenyl acetic acid (PAA) has been introduced in 2009 as a protein-bound substance. Different to IS and *p*CS, the protein binding in plasma is low (about 30%) (46). This molecule largely accumulates in plasma of ESRD patients (see **Tab. 3**) and interferes with nitric oxide production – a signaling molecule mediating neurotransmission, vasodilatation and cell defense – by mononuclear leucocytes (47). Furthermore, this solute is suspected to play a role in bone disorder in CKD by affecting proliferation, differentiation, mineralization and responsiveness to PTH of osteoclasts (48) and in immunodeficiency by inhibiting macrophage function (49).
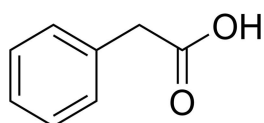
Fig. 4: Chemical structure of phenyl acetic acid.
MW: 136 Da.

III. <u>Renal replacement therapies</u>

The immediate goals of renal replacement therapies (RRT) are: i) to remove toxic waste products from blood (11), and ii) to correct the electrolyte, water and acid base abnormalities (5). RRT are hemodialysis (HD) and peritoneal dialysis (PD). During HD, blood is cleansed in an artificial kidney (hemodialyzer) made of a semi-permeable membrane (50), whereas during PD, the peritoneum is used as semi-permeable membrane (51). Therefore, both methods differ in terms of access: HD, vascular access; PD, peritoneal cavity access. As presented above, HD is much more common compared to PD (about 10 patients on HD for 1 on PD) (6).

Similarly to native kidneys, which combine filtration at the glomerulus with selective reabsorption across the tubule, artificial kidneys accomplish their role by dialyzing and filtering the blood across semi-permeable membranes driven by diffusion and convection (11). However, artificial kidneys are not able to correct the endocrine abnormalities of renal failure (5).

1) <u>Dialysis therapies</u>

Basic RRT were originally based either on purely diffusive – hemodialysis – or on purely convective principles – hemofiltration (HF). During convective treatment, the ultrafiltered plasma water is replaced by a substitution fluid with a composition similar to dialysate (52). This substitution can be performed upstream (pre-dilution) or downstream (post-dilution) from the hemofilter. Later, hemodiafiltration (HDF) was introduced, which cumulates both principles of HD and HF.

2) <u>Hemodialyzer and hemodialysis membranes</u>

Hemodialysis membranes are divided in three main categories according to materials: cellulose, modified cellulose, and synthetic polymers. Synthetic membranes are the gold standard for current hemodialyzers (53), which usually are hollow-fiber type and available as low- and high-flux membrane (13).

High-flux membranes are highly permeable to water (ultrafiltration coefficient > 20 mL/h/mmHg) and have larger pore sizes with a cut-off of about 50 kDa (low-flux membrane cut-off is about 10 kDa) (54) enabling the removal of middle molecules such as β_2m (11; 13). The development of high-flux membranes was driven by the desire to reach solute removal characteristics for artificial kidneys similar to those of the native organ (50). However, an increase of the membrane pore size to more effectively remove larger solutes is limited by serum albumin loss; albumin is essential for solute transport and maintenance of blood oncotic pressure (11). However, no upper limit of albumin loss during RRT has been defined so far (55).

Low-flux membranes are rather used during purely diffusion-based strategies (i.e., HD) whereas high-flux membranes are used for convective strategies (i.e., HF and HDF) and HD. In 2006, the NKF KDOQI guidelines recommend the use of high-flux dialysis (56).

Hemodialyzers can be characterized, amongst others, by the sieving coefficient and the mass transfer area coefficient (K_0A). This last term is a property of both the solute and the membrane. It reflects the maximum clearance possible at infinite blood and dialysate flow rates. The K_0A value may change during dialysis due to protein adsorbtion onto the membrane (decrease of permeability) or loss of membrane surface area due to coagulation of hollow fibers (11).

3) Hemodialysis in practice

Dialysis machines are designed to ensure patient safety during treatment. Ergonomic interfaces ensure their easy use by the medical staff. Dialysate, which is produced on-line by HD machines from reverse osmosis water and bicarbonate concentrates, is a buffered solution (physiologic pH) composed of sodium (Na^+), potassium (K^+), calcium (Ca^{2+}), magnesium (Mg^{2+}), chloride (Cl^-), and bicarbonate (HCO_3^-). During HD, blood and dialysate are pumped through the hemodialyzer. Weight-loss (or ultrafiltration flow rate, Q_{UF}) might be set by the staff and is automatically regulated during the dialysis session by dialysate affluent and effluent pumps (5).

Typical blood and dialysate flow rates (Q_B and Q_D, respectively) range from 200 to 400 mL/min and from 500 to 800 mL/min, respectively (57), depending on dialysis treatment and vascular access. Typical dialysis treatments are performed thrice a week during 4 h sessions and a Q_{UF} of about 10 mL/min (58).

IV. Clinical challenges

1) Inadequate removal of uremic toxins

The clearance of uremic toxins differs between the three toxin groups. Although urea is easily removed during hemodialysis, protein-bound uremic toxins, such as IS and pCS, and middle molecules, such as β_2m, are only poorly removed (22; 33; 59; 60; 61). Due to their high protein binding (90% to 95%) (22; 35) and high volume of distribution (33), both IS and pCS rather behave like middle molecules. Therefore, current dialysis strategies are not effective to remove such molecules (7). However, differences on the removal of uremic toxins between dialysis treatments have been reported.

The dialysis membrane type (low-flux *versus* high-flux, cellulosic *versus* synthetic) has no substantial impact on the removal of IS and pCS (22; 61). In contrast, dialysis strategies show large differences. Higher clearances are obtained with high-flux HD compared to PD (62) and

with pre- or post-dilution HDF compared to pre-dilution HF (60). Increasing the ultrafiltration flow rate improves the clearance but no difference is found neither between pre- and post-dilution HDF (60; 63) nor between HD and HDF on the short (64) and the long term (65).

In the case of β_2m, higher clearances and removal rates are reached by convective strategies, such as HDF and HF, as compared to HD (60; 63; 64; 66). The β_2m clearance increases proportionally during HDF while increasing the ultrafiltration flow rate (66). Furthermore, high-flux HD more effectively removes β_2m compared to PD (62) but long-term results are contradictory. Compared with HD, β_2m levels seem to be greater reduced with HDF (59; 65; 67) but clinical outcomes, as assessed by all-cause mortality and cardiovascular events are not significantly improved with HDF (67). Recent studies showed, however, better clinical outcomes with high-efficiency HDF (substitution volume > 17 L per session) as compared to HD and low-efficiency HDF (substitution volume < 17 L per session) (68; 69). Nocturnal dialysis, characterized by longer and more frequent dialysis sessions (8 h session, 6 nights per week), significantly reduces β_2m levels as compared to conventional HD (4 h session, thrice a week) (70).

2) <u>Worse clinical outcome in ESRD *versus* general population</u>

As reported by the ERA-EDTA registry in 2010 (6), adjusted survival probabilities of incident RRT patients is low: 95.8%, 87.7%, 79.0%, and 57.1%, after 90 days, 1, 2, and 5 years, respectively. The survival probability is strongly dependent on age. Renal transplant patients have a largely higher long term survival rate as compared to patients on hemodialysis or peritoneal dialysis (about 80% *versus* about 50% after 5 years, respectively). Therefore, the life expectancy of ESRD patients is largely decreased when compared to the general population (see **Fig. 5**). The two main causes of death for ESRD patients is CVD (about 40%) and infection (about 10%), as reported in 2012 by the USRDS (71).
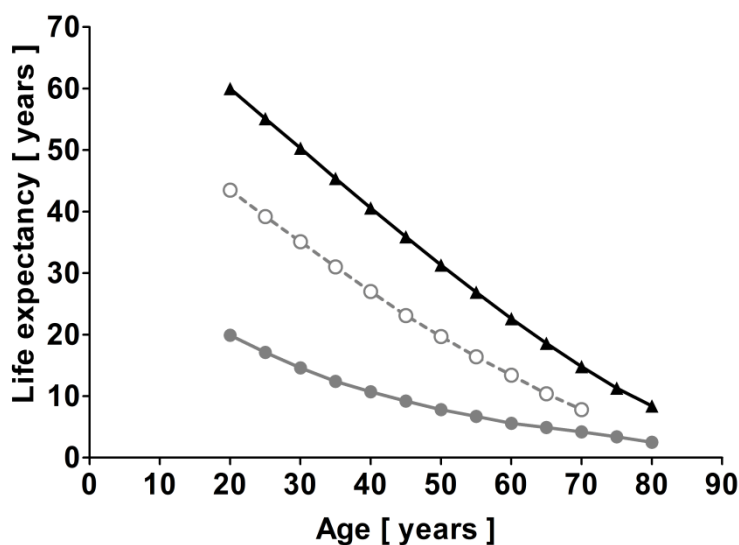
Fig. 5: Expected remaining lifespan of the general population in 2005 and of prevalent dialysis and transplant patients in 2009 and 2010 (including mortality of the first 90 days).

Data of life expectancy were collected from (6) for the general population (▲), the ESRD patients on maintenance hemodialysis (●), and the transplanted ESRD patients (○).

3) <u>Albumin binding and impaired drug binding in CKD</u>

Human serum albumin (HSA, MW = 66.5 kDa) is the most abundant plasma protein with a concentration of about 570 µM (38 g/L) (37; 72). It is a carrier protein for metallic ions and many hydrophobic compounds in plasma like drugs, fatty acids, hormones, and waste products (73; 74; 75; 76). Uremic toxins are able to bind specifically to Sudlow's site I, like 3-carboxy-4-methyl-5-propyl-2-furanpropionic acid (CMPF) (77), and site II of HSA (78), like IS and pCS (77; 79), thereby leading to impaired binding of drugs potentially causing dosage problems (1; 46; 80; 81; 82).

V. <u>The receptor-ligand binding theory</u>

Proteins like albumin present binding sites on their surface. The binding of ligand L to receptor R is based on the law of mass action (83). It assumes that binding is reversible:

$$R + L \underset{k_{off}}{\overset{k_{on}}{\rightleftharpoons}} RL$$
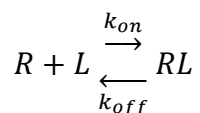
When equilibrium is reached, new ligand-receptor complexes are formed at the same rate at which ligand-receptor complexes dissociate. Thus, the equilibrium dissociation constant (K_D), inverse of the equilibrium association constant (K_A), is given by **Eq. 1**.

$$\frac{[L].[R]}{[RL]} = \frac{k_{off}}{k_{on}} = K_D = \frac{1}{K_A}$$

Eq. 1: Definition of the equilibrium constants (84)**.**
Where *[L]* and *[RL]* are the free and bound ligand concentration, respectively; k_{on} and k_{off} the association and dissociation rate constants.

If the receptor has a high affinity for the ligand, then K_D will be low and a low concentration of ligand will occupy half of the receptors (in that case *[L] = K_D*). This model assumes that all receptors are equally accessible to the ligands, the receptors are either free or bound to the ligand, the binding does not alter the ligand or receptor, and that the binding is reversible (84).

Ligands may bind to other sites than to the receptors of interest. Binding to the receptor of interest is called **specific binding**, while binding to other sites is called **nonspecific binding**. The latter is usually directly proportional to the ligand concentration. The **total binding** is the sum of specific and nonspecific binding as shown in **Fig. 6**. It can be assumed that specific binding only happens at low ligand concentrations. The specific binding is limited by the maximal available binding sites (B_m).
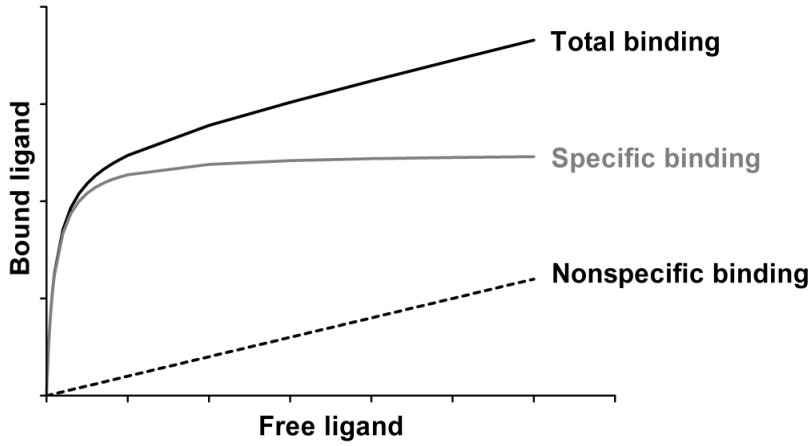
Fig. 6: Representation of the total, specific and nonspecific ligand binding to receptors.

Since uremic toxins, such as IS or *p*CS, bind specifically to albumin on Sudlow's site II (79; 85), the law of mass action applies. At high concentrations, nonspecific binding will occur as if the toxins will be captured by the protein tertiary structure. Since the IS and the *p*CS concentration is low in uremic patients (about 80 and 100 µM, respectively (64)) compared to the albumin concentration (about 570 µM (37)), the bound toxin concentration is given by **Eq. 2** (84):

$$[RL] = \frac{B_m \times [L]}{K_D + [L]}$$

Eq. 2: One site specific binding equation.
Where *[RL]* is the bound ligand concentration [M], *[L]* the free ligand concentration [M], B_m the binding site concentration [M], and K_D the dissociation constant [M].

From this equation, it is possible to calculate the protein bound fraction (PBF) of a given ligand (see the Appendix for the complete demonstration; **Eq. 3**).

$$PBF = \frac{\frac{K_D}{B_m} + \frac{[L_T]}{B_m} + 1 - \sqrt{\left(\frac{K_D}{B_m} + \frac{[L_T]}{B_m} + 1\right)^2 - 4.\frac{[L_T]}{B_m}}}{2.\frac{[L_T]}{B_m}}$$

Eq. 3: Relationship between PBF, binding constants, and ligand concentration for a one site specific binding reaction.
Where *PBF* is the protein bound fraction [%], *[L_T]* the total ligand concentration [M], B_m the binding site concentration [M], and K_D the dissociation constant [M].

This equation, which is adapted from Meyer et al. (86), describes the PBF of a ligand (in the present case a uremic toxin) as a function of the binding constants K_D and B_m, specific to the ligand and the receptor at a constant toxin concentration. **Fig. 7** has been obtained from this equation by varying the total toxin concentration *[L_T]* in the ratio $\alpha = [L_T]/B_m$.
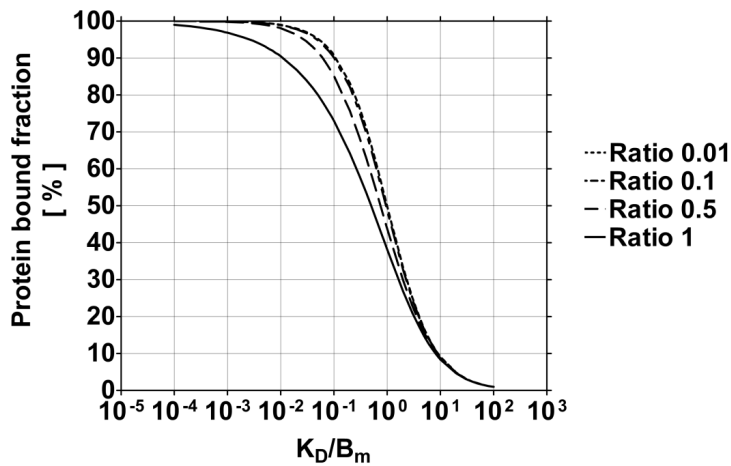
Fig. 7: Dependence of the PBF on the ratio K_D/B_m for different toxin-proteins ratio.
This figure was obtained by varying the ratio $[L_T]/B_m$ from 0.01 to 1 in **Eq. 3**.

This figure yields important information to understand the protein binding of uremic toxins in human plasma and the situation during dialysis. The PBF indeed corresponds to the fraction retained in blood during RRT. The PBF decreases by increasing the ratio K_D/B_m. This happens by increasing K_D (i.e. decreasing the binding affinity) and/or decreasing B_m (i.e., removing binding sites or diluting blood/plasma). It is important to note that diluting plasma will not change the ratio $[L_T]/B_m$ since both total binding capacity and total toxin concentration are decreased proportionally. During dialysis, the toxin is removed, $[L_T]$ and, consequently, the ratio $[L_T]/B_m$ decreases, which in turn increases the PBF. In other words, the toxin removal decelerates during dialysis.

VI. <u>Aim of the study</u>

Based on conventional dialysis strategies, purpose of the present thesis was to develop a dialysis method which more effectively removes protein bound uremic toxins. Focus was the development of a means to reduce protein binding of such solutes in order to increase their dialytic clearances with the potential goal to improve clinical outcomes of hemodialysis patients.

MATERIALS AND METHODS

I. Materials

1) Reagents

a. Uremic toxins

IS and **PAA** were purchased from Sigma-Aldrich (indoxylsulfate potassium salt, ref. I3875; phenylacetic acid, 99%, ref. P16621; Steinheim, Germany).

As a kind gift from Miss N. Meert, ***pCS*** was synthesized by the laboratory of Organic & Bio-organic Synthesis of the University Ghent (Belgium).

b. Chemicals

Ammonium formate (NH_4COOH), **tetrabutylammonium hydrogensulfate** (TBA), **heparin**, **lipopolysaccharide** (LPS), **phosphate buffered saline** pH 7.4 (PBS), **4-(2-Hydroxyethyl)piperazine-1-ethanesulfonic acid N-(2-Hydroxyethyl)piperazine-N′-(2-ethanesulfonic acid)** (HEPES), **glucose** , **N-Formyl-Nle-Leu-Phe-Nle-Tyr-Lys** (hexapeptide), **activated charcoal**, and **HSA** were purchased from Sigma-Aldrich (ammonium formate for mass spectrometry, ≥99.0%, ref. 70221, Fluka analytical; tetrabutylammonium hydrogensulfate 97%, ref. 155837; heparin sodium salt from porcine intestinal mucosa, ref. H3149; Lipopolysaccharides from *Salmonella enterica* serotype minnesota Re 595, ref. L9764; phosphate buffered saline powder, pH 7.4, ref. P3813; HEPES, ≥99.5% by titration, ref. H3375; D-(+)-glucose monohydrate for microbiology, ≥99.0%, ref. 49159; N-Formyl-Nle-Leu-Phe-Nle-Tyr-Lys, ≥97%, ref. F0267; DARCO®, 20-40 mesh particle size, granular, ref. 242268; albumin from human serum, lyophilized powder, fatty acid free, globulin free, ≥99.0%, ref. A3782).

Phenylalanine (Phe), **di-potassium hydrogen phosphate** (K_2HPO_4), **sodium chloride** (NaCl), **potassium chloride** (KCl), **magnesium chloride** ($MgCl_2$), **Titriplex® III** (EDTA), **PBS pH 7.2 tablets**, **sodium acetate** (CH_3COONa), and **ammonium acetate** (CH_3COONH_4) were purchased from Merck (DL-phenylalanine for biochemistry, ref. 107257; di-Potassium hydrogen phosphate anhydrous for analysis EMSURE®, ref. 105104; sodium chloride for analysis EMSURE® ACS, ISO, Reag. Ph Eur, ref. 106404; potassium chloride for analysis EMSURE®, ref. 104936; magnesium chloride hexahydrate for analysis EMSURE® ACS, ISO, Reag. Ph Eur, ref. 105833; ethylenedinitrilotetraacetic acid, disodium salt dihydrate for analysis, ® ACS, ISO, Reag. Ph Eur, ref. 108418; buffer tablets pH 7.2 for preparing buffer solution according to WEISE for staining of blood smears, ref. 109468; sodium acetate anhydrous for analysis EMSURE® ACS, Reag. Ph Eur, Ref. 106268; ammonium acetate Fractopur®, Ref. 116103; Darmstadt, Germany).

Sodium citrate (NaCitrate) was purchased from Carl Roth GmbH (tri-sodium citrate dehydrate Rotipuran®, ≥99% for analysis ACS, ref. 3580.1; Carl Roth GmbH, Karlsruhe, Germany).

Dihydrorhodamine 123 (D123) was purchased from Invitrogen (molecular probes®, 10 mg, ref. D-632).

c. Solutions

Saline was purchased from B.Braun Melsungen (NaCl 0.9% B.Braun, Ecotainer®, ref. 3570160; or isotonic sodium chloride solution, Perfuflac® N, ref. 6796; Melsungen, Germany).

Deionized ultrapure water was either purchased from B.Braun Melsungen (Aqua B.Braun, ref. 0082479E), or prepared with a Barstead Nanopure water preparation system (D11931, Thermo Scientific, Langenselbold, Germany).

HPLC water was purchased from VWR International (water hipersolv chromanorm® for HPLC, ref. 23595.328, Darmstadt, Germany).

Dialysate for *in vitro* dialysis experiments involving mini-dialyzers was prepared with a Nikkiso DBB03 apparatus from bicarbonate concentrate.

Dialysate acid and **alkaline concentrates** were purchased from B.Braun Avitum AG (SW 196 A, ref. 3273; alkaline bicarbonate concentrate 8.4%, ref. 169; Melsungen, Germany).

Formic acid, **acetonitrile**, **sodium hydroxide** (NaOH), **ethanol** (EtOH) **May-Grünwald's staining solution**, **Giemsa solution**, and **acetic acid** (CH_3COOH) were purchased from Merck (EMSURE®, 98-100% purity, ref. 1.00264; LiChrosolv® acetonitrile gradient grade for liquid chromatography, ref. 100030; sodium hydroxide solution, for 1000 mL, c(NaOH) = 1 mol/L = 1 N, Titrisol®, ref. 109956; absolute for analysis EMSURE® ACS, ISO, Reag. Ph Eur, ref. 100983; May-Grünwald's eosine-methylene blue solution modified for microscopy, ref. 101424; *Giemsa*'s azur eosin methylen blue solution for microscopy, ref. 109204; acetic acid, for 500 mL, c(CH_3COOH) = 1 mol/L = 1 N, Titrisol®, ref. 109951).

Dimethyl sulfoxide (DMSO) was purchased from Sigma-Aldrich (Hybri-Max™, sterile-filtered, BioReagent, suitable for hybridoma, ≥99.7%, ref. D2650).

PharmLyse solution was performed by BD Bioscience (ref. 555899, Heidelberg, Germany)

HSA 20% solution was performed by Biotest (Albiomin® 20%; Dreieich, Germany).

d. Self prepared solutions

Heparin stock solution (**350 IU/mL)** was prepared by dissolving heparin in saline and was readily stored at 4 °C for maximum 4 weeks.

NaCitrate stock solution (**3.8% w/w**) was obtained by dissolving NaCitrate in saline and was stored at -20 °C.

PBS solution (**10 mM, pH 7.4**) was prepared by dissolving one pack of PBS in 1 L ultrapure water; this solution was stored at room temperature for few days. **PBS solution (1x PBS, pH 7.2)** was prepared by dissolving one buffer tablet pH 7.2 in 1 L ultrapure water.

D123 stock solution (**200 μM**) was prepared by dissolving one vial D123 in 1.45 mL DMSO. This solution was then diluted 1:100 in DMSO and 100 μL aliquots were stored at -30 °C protected from light. Before use, one aliquot was mixed with 9.90 mL 30 mM HEPES buffer pH 7.4 (final concentration 2 μM D123).

HEPES buffer (**30 mM**, calcium free) was prepared by dissolving 14.30 g HEPES, 12.86 g NaCl, 1.50 g KCl, 0.41 g $MgCl_2$, and 4.00 g glucose in 1.6 L ultrapure water, and adjusted to pH 7.4 with NaOH. Then, ultrapure water was added to a final volume of 2 L. Finally, it was filtered through a 0.20 μm sterile filter. Aliquots (50 mL) were stored at -20 °C.

HH-Ca^{2+}-buffer was prepared by dissolving 7.15 g HEPES, 6.43 g NaCl, 0.75 g KCl, 0.203 g $MgCl_2$, and 2 g glucose in 1 L ultrapure water.

Hexapeptide solution (**100 μM**) was prepared by dissolving 1 mg hexapeptide in 12.14 mL DMSO and 10 μL aliquots were stored at -30 °C. Before use, one aliquot was diluted in 990 μL 30 mM HEPES buffer pH 7.4 (final concentration 1 μM).

EDTA solution (**100 mM**) was prepared by diluting 37.2 g EDTA in 1 L pyrogen free saline, aliquoted in 50 mL sterile Falcon tubes and stored at -20 °C. **EDTA solution (20 mM)** was obtained by diluting EDTA 100 mM 1:5 with saline.

LPS working solution (**10 μg/mL**) was prepared by dissolving LPS in 5 mL 20 mM EDTA pH 7.4 which then was completed to 100 mL with HH-Ca^{2+}-buffer (500 mg/L LPS stock solution). Before use, LPS working solution was made by diluting the parent solution 1:50 with the HH-Ca^{2+}-buffer.

NaCl stock solution (**5.00 M**) was prepared by dissolving 1,461 g NaCl in 5 L ultrapure water.

Giemsa working solution was obtained by mixing 4 mL Giemsa solution with 80 mL PBS pH 7.2.

PAA stock solution (**100 mM**) was prepared by diluting 0.136 g PAA in 10 mL 20% EtOH / 80% H_2O (v/v), pH was neutralized with NaOH.

Phe solution (**8 mg/mL**) was prepared in saline.

e. Biologic fluids

Frozen human citrate-plasma was obtained from the Bavarian Red Cross blood donor service (Munich, Germany).

Human whole blood was freshly donated by healthy volunteers into transfer bags (COMPOFLEX® 600 mL, ref. 501108; Fresenius HemoCare, Bad Homburg, Germany) prefilled with 5 IU/mL heparin.

Normal healthy plasma was separated from human whole blood by centrifugation (2,000 *g*, 10 min, 5 °C).

Uremic plasma was separated by centrifugation (2,000 *g*, 10 min, 5 °C) from blood drawn into EDTA-tubes or heparinized syringes (60 mL, 5 IU/mL) of ESRD patients of a single dialysis

center (Dialysis center, Elsenfeld, Germany) after having obtained approval from the competent review board (ethics committee of the University Hospital Würzburg, code AZ 64/12) and written informed consent from the patients.

2) <u>Laboratory equipments</u>

YM30 filter units were purchased from Millipore (Centrifree® ultrafiltration unit with ultracel YM-T membrane, red. 4104, Merck; Darmstadt, Germany).

30 kDa filter units were purchased from VWR international (VWR centrifugal filter, modified PES 30k, 500 µL, low protein binding, ref. 516-0231 and ref. 516-0232).

HPLC glass vials were purchased from Chromacol (ref. 2-CRV, ref. 1.1-CTVG, United Kingdom).

Syringe filters 0.20 µm were purchased from Sartorius (Minisart sterile filter, ref. 17597K; Sartorius Stedim Biotech GmbH, Goettingen, Germany).

Transfusion set was purchased from Codan (Transfusion set for blood or blood components, ref. 45.4424; CODAN Medical devices, Lensahn, Germany)

EDTA S-Monovette® and **lithium heparin S-Monovette®** were purchased from Sarstedt (S-Monovette® 2.7 mL K3E and S-Monovette® 7.5 mL K3E, ref. 05.1167 and ref. 01.1605.001; S-Monovette® 2.7 mL LH, ref. 05.1553.001; Nümbrecht, Germany).

Tubing systems for dialysis were purchased either by Promedt (Medizintechnik Promedt GmbH, Tornesch, Germany) or by Nikkiso (Nikkiso Medical GmbH, Hamburg, Germany).

Hemodialysis membranes used either in mini- (housing Ø 8mm) or standard-dialyzers are presented in **Tab. 5**.

Membrane type	Purchaser
Cuprophan®, low-flux cellulosic membrane, 6 kDa cut-off PUREMA® H dialyzer, high-flux polyethersulfone membrane PUREMA® L dialyzer, low-flux polyethersulfone membrane DIAPES® HF800, high-flux polyethersulfone membrane DIAPES® LF100, low-flux polyethersulfone membrane	**Membrana GmbH, Wuppertal, Germany**
Polyamix™, high-flux polyarylethersulfone, polyvinylpyrrolidone, polyamide blend membrane	**Gambro Dialysatoren GmbH, Hechingen, Germany**
Helixone®, high-flux polyethersulfone membrane	**Fresenius Medical Care, Bad Homburg, Germany**

Tab. 5: Hemodialysis membranes used during dialysis experiments

3) <u>Analysis tools</u>

Pressures and temperature during *in vitro* dialysis experiments were recorded with a **MSR-Manager system** (LAB-Box1; Hitec Zang GmbH, Herzogenrath, Germany) driven by a LabVision software version 2.6 (Hitec Zang GmbH).

Reversed-phase high pressure liquid chromatography (RP-HPLC) was performed using a Gynkotek apparatus (Germering, Germany) with a HPLC pump model M480 and a column

thermostat STH 585. A degasser ERC-3315 (ERC GmbH, Riemerling, Germany) was built in the system. Detectors were a spectrofluorometric RF-551 detector (Shimadzu, Kyoto, Japan) and an UV-VIS detector UVD 340 U (Dionex GmbH, Germering, Germany). A C18 column was used (ProntoSIL® Hypersorb, 250 x 4.6 mm, ODS 3.0 µm; Bischoff chromatography, Leonberg, Germany) with a guard column (HPLC guard cartridge system, Security Guard™; Phenomenex, USA) for all uremic toxins.

The **external pumps** were IPC and MCP pumps with CA or Pro-381 heads from ISMATEC (IDEX Health & Science, Wertheim-Mondfeld, Germany).

Centrifuge apparatus: bench top centrifuge Z 513 K (Hermle Labortechnik GmbH, Wehingen, Germany) and Eppendorf 5414 centrifuge (Eppendorf Vertrieb Deutschland GmbH, Wesseling-Berzdorf, Germany).

pH meter inoLab pH Level 2 (WTW, Weilheim, Germany).

A DBB-03 **dialysis machine** (Nikkiso Medical GmbH) served for the *ex vivo* experiments with human blood or plasma as well as for the animal experiments; a Formula 2000 (Bellco, Mirandola, Italy) was used for the pilot experiments in aqueous solution.

Blood gas analysis (BGA) was performed with an AVL-OMNI 9 and a COBAS b 123 apparatus (Roche Roche Diagnostics GmbH, Mannheim, Germany).

The **total protein concentration** (TP) was determined with a COBAS C111 apparatus (Roche Roche Diagnostics GmbH).

The **albumin concentration** was measured using laser nephelometry (BN ProSpec, Siemens, Germany).

Conductivity was measured using a CDM83 apparatus (Radiometer Copenhagen, Copenhagen, Denmark).

Flow cytometry was performed with a FACScan apparatus (BD Bioscience, Heidelberg, Germany).

Microscopic observations were performed using a Laborlux 12 microscope (Leitz) and pictures were taken with an AxioCam MRc camera (Zeiss) and an AxioVision software (version 4.7.0.0, Carl Zeiss Imaging Solutions).

Spectrophotometry was performed using a UV-1650PC spectrophotometer (Shimadzu Corporation, Kyoto, Japan).

The **cell count** in blood was measured with an ABX Pentra 60 cell counter (Agon Lab AG, Reichenbach/Stuttgart, Germany) and **lactate dehydrogenase** (LDH) concentration was measured enzimatically (IDEXX Laboratories, Ludwigsburg, Germany).

4) <u>Analytical software</u>

The binding constants K_D and B_m were determined with the software **GraphPad Prism** (version 3.00 for Windows; GraphPad Software, San Diego California USA). Linear regression applying either a one site specific binding equation or a one site total binding equation was performed (see **Eq. 2** and **Eq. 4**, respectively):

$$[RL] = \frac{B_m \times [L]}{K_D + [L]} + (NS \times [L])$$

Eq. 4: One site total binding equation.
Where *[RL]* is the bound ligand concentration, *[L]* the free ligand concentration, B_m the binding site concentration, K_D the dissociation constant, and *NS* the non specific binding coefficient.

Statistical analyses were performed with either **MINITAB®** release 14.20 for Windows (Minitab Ltd, Coventry, United Kingdom) or with **GraphPad Prism.**
The HPLC measurements were analyzed by **Chromeleon** software (version 6.80; Dionex Corporation, Sunnyvale, USA).

II. Methods

1) Standard operating procedures

Measurements of biological parameters have been mostly performed according to the laboratory's standard operating procedures.

a. Free hemoglobin concentration

The free hemoglobin concentration was determined by spectrophotometry. Plasma was isolated, diluted 1:5 in saline and transferred in 1 cm PMMA cells. Firstly, the hemoglobin (Hb) concentration was determined by measuring the optical density (OD) at a wavelength (λ) of 546 nm using a reference in saline. The free hemoglobin concentration was calculated according to the Beer-Lambert equation (87):

$$C = \frac{OD_{546}}{\varepsilon \times l} \times DF$$

Eq. 5: Beer Lambert equation to determine the free hemoglobin concentration (87)**.**
Where *C* is the free Hb concentration [g/dL], OD_{546} the optical density at λ = 546 nm, ε the Hb extinction coefficient at λ = 546 nm (ε = 8.37 dL/g/cm), *l* the cell length equal to 1 cm, and *DF* the dilution factor of the sample.

Secondly, the free Hb concentration was measured according to the method of Cripps (88) allowing a better estimation at low concentrations. Free Hb concentration was determined by measuring the OD at λ = 560 nm, λ = 576 nm, and λ = 592 nm and calculated according to:

$$C = (2 \times OD_{576} - OD_{560} - OD_{592}) \times k \times DF$$

Eq. 6: Calculation of the free hemoglobin concentration according to Cripps (88)**.**
Where *C* is the free Hb concentration in [mg/dL], OD_{576}, OD_{560}, and OD_{592} the optical density at λ = 576, 560, and 592 nm, respectively, *k* a constant (k = 99.8 mg/dL), and *DF* the dilution factor of the sample.

b. Hemolysis

Hemolysis referred to the amount of free hemoglobin (plasma Hb) expressed in % of the total hemoglobin (blood Hb).

c. Thrombin-antithrombin III

The thrombin-antithrombin III (TAT) concentration was measured by ELISA assay (Enzygnost TAT micro, ref. OWMG 15; Siemens, Marburg Germany). Blood samples (1.8 mL) were stopped with 0.2 mL 3.8% NaCitrate in 3.5 mL polystyrene tubes on ice. Then, plasma aliquots were stored at -20 °C after isolation.

d. Complement component 5a

The complement component 5a (C5a) concentration was measured by ELISA assay (DRG C5a ELISA, ref. EIA-3327; DRG Instruments GmbH, Marburg, Germany). Blood samples (1.8 mL) were stopped with 0.2 mL 100 mM EDTA solution in 3.5 mL polystyrene tubes on ice. Then, plasma aliquots were stored at -20 °C after isolation.

e. Cell count

Samples were measured in duplicate immediately after sampling. Leucocyte (WBC), erythrocyte (RBC), platelet (PLT), and basophilic granulocyte counts were determined by impedance. The hematocrit level (Hct) was calculated from these values. Lymphocyte, monocyte, neutrophilic, and eosinophilic granulocyte counts were determined by impedance and light scattering. The total Hb concentration (tHb) was determined by measuring the OD_{550} after cell lysis.

f. Measurement of the uremic toxin concentration by RP-HPLC

i. Sample preparation

The **total toxin concentration** was determined in plasma samples diluted 1:5 (final volume 5 mL) in saline. Then, proteins were heat denatured (30 min at 95 °C) and, subsequently, cooled on ice for 10 min. A 1 mL sample was transferred into YM30 filter units and centrifuged for 60 min at 2,000 g and 5 °C. This protocol was further refined as follows. Plasma samples were diluted 1:5 in PBS pH 7.4 (final volume 0.5 mL), proteins were heat denatured and cooled as given above. The sample was transferred into an Eppendorf cup and centrifuged at 10,000 g and room temperature for 5 min to pellet precipitated proteins. The resulting clear supernatant was filtered through 30 kDa filter units (from VWR) and centrifuged for 30 min at 10,000 g and room temperature to remove larger proteins. Finally,

filtrate was transferred into HPLC vials and measured by RP-HPLC. Standard curves were generated in human plasma using the same preparation method.

The **free toxin concentration** was determined in plasma samples directly filtered through YM30 (1 mL) or 30 kDa units (0.5 mL, VWR) for 30 min at 10,000 g and room temperature. The filtrate was transferred into HPLC vials and measured by RP-HPLC. Standard curves were produced in saline or PBS pH 7.4 since no difference was seen compared with a standard curve in plasma filtrate.

ii.   Measurements

RP-HPLC detection parameters were Ex.280 nm / Em.340 nm and Ex.264 nm / Em.290 nm for **IS** and **pCS**, respectively. Elution gradients started from 15% to 25% eluent B within 10 min at 1 mL/min and 30 °C; eluent A was 50 mM NH_4COOH buffer pH 3.4 adjusted with formic acid, eluent B was acetonitrile. Retention times in such conditions were about 5.1 and 6.8 min for IS and pCS, respectively.

PAA was detected with UV-VIS at $\lambda = 259$ nm and 30 °C with flow rate of 1 mL/min. Retention time was about 14 min. As an internal standard, 1.5 mg/mL Phe was used. Gradient: from 5% to 60% eluent B within 20 min. Eluent A: 4 mM TBA + 10 mM K_2HPO_4 in HPLC water at pH 7.0 (with NaOH), Eluent B: 80% acetonitrile + 20% A (v/v).

g. **Dialysis experiments**

For all dialysis experiments involving standard or mini-dialyzers, the dialyzer and tubing system were initially rinsed with 1 L saline in single pass at appropriate flow rate (NB: in the case of mini-dialyzer setups, the circuit was rinsed with 100 mL saline only). Then, the circuit was closed, the dialysate circuit was connected and the system was recirculated for at least 20 min. The tubing system was filled with blood or plasma, respectively. In the case of standard dialysis with blood, blood was added to reach a pre-determined total blood volume within the system. Finally, the venous line was connected to the blood reservoir and the dialysis session started.

Note: *For the dialysis experiments involving the serial dialyzers setup, the external tubing system of the first cartridge was rinsed in single pass with saline and then closed. Consecutively, fluid in this closed loop was pumped at the appropriate flow rate until the end of the experiment.*

h. **Blood smears**

Blood smears were analyzed on microscope slides after May-Grünwald Giemsa staining. Staining was performed as follows. After drying, blood smears were immerged for 3 min in May-Grünwald staining solution. Then, the May-Grünwald staining solution was diluted 1:1 in PBS pH 7.4 and microscope slides were further immerged for 1 to 2 min. They were immerged 15 to 20 min in the Giemsa working solution, well rinsed with PBS pH 7.2 and finally air-dried.

2) **Statistical analysis**

If normally distributed, comparison of two groups was performed with the Student's t-test. To compare more groups, a one way ANOVA followed by Tukey's *post-hoc* test was applied. If not normally distributed, the Mann-Whitney-U-test was used. Correlation was assessed with the Pearson test. A P-value < 0.05 was considered to be significant (software: Minitab® and GraphPad Prism). Results are always given as mean ± SD.

3) **Experimental part**

Physiological Na^+ and Cl^- concentrations in human plasma are 140 ± 5 and 100 ± 5 mM respectively, corresponding to a physiological NaCl concentration ([NaCl]) of 120 mM whereas saline has a concentration of 154 mM for both Na^+ and Cl^- (308 mOsm/L). Thus, isotonic [NaCl] will refer to "0.15 M NaCl".

a. *In vitro* **uremic toxin binding experiments**

i. Effect of storage conditions

Blood from eight ESRD patients was drawn in EDTA-tubes before dialysis and plasma was separated. An aliquot (1 mL) was taken to determine total and free IS and *p*CS concentrations while, another aliquot was frozen at -20 °C for 6 months and then thawed to repeat the measurements.

Heparinized plasma (5 IU/mL) was isolated from blood of two healthy volunteers (n = 2) and kept either in the fridge or at -20 °C overnight. IS and PBS pH 7.4 were added to the fresh and the thawed plasma (650 µL plasma, 900 µL final volume) to reach 22, 44, 111, 222, and 444 µM IS (corresponding to an albumin/toxin ratio ranging from 0.05 to 1.0). An aliquot of each sample was taken to measure total and free IS concentrations as well as the albumin concentrations. The binding constants K_D and B_m were determined using **Eq. 2**.

ii. Uremic toxin binding affinity in uremic plasma

Blood from 49 ESRD patients was collected in EDTA-tubes pre- and post-dialysis; plasma was separated at 2,000 g for 10 min. Four hour dialysis sessions were performed in HD or HDF modus. Free and total IS and pCS were determined in these samples. The binding properties were assessed by non linear regression using a one site specifying binding equation (**Eq. 2**) by considering each sample as part of a uremic "pool".

iii. Pilot binding studies of IS, pCS, and PAA in normal human plasma

The effect of toxin concentration and increased [NaCl] on different uremic toxins was tested in normal human plasma isolated from heparinized blood (5 IU/mL). Toxin concentrations were 5, 10, 25, 50, 100, and 200 µM for both IS and pCS, 100, 200, 500, 1000, 2000, and 4000 µM for PAA. [NaCl] was 0.15, 0.30, 0.50, and 1.00 M.

Binding studies involving IS and PAA with 0.15, 0.30, and 0.50 M NaCl were performed by mixing plasma with a cocktail of IS and PAA; whereas with 1.00 M NaCl, pCS was also added. Experiments involving pCS at 0.15, 0.30, and 0.50 M NaCl were performed with pCS only. Firstly, toxins were added to 1.5 mL plasma and incubated for 1 h at room temperature. Then, 5.00 M NaCl solution and saline were added to reach the target [NaCl] and a final volume of 3.0 mL (final plasma dilution 1:2). Again, samples were incubated for 1 h at room temperature. Free and total toxin concentrations were measured using RP-HPLC.

iv. Determination of the binding constants of IS in HSA solution

Fatty acid free HSA (8.5 g/L stock solution) was mixed 1:1 with IS, PBS pH 7.4, and 5.00 M NaCl (final volume: 1 mL; final concentrations: HSA, 4.25 g/L; IS, 2.5, 5.0, 7.5, 10, 15, and 25 µM; NaCl, 0.15, 0.30, 0.50, and 0.75 M) and incubated for 30 min at room temperature. The toxin-albumin ratio was kept < 0.40 mol/mol. Free and total toxin concentrations were measured using RP-HPLC. The binding constants K_D and B_m were determined using **Eq. 2**. B_m was set constant and equal to the HSA concentration (65 µM). Two independent experiments were performed (n = 2). Scatchard plot analysis was performed on the free and bound IS concentrations.

v. Determination of the binding constants of IS, pCS, and PAA in normal human plasma

Experiments involving IS were performed with 0.5 mL citrate-plasma after removal of fat aggregates with a transfusion set. Plasma was incubated for 30 min at room temperature and different [NaCl] in PBS pH 7.4 ([NaCl]: 0.15, 0.30, 0.50, and 0.75 M). IS was added to reach a final concentration of 8, 15, 23, 30, 90, and 150 µM. The volume of PBS pH 7.4 was

adjusted with respect to the IS and NaCl volumes so that the plasma was always 1:2 diluted. The toxin-albumin ratio was kept ≤ 1.0 mol/mol to avoid non-specific binding. Experiments involving pCS were performed as already described (refer to "Pilot binding studies of IS, pCS, and PAA in normal human plasma"). Both toxins were studied separately in order to avoid competition for the binding sites. Three independent experiments were performed using plasma of three different donors (n = 3).

Experiments involving PAA were performed with either 3.48 mL (for 0.15 M NaCl) or 3.08 mL citrate-plasma (for 0.40, 0.50, and 0.65 M NaCl). PAA (100 mM stock solution, final concentrations: 0.025, 0.1, 0.5, 1.0, 2.0, 4.0, and 8.0 mM) was added with saline, 5.00 M NaCl and Phe (0.4 mg/mL final concentration) to reach a final volume of 4 mL. Toxin and plasma were incubated for 1 h at room temperature. This experiment was performed in triplicate with the plasma of the same donor.

Free and total toxin concentrations have been measured by RP-HPLC. The binding constants K_D and B_m were determined using **Eq. 2** for IS and pCS and **Eq. 4** for PAA.

For IS, the ratio K_D/B_m was calculated from the experimental free and bound IS concentrations. The ratio K_D/B_m was used as input to calculate the theoretical PBF using **Eq. 3**. Theoretical and experimental PBF were compared at low toxin-albumin ratio. The PBF was determined as follows: in the theoretical approach, the toxin-albumin ratio was set at 0.1; in the experimental approach, the toxin-albumin ratio was obtained from the measured total toxin and albumin concentrations.

vi.   Binding studies of IS and pCS in uremic plasma

7.5 mL blood from 15 ESRD patients was collected before dialysis in EDTA-tubes, plasma was separated and stored at -30 °C. For the binding experiments, 0.5 mL of uremic plasma was incubated for 30 min at different [NaCl] (0.15, 0.30, 0.50, and 0.75 M NaCl) in PBS pH 7.4 at room temperature. The volume of PBS was adjusted with the NaCl volume so that the plasma was always 1:2 diluted. For each sample, free and total IS and pCS concentrations were measured by RP-HPLC. K_D of uremic plasma proteins for IS and pCS was estimated according to **Eq. 3** and considering [HSA] = 286 µM after 1:2 dilution (37), thus, hypothesizing B_m being constant at 286 µM.

vii.   Effect of plasma dilution on the binding properties

These experiments were performed in citrate-plasma with a final dilution of either 1:2 or 1:10. Plasma (0.5 or 0.1 mL) was diluted with PBS pH 7.4, NaCl solution, and IS solution to reach a final [NaCl] of 0.15 and 0.50 M and a final volume of 1.0 mL. To 1:2-diluted plasma samples IS was added to obtain the same concentrations as described above (refer to "Determination of the binding constants of IS, pCS, and PAA in normal human plasma"). 1:10-diluted samples contained only one fifth of IS. The samples were incubated for 30 min at room temperature, further analyzed by RP-HPLC, and binding constants K_D and B_m were

determined as previously described. Scatchard plot analysis was performed on the free and bound IS concentrations.

viii. Effect of the temperature on the PBF of IS

Experiments were performed with plasma of two different ionic strengths. Firstly, 17.5 mL freshly donated heparinized (5 IU/mL) plasma from a single healthy donor was diluted with the same volume of PBS pH 7.4. Secondly, to prepare plasma with higher ionic strength, 17.5 mL heparinized plasma was mixed with half of the volume (8.75 mL) of PBS pH 7.4 and half of the volume (8.75 mL) of a 2.00 M NaCl solution resulting in 1:2 diluted plasma with 0.61 M [NaCl]. Both preparations were dialyzed (2.1 mL/min) at 25 and 37 °C against a solution of 150 µM IS with the corresponding ionic strength (0.15 and 0.61 M NaCl) using a mini-dialyzer with a low-flux dialysis membrane (Cuprophan®, 125 cm² membrane surface area; inner and outer compartment each 4.6 mL, respectively). Samples for the measurement of the total toxin concentration were collected from both compartments when the equilibrium was reached (1 h). The equilibrium point previously was determined during a pilot experiment with 12 mL plasma and the toxin solution during 150 min. Plasma runs through the dialyzer were calculated according to:

$$\tau = t \times \frac{Q}{V}$$

Eq. 7: Calculation of blood or plasma runs through the dialyzer.
Where τ is the number of plasma or blood runs, t the dialysis duration [min], Q the flow (plasma or blood) rate [mL/min], and V the fluid (plasma or blood) volume [mL].

ix. Effect of different ion species on the PBF of IS in uremic plasma

Two separate experiments (n = 2) were performed with plasma of the same uremic patient. Plasma (1 mL) was mixed with different solutions (final volume 1.75 mL) to compare the influence of the ion species and pH value on the PBF of IS. Therefore different stock solutions were prepared: 3.00 M NaCl, 3.00 M KCl, 0.15 M CH$_3$COONa pH 4.85 adjusted with CH$_3$COOH, and 0.15 M CH$_3$COONH$_4$ pH 4.85 adjusted with CH$_3$COOH. Eight different plasma preparations were compared: native plasma diluted with saline, plasma + 0.50 M NaCl, plasma + 0.50 M KCl, plasma + 0.25 M NaCl + 0.25 M KCl, plasma with pH decreased to about 5.4 using either 0.15 M CH$_3$COONa or 0.15 M CH$_3$COONH$_4$ stock solutions and with either 0.15 or 0.50 M NaCl. Total and free toxin concentrations were measured.

b. __Dialysis experiments in aqueous solution__

Dialysis experiments in saline were performed using a modified Bellco Formula 2000 dialysis apparatus; the setup illustrated in **Fig. 8** was initially used. Samples were taken from the blood reservoir (BR), arterial (ART), and venous (VEN) accesses. System pressures were monitored at the blood and dialysate inlet and outlet of the dialyzer.
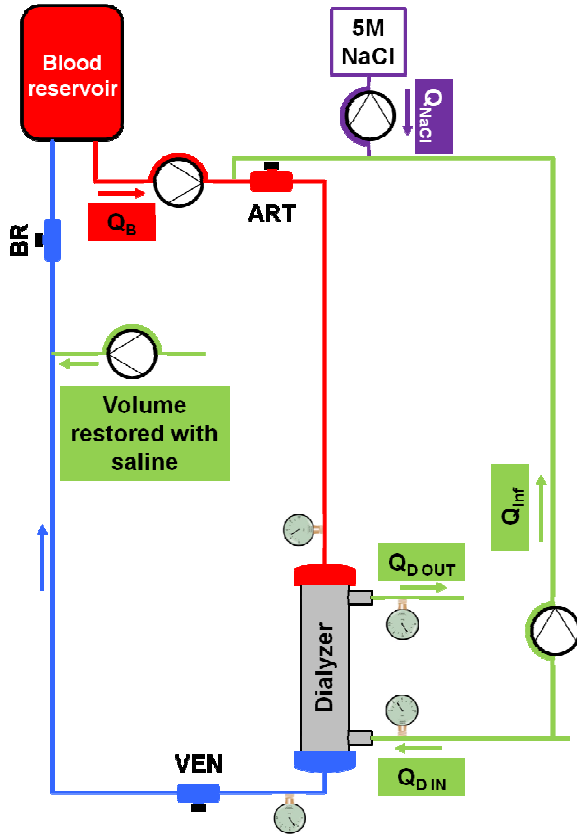
Fig. 8: Standard pre-dilution HDF, initial setup.
The fluid is pumped from the blood bag through the dialyzer. The substitution fluid is driven into the blood stream; the ionic strength of the substituate is increased by adding (flow rate Q_{NaCl}) a 5.00 M NaCl solution. The excess volume is removed by adjusting the ultrafiltration flow rate Q_{UF}. The fluid volume in the blood reservoir is monitored and kept constant by automatically restoring with saline the volume lost by Q_{UF}.

To determine the ionic strength of the solution contained in the blood line, the conductivity was measured. The conductivity σ is directly proportional to the ion concentration according to Kohlrausch's law (89):

$$\sigma = \sum \lambda_i \cdot [X_i]$$

Eq. 8: Kohlrausch's law (89)**.**
Where λ_i is the ionic molar conductivity [S.m^2/mol] and *[X_i]* the concentration of the ion *i* [mol/m^3].

A standard conductivity curve was generated in deionized water at room temperature by diluting a 5.00 M NaCl solution to 0.10, 0.25, 0.50, 1.00, 2.50, and 5.00 M NaCl.

i. Standard HDF – stability of ionic strength

Initial dialysis experiments were performed in pre-dilution HDF (pre-HDF, **Fig. 8**) modus using a PUREMA® H dialyzer (1.8 m² membrane surface area) and with 525 mL saline in the blood circuit. Machine settings were Q_B = 300 mL/min, Q_D = 500 mL/min, substituate flow rate Q_{inf} = 160 mL/min, and Q_{UF} = 40 mL/min. The dialysate temperature was set to 37 °C. In a first experiment, the saline was recirculated for 30 min. Then, saline (0.15 M) was injected into the substitution fluid at Q_{NaCl} = 5, 10, 15, 20, and 25 mL/min, waiting 15 min for equilibration after flow rate alteration and before sampling. In a second experiment, a 5.00 M NaCl solution was injected during 4 h at Q_{NaCl} = 25 mL/min. Samples were drawn after 5, 30, 60, 120, 180, and 240 min to measure conductivity.

ii. Standard HDF – effect of Q_{inf}

This experiment was performed using the same hemodialyzer and machine settings as described above (refer to "Standard HDF – stability of ionic strength"). A 5.00 M NaCl solution was infused into the substitution fluid at Q_{NaCl} = 5, 10, 15, 20, 25, and 30 mL/min, waiting 15 min for equilibration after flow rate alteration and before sampling. Samples were drawn at the BR, ART, and VEN accesses to measure conductivity. In a first experiment, Q_{inf} and Q_{UF} were 160 and 40 mL/min, respectively; whereas in a second experiment, they were set to 50 and 30 mL/min, respectively.

iii. Standard HDF – modification of the dialysis setup

In a next step, the dialysis setup was modified (see **Fig. 9**) so that the external pump, which infused the 5.00 M NaCl solution, simultaneously removed substitution fluid at the same flow rate Q_{NaCl} to keep Q_{inf} constant. Dialysis experiment was performed in pre-HDF modus as described above (see "Standard HDF – stability of ionic strength"). Samples were taken with the BR, ART, and VEN accesses to measure conductivity.

iv.   Standard HDF – effect of Q_B and Q_D

This pre-HDF experiment (**Fig. 8**) was performed using a PUREMA® H dialyzer (1.8 m² membrane surface area) and with 525 mL saline in the blood circuit. Machine settings were Q_B = 200, 300, 400, and 500 mL/min, Q_D = 500 and 800 mL/min, Q_{inf} = 160 mL/min, and Q_{UF} = 40 mL/min. Dialysate temperature was set to 37 °C. After 30 min recirculation, the 5.00 M NaCl solution was infused into the substitution fluid at Q_{NaCl} = 5, 10, 15, 20, and 25 mL/min, waiting 15 min for equilibration after flow rate alteration and before sampling. Samples were drawn with the BR, ART, and VEN accesses to measure conductivity.

v.   Serial dialyzers – stability of ionic strength

Three pre-HDF sessions lasting 2 h were performed with 1 L saline using two serial dialyzers as presented in **Fig. 10**: the first cartridge contained DIAPES® HF800 membranes (1.4 m²); the second cartridge contained PUREMA® H membranes (1.7 m²). Flow rates used are given in **Tab. 6**. Samples (2 mL) were drawn at the first dialyzer blood outlet (BM, also second dialyzer blood inlet), second dialyzer blood outlet (VEN), first dialyzer dialysate inlet (IN) and outlet (OUT) after 0, 15, 30, 60, 90, and 120 min to monitor the [NaCl].

Session	Q_B	Q_D	Q_{UF}	Q_{inf}	Q_{ex}	Q_{NaCl}
1	150	500	0	75	200	14.4
2	150	500	0	75	225	16.2
3	150	500	0	75	250	18.0

Tab. 6: Flow rate used to determine the stability of the ionic strength during pre-dilution HDF with the serial dialyzers setup.

Flow rates are given in [mL/min]. The dialysis sessions correspond to: 1) $Q_{ex} < (Q_B + Q_{inf})$, 2) $Q_{ex} = (Q_B + Q_{inf})$, and 3) $Q_{ex} > (Q_B + Q_{inf})$. Abbreviations: Q_B, blood flow rate; Q_D, dialysate flow rate (second cartridge); Q_{UF}, ultrafiltration flow rate (weight-loss); Q_{inf}, substitution fluid flow rate; Q_{NaCl}, 5.00 M NaCl solution infusion flow rate; Q_{ex}, dialysate flow rate (closed loop) of the first cartridge.
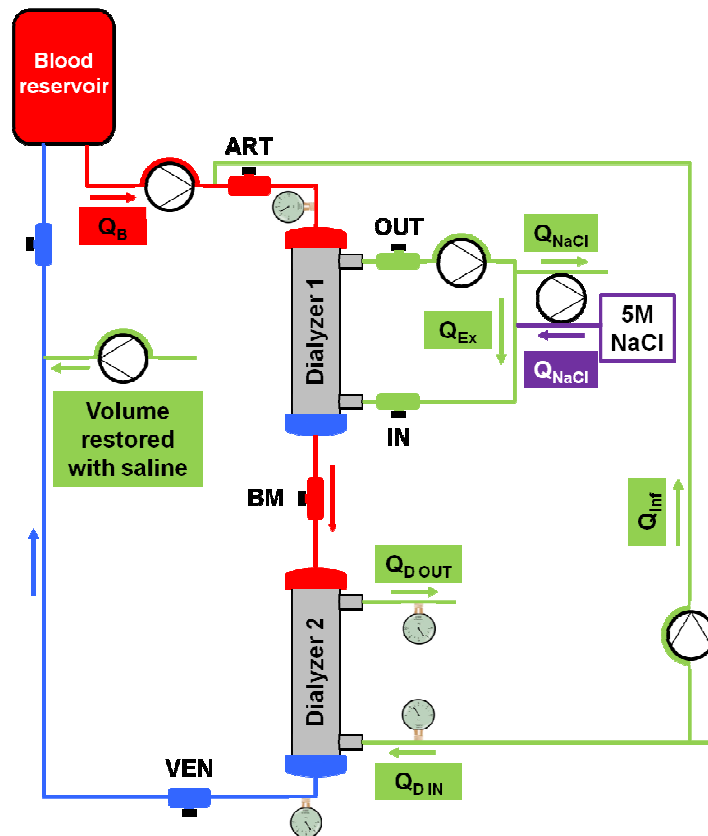
Fig. 10: Serial dialyzers setup in pre-dilution HDF.

The standard pre-HDF setup (**Fig. 9**) was improved by adding a second cartridge in which the dialysate circuit is connected in a closed loop (here "dialyzer 1") and filled with saline; the solution is pumped counter-current the blood stream with a flow rate Q_{ex}. The ionic strength is increased in the closed loop by substituting saline with 5.00 M NaCl solution. Thus, the ionic strength in the blood stream is increased by diffusion through the semi-permeable membrane. All experiments involving the serial dialyzers setup were performed on a Nikkiso DBB03 dialysis apparatus.

vi.   Serial dialyzers – influence of Q_{ex}

The impact of the dialysate flow rate in the first cartridge Q_{ex} on the [NaCl] was studied in 525 mL human whole blood using different flow rates (**Tab. 7**). Machine settings (Q_B, Q_D, Q_{inf}, and Q_{UF}) and hemodialyzers were the same as above (refer to "Serial dialyzers – stability of ionic strength"). The dialysate temperature was set to 39 °C. As exposed in **Fig. 10**, [NaCl] was measured in the first dialyzer blood outlet (BM) and first dialyzer dialysate outlet (IN).

	Q$_{ex}$ [mL/min]				
	100	**200**	**300**	**400**	**500**
Q$_{NaCl}$ **[mL/min]**	3.1	6.2	9.3	12.4	15.5
	7.2	14.4	21.6	28.9	36.1
	12.4	24.7	37.1	49.5	61.9

Tab. 7: Flow rates used to determine the influence of *Q$_{ex}$* on the ionic strength in blood.

Abbreviations: Q$_{NaCl}$, 5.00 M NaCl solution infusion flow rate; Q$_{ex}$, dialysate flow rate (closed loop) of the first cartridge.

vii.   Serial dialyzers with transmembrane pre-dilution

In a first experiment, the serial dialyzers setup with transmembrane pre-dilution HDF (SDial-TM pre-HDF, **Fig. 11**) was tested with saline at Q$_B$ = Q$_{ex}$ = 150 mL/min, Q$_D$ = 500 mL/min, Q$_{inf}$ = 75 mL/min, and Q$_{UF}$ = 0 mL/min. The dialysate temperature was set to 39 °C. Filters were the same as already described (see "Serial dialyzers – stability of ionic strength"). After 10, 20, and 30 min of dialysis with Q$_{NaCl}$ = 6.5 mL/min, 3 mL samples for [NaCl] measurement were drawn BM, IN, and OUT. The same was repeated with Q$_{NaCl}$ = 10.8 mL/min.

In a second experiment, the [NaCl] was measured during different sessions (see flow rates in **Tab. 8**). Samples were drawn over 3 min (interval of 1 min), waiting 15 min for equilibration after flow rate alteration and before sampling. Note: [NaCl]$_{OUT}$ for the third setting was not measured.

Session	Q$_B$	Q$_D$	Q$_{UF}$	Q$_{inf}$	Q$_{ex}$	Q$_{NaCl}$
1	150	500	0	75	25	13.5
2	150	500	0	75	200	17.0
3	300	500	0	75	200	27.0

Tab. 8: Flow rates used to determine the stability of the ionic strength with SDial-TM pre-HDF.

Flow rates are given in [mL/min]. Abbreviations: Q$_B$, blood flow rate; Q$_D$, dialysate flow rate (second cartridge); Q$_{UF}$, ultrafiltration flow rate (weight-loss); Q$_{inf}$, substitution fluid flow rate; Q$_{NaCl}$, 5.00 M NaCl solution infusion flow rate; Q$_{ex}$, dialysate flow rate (closed loop) of the first cartridge.
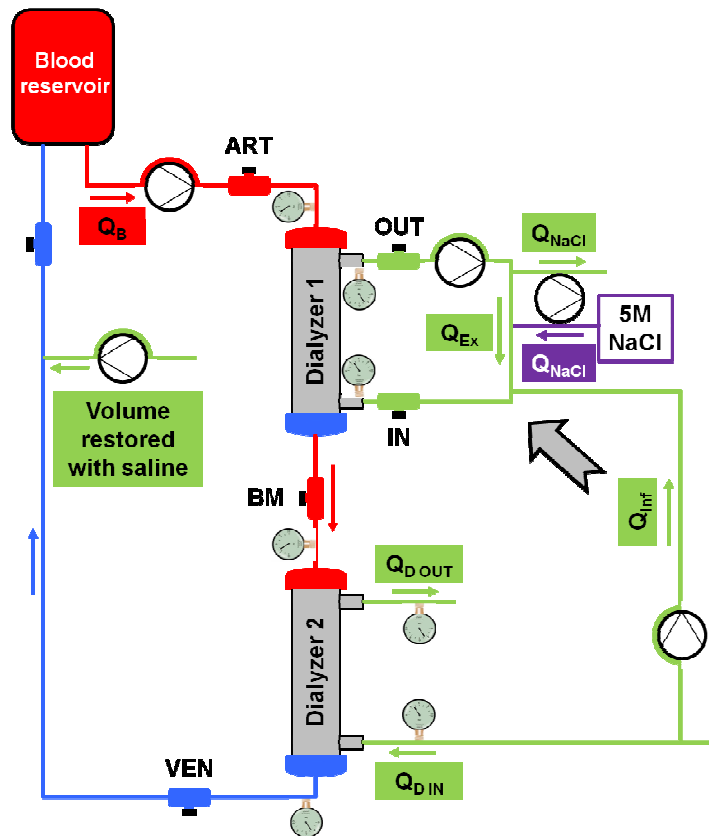
c. *Ex vivo* hemocompatibility of increased ionic strength

i. Cell damage in single pass dialysis

Human heparinized blood (5 IU/mL; pool from 3 donors) was dialyzed ($Q_B = Q_D = 4.3$ mL/min) in single pass against different dialysate solutions (0.15, 0.40, 0.50, 0.60, 0.75, and 1.00 M NaCl) using a mini-module setup (**Fig. 12**; containing Polyamix™ membranes, 258 cm² effective surface area) in order to test increasing $[NaCl]_{blood}$. Blood (8 mL) subjected to increased ionic strength was collected in Petri dishes and then incubated for 240 min at 37 °C under agitation (70 rpm). Samples (1 mL) were taken after 0, 15, 30, 60, 90, 120, and 240 min to measure cell count and hemolysis. Na^+ and Cl^- concentrations were measured in blood in the last sample (240 min).

Hemolysis levels resulting from this experiment were compared to a reference: 3 mL human heparinized blood (5 IU/mL) from 21 volunteers (n = 21) was diluted with 1.44 mL of a mix of saline and 2.00 M NaCl in order to increase $[NaCl]_{blood}$. Blood of the references was incubated at room temperature for 1 h. Finally, free Hb, tHb and cell counts were determined.
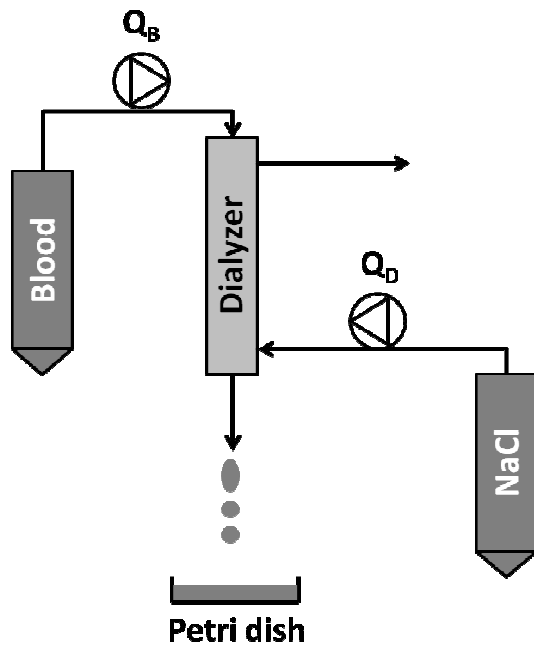
Fig. 12: Setup for single pass experiment of blood with NaCl solution.
Blood is pumped from a plastic tube through a mini-dialyzer in which a NaCl solution flows counter-currently. [NaCl] increases in blood within the dialyzer.

Blood smears at different [NaCl] were performed in human blood, after setting Hct and heparin concentration to 32% and 10 IU/mL, respectively, as follows: blood was diluted 1:10 in plastic tubes with different NaCl solutions to reach a final concentration of 0.15, 0.25, 0.50, and 0.75 M NaCl.

In order to study the blood cell morphology before and after contact with high ionic strength, human heparinized blood was dialyzed ($Q_B = Q_D = 4.1$ mL/min) in single pass using a setup with serial mini-dialyzers (**Fig. 13**; containing Helixone® membranes, 239 cm² effective surface area). In the first cartridge, the same dialysate solutions as above were used to increase $[NaCl]_{blood}$; in the second cartridge blood was dialyzed against fresh dialysate to bring back to physiological ionic strength. Blood samples were drawn in the second dialyzer inlet and outlet to measure cell count; 15 min have been waited for equilibration after [NaCl] alteration and before sampling. Blood smears were also performed.
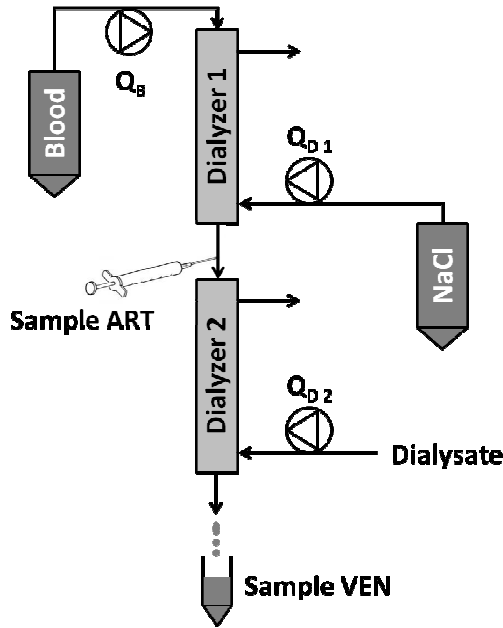
Fig. 13: Serial dialyzers setup for single pass experiment of blood with NaCl solution.
Blood is pumped from a plastic tube through a first mini-dialyzer in which a NaCl solution flows counter-currently to increase [NaCl] in blood. Then, blood passes a second dialyzer in which counter-currently flowing dialysate to restitute physiological ionic strength in blood.

ii. Effect of blood volume on hemolysis and cell count

Dialysis experiments were performed using PUREMA® H dialyzer (1.7 m² membrane surface area) in heparinized human blood (5 IU/mL) with Q_B = 150 mL/min, Q_D = 500 mL/min, Q_{UF} = 10 mL/min, and Q_{inf} = Q_{NaCl} (150 mL/min) using standard pre-HDF (**Fig. 9**). [NaCl] in the substitution fluid ([NaCl]$_{SUB}$) was increased to 1.00 M. Blood volume was either 500 (one single donor) or 1500 mL (pool from 3 donors). ART and VEN samples were taken after 0, 15, 30, 60, 90, 120, and 180 min. Cell count and hemolysis were measured only in venous samples, whereas BGA and ion concentrations were measured in both arterial and venous samples. Pressures were recorded online. Two separate experiments were performed (n = 2). Blood runs were calculated according to **Eq. 7**. The transmembrane pressure (TMP) was calculated according to **Eq. 9** (90) :

$$TMP = \frac{P_{blood}^{inlet} + P_{blood}^{outlet}}{2} - \frac{P_{dialysate}^{inlet} + P_{dialysate}^{outlet}}{2}$$

Eq. 9: Calculation of the transmembrane pressure.

iii. Maximizing the NaCl concentration in blood

Standard pre-dilution HDF pilot experiments were performed using a PUREMA® H dialyzer (1.7 m² membrane surface area) in human heparinized blood (500 mL; 5 IU/mL) with Q_B = 150 mL/min, Q_D = 500 mL/min, and Q_{UF} = 0 mL/min. Different settings and infusion flow rates were tested (**Tab. 9**). Samples were drawn after 0, 15, 30, 60, 90, 120, 150, and 180 min to perform BGAs (samples ART and VEN), cell counts and hemolysis measurements (samples VEN only).

Setting	NaCl solution infused	Q_{NaCl}	Q_{inf}	Target $[NaCl]_{blood}$
Single infusion (Fig. 9)	0.15 M	14.5	50	0.15 M
Single infusion (Fig. 9)	1.00 M	150	150	0.50 M
Spread infusion (Fig. 14)	1.00 M	150	150	0.50 M
Single infusion (Fig. 9)	1.55 M	14.5	50	0.50 M

Tab. 9: Settings and flow rates tested to determine the maximal [NaCl] in blood.
Flow rates are given in [mL/min]. Abbreviations: Q_{inf}, substitution fluid flow rate; Q_{NaCl}, NaCl solution infusion flow rate; $[NaCl]_{blood}$, NaCl concentration in blood after increased ionic strength.
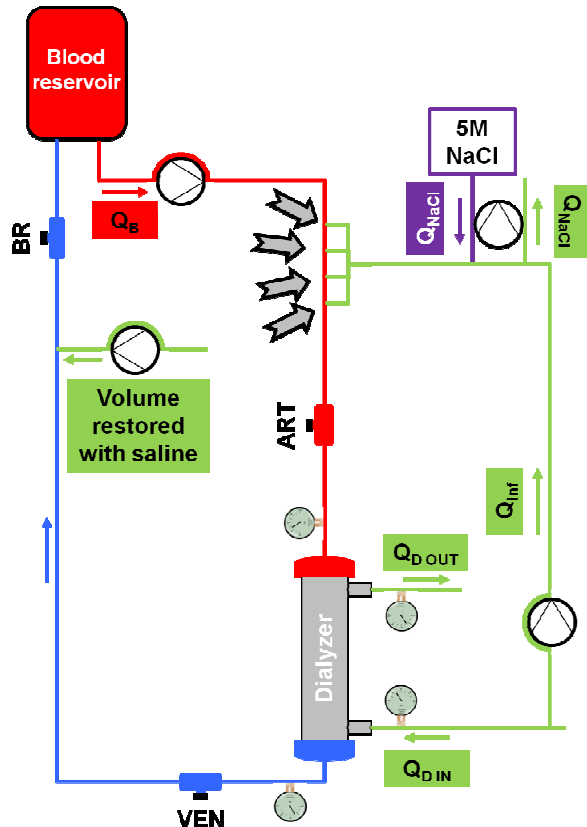
Fig. 14: Standard pre-dilution HDF with spread infusion of the substitution fluid.
To perform the spread infusion (see grey arrows), the substituate line was connected to the blood line at 4 different accesses.

iv. Role of the first-cartridge membrane in the osmotic shock

A HD pilot experiment (n = 1) using the serial dialyzers setup (**Fig. 10**) was performed over 4 h with Q_B = 150 mL/min, Q_D = 500 mL/min, and Q_{UF} = Q_{inf} (0 mL/min) and with 525 mL heparinized blood (10 IU/mL; pool of 2 donors) after adjustment of the Hct to 32% with saline. Dialysate temperature was set to 39 °C. The first cartridge contained DIAPES® LF100 membranes (1.4 m²) and the second cartridge contained PUREMA® H membranes (1.7 m²). The first part of the experiment was performed with Q_{ex} = 300 mL/min (> Q_B) leading to $[NaCl]_{IN\ 1}$ ≈ 0.55 M, whereas the second part was performed with Q_{ex} = 50 mL/min (< Q_B) leading to $[NaCl]_{IN\ 1}$ ≈ 1.17 M. Between both parts, the tubing systems and both cartridges were replaced with new ones, and blood from the same pool was used. In each experiment 5.00 M NaCl was infused during the first 2 h (Q_{NaCl} = 11 mL/min) while the remaining 2 h were performed in isotonic conditions (Q_{NaCl} = 0 mL/min). Samples were taken after 0, 15,

30, 45, 60, 90, 120, 135, 150, 180, 210, and 240 min. The [NaCl] was measured in both arterial and venous samples; cell count and hemolysis were determined only in venous samples. Pressures and the temperature were monitored online. The TMP of each hemodialyzer was calculated according to **Eq. 9**.

v. Comparison between standard and serial dialyzers pre-dilution HDF

Dialysis treatments were performed during 2 h in pre-HDF modus with human whole blood (525 mL) after adjustment of Hct, heparin, and TP to 32%, 10 IU/mL, and 65 g/L with saline, heparin, and 20% HSA solution, respectively. Flow rates were: Q_B = 150 mL/min, Q_D = 500 mL/min, Q_{inf} = 75 mL/min, Q_{ex} = 225 mL/min, and Q_{UF} = 0 mL/min. The same hemodialyzers as already described (refer to "Serial dialyzers – stability of ionic strength") were used. During standard pre-HDF (**Fig. 9**), different $[NaCl]_{SUB}$ were tested: 0.15, 0.75, 1.00 (Q_{inf} = 50 mL/min), and 1.20 M NaCl, which corresponds to $[NaCl]_{blood}$ = 0.15, 0.36, 0.36, and 0.50 M NaCl, respectively. For this purpose, the external pump provided 5.00 M NaCl solution flow rates Q_{NaCl} of 0, 10, 9.5, and 16 mL/min, respectively. During serial dialyzers pre-dilution HDF (SDial pre-HDF, **Fig. 10**), Q_{NaCl} was set to 0, 16, 20, and 30 mL/min to provide $[NaCl]_{blood}$ of 0.15, 0.36, 0.50, and 0.75 M, respectively. The dialysate temperature was set to 39 °C. Blood was recirculated for 5 min before starting the experiment (NaCl pump start). ART (standard pre-HDF) and BM (SDial pre-HDF) samples (1 mL) were drawn after 0, 15, 30, 45, 60, 90, and 120 min to measure [NaCl]. VEN samples (7.5 mL) for cell count, free Hb, [NaCl], C5a concentration, and TAT concentration were drawn simultaneously. Pressures were monitored online: blood ART and VEN, dialysate inlet and outlet (second cartridge only); TMP was calculated with **Eq. 9**.

vi. Serial dialyzers transmembrane pre-dilution HDF

The serial dialyzers setup as described above (**Fig. 10**) was compared to the SDial-TM pre-HDF (see **Fig. 11**) using 0.50 M $[NaCl]_{blood}$. Dialysis parameters, blood preparation and sampling were the same as above mentioned (see "Comparison between standard and serial dialyzers pre-dilution HDF"). Several pressure transducers were added to separately detect the TMP of both filters. Three separate experiments (n = 3) were performed.

Fig. 15: Experimental setting of serial dialyzers transmembrane pre-dilution HDF.

d. <u>Removal of uremic toxins by dialysis</u>

i. <u>Clearance measurement in a miniaturized setup</u>

Single pass dialysis experiments were performed with mini-dialyzers containing Polyamix™ membranes (258 cm² effective surface area) at Q_B = 4.3 and 5.7 mL/min. This setup corresponded to $Q_{B\ eq}$ = 300 and 400 mL/min, respectively, when extrapolated to a membrane surface area of 1.8 m² according to **Eq. 10**:

$$Q_1 = \frac{A_1 \times Q_2}{A_2}$$

Eq. 10: Flow rate extrapolation from minituarized to standard setup.

The mini-dialyzer and tubing system were initially rinsed with saline for 20 min. Then, a 20 µM aqueous IS solution was dialyzed (Q_B = 4.3 mL/min) at room temperature against dialysate in counter-current flow. Arterial and venous samples were taken after 5, 6, and 7 min to measure the IS concentration. The same was repeated with Q_B = 5.7 mL/min (Q_D = 8.33 and 10.9 mL/min for Q_B = 4.3 and 5.7 mL/min, respectively). In a next step, the system was rinsed with saline and heparinized plasma (5 IU/mL) from healthy donors spiked with 20

µM IS was used applying the same method. Finally, the system was rinsed with saline and the first trial in aqueous solution was repeated. The free IS fraction was also determined in arterial samples. The instantaneous clearance of IS was calculated according to **Eq. 11**:

$$K = Q_B \cdot \frac{C_{ART} - C_{VEN}}{C_{ART}}$$

Eq. 11: Instantaneous clearance (91)**.**
Where K is the clearance [mL/min], Q_B the blood flow rate [mL/min], C_{ART} and C_{VEN} the arterial and venous concentrations, respectively.

The calculated clearance from the free toxin fraction was determined according to **Eq. 12**:

$$K_{est} = K_{aqueous} \times FF$$

Eq. 12: Estimated clearance of the free toxin fraction.
Where K_{est} is the blood or plasma estimated clearance [mL/min], $K_{aqueous}$ the aqueous clearance of the compound [mL/min], and FF the free toxin fraction.

ii. Comparison of HD, HDF, and increased ionic strength HDF in healthy plasma

IS (final concentration: 90 µM) and heparin (5 IU/mL) were added to freshly frozen human citrate plasma. After one hour incubation at room temperature, *in vitro* dialysis using the conditioned plasma (about 115 mL) and mini-dialyzers (31 mL; housing containing Polyamix™ membranes, 258 cm² effective surface area; two blood flow rates Q_B = 4.3 and 5.7 mL/min corresponding to $Q_{B\,eq}$ = 300 and 400 mL/min, respectively, when extrapolated (**Eq. 10**) to a membrane surface area of a 1.8 m² dialyzer) was performed at room temperature in three different modes (**Fig. 16**): i) HD, ii) pre-HDF with infusion of saline, and iii) pre-HDF with infusion of 1.00 M NaCl (final concentration in plasma: 0.36 and 0.32 M for $Q_{B\,eq}$ = 300 and 400 mL/min, respectively). During HDF Q_{inf} was 1.4 mL/min (corresponding to $Q_{inf\,eq}$ = 100 mL/min when extrapolated (**Eq. 10**) to the membrane surface area of a 1.8 m² dialyzer). Dialysate was prepared by a Nikkiso DBB 03 dialysis machine from bicarbonate and electrolyte concentrate. The counter-current dialysate flow rates were Q_D = 8.3 and 11.0 mL/min (corresponding to $Q_{D\,eq}$ = 580 and 770 mL/min, respectively) at $Q_{B\,eq}$ = 300 and 400 mL/min, respectively. After equilibration of the toxins in the plasma during recirculation for 10 min, a baseline sample was drawn and the treatment simulation was started. Further samples were drawn at 20, 50, 85, and 180 min when using $Q_{B\,eq}$ = 300 mL/min and at 15, 40, 65, and 140 min when using $Q_{B\,eq}$ = 400 mL/min. The total IS concentration and the albumin concentration were measured.
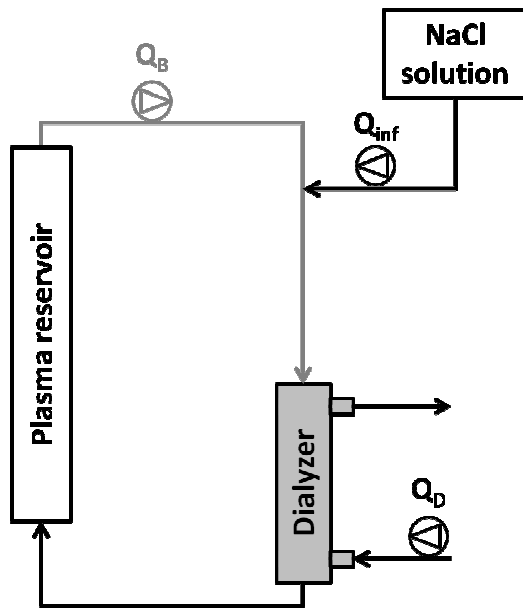
Fig. 16: Mini-module dialysis setup used to compare HD, HDF, and increased ionic strength HDF.
During HD, Q_{inf} was set to 0 mL/min whereas during HDF, either saline or 1.00 M NaCl solution was infused at a flow rate $Q_{inf\,eq}$ = 100 mL/min.

Kinetics of the IS removal from plasma was interpolated using non linear regression of an exponential decay curve (**Eq. 13**). The interest of such a calculation is presented in the Appendix (see "Interest of calculating the blood runs through the dialyzer").

$$C = C_0 . e^{-\gamma . \tau}$$

Eq. 13: Interpolation of toxin removal during dialysis (84).
Where C is the remaining toxin concentration [% of C_0], C_0 the toxin concentration at the beginning of the experiment set equal to 100%, τ the number of blood runs through the dialyzer calculated according to **Eq. 7**, and γ the removal rate [%/run].

Since the volume is constant in the plasma reservoir (including tubing), dialysate is able to flow into the plasma when samples are drawn. The toxin concentration was therefore calculated with correction because of dilution due to sampling. Three independent experiments (n = 3) were performed. The removal rates (γ; **Eq. 13**) and removal ratio (RR; **Eq. 14**) were determined from each replicate.

$$RR = \frac{C_0 - C_f}{C_0} \times 100$$

Eq. 14: Removal ratio (64).
Where RR is the removal ratio [%], C_0 and C_f the toxin concentrations at the beginning and at the end of the experiment [µM], respectively.

iii. Removal rates in uremic and normal plasma using the mini setup

Plasma from three healthy volunteers (n = 3) and three patients on maintenance hemodialysis (n = 3) was freshly prepared from heparinized blood (5 IU/mL) and stored overnight in the fridge. IS and pCS were added to reach a final concentration of 100 and 130 µM, respectively, taking the native total toxin concentration into account. *In vitro* pre-HDF at

$Q_{B\ eq}$ = 300 mL/min and the determination of total toxin concentrations were performed as described above (refer to "Comparison of HD, HDF, and increased ionic strength HDF in healthy plasma"). The experiment was done in two parts: during the first 90 min, saline was infused into the plasma. After 90 min, the infusion solution was switched to 1.00 M NaCl (0.36 M final concentration in plasma). The albumin concentration was measured before and after the experiment to quantify the albumin loss. The toxin removal rate was determined according to **Eq. 13**.

iv.   Complete removal of IS and *p*CS with HDF

Pre-dialysis uremic plasma (40 mL) from one patient (n = 1) on maintenance hemodialysis was separated from heparinized blood (5 IU/mL) and dialyzed against fresh dialysate with a mini-dialyzer (31 mL; housing containing Helixone® membranes, 250 cm² effective surface area) in pre-HDF modus with a 1.00 M NaCl infusion. Flow rates were Q_B = 5.7 mL/min, Q_D = 10.5 mL/min, and Q_{inf} = 1.4 mL/min (resulting in 0.32 M NaCl in plasma). Samples were taken at the dialyzer blood outlet after 0, 2, 10, 25, 40, 60, 80, and 100 plasma runs (corresponding to 0, 11, 53, 134, 214, 320, 427, and 534 min, respectively; **Eq. 7**) to measure total IS and *p*CS concentrations. The results were calculated with correction because for dilution due to sampling (see above).

v.   Standard *versus* serial HD

Heparinized plasma (5 IU/mL) from different donors was pooled and IS was added to reach about 100 µM. The added volume was only about 5% of the final volume. Then, the plasma was incubated for at least 15 min at room temperature to allow equilibration. The same mini-dialyzers as above (refer to "Complete removal of IS and *p*CS with HDF") were used to compare standard and serial HD (**Fig. 17**) at room temperature with the same conditioned plasma. Flow rates were set at Q_B = 5.7 mL/min and Q_D = 10.5 mL/min. After rinsing both setups in single-pass with saline, they were filled with conditioned plasma (standard HD: 31 mL, serial HD: 35 mL) which recirculated for 10 min without dialysate flow. Subsequently, the experiment was started and venous samples were drawn after 0, 30, 60, 120, 180, 240, and 300 min to measure the total IS concentration. Two independent experiments were performed with different plasma pools (n = 2). The concentration was calculated with correction because for dilution due to sampling (see above), and the number of blood runs was calculated (**Eq. 7**) from the respective plasma volumes.
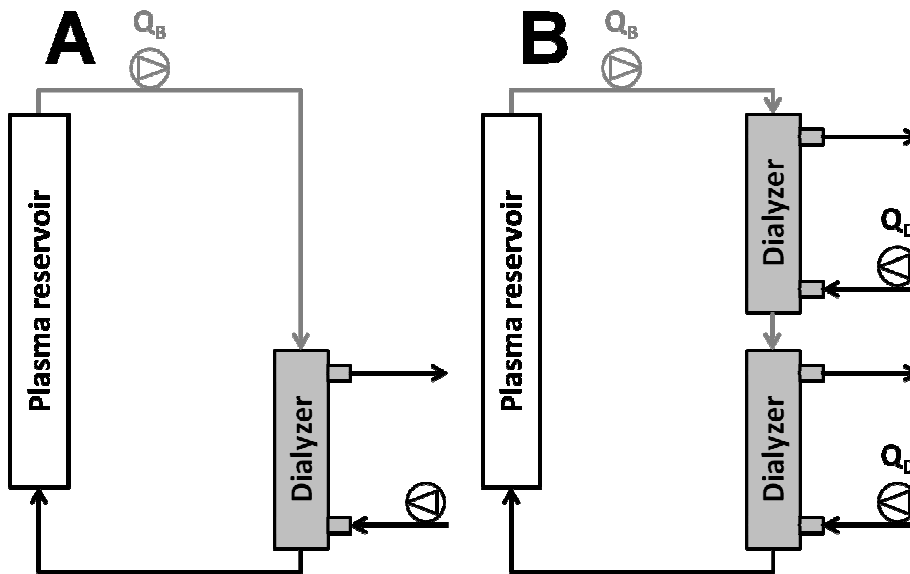
Fig. 17: Mini-dialyzers setup to compare standard HD (A) and serial HD (B).
Serial HD consists of two hemodialyzers in series with independent dialysate circuits.

vi. Toxin removal using a standard dialysis machine

Before each experiment, 850 mL human citrated plasma was filtered through a transfusion set to remove fat aggregates and heparin was added (final concentration: 10 IU/mL). From this preparation, 50 mL plasma was drawn and mixed with 12.5 mL of 10 mM IS solution to prepare 4 syringes each containing 15 mL conditioned plasma (2 mM IS). The remaining plasma (800 mL) was mixed with 2 mM IS solution to reach a 100 µM IS final concentration.

One single setup was assembled to allow switching between three different HDF modi (see **Fig. 18**): standard pre-HDF (refer to **Fig. 9**) and SDial pre-HDF (refer to **Fig. 10**) with or without charcoal adsorber. To increase [NaCl]$_{blood}$ to 0.50 M, a 5.00 M NaCl solution was used to replace part of the substitution fluid in case of standard pre-HDF or part of the saline in case of SDial pre-HDF. Flow rates were: Q_B = 150 mL/min, Q_D = 500 mL/min, Q_{ex} = 300 mL/min, Q_{inf} = 75 mL/min, net ultrafiltration flow rate Q_{UF} = 0 mL/min. Both serial hemodialyzers had a high-flux polyethersulfone dialysis membrane (PUREMA® H, 1.7 m²). The dialysate temperature was set at 39 °C.

The blood circuit was filled with conditioned plasma which was recirculated for 5 min. Subsequently, pre-HDF was performed for each setup during 30 min. After testing one setting, it was switched randomly to the next and plasma again was recirculated for 5 min. Samples were taken after 5, 10, 15, 20, and 30 min at the first dialyzer blood inlet (ART), first dialyzer blood outlet (BM; corresponding also to the second dialyzer blood inlet), and second dialyzer blood outlet (VEN) to measure [NaCl] and total IS concentration. Temperature and pressures were monitored online. Three experiments (n = 3) were performed with each setting.
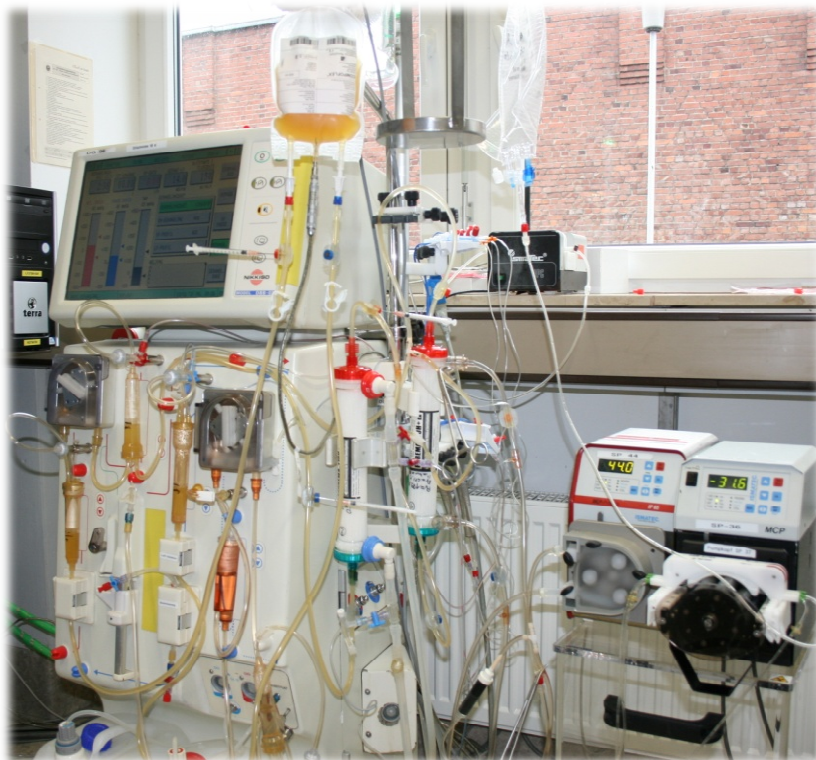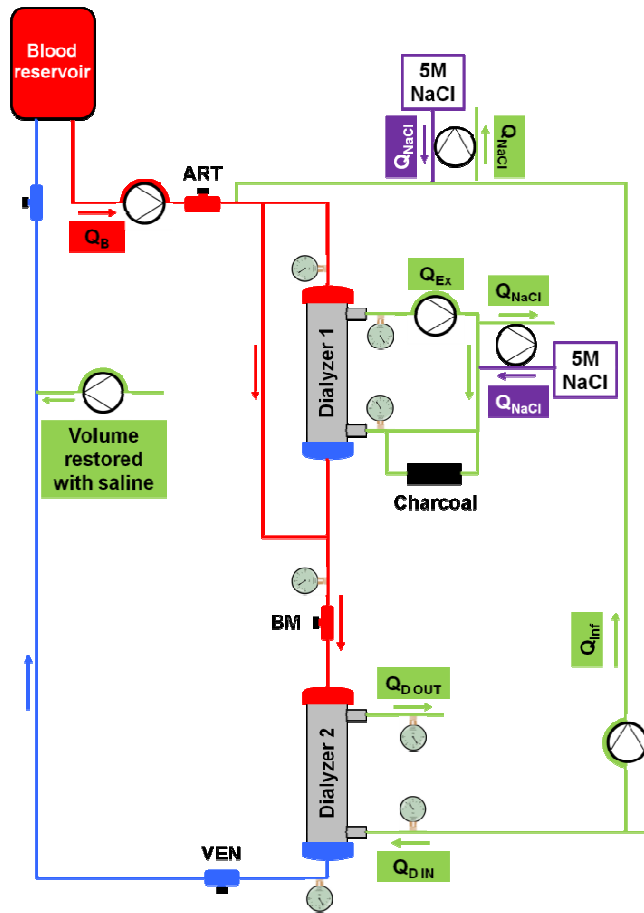
Fig. 18: Dialysis setup used to switch from standard pre-dilution HDF (dialyzer 1 in bypass) to serial dialyzers pre-dilution HDF with or without charcoal adsorber.
NaCl was infused either within the substitution line or within the external loop. Top, schema; bottom, experimental setting.

e. **Experimental transfer into the animal model**

Animal experiments were performed adhering to the German Protection of Animals Act. After having received approval from the district government of Lower Franconia (registration no. 55.2-2531.01-17/09), four female Merino sheep (mean weight 42.8 ± 3.0 kg) were enrolled for the trials.

i. RBC resistance to increased ionic strength under static conditions

Blood from four sheep was drawn (30 mL) via the dialysis catheter before the dialysis experiments and anticoagulated with heparin (5 IU/mL). As already described in "Cell damage in single pass dialysis", 3 mL blood was mixed with 1.44 mL of saline and 2.00 M NaCl in order to increase $[NaCl]_{blood}$ to 0.15, 0.20, 0.25, 0.35, 0.50, 0.60, and 0.75 M. Samples were incubated at room temperature for 1 h and hemolysis was determined.

ii. RBC resistance to increased ionic strength under dynamic conditions

Heparinized blood (100 mL, 5 IU/mL) from two human healthy donors (n = 2) and from 2 sheep (70 mL) was drawn in order to perform standard pre-HDF with infusion of saline or 1.20 M NaCl solution in a mini-dialyzers setting (see **Fig. 16** and **Fig. 19**; housing containing PUREMA® H membranes, 250 cm² effective surface area). Hct in human blood was adjusted to 30% with saline. Dialysis parameters were: Q_B = 5.6 mL/min, Q_{inf} = 2.8 mL/min, and Q_D = 10 mL/min corresponding to $Q_{B\ eq}$ = 400 mL/min, $Q_{inf\ eq}$ = 200 mL/min, and $Q_{D\ eq}$ = 800 mL/min, respectively (**Eq. 10**). The tubing systems were filled with blood (31 mL) and venous samples were taken after 30, 60, 90, 120, and 180 min to determine hemolysis. Arterial and venous samples were taken post-dialysis to measure the respective [NaCl].
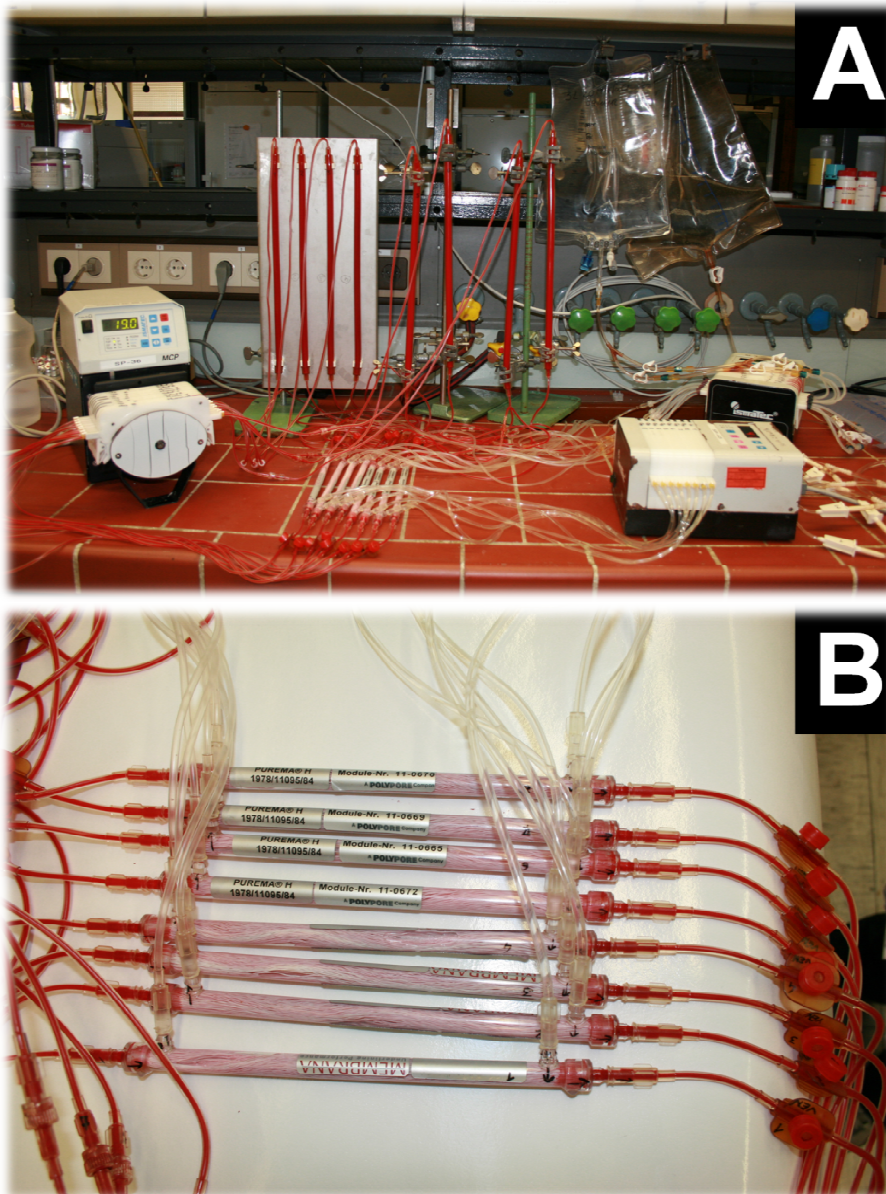
Fig. 19: Experimental *in vitro* HDF setup filled with blood (A). Detail of the mini-dialyzers (B).

iii. *In vivo* pre-dilution HDF experiments

Pre-dilution HDF was performed in a randomized crossover fashion in the four sheep. The animals were instrumented and anticoagulated as already described by Krieter et al. (92). Briefly, vascular access was achieved with a 20 cm double lumen dialysis catheter inserted into one jugular vein by Seldinger technique after local anesthesia. To avoid hypotension the priming fluid within the extracorporeal circuit (400 mL) was administered to the sheep at the start of dialysis. For anticoagulation, an initial bolus dose of 10,000 units of unfractionated heparin and a continuous injection of 0.015 M NaCitrate were used. During the experiments, the sheep were observed for symptoms of adverse reactions and blood pressure was monitored via tail cuff (neonatal cuff no. 4) by using the DINAMAP® PRO 100 (Critikon, Tampa, USA) device.

Two hours pre-dilution HDF were performed using the two setups as already illustrated: standard pre-HDF (**Fig. 9**; PUREMA® H membranes, 1.9 m²) and SDial-TM pre-HDF (**Fig. 11**; first cartridge, PUREMA® L membranes, 1.8 m²; second cartridge, PUREMA® H membranes, 1.9 m²). Flow rates were: Q_B = 150 mL/min, Q_D = 500 mL/min, Q_{inf} = 75 mL/min, Q_{ex} = 200 mL/min, and Q_{UF} = 0 mL/min. The dialysate temperature was set at 37 °C. $[NaCl]_{blood}$ was increased after an initial 30 min baseline period of standard pre-HDF using online prepared substitution fluid in order to reach the following $[NaCl]_{blood}$: standard pre-HDF 0.36 M and 0.45 M (corresponding to about 0.75 M and 1.10 M $[NaCl]_{SUB}$, respectively) and SDial-TM pre-HDF 0.36 M and 0.60 M. Blood samples were drawn from the extracorporeal circuit before the substitution line (ART), before the second dialyzer blood inlet (BM), and after the second dialyzer outlet (VEN) to measure whole blood cell count, free Hb, LDH concentration, BGA, and electrolyte concentration (Na^+, Cl^-, K^+, Ca^{2+}, HCO_3^-).

Fig. 20: Animal model of pre-dilution HDF.
A, Hemodiafiltration apparatus; B, standard pre-HDF; C, SDial-TM pre-HDF.

RESULTS

I. Binding of uremic toxins in human biological fluids

1) Effect of storage conditions

In order to assess the influence of sample freezing on the binding properties of IS and pCS in human plasma, two experiments have been performed. In the first one, total and free toxin concentrations were measured in the same uremic plasma samples before and after storage for 6 months at -20 °C. In the second one, the binding constants K_D and B_m for IS were calculated in normal plasma before and after freezing.
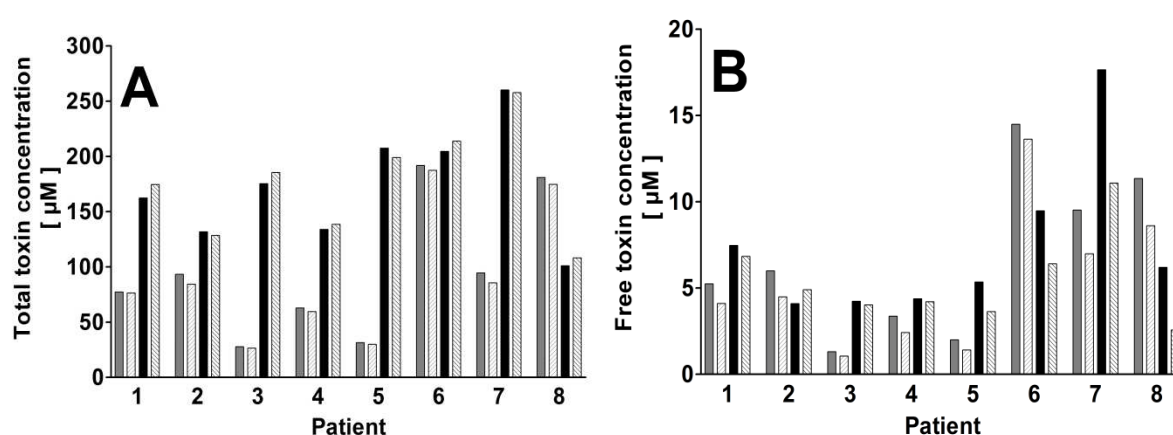
Fig. 21: Effect of freezing on total and free toxin concentrations.
IS (■, ▨) and pCS (■, ▨) concentrations were measured in plasma from 8 ESRD patients before (full bars) and after (hatched bars) freezing at -20 °C for 6 months. A, total concentration; B, free concentration.

In uremic plasma (see **Fig. 21**), the PBF of IS was higher ($P < 0.001$) after freezing (93.3 ± 1.6% *versus* 94.5 ± 1.5% before and after freezing, respectively) resulting from a decrease of the total (95 ± 62 *versus* 91 ± 60 µM before and after freezing, respectively; $P < 0.01$) and free concentrations (6.7 ± 4.7 *versus* 5.3 ± 4.3 µM before and after freezing, respectively; $P < 0.01$). In the case of pCS, the PBF (95.8 ± 1.6% *versus* 97.0 ± 0.9% before and after freezing, respectively; $P = 0.06$), total toxin concentration (172 ± 51 *versus* 176 ± 49 µM before and after freezing, respectively; $P = 0.21$), and free toxin concentration (7.4 ± 4.6 *versus* 5.5 ± 2.7 µM before and after freezing, respectively; $P = 0.06$) were constant. The variability between patients of total and free toxin concentrations was high for both IS (range 27.8 to 191.9 µM and 1.3 to 14.5 µM for total and free toxin concentration, respectively) and pCS (range 101.1 to 257.8 µM and 4.1 to 17.6 µM for total and free toxin concentration).

In normal plasma, the freezing of plasma did not change K_D (14.3 ± 5.3 *versus* 14.7 ± 7.5 µM before and after freezing, respectively) but decreased B_m (614 ± 47 *versus* 565 ± 33 µM before and after freezing, respectively). The HSA concentration was however constant after freezing (32.3 ± 1.5 *versus* 32.6 ± 1.9 g/L).

2) **Determination of the uremic toxin binding affinity in uremic plasma**
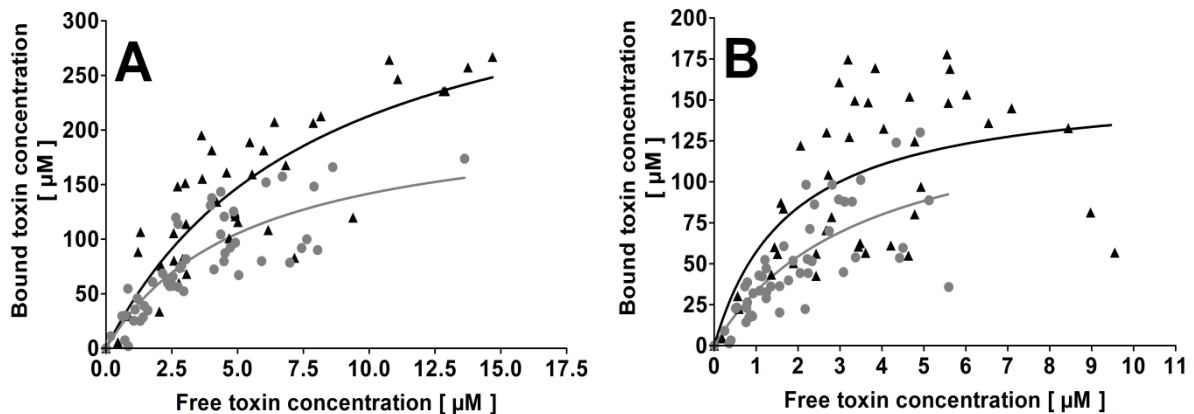
Fig. 22: Binding study of native uremic plasma pre- and post-dialysis.
Binding curves of IS (●) and *p*CS (▲) in plasma of ESRD patients (n = 49) were obtained by measuring bound and free toxin concentrations pre (A) and post (B) dialysis session.

Mean IS and *p*CS concentrations were 82.0 ± 46.3 (range of 2.9 to 187.4 µM) and 139.3 ± 84.9 µM (range of 1.8 to 372.3 µM), respectively. Binding constants in uremic plasma were pre-dialysis $K_D = 5.3 \pm 1.7$ and 8.0 ± 2.4 µM for IS and *p*CS, respectively, and $B_m = 217 \pm 36$ and 384 ± 64 µM for IS and *p*CS, respectively. Post-dialysis $K_D = 3.5 \pm 1.5$ and 1.8 ± 1.0 µM for IS and *p*CS, respectively, and $B_m = 151 \pm 37$ and 160 ± 29 µM for IS and *p*CS, respectively.
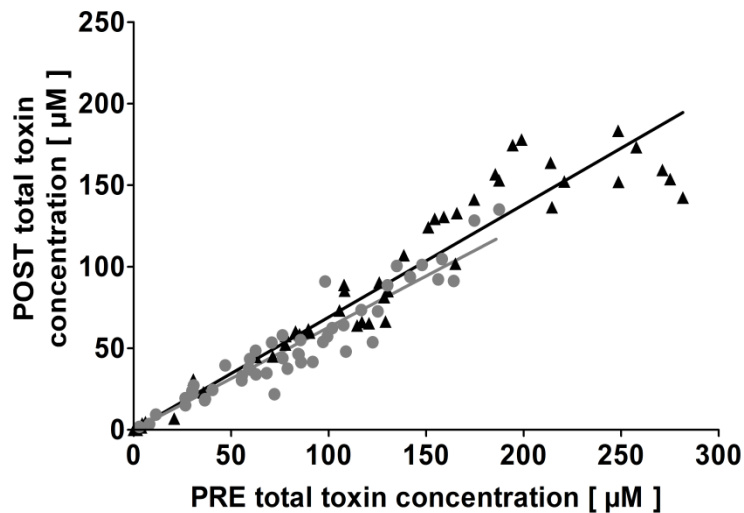
Fig. 23: Comparison between pre- and post-dialysis total toxin concentrations in uremic plasma.
IS (●) and *p*CS (▲) total concentrations were measured in plasma of 49 ESRD patients.

As shown in **Fig. 23**, pre- and post-dialysis total toxin concentrations were highly correlated for both IS ($r^2 = 0.89$, $P < 0.001$) and *p*CS ($r^2 = 0.91$, $P < 0.001$). In this cohort of patients, the removal rates were $37 \pm 2\%$ and $31 \pm 2\%$ for IS and *p*CS, respectively. However, no correlation was found between IS and *p*CS concentrations neither pre- nor post-dialysis.

3) <u>Pilot binding studies of different uremic toxins in normal plasma</u>

The influence of the [NaCl] on the binding of the uremic toxins IS, pCS, and PAA was studied in a pilot experiment in normal human plasma. As shown in **Fig. 24** at a given toxin concentration, the PBF of all three toxins decreased ($P < 0.05$) with increasing ionic strength.
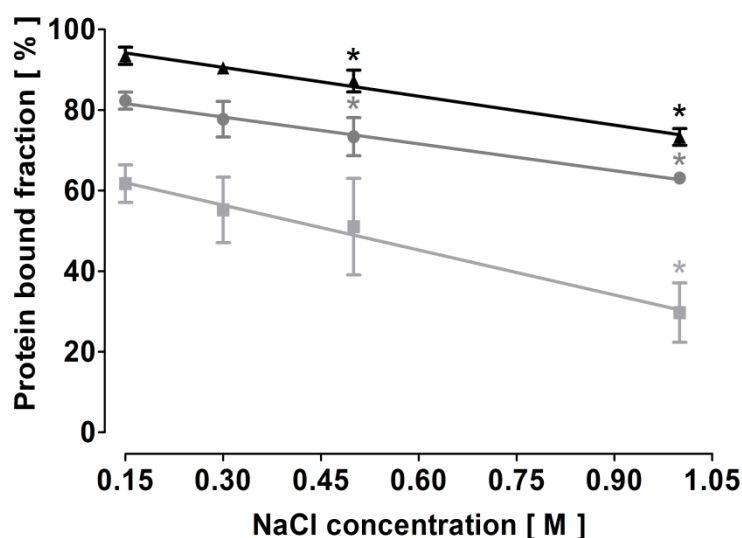
Fig. 24: PBF of uremic toxins *versus* the [NaCl] in human plasma.
Uremic toxins were added to normal human plasma to 100 µM for both IS (—●—, n = 4) and pCS (—▲—, n = 3), and to 200 µM for PAA (—■—, n = 3). The PBF of all three toxins was negatively correlated with the ionic strength ($r^2 = 0.99$, $P < 0.01$): IS, PBF = -22.2 × [NaCl] + 84.9; pCS, PBF = -23.9 × [NaCl] + 97.8; PAA, -37.2 × [NaCl] + 67.6; with *PBF* in [%] and *[NaCl]* in [M]. Results are mean ± SD; *, $P < 0.05$ *versus* 0.15 M NaCl.

Since the HSA concentration was constant in all samples, the results were compared to the model presented in **Fig. 7** hypothesizing a B_m = 300 µM = HSA concentration and no protein denaturation despite increasing [NaCl]. The binding affinity for the most relevant uremic toxins, here IS and pCS, was estimated:

[NaCl]	IS (α = 0.33)			pCS (α = 0.33)		
	PBF	K_D/B_m	K_D	*PBF*	K_D/B_m	K_D
0.15 M	82%	0.16	48 µM	92%	0.06	18 µM
0.30 M	78%	0.21	63 µM	88%	0.10	30 µM
0.50 M	73%	0.28	84 µM	84%	0.14	42 µM

Tab. 10: Estimated binding affinity of the uremic toxins IS and *p*CS in normal plasma at different ionic strength.
The binding affinity K_D of IS and pCS for plasma proteins was calculated according to **Eq. 3** from the measured PBF at a toxin-albumin ratio of 0.33. Abbreviations: α, toxin-albumin ratio; PBF, protein bound fraction; [NaCl], sodium chloride concentration.

As shown in **Fig. 25**, the PBF of the three uremic toxins is strongly dependant on the toxin concentration itself.
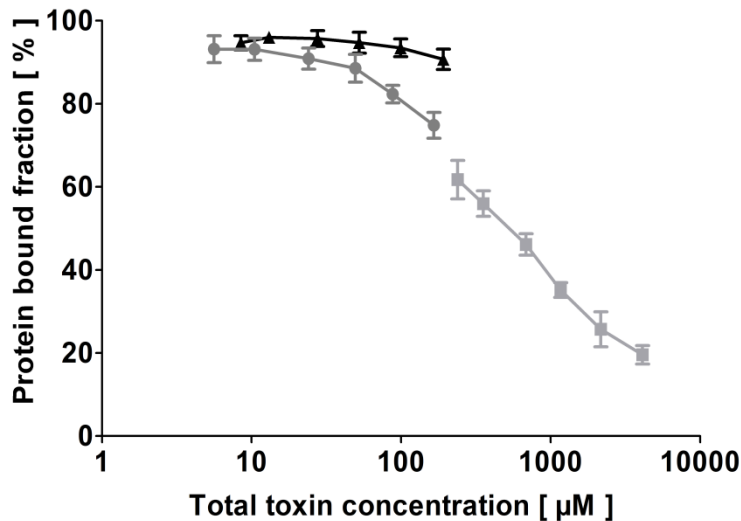
Fig. 25: PBF of three uremic toxins *versus* their concentration in normal human plasma.
The PBF is shown for IS (⬤ , n = 4), *p*CS (▲ , n = 3) and PAA (◼ , n = 3). Means ± SD are given.

4) Effect of sodium chloride on plasma proteins

a. Effect of NaCl on the IS binding ability of HSA

In fatty acid free HSA solution at pH 7.4 and room temperature IS was bound to one high affinity binding site as demonstrated by Scatchard plot (**Fig. 26**, B). Furthermore, no denaturation of the binding sites was noted while increasing the [NaCl]. Measured HSA concentration in the stock solution was 8.5 ± 0.1 g/L (128 ± 2 µM). As determined from the binding curves (**Fig. 26**, A), K_D was positively correlated (r^2 = 1.00, *P* < 0.001) with the ionic strength: K_D = 8.7 ± 0.6, 17.4 ± 3.4, 27.2 ± 3.8, and 40.8 ± 10.8 µM at 0.15, 0.30, 0.50, and 0.75 M NaCl, respectively; K_D = 53.0 × [NaCl] + 1.0 (r^2 = 0.89) with K_D in [µM] and *[NaCl]* in [M].
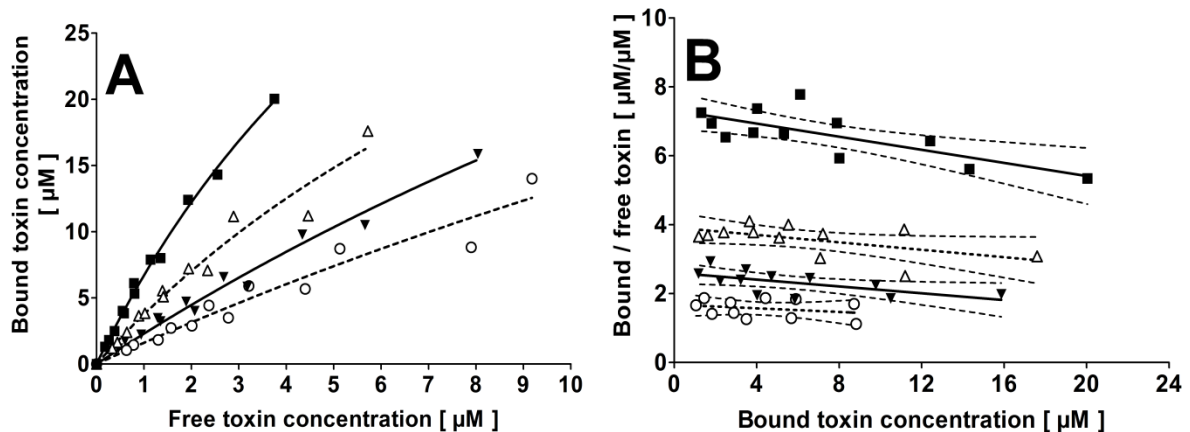
Fig. 26: Binding of IS on HSA at different ionic strengths.
Binding experiments (n = 2) were performed in 4.25 g/L HSA solution (8.5 g/L stock solution) at room temperature, pH 7.4, and with 0.15 (◼), 0.30 (△), 0.50 (▼), and 0.75 M (○) NaCl. A, binding curves; B, Scatchard plot.

b. **Effect of NaCl on the binding ability of normal plasma for IS, *p*CS, and PAA**

The binding affinity and capacity of normal human plasma for IS, *p*CS, and PAA was determined at room temperature and pH 7.4 by ultrafiltration.
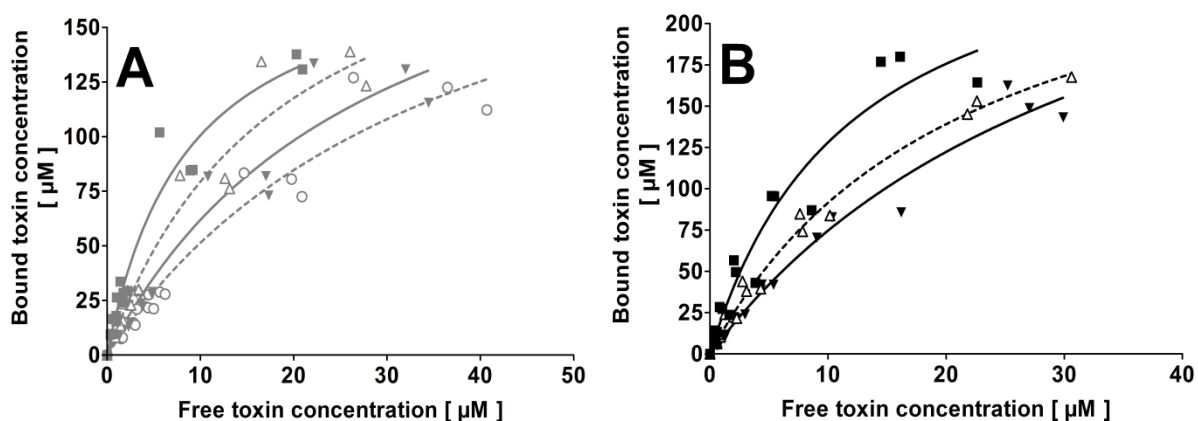
Fig. 27: Binding of IS and *p*CS in normal human plasma at different ionic strengths.
Binding experiments were performed in half-diluted human plasma from three different donors (n = 3) with IS (A) and *p*CS (B) at room temperature, pH 7.4, and with 0.15 (■), 0.30 (△), 0.50 (▼), and 0.75 M (○) NaCl.

As shown in **Fig. 27**, binding properties of human plasma were altered for both IS and *p*CS. A similar effect was seen for PAA (see binding curves in Appendix, **Fig. 81**). Increasing the ionic strength was positively correlated with K_D for IS ($r^2 = 0.98$, $P < 0.05$) but not for PAA ($r^2 = 0.78$, $P = 0.11$) as shown in **Fig. 28**. Correlation was not assessed for *p*CS because too few data were collected. Furthermore, K_D for IS and *p*CS was increased ($P < 0.05$) when [NaCl] was greater than 0.30 M.
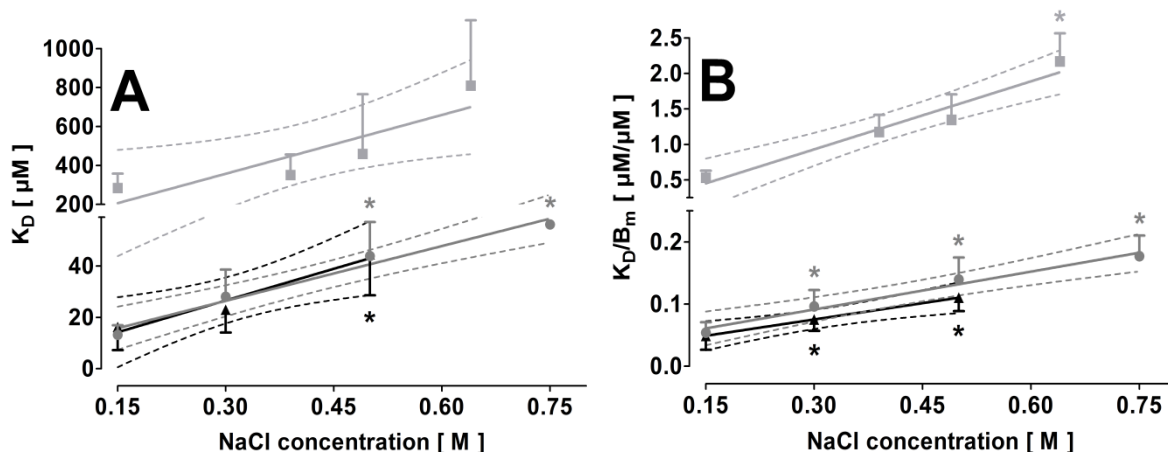
Fig. 28: Effect of [NaCl] on the binding constants of uremic toxins in normal human plasma.
The effect of increased ionic strength on K_D (A) and on the ratio K_D/B_m (B) at 25 °C and pH 7.4 is shown. The binding constants were determined using a one site specific binding equation (**Eq. 2**) for both IS (—●—) and *p*CS (—▲—). For PAA (—■—), a one site total binding equation (**Eq. 4**) was applied. Plots (mean ± SD, n = 3) were interpolated with linear regression: IS, $K_D = 71.2 \times$ [NaCl] + 5.1 ($r^2 = 0.82$) and $K_D/B_m = 0.20 \times$ [NaCl] + 0.03; *p*CS, $K_D = 82.4 \times$ [NaCl] + 1.9 ($r^2 = 0.58$) and $K_D/B_m = 0.18 \times$ [NaCl] + 0.02 ($r^2 = 0.68$); and PAA, $K_D = 1007 \times$ [NaCl] + 55.3 ($r^2 = 0.41$) and $K_D/B_m = 3.19 \times$ [NaCl] - 0.03 ($r^2 = 0.81$); with K_D in [µM] and *[NaCl]* in [M]. *, $P < 0.05$ *versus* 0.15 M NaCl.

For both IS and pCS, B_m was not different with increasing ionic strength: IS, B_m = 250 ± 48, 290 ± 57, 317 ± 62, and 326 ± 69 µM at 0.15, 0.30, 0.50, and 0.75 M NaCl, respectively; pCS, B_m = 324 ± 34, 296 ± 49, and 401 ± 120 µM at 0.15, 0.30, and 0.50 M NaCl, respectively. Since experiments with PAA were performed with different plasma volumes, change of B_m was impossible to assess. Thus, increasing the ionic strength was positively correlated with the ratio K_D/B_m for both IS (r^2 = 0.98, $P < 0.01$) and PAA (r^2 = 0.95, $P < 0.05$). This corresponded to a 2.2 fold increase of the ratio for IS, 2.3 fold for pCS, and 3.5 fold for PAA when [NaCl] was increased from 0.15 to 0.50 M. The ratio K_D/B_m was significantly increased with [NaCl] ≥ 0.30 M for both IS and pCS, and [NaCl] > 0.50 M for PAA.
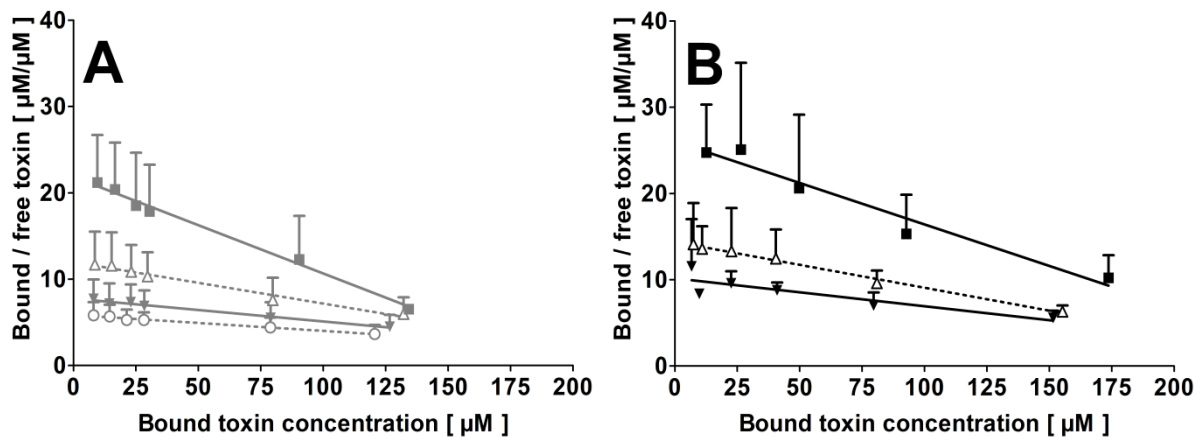
Fig. 29: Scatchard plot deriving from the binding studies on uremic toxins in normal human plasma.
The Scatchard plot is shown for IS (A) and pCS (B) as mean ± SD (n = 3) with 0.15 (■), 0.30 (△), 0.50 (▼), and 0.75 M (○) NaCl. Regression coefficients r^2 are: A, 0.55, 0.41, 0.33, and 0.36 at 0.15, 0.30, 0.50, and 0.75 M NaCl, respectively; B, 0.49, 0.50, and 0.36 at 0.15, 0.30, and 0.50 M NaCl, respectively.

Scatchard plot analysis (**Fig. 29**) confirmed that IS and pCS were bound to one binding site in normal human plasma in the range of 0.15 to 0.75 M [NaCl]. Scatchard plot analysis of PAA demonstrated that two different classes of binding sites were involved in the binding (see Appendix, **Fig. 82**) with different binding affinities: a high affinity binding site and a low affinity binding site corresponding to the unspecific binding.

[NaCl] [M]	K_D [µM]	B_m [µM]	K_D/B_m	Theoretical PBF at α = 0.1	Experimental PBF at α = 0.1
0.15	13.2 ± 3.7	250 ± 48	0.05 ± 0.02	94 ± 2%	95 ± 1%
0.30	28.1 ± 18.4	290 ± 57	0.10 ± 0.03 [a]	90 ± 2% [a]	91 ± 2% [a]
0.50	43.9 ± 13.2 [a]	317 ± 62	0.14 ± 0.04 [a,b]	87 ± 3% [a,b]	87 ± 3% [a,b]
0.75	56.2 ± 2.0 [a,b]	326 ± 69	0.18 ± 0.03 [a,b,c]	84 ± 3% [a,b,c]	84 ± 2% [a,b]

Tab. 11: Binding constants K_D and B_m and the PBF of IS incubated at room temperature in 1:2-diluted normal human plasma.
Abbreviations: [NaCl], sodium chloride concentration; α, toxin-albumin ratio; PBF, protein bound fraction. Values are mean ± SD (n = 3). Higher [NaCl] significantly increased K_D resulting in a decreased PBF. At low toxin concentration, both experimental and theoretical PBF, as predicted by **Eq. 3**, were similar ($P > 0.05$). The effects of an increased [NaCl] and plasma dilution on the PBF of IS, as assessed by **Eq. 3**, are also shown. [a], $P < 0.05$ *versus* 0.15 M NaCl; [b], $P < 0.05$ *versus* 0.30 M NaCl; [c], $P < 0.05$ *versus* 0.50 M NaCl.

As presented in **Tab. 11**, the PBF of IS in normal plasma could be accurately predicted by **Eq. 3**. Experimental and theoretical values did not differ.

c. Effect of NaCl on the PBF in uremic plasma

Normal plasma was incubated at IS concentrations ranging from 9.5 to 161.2 µM (mean = 56.7 ± 54.5 µM) and *p*CS concentrations ranging from 6.9 to 186.1 µM (mean = 61.6 ± 63.4 µM), whereas native toxin concentrations in uremic plasma ranged from 23.5 to 136.6 µM (mean = 69.5 ± 35.5 µM) and from 30.6 to 135.4 µM (mean = 90.2 ± 27.9 µM) for IS and *p*CS, respectively. Thus, the toxin concentrations were not different between uremic and normal plasma.
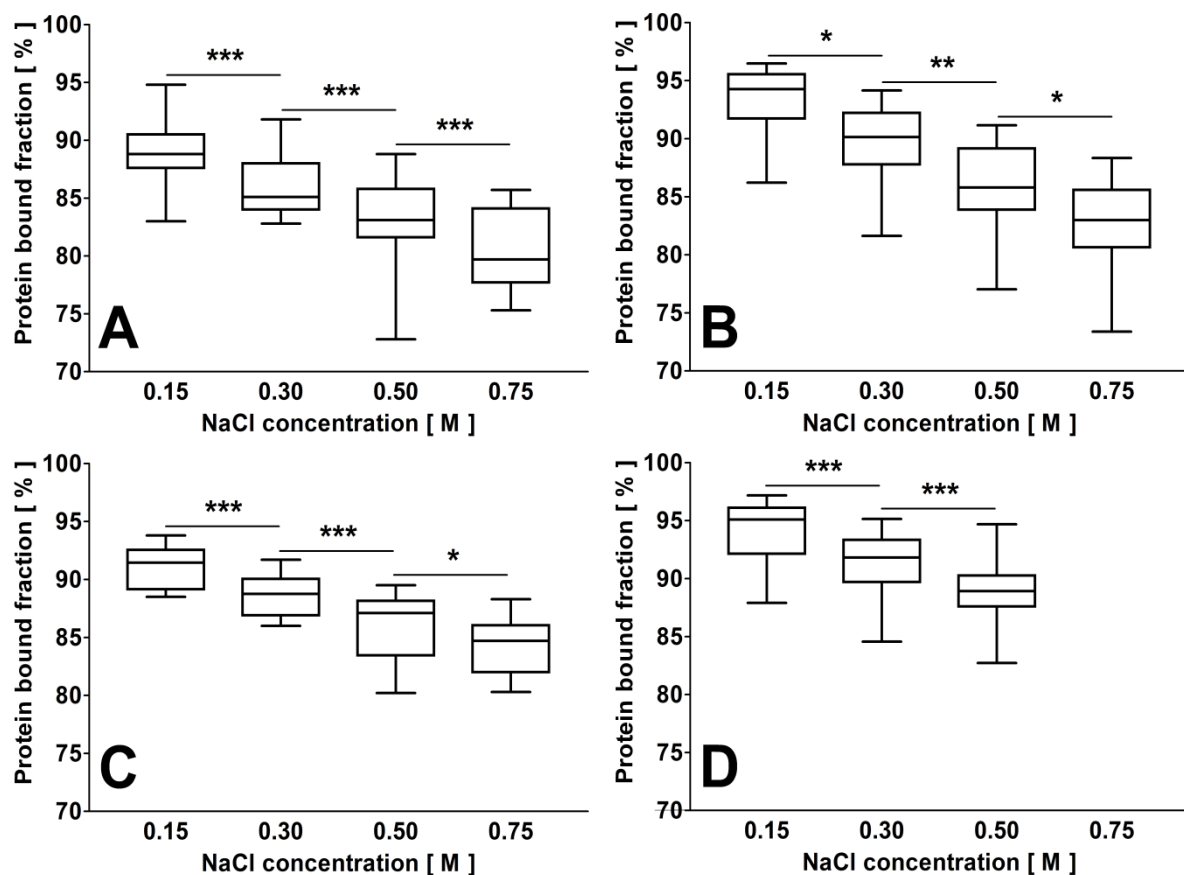
Fig. 30: Effect of increased ionic strength on the PBF of IS and *p*CS in both uremic and normal plasma.
The PBF was determined in uremic (A and C, n = 15, native toxin concentration) and normal plasma (B and D, 3 different donors with 6 different toxin concentrations, i.e., n = 18) at room temperature and at pH 7.4 for IS (A and B) and *p*CS (C and D). Increased ionic strength decreased the PBF of IS and *p*CS in both uremic and normal plasma. *, $P < 0.05$; **, $P < 0.01$; and ***, $P < 0.001$. Part D: the effect of 0.75 M NaCl in normal plasma on *p*CS has not been studied.

The PBF of both IS and *p*CS decreased ($P < 0.05$) in plasma of uremic and healthy individuals with increasing ionic strength (**Fig. 30**). In normal plasma, the PBF of IS at 0.15 and 0.30 M NaCl was about 4% higher than in uremic plasma ($P < 0.01$); the PBF of *p*CS was always about 3% higher in normal plasma than uremic one ($P < 0.05$).

Because of the high patient intervariability and the small population (n = 15; see Appendix, **Fig. 83**), the K_D of uremic plasma proteins for both IS and pCS was assessed according to **Eq. 3** with an experimental albumin concentration of 286 µM after 1:2 dilution, hypothesizing B_m being constant at 286 µM, increasing the [NaCl] in uremic plasma correlated with increased K_D: IS, K_D = 27.3 ± 8.6, 37.1 ± 10.6, 46.5 ± 16.9, and 55.9 ± 15.3 µM at 0.15, 0.30, 0.50, and 0.75 M NaCl, respectively (r^2 = 0.40, P < 0.001); pCS, K_D = 20.1 ± 5.3, 26.5 ± 4.9, 33.5 ± 8.7, and 39.7 ± 9.4 µM at 0.15, 0.30, 0.50, and 0.75 M NaCl, respectively (r^2 = 0.51, P < 0.001). Linear regression of the results on uremic plasma led to K_D = 47.0 × [NaCl] + 21.7 (r^2 = 0.99) and K_D = 32.6 × [NaCl] + 16.0 (r^2 = 0.99) for IS and pCS, respectively, with K_D in [µM] and *[NaCl]* in [M].

5) Influence of other parameters on plasma binding ability for IS

a. Plasma dilution

Binding constants K_D and B_m were determined in normal human plasma at two different plasma dilutions: 1:2- and 1:10-diluted plasma (see **Fig. 84** in Appendix). Results are presented in **Fig. 31**.
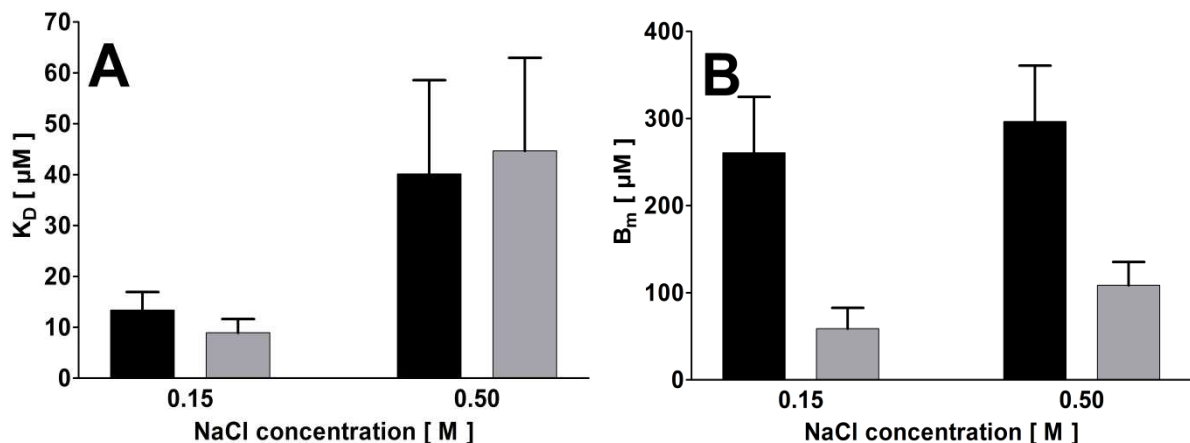
Fig. 31: Binding constants of IS determined at different plasma dilutions and ionic strengths.
The binding constants K_D (A) and B_m (B) were calculated at 0.15 and 0.50 M NaCl in plasma 1:2-diluted (■) or 1:10-diluted (▨) at room temperature and pH 7.4. Results are mean ± SD (n = 3).

For a given [NaCl], dilution did not affect the binding affinity K_D with respect to the 1:2 and 1:10 dilutions. In contrast, the number of binding sites B_m was decreased (P < 0.05) by dilution without a difference between 0.15 and 0.50 M NaCl. B_m decreased with dilution and was in the range of the albumin concentration: 238 ± 90 µM for a dilution factor of 2 (corresponding to 48 ± 18 µM for a dilution factor of 10). Thus, both dilution and increased ionic strength decreased the PBF of IS in normal human plasma (**Tab. 12**). Experimental and theoretical PBFs were highly correlated (r^2 = 0.98, P < 0.0001). Scatchard plot analysis of these data confirmed a stoichiometry of 1 for IS in human plasma (**Fig. 32**) at both [NaCl].
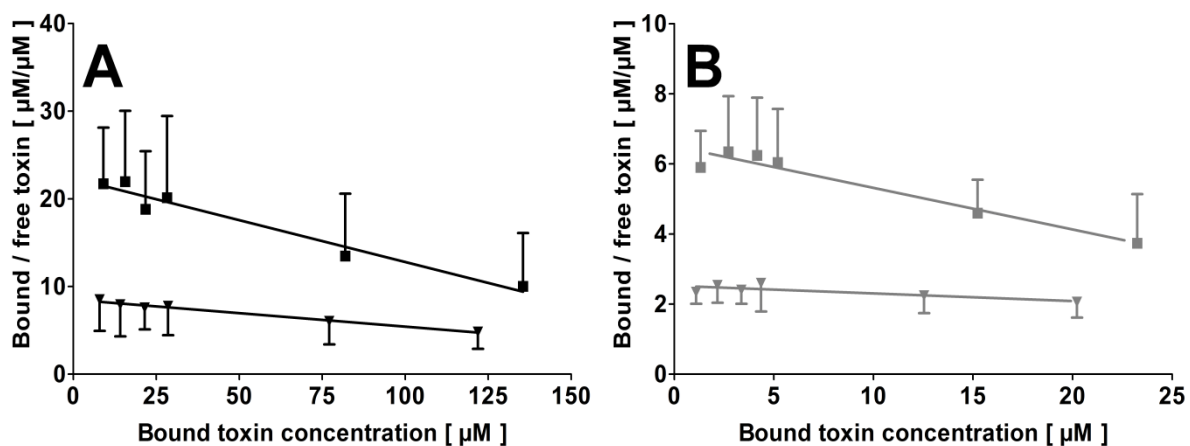
Fig. 32: Scatchard plot deriving from the binding studies on IS in normal human plasma at different dilutions and ionic strengths.

The Scatchard plots are shown for IS incubated in plasma with 1:2 (A) or 1:10 dilution (B) as mean ± SD (n = 3) with 0.15 (■) and 0.50 M (▼) NaCl. Regression coefficients r^2 are: A, 0.34 and 0.21 at 0.15 and 0.50 M NaCl, respectively; B, 0.40 and 0.11 at 0.15 and 0.50 M NaCl, respectively.

[NaCl] [M]	DF	K_D [µM]	B_m [µM]	K_D/B_m	Theoretical PBF α = 0.1 [%]	Experimental PBF α = 0.1 [%]
0.15	1:2	13.4 ± 3.6	261 ± 64	0.05 ± 0.02	94 ± 2	95 ± 2 [c]
0.50	1:2	40.1 ± 18.4	297 ± 64	0.13 ± 0.05 [b]	87 ± 4 [b]	88 ± 4 [b]
0.15	1:10	8.9 ± 2.7	59 ± 24 [a]	0.16 ± 0.02 [a]	85 ± 1 [a]	86 ± 3 [a]
0.50	1:10	44.7 ± 18.3	109 ± 27 [a]	0.41 ± 0.11 [a, b]	70 ± 5 [a, b]	73 ± 6 [a, b]

Tab. 12: Binding constants K_D and B_m and PBF of IS incubated at room temperature in 1:2- and 1:10-diluted normal human plasma.

Abbreviations: [NaCl], sodium chloride concentration; DF, dilution factor; α, toxin-albumin ratio; PBF, protein bound fraction. Values are mean ± SD (n = 3). Plasma dilution only influenced B_m and, thus, the ratio K_D/B_m. The effects of increased [NaCl] and plasma dilution on the PBF of IS, as assessed by **Eq. 3**, are also shown. [a] $P < 0.05$ versus dilution factor 1:2; [b] $P < 0.05$ versus 0.15 M NaCl; [c] $P < 0.05$ theoretical versus experimental bound fraction.

b. __Temperature__

In a pilot experiment, the equilibrium point of equilibrium dialysis using a mini-dialyzer apparatus was assessed by measuring the IS concentration within the aqueous compartment (thus corresponding to the free toxin concentration). Using 12 mL plasma, 50 µM IS solution and Q_B = 2.2 mL/min, the free IS concentration decreased within the first 10 runs through the dialyzer and reached equilibrium (**Fig. 33**). Using a smaller volume (4.6 mL), the equilibrium was largely reached after 1 h, corresponding to 28 runs.
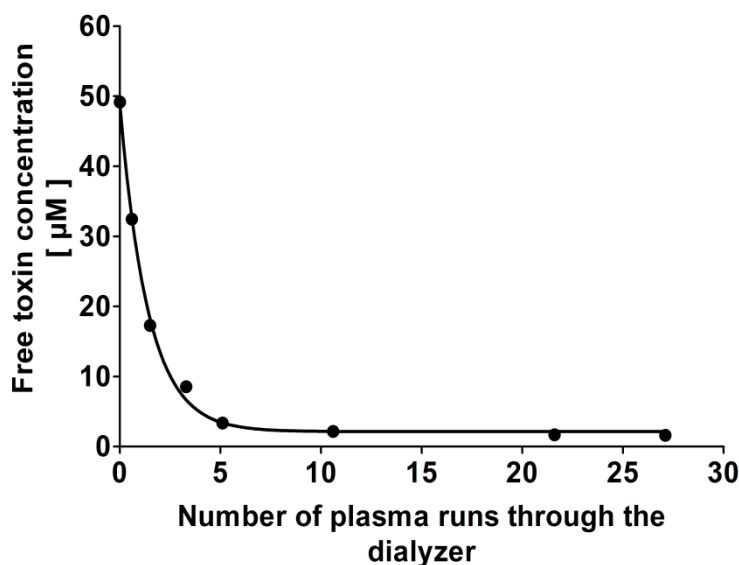
Fig. 33: Decrease of the IS concentration in the aqueous compartment during equilibrium dialysis.
Regression coefficient is r^2 = 1.00.

This setup was used to assess the PBF of IS in normal plasma at 25 and 37 °C and at 0.15 and 0.61 M NaCl. In plasma from a single donor, an increase in the temperature from 25 to 37 °C significantly decreased the PBF of IS in 0.15 M NaCl as well as in 0.61 M NaCl solution (91 ± 2% to 85 ± 2%, $P < 0.01$; and 85 ± 2% to 79 ± 2%, $P < 0.001$; respectively).

c. Influence of other ion species
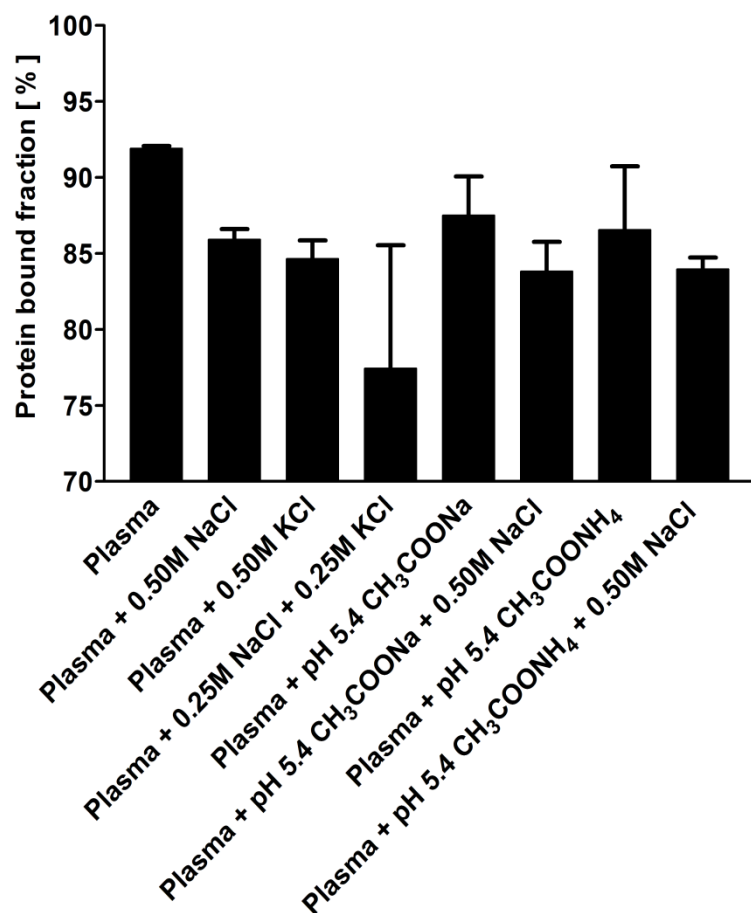
Fig. 34: Influence of different ion species on the PBF of IS in uremic plasma.
The PBF is represented for different treatments of the plasma as mean ± SD (n = 2). Increasing the ionic strength and decreasing the pH both decreased the PBF of IS in uremic plasma; however, both effects did not cumulate.

The influence of different ion species on the PBF of IS was studied *in vitro* in uremic plasma. The PBF was decreased (about 8%) with addition of either NaCl or KCl as compared to native plasma (**Fig. 34**). At similar ionic strength, mixing NaCl and KCl did not further decrease the binding (the high variability was due to a manipulation error). Decreasing the pH to 5.4 with an acetate buffer also reduced the protein binding (PBF about 5% lower compared to native plasma) and adding NaCl at lower pH further decreased the PBF of IS. The latter effect is of the same magnitude as simply increasing ionic strength with NaCl only.

II.   Modification of the ionic strength in aqueous solution applied on a dialysis machine

A standard curve of the conductivity *versus* the [NaCl] in deionized water is presented in **Fig. 35**.
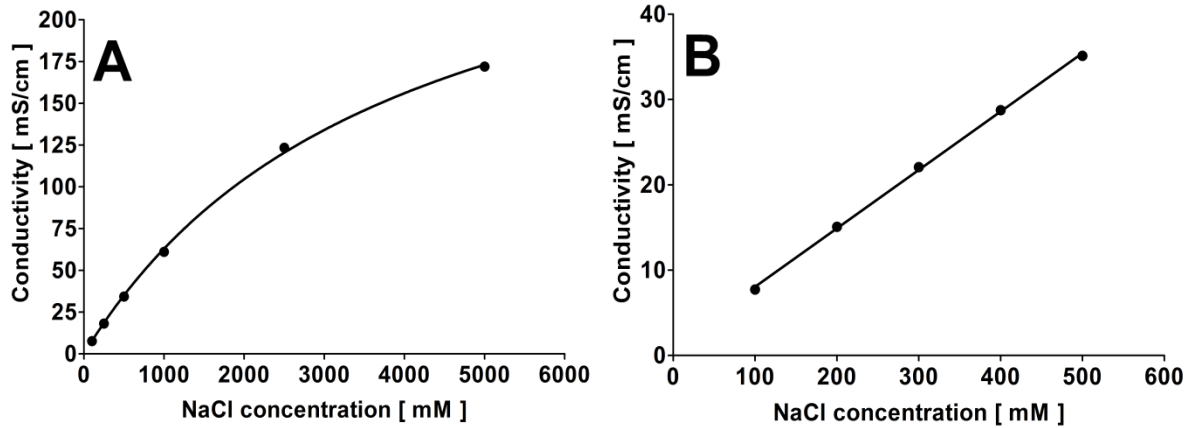
Fig. 35: Standard curve of the conductivity *versus* the [NaCl].
The conductivity was measured in deionized water (A) in the range of 0.10 to 5.00 M NaCl. The corresponding linearization in the range of 0.10 to 0.50 M NaCl was calculated (B).

The relationship between the [NaCl] expressed in [mM] and the conductivity σ expressed in [mS/cm] in the range of 0.10 to 5.00 M NaCl was:

$$[NaCl] = \frac{3878 \times \sigma}{307.4 - \sigma} \Leftrightarrow \sigma = \frac{307.4 \times [NaCl]}{3878 + [NaCl]}$$

When $10 \leq \sigma \leq 35$ mS/cm, it was possible to use linear regression. The following relationship was found:

$$[NaCl] = \frac{\sigma - 1.218}{0.06842} \Leftrightarrow \sigma = 0.06842 \times [NaCl] + 1.218$$

Thus, the [NaCl] can be rapidly assessed by measuring the conductivity when $10 \leq \sigma \leq 35$ mS/cm corresponding to the range of 0.10 to 0.50 M NaCl, by:

$$[NaCl] \approx 13.6 \times \sigma$$

Eq. 15: Estimation of the NaCl concentration from the conductivity in aqueous solution.
Where *[NaCl]* is the NaCl concentration in [mM] and σ the conductivity of the solution in [mS/cm].

1) **Standard pre-dilution HDF**

a. **Ionic strength stability**
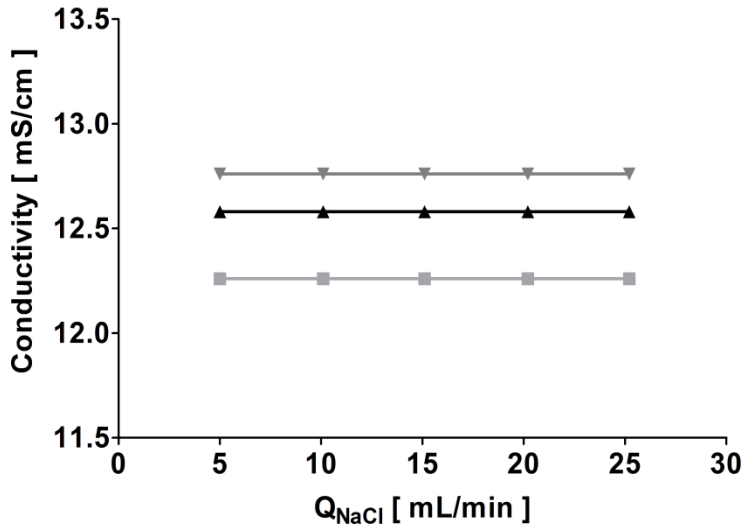
Fig. 36: Course of the conductivity in aqueous solution during infusion of NaCl. The conductivity was measured in the blood reservoir (⬛), in the arterial line (▲), and in the venous line (▼) during standard pre-dilution HDF on a dialysis machine. Infusion of saline did not change conductivity over time.

During infusion of saline into the substitution fluid (**Fig. 36**), the conductivity stayed constant at all sampling sites independently of the infusion flow rate of saline (Q_{NaCl}). The lowest conductivity was measured in the blood reservoir and the highest in the venous line but this difference was minimal (0.5 mS/cm).
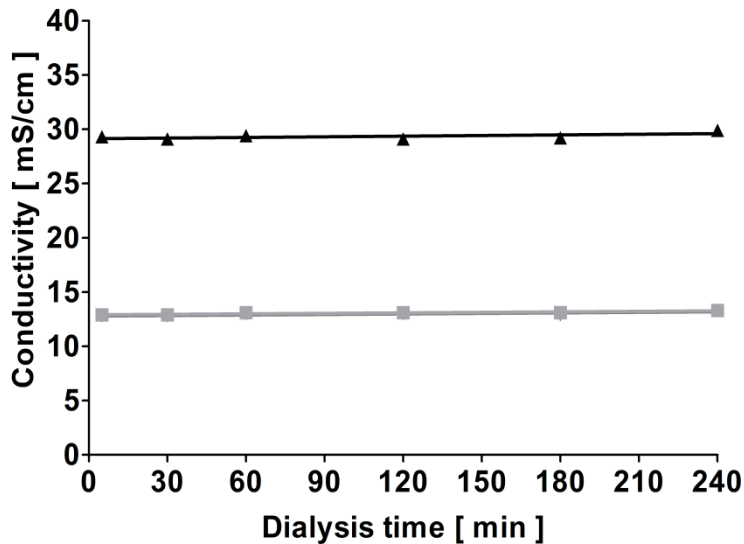
Fig. 37: Course of the conductivity in aqueous solution during infusion of 5.00 M NaCl over 4 h. Standard pre-dilution HDF was performed on a dialysis machine with Q_{NaCl} = 25 mL/min. The conductivity was measured in the blood reservoir (⬛), in the arterial line (▲), and in the venous line (▼) over time. The conductivity was higher in the arterial line as compared to the blood reservoir and the venous line (both were exactly similar).

When infusing 5.00 M NaCl at a constant flow rate Q_{NaCl}, the conductivity was steady over the 4 h dialysis session at 13.1 ± 0.2, 29.3 ± 0.3, and 13.0 ± 0.2 mS/cm in the blood reservoir, arterial, and venous line, respectively (**Fig. 37**) (corresponding to about 178 ± 3, 398 ± 4, and 177 ± 3 mM NaCl, respectively (**Eq. 15**)).

b. __Influence of Q_{inf} on the ionic strength__
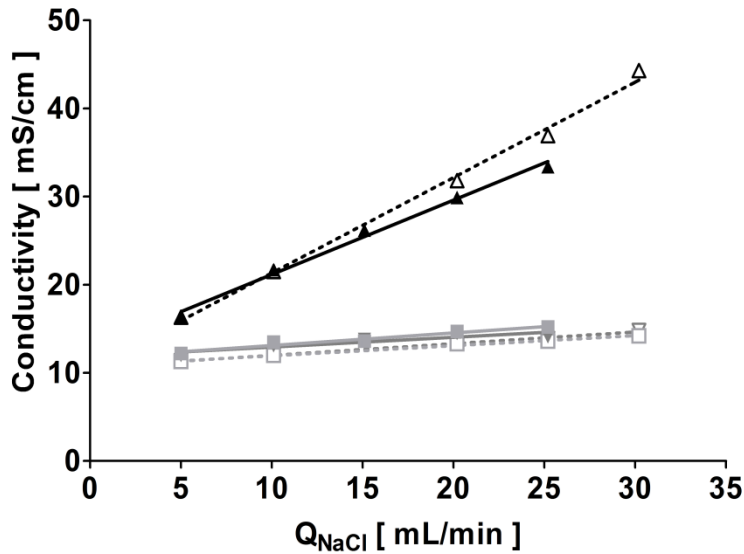
Fig. 38: Course of the conductivity with Q_{inf} and Q_{NaCl}. The conductivity was measured during standard pre-dilution HDF on dialysis machine at Q_{inf} = 160 mL/min (solid lines) and Q_{inf} = 50 mL/min (dotted lines) in the blood reservoir (━■━, ┄□┄), in the arterial line (━▲━, ┄△┄), and in the venous line (━▼━, ┄▽┄). The infusion flow rate of the 5.00 M NaCl solution Q_{NaCl} was adjusted between 5 and 30 mL/min. Increasing Q_{NaCl} positively correlated ($P < 0.05$) with the conductivity.

Increasing Q_{NaCl} (see **Fig. 38**) positively correlated with the conductivity within the blood reservoir (Q_{inf} = 50 mL/min, r^2 = 0.99, $P < 0.001$; Q_{inf} = 160 mL/min, r^2 = 0.95, $P < 0.01$), the arterial line (both Q_{inf}, r^2 = 0.99, $P < 0.001$), and the venous line (Q_{inf} = 50 mL/min, $P < 0.001$; Q_{inf} = 160 mL/min, r^2 = 0.81, $P < 0.05$). Increasing Q_{inf} did not influence the arterial conductivity ($P = 0.22$), whereas the conductivity in the blood reservoir and in the venous line was higher ($P < 0.05$) with Q_{inf} = 50 mL/min.
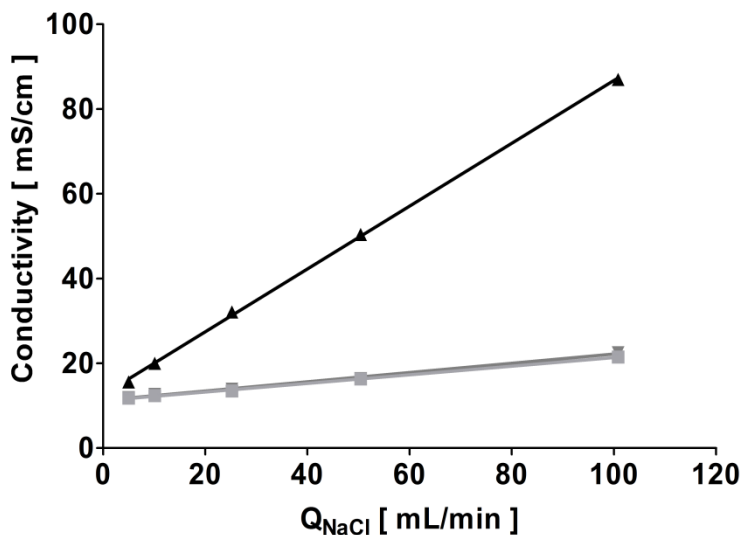
Fig. 39: Course of the conductivity with Q_{NaCl} after modification of the setup. The conductivity was measured in the blood reservoir (━■━), in the arterial line (━▲━), and in the venous line (━▼━). In this standard HDF set-up, a 5.00 M NaCl solution was infused at the same flow rate Q_{NaCl} while substitution fluid was removed. Increasing Q_{NaCl} positively correlated (r^2 = 0.99, $P < 0.0001$) with the conductivity.

After modification of the setup, higher Q_{NaCl} could be studied. The conductivity within the blood reservoir, the arterial and venous line was positively correlated (r^2 = 0.99, $P < 0.0001$) with the infusion flow rate of the 5.00 M NaCl solution. In this experiment the maximal conductivity reached was 87.0 and 22.5 mS/cm in the arterial and venous line, respectively, corresponding to approximately 1183 and 306 mM NaCl, respectively (**Eq. 15**).
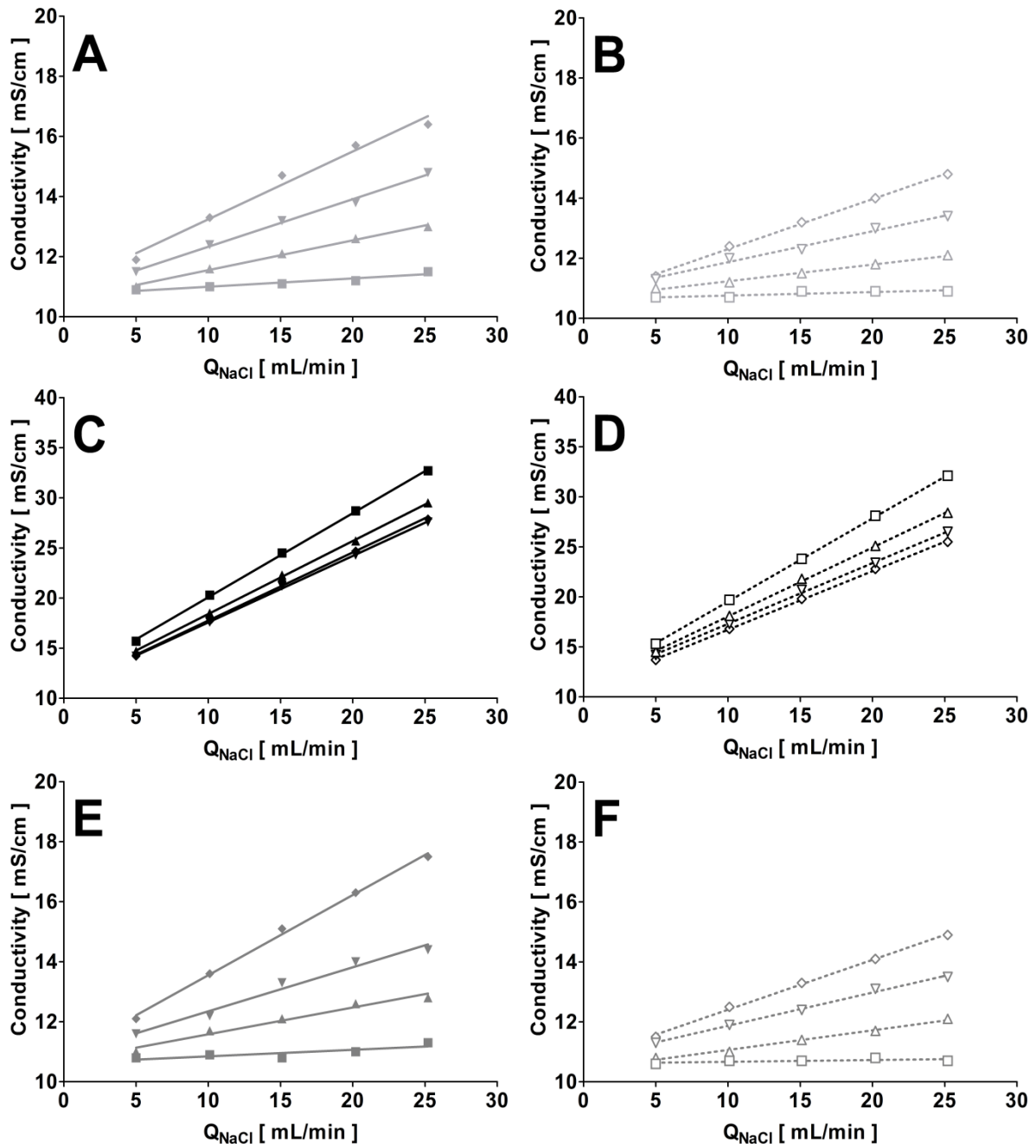
Fig. 40: Influence of Q_B and Q_D on the conductivity in aqueous solution.
The conductivity was measured during standard pre-dilution HDF with Q_D = 500 mL/min (A, C, and E) and Q_D = 800 mL/min (B, D, and F) in the blood reservoir (A-B, hell grey), the arterial line (C-D, black) and the venous line (E-F, dark grey) at different blood rates: Q_B = 200 (■), 300 (▲), 400 (▼), and 500 mL/min (◆).

For all Q_B and both Q_D, conductivity positively correlated ($r^2 > 0.92$, $P < 0.01$) with Q_{NaCl}, except at Q_B = 200 mL/min in the blood reservoir (only for Q_D = 800 mL/min, $r^2 = 0.75$, P = 0.06) and in the venous line (Q_D = 500 mL/min, $r^2 = 0.70$, P = 0.08; Q_D = 800 mL/min, r^2 = 0.45, P = 0.21) for which no correlation was found. Furthermore, increasing Q_B positively correlated with the conductivity in the blood reservoir (Q_D = 500 mL/min, $r^2 = 0.99$, $P < 0.01$;

Q_D = 800 mL/min, r^2 = 0.99, P < 0.0001) and the venous line (Q_D = 500 mL/min, r^2 = 0.98, P < 0.01; Q_D = 800 mL/min, r^2 = 0.99, P < 0.01). In the arterial line, however, the conductivity was not correlated with Q_B (r^2 = 0.78, P = 0.12) at Q_D = 500 mL/min, although, it negatively correlated with Q_B (r^2 = 0.94, P < 0.05) at Q_D = 800 mL/min.

2) Serial dialyzers setup

a. Ionic strength stability in pre-dilution HDF

In order to determine the stability of the [NaCl] over time with the serial dialyzers (SDial) setup in pre-dilution HDF, the ionic strength was monitored in all compartments at different dialysate flow rates in the first cartridge (Q_{ex}).
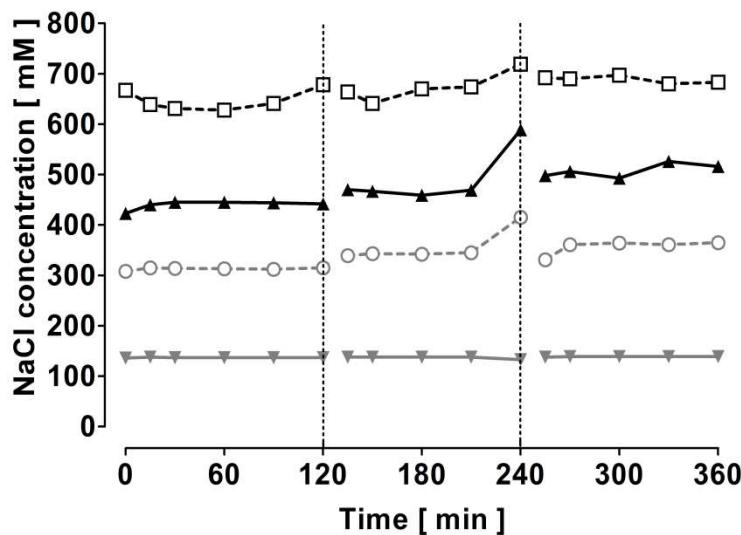
Fig. 41: Ionic strength stability during HDF using the SDial setup.
The [NaCl] was measured in different locations of the setup: BM (▲), VEN (▼), IN (□), and OUT (○). Three dialysis sessions (2 h) have been performed: 0 – 120 min, Q_{ex} < Q_B + Q_{inf}; 120 – 240 min, Q_{ex} = Q_B + Q_{inf}; and 240 – 360 min, Q_{ex} > Q_B + Q_{inf}.

The [NaCl] was constant over time in all compartments independently of the flow rates. Venous ionic strength was isotonic. The [NaCl] measured in the first dialyzer dialysate inlet (IN) was higher than the arterial one indicating an incomplete diffusion of the Na^+ and Cl^- ions through the dialysis membrane; increasing Q_{ex} reduced the difference between [NaCl]$_{IN}$ and [NaCl]$_{BM}$: [NaCl]$_{IN}$ / [NaCl]$_{BM}$ = 1.45 ± 0.05, 1.38 ± 0.10, and 1.36 ± 0.05 for Q_{ex} = 200, 225, and 250 mL/min, respectively.

b. Influence of Q_{ex}

The impact of Q_{ex} on the difference between first dialyzer blood outlet (BM) and dialysate inlet (IN) ionic strengths was determined in blood. Increasing Q_{ex} was negatively correlated with the difference between both concentrations: [NaCl]$_{IN}$ / [NaCl]$_{BM}$ = 1.74 ± 0.70, 1.44 ± 0.02, 1.27 ± 0.03, 1.22 ± 0.07, and 1.16 ± 0.14 for Q_{ex} = 100, 200, 300, 400, and 500 mL/min (r^2 = 0.88, P < 0.05).

3) **Simulation of the NaCl concentration**

a. **Standard pre-dilution HDF**

i. Comparison to experimental data

A simulation of the [NaCl] during standard pre-dilution HDF, based on an iterative procedure (see corresponding algorithm in Appendix, **Fig. 85**) using the parameters of the Bellco Formula 2000 dialysis machine, was performed and compared to the results presented in **Fig. 40**. The mean mass transfer area coefficient of a Nipro Pureflux® 170 H filter (PUREMA® H membrane, 1.7 m² membrane surface area) was determined from the specification data sheet (93) and calculated from the instantaneous clearances according to **Eq. 16** (11). The mean K_0A for this hemofilter was 1152 mL/min.

$$K_0A = \frac{Q_B \cdot Q_D}{Q_B - Q_D} \cdot \ln\left(\frac{Q_D \cdot (Q_B - K)}{Q_B \cdot (Q_D - K)}\right)$$

Eq. 16: Calculation of the mass transfer area coefficient from measured clearances (11).
Where K_0A is the mass transfer area coefficient [mL/min]; Q_B and Q_D are the blood and dialysate flow rates [mL/min], respectively, and K the clearance [mL/min].
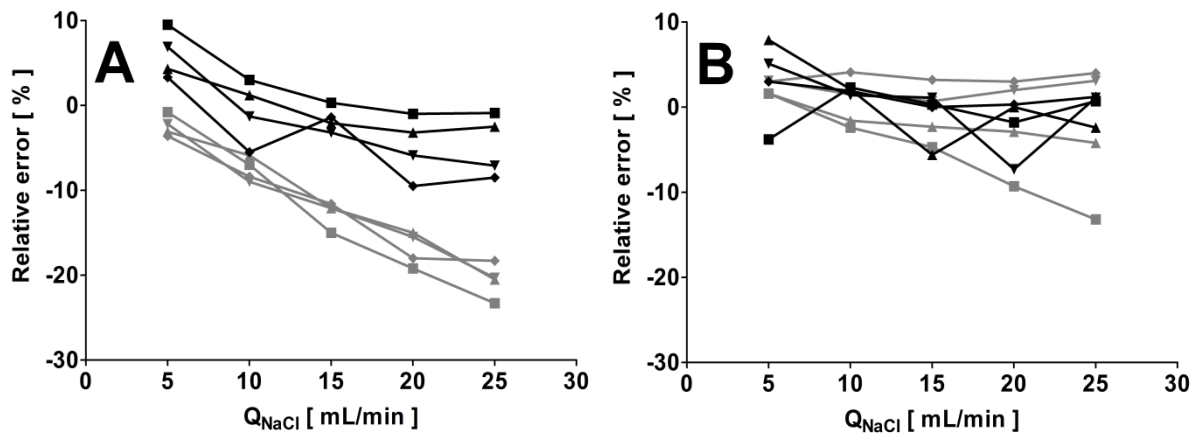
Fig. 42: Relative error between experimental and simulated [NaCl] during standard pre-dilution HDF.
Relative errors were calculated as *error = ([NaCl]$_{experiment}$ − [NaCl]$_{simulation}$) / [NaCl]$_{experiment}$*: A, Q_D = 500 mL/min; and B, Q_D = 800 mL/min; arterial (▬▬▬) and venous [NaCl] (▬▬▬); Q_B = 200 (■), 300 (▲), 400 (▼), and 500 mL/min (◆). Simulations fitted well with experimental data.

As shown in **Fig. 42**, the simulation fitted well the experimental results (relative error of ± 10%) at Q_D = 800 mL/min for both arterial and venous [NaCl] ([NaCl]$_{ART}$ and [NaCl]$_{VEN}$, respectively), and at Q_D = 500 mL/min for the [NaCl]$_{ART}$. For Q_{NaCl} > 15 mL/min and Q_D = 500 mL/min, [NaCl]$_{VEN}$ was, however, overestimated by the simulation (relative error > 10%). Simulations highly correlated with the experiment (Q_D = 500 mL/min, r^2 = 0.98, P < 0.0001 and r^2 = 0.93, P < 0.0001 for [NaCl]$_{ART}$ and [NaCl]$_{VEN}$, respectively; Q_D = 800 mL/min, r^2 = 0.99, P < 0.0001 and r^2 = 0.82, P < 0.0001 for [NaCl]$_{ART}$ and [NaCl]$_{VEN}$, respectively) and confirmed

that increasing Q_B reduces the clearance of the semi-permeable membrane leading to an accumulation of NaCl in the blood reservoir.

ii. Influence of K_0A on the removal of NaCl excess
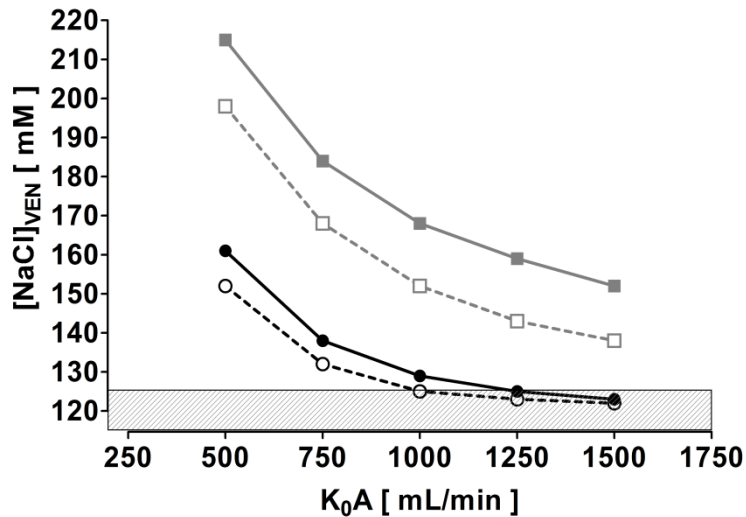
Fig. 43: Influence of K_0A on the venous [NaCl] during standard pre-dilution HDF.
The [NaCl]$_{VEN}$ was assessed by using the simulations of standard pre-dilution HDF with varying blood and dialysate flow rates: Q_B = 200 (━●━, --○--) and 500 mL/min (━■━, --□--), Q_D = 500 (solid line) and 800 mL/min (dotted line). The [NaCl] in the dialysate was set to 120 mM. The hatched area corresponds to physiologic [NaCl] in blood, being in the range of 115 to 125 mM. Q_{inf} = Q_{NaCl} = 10 mL/min, Q_{UF} = 0 mL/min. NaCl accumulates in blood when decreasing K_0A.

As shown in **Fig. 43**, increasing K_0A reduced [NaCl]$_{VEN}$ reaching physiologic concentrations at low Q_B. Whereas at high Q_B and in the range 500 < K_0A < 1500 mL/min, [NaCl]$_{VEN}$ was higher than 140 mM. Increasing the dialysate flow rate decreased the [NaCl].

b. **Serial dialyzers setup**

i. With pre-dilution HDF

A simulation of the [NaCl] during pre-dilution HDF with the SDial setup (see corresponding algorithm in Appendix, **Fig. 87**) using the parameters of the Nikkiso DBB-03 apparatus has been performed and compared to the results presented in **Fig. 41**. The K_0A of urea for DIAPES® BLS 714 G and Xenium® 170 H filters was determined based on clearance measurements presented on the respective data sheets and **Eq. 16**: $K_0A_{BLS\ 714\ G}$ = 635 mL/min and $K_0A_{Xenium\ 170\ H}$ = 1483 mL/min. Mean [NaCl]$_{BM}$ ([NaCl] in the blood line between both cartridges) and [NaCl]$_{VEN}$ acceptably matched the simulation ([NaCl]$_{BM}$, 443 ± 2 *versus* 431 mM, 491 ± 55 *versus* 472 mM, and 508 ± 13 *versus* 509 mM; [NaCl]$_{VEN}$, 137 ± 1 *versus* 134 mM, 137 ± 2 *versus* 136 mM, and 139 ± 0 *versus* 137 mM; for Q_{ex} = 200, 225, and 250 mL/min, respectively; experiment *versus* simulation) whereas [NaCl]$_{IN}$ and [NaCl]$_{OUT}$ ([NaCl] in the first cartridge dialysate inlet and outlet, respectively) were underestimated by the simulation ([NaCl]$_{IN}$, 643 ± 20 *versus* 558 mM, 674 ± 28 *versus* 593 mM, and 688 ± 7 *versus*

624 mM; accordingly, $[NaCl]_{OUT}$, 314 ± 1 *versus* 218 mM, 357 ± 33 *versus* 252 mM, and 356 ± 14 *versus* 285 mM).

The simulation was also compared to the results presented above ("Influence of Q_{ex}"). It generally underestimated the experimental results of about 15 ± 21 mM (BM) and 65 ± 12 mM (IN) but similar ratios $[NaCl]_{IN}$ / $[NaCl]_{BM}$ were obtained: simulation $[NaCl]_{IN}$ / $[NaCl]_{BM}$ = 1.68 ± 0.21, 1.28 ± 0.06, 1.18 ± 0.03, 1.14 ± 0.02, and 1.12 ± 0.02 for Q_{ex} = 100, 200, 300, 400, and 500 mL/min, respectively.

ii. With transmembrane pre-dilution HDF

The simulation of the SDial setup with transmembrane pre-dilution (see corresponding algorithm in Appendix, **Fig. 88**) was compared to experimental results for Q_B = Q_{ex} = 150 mL/min, Q_D = 500 mL/min, Q_{inf} = 75 mL/min, Q_{NaCl} = 6.5 and 10.8 mL/min. Again, the $[NaCl]_{BM}$ acceptably matched the simulation: 250 ± 19 *versus* 264 mM and 351 ± 23 *versus* 358 mM for Q_{NaCl} = 6.5 and 10.8 mL/min, respectively, experiment *versus* simulation; whereas the simulation underestimated $[NaCl]_{IN}$ and $[NaCl]_{OUT}$: $[NaCl]_{IN}$, 333 ± 45 *versus* 285 mM and 433 ± 12 *versus* 393 mM for Q_{NaCl} = 6.5 and 10.8 mL/min, respectively; $[NaCl]_{OUT}$, 184 ± 38 *versus* 158 mM and 233 ± 12 *versus* 182 mM for Q_{NaCl} = 6.5 and 10.8 mL/min, respectively.
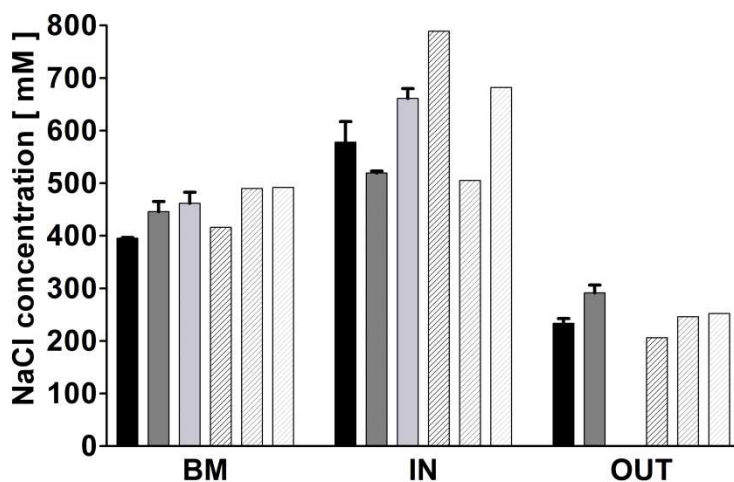
Fig. 44: Comparison between simulation and experimental [NaCl] for the SDial setup.
The [NaCl] was measured in aqueous solution (full bars) and compared to the simulation (hatched bars) for Q_B = 150 mL/min and Q_{ex} = 25 mL/min (■), Q_B = 150 mL/min and Q_{ex} = 200 mL/min (■), and Q_B = 300 mL/min and Q_{ex} = 200 mL/min (▨).

In this second experimental part (**Fig. 44**), the simulations approximated well $[NaCl]_{BM}$, $[NaCl]_{IN}$, and $[NaCl]_{OUT}$ at various Q_{ex} and Q_B with the SDial-TM pre-HDF.

iii. Serial dialyzers pre-HDF *versus* serial dialyzers transmembrane pre-HDF

Simulation of the $[NaCl]_{BM}$ and the $[NaCl]_{IN}$ (see **Fig. 11**) was performed to assess the influence of the transmembrane pre-dilution on the [NaCl] gradient between blood and dialysate in the first cartridge. Therefore, the K_0A of urea for DIAPES® BLS 714 G (first

dialyzer) and the one for Xenium® 170 H (second dialyzer) were considered; Q_B = 150 mL/min, Q_D = 500 mL/min, Q_{inf} = 75 mL/min, Q_{UF} = 0 mL/min, and Q_{NaCl} = 20 mL/min (5.00 M NaCl solution).

The results (see **Fig. 45**) indicated that the [NaCl] gradient decreased when increasing Q_{ex} and that the gradient largely decreased when using transmembrane pre-dilution as compared to normal pre-dilution.
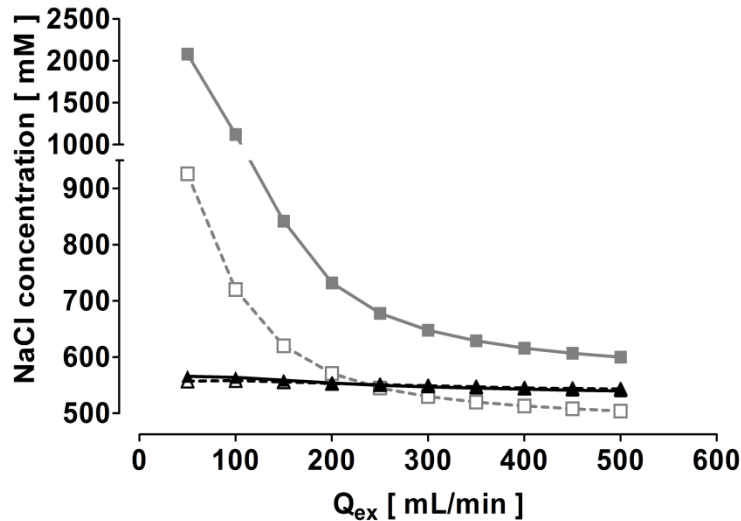
Fig. 45: Simulation of the influence of the mode of pre-dilution with the SDial setup on the [NaCl].
The simulation of the [NaCl] was performed for: SDial pre-HDF, [NaCl]$_{BM}$ (▬▲▬) and [NaCl]$_{IN}$ (▬■▬); and SDial-TM pre-HDF, [NaCl]$_{BM}$ (--△--) and [NaCl]$_{IN}$ (--□--). Dialysis parameters were: Q_B = 150 mL/min, Q_D = 500 mL/min, Q_{inf} = 75 mL/min, Q_{UF} = 0 mL/min, and Q_{NaCl} = 20 mL/min (5.00 M NaCl solution); K_0A first dialyzer = 635 mL/min, K_0A second dialyzer = 1483 mL/min. Transmembrane pre-dilution reduced greatly the concentration gradient in the first dialyzer.

III.   *Ex vivo* hemocompatibility of increased ionic strength

1) Cell damage after contact with NaCl

a.   Effect on red blood cells

In a first experiment, blood was dialyzed against different NaCl solutions so that [NaCl]$_{blood}$ was increased to 0.15, 0.26, 0.39, 0.48, 0.58, and 0.75 M. During 240 min incubation at 37 °C with increased ionic strength, hemolysis was steady. Hemolysis was plotted against [NaCl]$_{blood}$. In a second experimental setup, blood was incubated 1 h at room temperature after dilution with different NaCl solutions to increase ionic strength. Results are presented in **Fig. 46**.
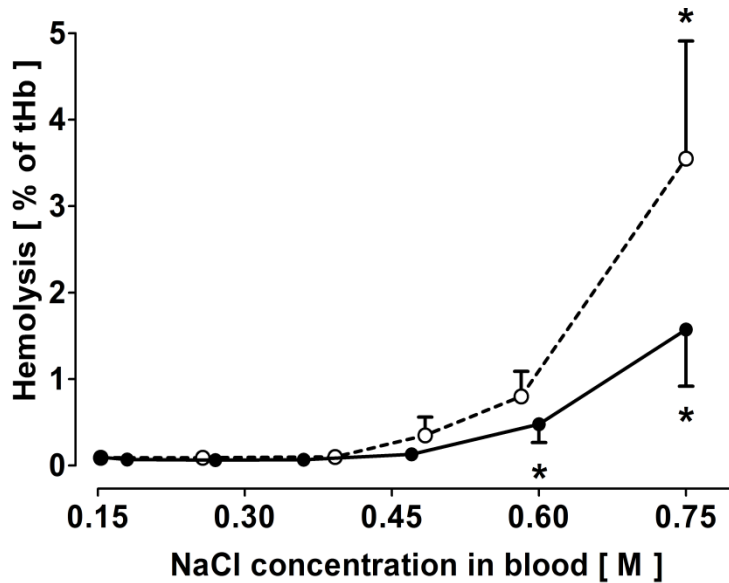
Fig. 46: Hemolysis in human blood after contact with NaCl. Hemolysis was studied during single pass dialysis (--O--) and blood dilution (--●--); results are presented as mean ± SD (n = 7 and n = 21, respectively). *, $P < 0.05$ *versus* 0.15 M NaCl. Hemolysis non linearly increased with higher $[NaCl]_{blood}$.

In both experimental settings, no hemolysis was seen after exposure to [NaCl] ranging from 0.15 to 0.50 M. When $[NaCl]_{blood}$ was further increased, hemolysis enhanced exponentially with the [NaCl]. This increase was faster during the single pass dialysis experiment compared to the static experiment in test tubes.
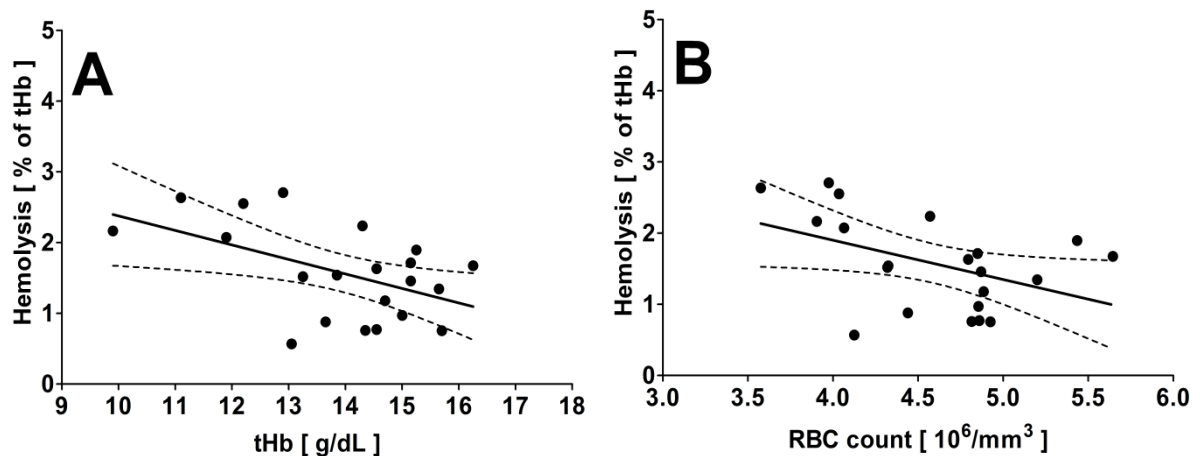
Fig. 47: Hemolysis in human blood after contact with 0.75 M NaCl. Blood from single donors (n = 21) was diluted with different NaCl solution to reach a final concentration of 0.75 M NaCl and incubated 1 h at room temperature. Hemolysis is presented *versus* either tHb level (A) or the RBC count (B). Solid line: linear regression; dotted lines: 95% confidence interval. Hemolysis negatively correlated with tHb and RBC count.

As presented in **Fig. 47**, hemolysis in blood with 0.75 M NaCl slightly negatively correlated with the RBC count ($r^2 = 0.20$, $P < 0.05$) and tHb level ($r^2 = 0.26$, $P < 0.05$). No correlation was found neither between hemolysis and mean cell volume ($P = 0.63$) nor between RBC count or tHb level and hemolysis at lower $[NaCl]_{blood}$. RBC count and tHb levels highly correlated ($r^2 = 0.83$, $P < 0.0001$).
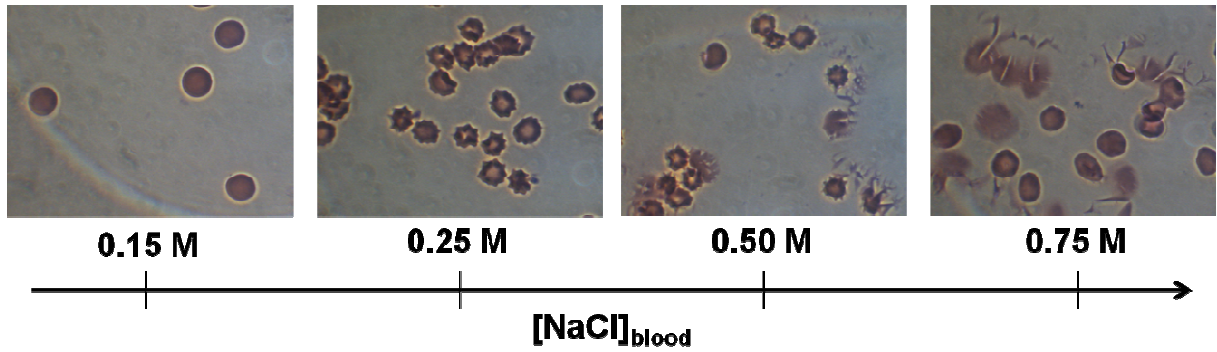
Fig. 48: May-Grünwald staining of blood smears at different [NaCl].
Optical microscopy (×100) of RBC after staining. Blood was diluted 1:10 with different NaCl solutions.

Blood samples at different [NaCl]$_{blood}$ were stained with May-Grünwald solution as shown in **Fig. 48**. Normal morphology of RBC was visible at physiologic [NaCl]$_{blood}$. When the ionic strength was increased to 0.25 M NaCl, exclusively echinocytes were seen but cells were still intact. At [NaCl]$_{blood}$ ≥ 0.50 M, both echinocytes and blasted cells (hemoglobin release) were visible.
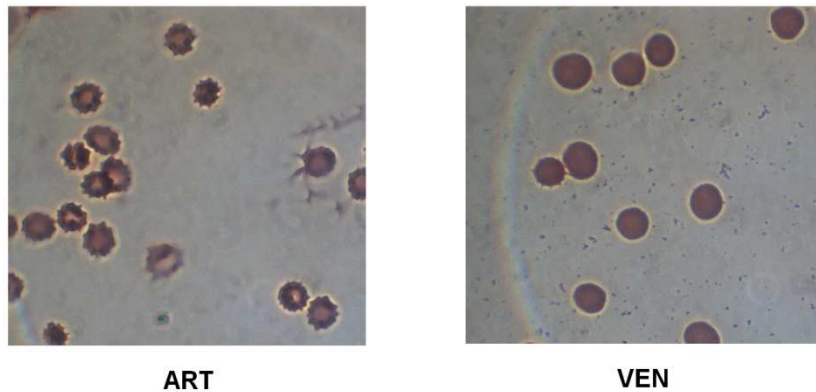
Fig. 49: May-Grünwald staining of blood smears of arterial and venous samples during dialysis.
The arterial (ART) [NaCl] was about 0.50 M, venous (VEN) [NaCl] was physiologic. Optical microscopy (×100).

During dialysis, echinocytes were prevalent in arterial samples when [NaCl]$_{blood}$ was about 0.50 M, whereas a normal morphology was seen in venous samples where [NaCl]$_{blood}$ was physiologic (0.15 M).

b. Effect on white blood cells
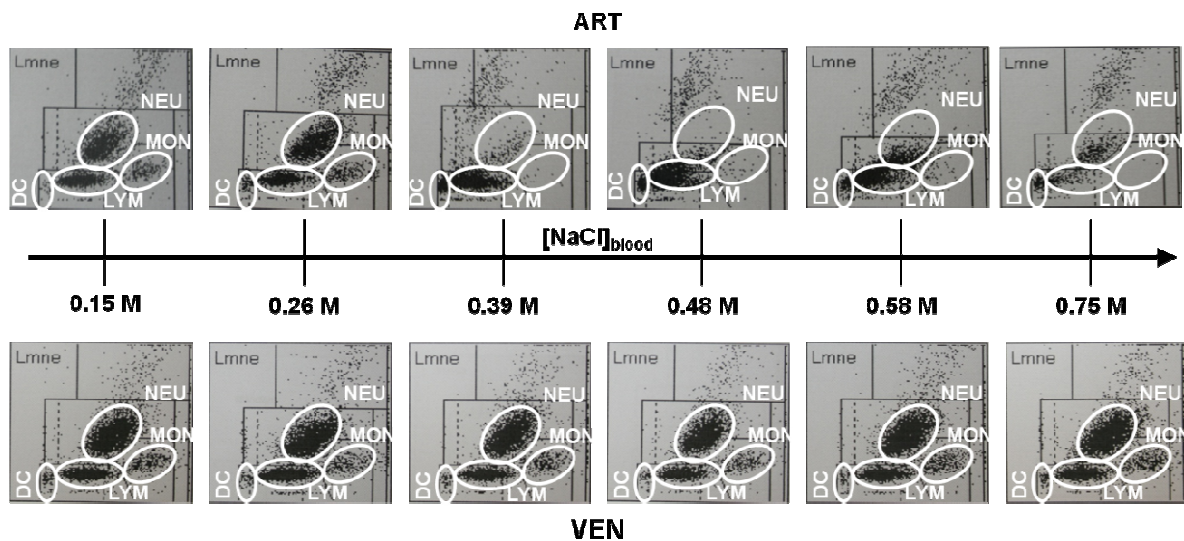
Fig. 50: Dot plots of WBC subpopulations subjected to NaCl.
Dot plots of WBC subpopulations were obtained from arterial (increased ionic strength) and venous (physiologic ionic strength) blood samples after contact with different [NaCl] during single pass dialysis. Four areas are highlighted: dead cells (DC, bottom left), lymphocytes (LYM, bottom middle), granulocytes (NEU, top) and monocytes (MON, bottom right).

With $[NaCl]_{blood} \leq 0.26$ M, no change in the WBC subpopulations was observed (**Fig. 50**) neither in arterial nor in venous samples. With $[NaCl]_{blood} \geq 0.39$ M, the arterial dot plots changed significantly: the monocyte, granulocyte neutrophiles and basophiles subpopulations seem to vanish since granularity and cell size decreased; the proportion of lymphocyte- and dead cells increased. This abnormality was more pronounced with higher $[NaCl]_{blood}$. These changes were, however, not visible in corresponding venous samples in which normal dot plots were obtained similar to those found in arterial blood with $[NaCl]_{blood}$ = 0.15 M.

2) Effect of the blood volume on the *ex vivo* results

Hemolysis rates and cell counts were studied during *ex vivo* standard pre-HDF experiments using two different blood volumes: 500 and 1500 mL.

$[NaCl]_{ART}$ was higher ($P < 0.05$, **Tab. 13**) in the experiment using 500 mL blood compared to the one with 1500 mL blood (489 ± 35 *versus* 464 ± 19 mM, respectively) whereas $[NaCl]_{VEN}$ was similar ($P = 0.06$; 135 ± 6 *versus* 140 ± 5 mM, respectively). Hct and tHb were higher in the experiments with 500 mL blood but these differences depended only on the donor variability. Arterial Ca^{2+} and K^+ as well as venous Ca^{2+} concentrations were not different ($P > 0.05$) between both experiments but venous K^+ concentration was lower ($P < 0.01$) in 1500 mL blood.

		pH	pO$_2$ [mmHg]	pCO$_2$ [mmHg]	HCO$_3^-$ [mM]	Na$^+$ [mM]	K$^+$ [mM]	Ca^{2+} [mM]	Cl$^-$ [mM]	tHb [g/dL]	Hct [%]
500mL	ART	7.22 ± 0.06	112.1 ± 27.8	25.8 ± 8.3	10.1 ± 1.9	513 ± 36	0.62 ± 0.19	0.47 ± 0.06	465 ± 34	-	-
	VEN	7.17 ± 0.07	101.8 ± 18.8	77.5 ± 13.5	27.5 ± 0.9	158 ± 6	2.65 ± 0.40	1.13 ± 0.06	112 ± 5	18.1 ± 1.1	52.9 ± 3.7
1500mL	ART	7.18 ± 0.05	97.2 ± 33.5	27.5 ± 2.8	10.1 ± 1.0	491 ± 19	0.56 ± 0.16	0.48 ± 0.03	437 ± 19	-	-
	VEN	7.12 ± 0.04	88.6 ± 24.6	89.3 ± 6.8	28.2 ± 1.0	163 ± 6	2.26 ± 0.11	1.17 ± 0.02	116 ± 5	15.8 ± 0.4	47.4 ± 0.9

Tab. 13: Arterial and venous ion concentrations, pH, gas saturation, hemoglobin and hematocrit during *ex vivo* standard pre-dilution HDF.

Results are presented as mean ± SD (2 independent experiments, 6 measurements, i.e. n = 12) of dialysis experiments performed with 500 mL and 1500 mL blood.
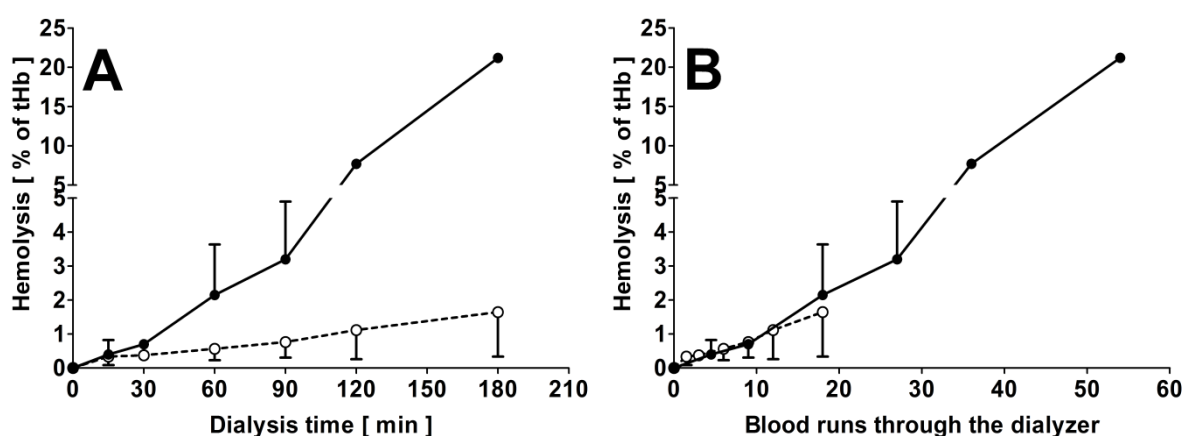
Fig. 51: Effect of the blood volume on the hemolysis during *ex vivo* standard pre-dilution HDF.

Hemolysis rates *versus* time (A) and *versus* blood runs through the dialyzer (B) are presented for dialysis sessions with either 500 mL (—●—) or 1500 mL (--○--) blood. Means ± SD (n = 2) are given.

When ploting the hemolysis *versus* time (**Fig. 51**, A), the rate was higher when using 500 mL blood compared with 1500 mL blood. Post-dialysis (180 min) hemolysis levels were 21.2 ± 0.6% and 1.6 ± 1.3%, respectively. When ploting the same experimental values *versus* blood runs through the dialyzer according to **Eq. 7** (**Fig. 51**, B), the hemolysis rate was similar between both blood volumes.
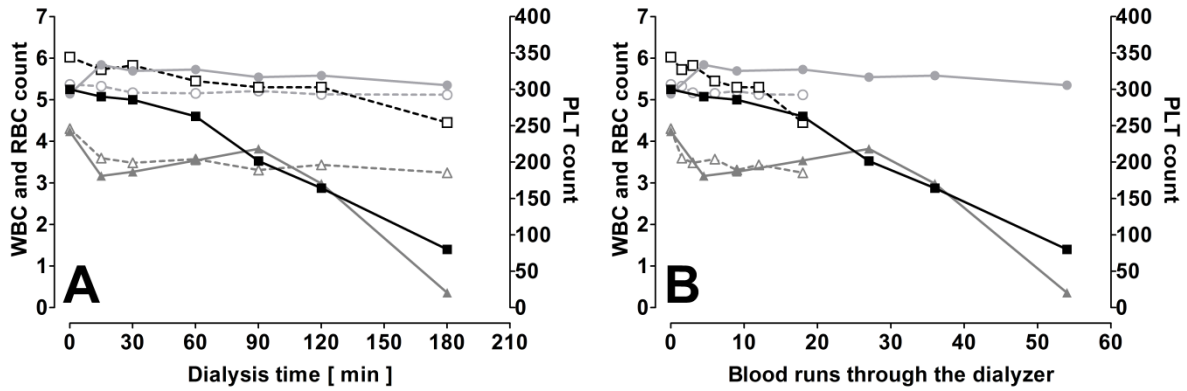
Fig. 52: Effect of the blood volume on the cell count during *ex vivo* standard pre-dilution HDF.
Mean (n = 2) cell counts *versus* time (A) and *versus* blood runs through the dialyzer (B) are presented for WBC [$\times 10^3$/mm^3] (━■━, --□--), RBC [$\times 10^6$/mm^3] (━●━, --○--), and PLT [$\times 10^3$/mm^3] (━▲━, --△--). Experiments were performed with 500 mL (solid lines) or 1500 mL blood (dotted lines).

When using 500 mL blood, the mean WBC and PLT counts were decreased after 180 min treatment, whereas only a slight decrease was observed when using a larger blood volume (**Fig. 52**, A). However, when comparing the results for the same mechanical stress, i.e., number of passages through the blood pump (**Fig. 52**, B), the results were similar. This observation was confirmed by similar findings for the WBC subpopulations in the dot plots (**Fig. 53**).
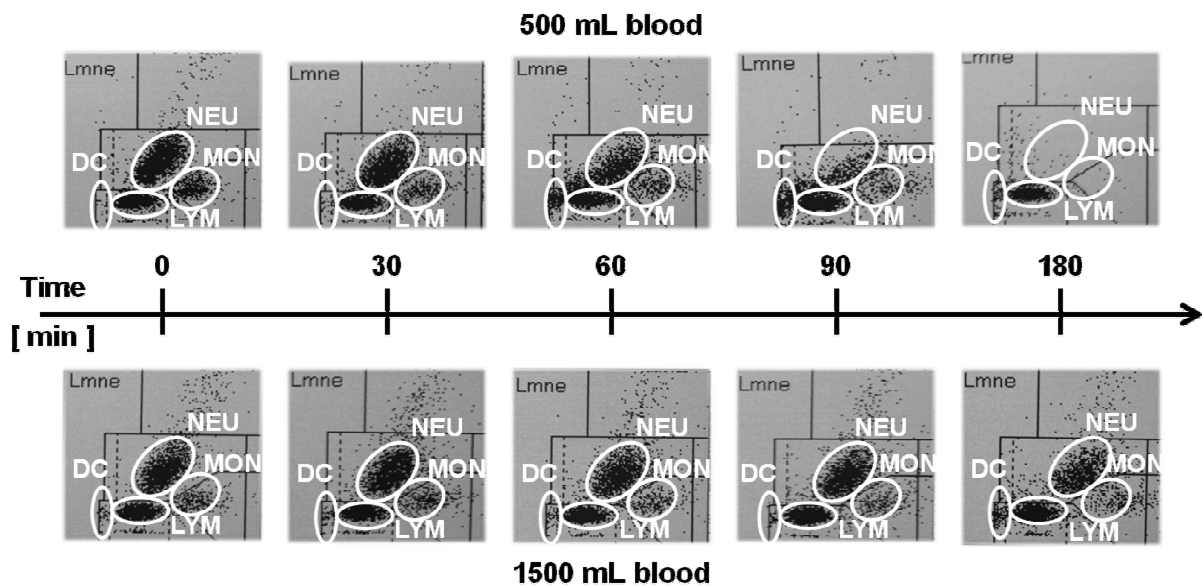
Fig. 53: Dot plots of the WBC subpopulations during standard pre-dilution HDF with different blood volumes.
Four areas are highlighted: dead cells (DC, bottom left), lymphocytes (LYM, bottom middle), granulocytes (NEU, top), and monocytes (MON, bottom right).
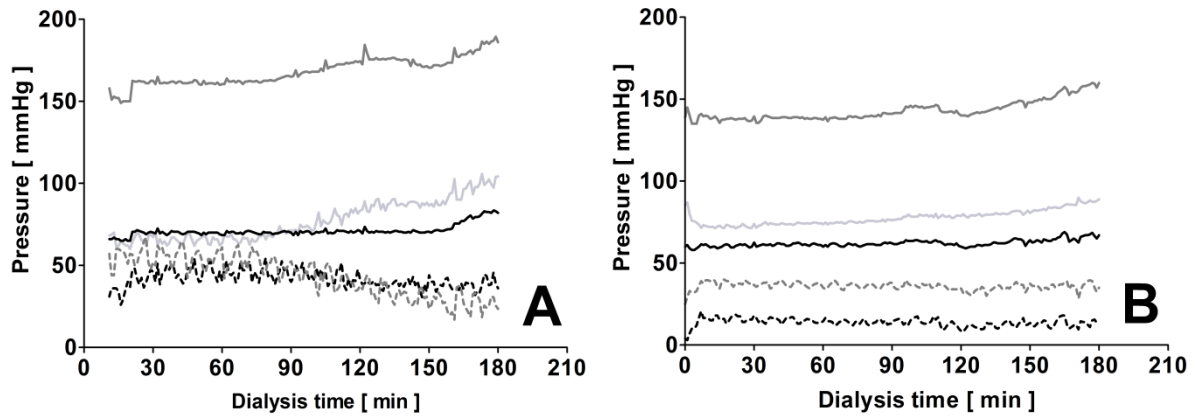
Fig. 54: Effect of the blood volume on the pressures during standard pre-dilution HDF.
Mean (n = 2) pressures recorded were: arterial (⎯⎯), venous (▬▬), dialysate inlet (▪▪▪▪), dialysate outlet (▪▪▪▪), and TMP (⎯⎯). A, 500 mL blood; B, 1500 mL blood.

Arterial, venous, dialysate inlet, and outlet pressures were higher for the experiment performed with low blood volume, maybe due to the higher Hct (52.9 ± 3.7% *versus* 47.4 ± 0.9%). The TMP was constant when using 1500 mL blood volume, whereas with 500 mL blood it increased after 90 min of dialysis because P_{IN} decreased and P_{ART} increased.

3) <u>Maximal NaCl concentration in blood</u>

Standard pre-HDF pilot experiments (n = 1) were performed in human blood while using different [NaCl] in the substitution fluid in order to determine the maximal admissible ionic strength under dynamic conditions.

Setting	Hct [%]	tHb [g/dL]	$[Na^+]_{ART}$ [mM]	$[Na^+]_{VEN}$ [mM]	$[Cl^-]_{ART}$ [mM]	$[Cl^-]_{VEN}$ [mM]
Single 0.15 M	43.3 ± 2.1	14.8 ± 0.6	141 ± 1	141 ± 1	103 ± 1	99 ± 2
Single 1.00 M	50.4 ± 2.7	17.2 ± 0.5	534 ± 9	155 ± 6	485 ± 7	110 ± 5
Spread 1.00 M	54.0 ± 4.5	18.5 ± 1.5	486 ± 37	161 ± 5	439 ± 36	115 ± 4
Single 1.55 M	38.2 ± 2.5	13.5 ± 0.6	444 ± 49	149 ± 8	390 ± 44	107 ± 7

Tab. 14: Hematocrit, hemoglobin and sodium chloride concentrations with a different setup of standard pre-dilution HDF.
Spread infusion was performed with four different accesses. Results are mean ± SD (single experiment, 7 measurements, i.e. n = 7).
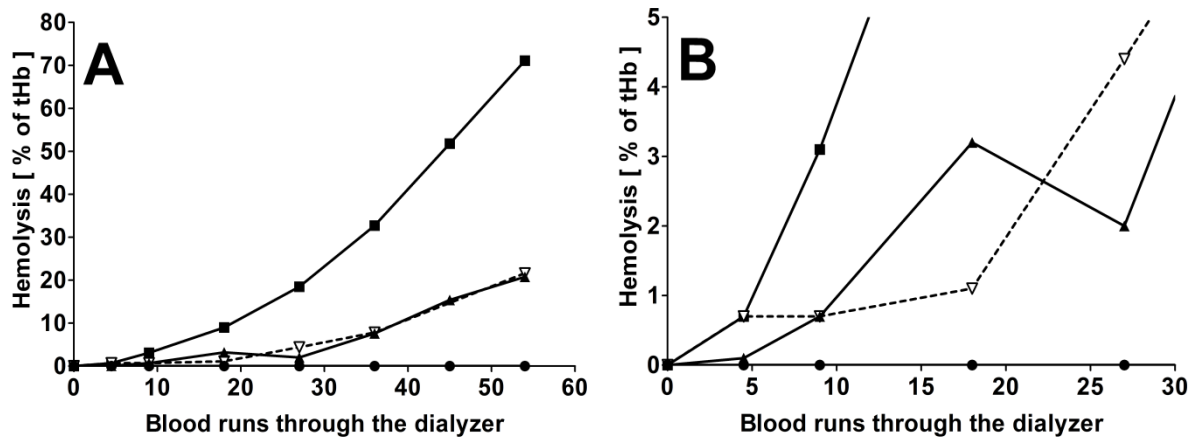
Fig. 55: Hemolysis in blood using different [NaCl] in the substitution fluid during standard pre-dilution HDF. Final $[NaCl]_{blood}$ was 0.50 M using three different $[NaCl]_{SUB}$: single (—▲—) and spread (--▽--) infusion of 1.00 M NaCl, and single infusion of 1.55 M NaCl (—■—). Reference: infusion of saline (—●—). A, hemolysis in blood *versus* blood runs through the dialyzer; B, detail of A. Results derived from a single pilot experiment (n = 1).

As shown in **Tab. 14**, $[NaCl]_{ART}$ reached about 0.51, 0.46, and 0.42 M when infusing a single 1.00 M NaCl solution, a spread 1.00 M NaCl solution, and a single 1.55 M NaCl solution in blood, respectively. When comparing the different settings, the higher the $[NaCl]_{SUB}$, the higher the hemolysis rate. There was no difference between single and spread infusion of the 1.00 M NaCl in blood.

4) <u>Role of the semi-permeable membrane in the osmotic shock</u>

In order to assess the impact of the semi-permeable membrane (first dialyzer) in the SDial setup on the protection against osmotic choc, hemodialysis treatments were performed in the same pool of human whole blood using this setup in HD-modus (Q_{inf} = 0 mL/min) and $[NaCl]_{blood}$ = 0.50 M. For that purpose, only the dialysate flow rate of the first dialyzer Q_{ex} was varied leading to two different [NaCl] at the first dialyzer dialysate inlet: 0.55 *versus* 1.10 M NaCl. After 120 min dialysis with increased ionic strength, blood was further dialyzed (120 min) under physiologic conditions (0.15 M NaCl).
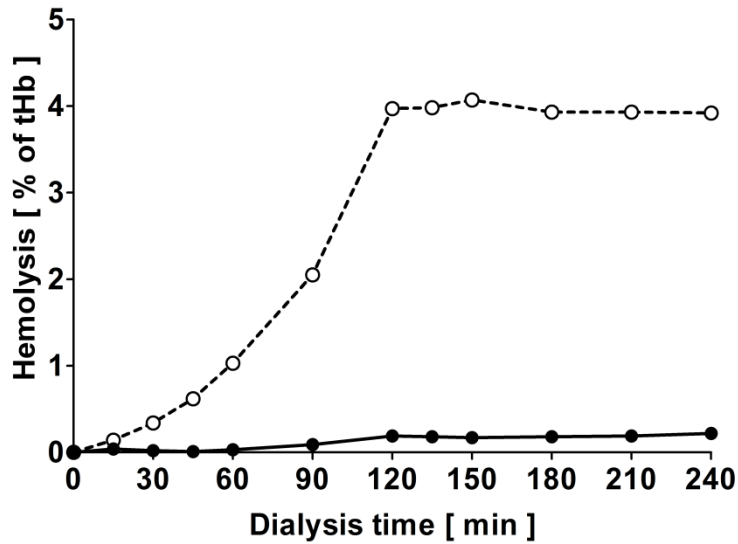
Fig. 56: Hemolysis rate during HD experiments with the SDial setup at 0.50 M NaCl.
Results are presented from a pilot experiment (n = 1) for Q_{ex} = 300 mL/min ($[NaCl]_{IN\ 1} \approx 0.55$ M, —●—) and Q_{ex} = 50 mL/min ($[NaCl]_{IN\ 1} \approx 1.10$ M, --○--). 0 to 120 min, $[NaCl]_{BM}$ = 0.50 M; 120 to 240 min, $[NaCl]_{BM}$ = 0.15 M. Time points correspond to 0.0, 4.3, 8.7, 13.2, 26.8, 36.0, 40.7, 45.5, 55.1, 64.7, and 74.5 blood runs through the dialyzer according to **Eq. 7**.

[NaCl] were measured as: BM, 498 ± 2 and 129 ± 0 mM between 0 − 120 min and 120 − 240 min, respectively, for Q_{ex} = 300 mL/min, and 526 ± 5 and 123 ± 1 mM between 0 − 120 min and 120 − 240 min, respectively, for Q_{ex} = 50 mL/min; VEN, 126 ± 1 and 124 ± 0 mM for Q_{ex} = 300 and 50 mL/min, respectively. Even though the $[NaCl]_{BM}$ was similar with both settings, the hemolysis was largely higher with the lowest Q_{ex} reaching 4.0% (*versus* 0.2%) after 120 min treatment, as shown in **Fig. 56**. Thus, with increasing [NaCl] gradient on the semi-permeable membrane, the hemolysis augmented. When infusion of 5.00 M NaCl was stopped (after 120 min treatment), hemolysis stayed constant.
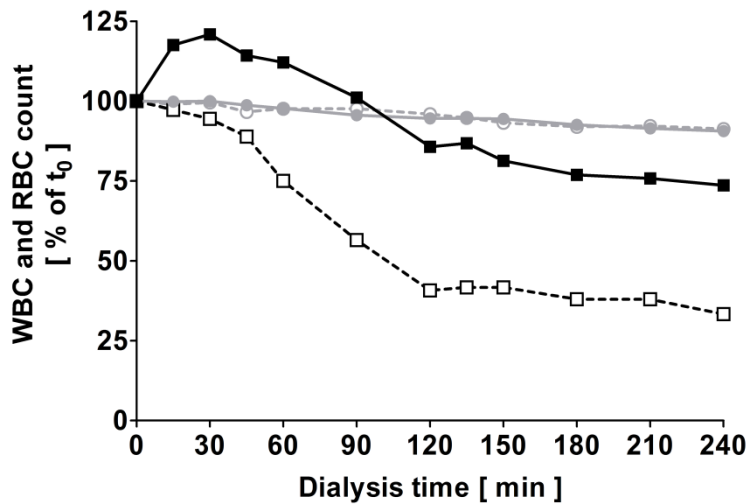
Fig. 57: Cell count during HD experiments with the SDial setup at 0.50 M NaCl.
WBC (—■—, --□--) and RBC counts (—●—, --○--) are presented for Q_{ex} = 300 mL/min (solid line) and Q_{ex} = 50 mL/min (dotted line). Values are expressed in % of the cell count of t = 0 min (n = 1). Time points correspond to 0.0, 4.3, 8.7, 13.2, 26.8, 36.0, 40.7, 45.5, 55.1, 64.7, and 74.5 blood runs through the dialyzer according to **Eq. 7**.

The WBC count decreased in both experiments within the first half but the reduction was faster for Q_{ex} = 50 mL/min (**Fig. 57**). Similarly to hemolysis, the WBC count stayed constant after stopping of the 5.00 M NaCl infusion. This finding was confirmed by the results of the dot plot (**Fig. 58**). The RBC count slightly decreased over the whole experiment.
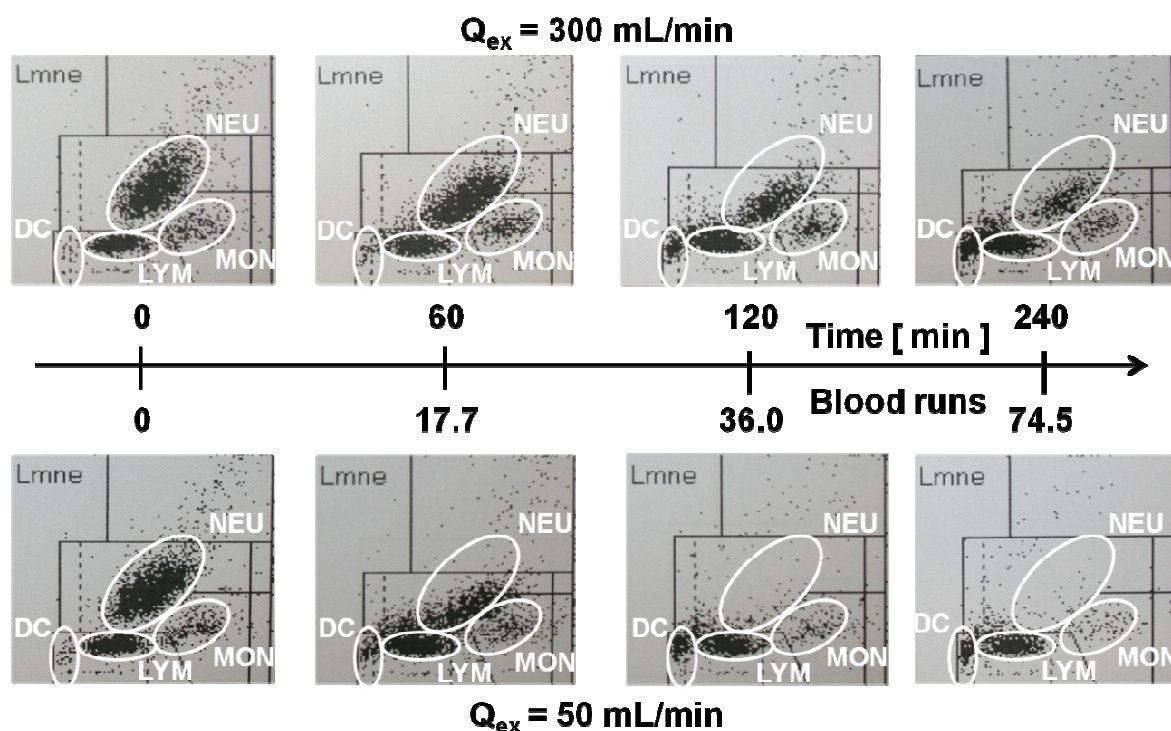
Fig. 58: Dot plots of the WBC subpopulations during HD experiments with the SDial setup at 0.50 M NaCl.
Four areas are highlighted: dead cells (DC, bottom left), lymphocytes (LYM, bottom middle), granulocytes (NEU, top), and monocytes (MON, bottom right).

		T	$P_{ART\,1}$	$P_{VEN\,1}$	$P_{IN\,1}$	$P_{OUT\,1}$	TMP_1	$P_{ART\,2}$	$P_{VEN\,2}$	$P_{IN\,2}$	$P_{OUT\,2}$	TMP_2
Q_{ex}=300 mL/min	0 – 120 min	35.4 ± 0.3	128 ± 2	94 ± 1	129 ± 3	123 ± 1	-15 ± 1	94 ± 1	57 ± 1	69 ± 1	59 ± 2	11 ± 1
	120 – 240 min	35.3 ± 0.1	123 ± 2	93 ± 1	91 ± 5	92 ± 5	17 ± 4	93 ± 1	57 ± 1	71 ± 2	56 ± 3	12 ± 1
Q_{ex}=50 mL/min	0 – 120 min	34.8 ± 0.2	134 ± 2	127 ± 2	155 ± 4	148 ± 4	-21 ± 2	127 ± 2	58 ± 0	64 ± 0	54 ± 3	34 ± 1
	120 – 240 min	35.3 ± 0.1	131 ± 1	120 ± 2	114 ± 6	119 ± 6	9 ± 4	120 ± 2	57 ± 1	64 ± 0	43 ± 2	35 ± 1

Tab. 15: Temperatures and pressures during HD experiments with the SDial setup at 0.50 M NaCl.
Abbreviations and units: T, temperature [°C]; P_{ART}, dialyzer blood inlet pressure [mmHg]; P_{VEN}, dialyzer blood outlet pressure [mmHg]; P_{IN}, dialyzer dialysate inlet pressure [mmHg]; P_{OUT}, dialyzer dialysate outlet pressure [mmHg]; and TMP, transmembrane pressure [mmHg].

Overall, the temperature was similar in both experiments (**Tab. 15**). Pressures at the first dialyzer were higher at low Q_{ex} (corresponding to high [NaCl] on the dialysate side) whereas pressures at the second filter were similar in both experiment. Interestingly, pressure at the dialysate side of the first dialyzer decreased when the infusion of 5.00 M NaCl solution was stopped resulting in a higher TMP: during the first 120 min, the TMP of the first dialyzer was negative in both experiments, whereas during the next 120 min, it was positive (see also **Fig. 59**). The TMP of the second dialyzer did not depend on the infusion of 5.00 M NaCl solution but was greater for Q_{ex} = 50 mL/min compared to Q_{ex} = 300 mL/min.
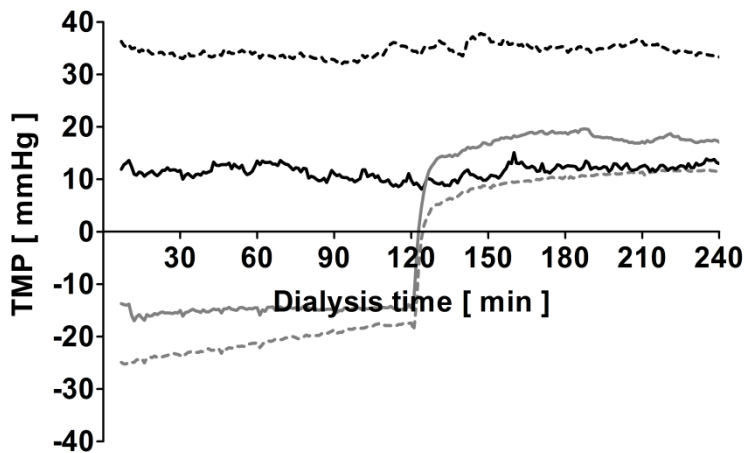
Fig. 59: TMP during HD experiments with the SDial setup at 0.50 M NaCl. TMP of dialyzer 1 (——, - - - -) and 2 (——, - - - -) for Q_{ex} = 300 mL/min (solid line) and Q_{ex} = 50 mL/min (dotted line).

5) Comparative *ex vivo* hemocompatibility

The *ex vivo* hemocompatibility of increased ionic strength was assessed for two dialysis setups using the flow rates of the animal model:

- Standard pre-dilution HDF (single dialyzer),
- Serial dialyzers pre-dilution HDF.

a. Standard *versus* serial dialyzers pre-dilution HDF

It is important to note that the serial dialyzers system is described according to the $[NaCl]_{blood}$ (also $[NaCl]_{BM}$) whereas the standard HDF is described according to the $[NaCl]_{SUB}$. The following concentrations were tested: standard pre-HDF, 0.15, 0.75, 1.00, and 1.20 M NaCl; SDial pre-HDF, 0.15, 0.36, 0.50, and 0.75 M NaCl.

Serial dialyzers pre-dilution HDF				Standard pre-dilution HDF			
$[NaCl]_{SUB}$	$[NaCl]_{blood}$		$[NaCl]_{VEN}$	$[NaCl]_{SUB}$	$[NaCl]_{blood}$		$[NaCl]_{VEN}$
	Target	Real			Target	Real	
120	120	125 ± 3	127 ± 3	120	120	126 ± 3	128 ± 2
120	360	377 ± 40	127 ± 4	750	360	336 ± 8	122 ± 2
120	500	474 ± 7	122 ± 4	1000	360	344 ± 18	122 ± 1
120	750	731 [*]	145 [*]	1200	500	463 ± 39	126 ± 5

Tab. 16: [NaCl] during both dialysis treatments.
Concentrations are given in [mM] as mean ± SD (n = 3). Abbreviations: $[NaCl]_{SUB}$, NaCl concentration in the substitution fluid; $[NaCl]_{blood}$, NaCl concentration in blood with increased ionic strength (standard pre-HDF: downstream the pre-dilution; SDial pre-HDF: second dialyzer blood inlet); $[NaCl]_{VEN}$, NaCl concentration in the venous line (blood downstream the second dialyzer). [*], n = 1.

Blood temperature was between 33.8 ± 0.4 and 35.2 ± 0.7 °C and was not different between the settings. The NaCl concentrations at the different samples sites of both setups are presented above (**Tab. 16**). Real $[NaCl]_{blood}$ largely matched the target $[NaCl]_{blood}$. For all settings, $[NaCl]_{blood}$ was increased (*P* < 0.0001) compared to physiologic controls.

Furthermore, settings with comparative ionic strength (SDial pre-HDF 0.36 M NaCl *versus* standard pre-HDF 0.75 and 1.00 M NaCl; SDial pre-HDF 0.50 M NaCl *versus* standard pre-HDF 1.20 M NaCl) also were similar. $[NaCl]_{VEN}$ was not different compared to the isotonic controls.
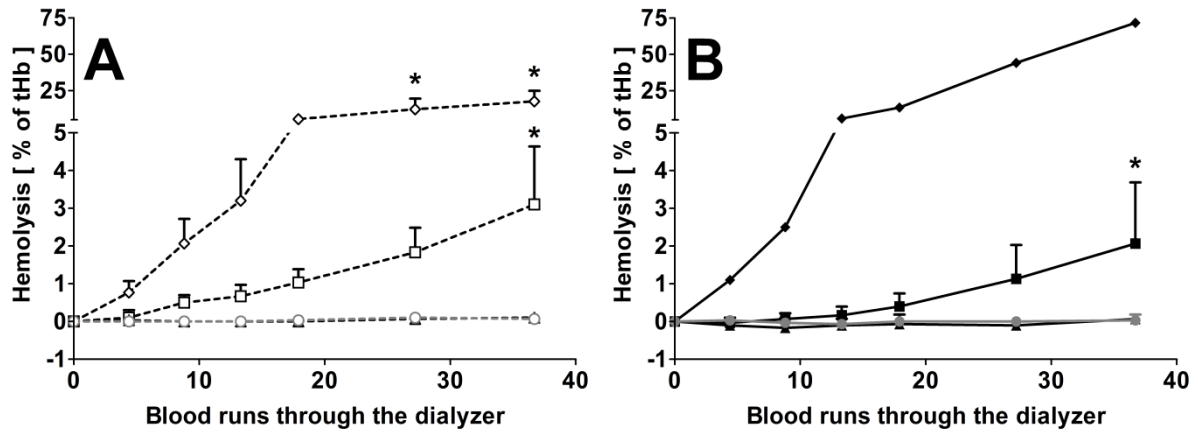
Fig. 60: *Ex vivo* **hemolysis in human heparinized blood during pre-dilution HDF at different [NaCl] and setups.** A, standard pre-HDF with substitution fluid of 0.15 (--○--), 0.75 (--△--), 1.00 (--□--), and 1.20 M NaCl (--◇--) corresponding to $[NaCl]_{blood}$ of 0.15, 0.36, 0.36, and 0.50 M, respectively; B, SDial pre-HDF with 0.15 (—●—), 0.36 (—▲—), 0.50 (—■—), and 0.75 M $[NaCl]_{blood}$ (—◆—). *, $P < 0.05$ *versus* t_0. The Y-axis is divided in two sections: -1% to 5% and 5% to 75%. Mean ± SD (n = 3).

As demonstrated in **Fig. 60**, a second serial hemodialyzer did not induce hemolysis itself. In the standard pre-HDF group (**Fig. 60**, A), no hemolysis was observed when increasing the ionic strength in the substitution fluid to 0.75 M NaCl. A further increase of the [NaCl] led to significant hemolysis after 120 min (corresponding to 36.7 blood runs) reaching 3.1 ± 1.5% and 17.6 ± 7.2% for 1.00 and 1.20 M $[NaCl]_{SUB}$, respectively. Post-dialysis hemolysis correlated with both $[NaCl]_{blood}$ and $[NaCl]_{SUB}$ ($r^2 = 0.47$, $P < 0.05$; and $r^2 = 0.43$, $P < 0.05$, respectively). In the SDial pre-HDF group (**Fig. 60**, B) increasing the ionic strength in blood to 0.36 M NaCl did not induce hemolysis. Hemolysis occurred when using 0.50 M or greater $[NaCl]_{blood}$. No correlation was found between post-dialysis hemolysis and $[NaCl]_{blood}$ ($r^2 = 0.18$, $P = 0.16$). Hemolysis after 60 min and 120 min dialysis was significantly higher ($P < 0.05$) for standard pre-HDF 1.20 M NaCl as compared to all other treatments. Only a single experiment was performed with the SDial pre-HDF and 0.75 M $[NaCl]_{blood}$ since hemolysis became unacceptably high not justifying further testing.

At the beginning of the dialysis experiments, WBC, RBC, and PLT counts were in the range of 4.3 ± 0.2 to 6.0 ± 2.7 ×10^3 cells /mm^3, 3.45 ± 0.51 to 4.19 ± 0.65 ×10^6 cells /mm^3, and 87 ± 10 to 163 ± 34 ×10^3 cells /mm^3, respectively; Hct and tHb were in the range of 31 ± 2% to 37 ± 6% and 10.4 ± 1.2 to 12.8 ± 1.7 g/dL, respectively. The WBC count (**Fig. 61**) was constant over time in the standard pre-HDF group with 0.15, 0.75, and 1.00 M $[NaCl]_{SUB}$, and in the SDial pre-HDF group with 0.15 and 0.36 M $[NaCl]_{blood}$. In standard pre-HDF 1.20 M $[NaCl]_{SUB}$ and in SDial pre-HDF 0.50 M $[NaCl]_{blood}$, the WBC count decreased ($P < 0.05$) at the end of the

dialysis session. When comparing all treatments, the post-dialysis (120 min) WBC count was significantly lower for standard pre-HDF 1.20 M NaCl and SDial pre-HDF 0.50 M NaCl; both were similar between each other. The WBC count was lower for standard pre-HDF 1.20 M NaCl as compared to the physiologic ionic strength already after 60 min treatment. Both RBC and PLT counts so that Hct and tHb were constant over time for all treatments. After 15 minutes, the C5a concentrations were below the detection limit for all treatments. The TAT concentrations were constant during all dialysis treatments (range 6 to 32 µg/L).
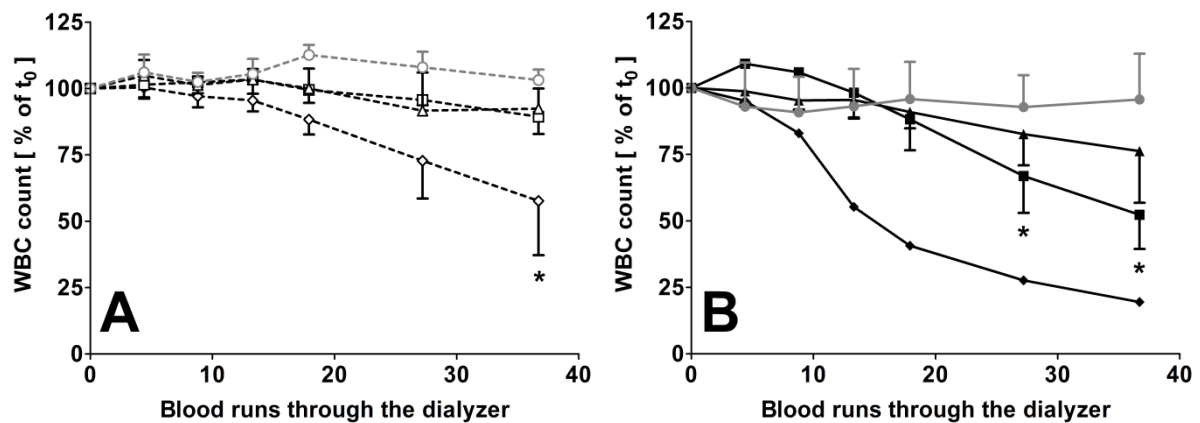
Fig. 61: *Ex vivo* WBC count in human heparinized blood during pre-dilution HDF at different [NaCl] and setups.
For both standard and SDial pre-HDF, the WBC count was decreased at the highest ionic strengths. A, standard pre-HDF with substitution fluid of 0.15 (--○--), 0.75 (--△--), 1.00 (--□--), and 1.20 M NaCl (--◇--) corresponding to $[NaCl]_{blood}$ of 0.15, 0.36, 0.36, and 0.50 M, respectively; B, SDial pre-HDF with 0.15 (--●--), 0.36 (--▲--), 0.50 (--■--), and 0.75 M $[NaCl]_{blood}$ (--◆--). Results are mean ± SD (n = 3, except for SDial pre-HDF 0.75 M NaCl (n = 1)); *, $P < 0.05$ *versus* t_0.

The dot plots of the WBC (**Fig. 62**) did not reveal any change during standard pre-HDF with 0.15 and 0.75 M $[NaCl]_{SUB}$ and during SDial pre-HDF with 0.15 and 0.36 M $[NaCl]_{blood}$. At higher $[NaCl]_{SUB}$, the monocyte and granulocyte counts decreased and dead cells increased. This phenomenon also occurred during SDial pre-HDF at higher $[NaCl]_{blood}$. The granulocyte and monocyte subpopulations completely disappeared during SDial pre-HDF with 0.50 M $[NaCl]_{blood}$ whereas few cells still were present in standard pre-HDF at 1.20 M $[NaCl]_{SUB}$.

As presented in **Fig. 63**, there was no visible change of the PLT volume histograms between 0 and 90 min of standard pre-HDF at 0.15, 0.75, and 1.00 M $[NaCl]_{SUB}$. The number of particles larger than 15 fL (corresponding to cell fragments or dead cells) increased after 45 min of standard pre-HDF at 1.20 M $[NaCl]_{SUB}$. In the SDial pre-HDF group, few of these particles were detected in the 120 min sample at 0.50 M $[NaCl]_{blood}$. Their number increased after 45 min SDial pre-HDF at 0.75 M $[NaCl]_{blood}$.
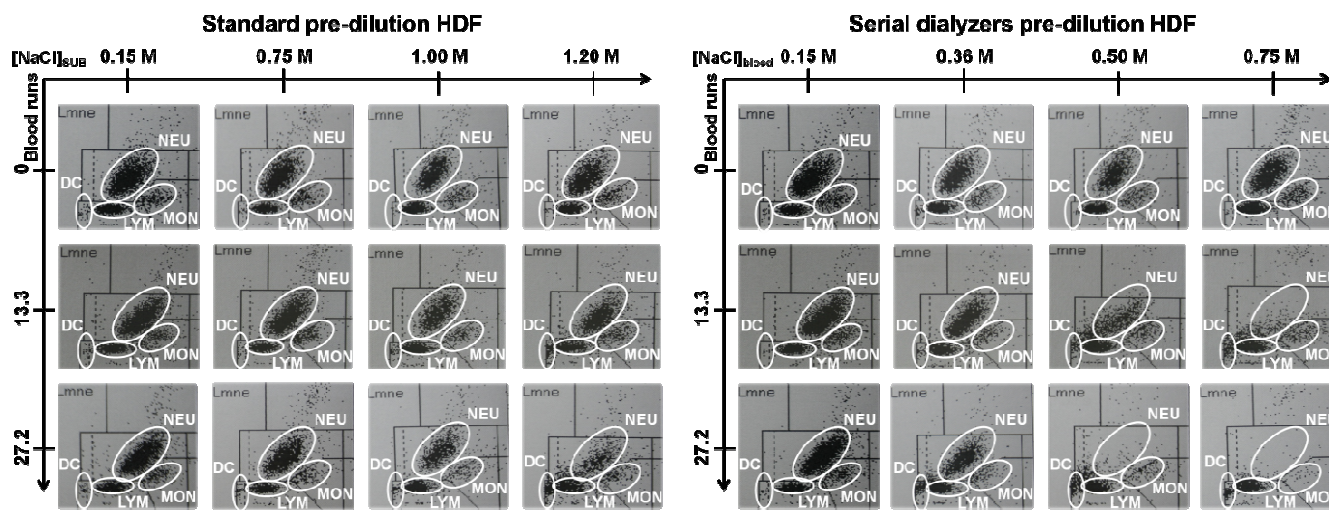
Fig. 62: Dot plots of the WBC subpopulations during pre-dilution HDF at different [NaCl] and setups.
Typical dot plots of 45 and 90 min samples compared to baseline for both dialysis setups: standard (left) and SDial pre-HDF (right). The X-axis represents the [NaCl] (standard pre-HDF, concentration in the substitution fluid; SDial pre-HDF, concentration in the blood). Four areas are highlighted: dead cells (DC, bottom left), lymphocytes (LYM, bottom middle), granulocytes (NEU, top), and monocytes (MON, bottom right).
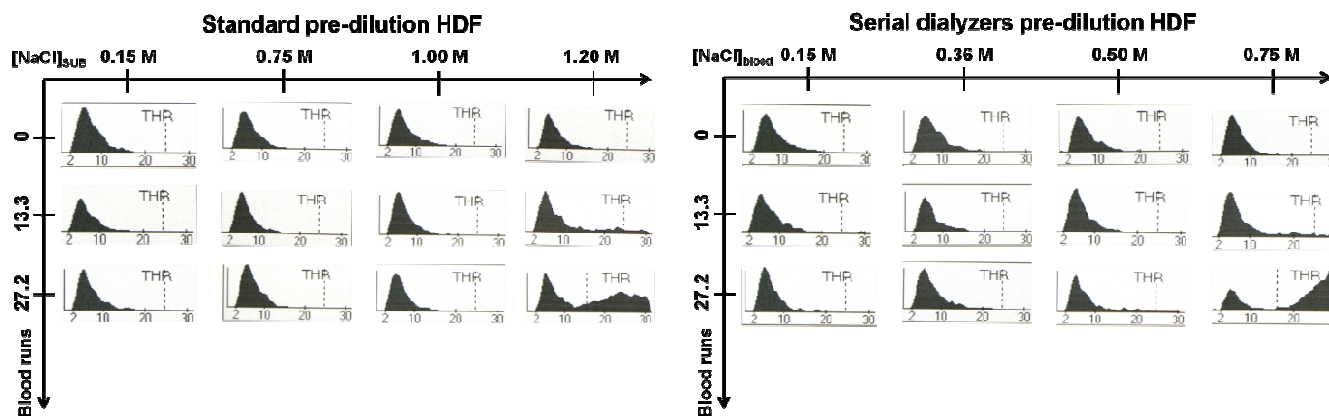
Fig. 63: Platelet volume histograms during pre-dilution HDF at different [NaCl] and setups.
Obtained during standard (left) and SDial pre-HDF (right) from samples drawn at 0, 45, and 90 min (0, 13.3, and 27.2 runs, respectively). The X-axis represents the [NaCl] (standard pre-HDF, concentration in the substitution fluid; SDial pre-HDF, concentration in the blood).
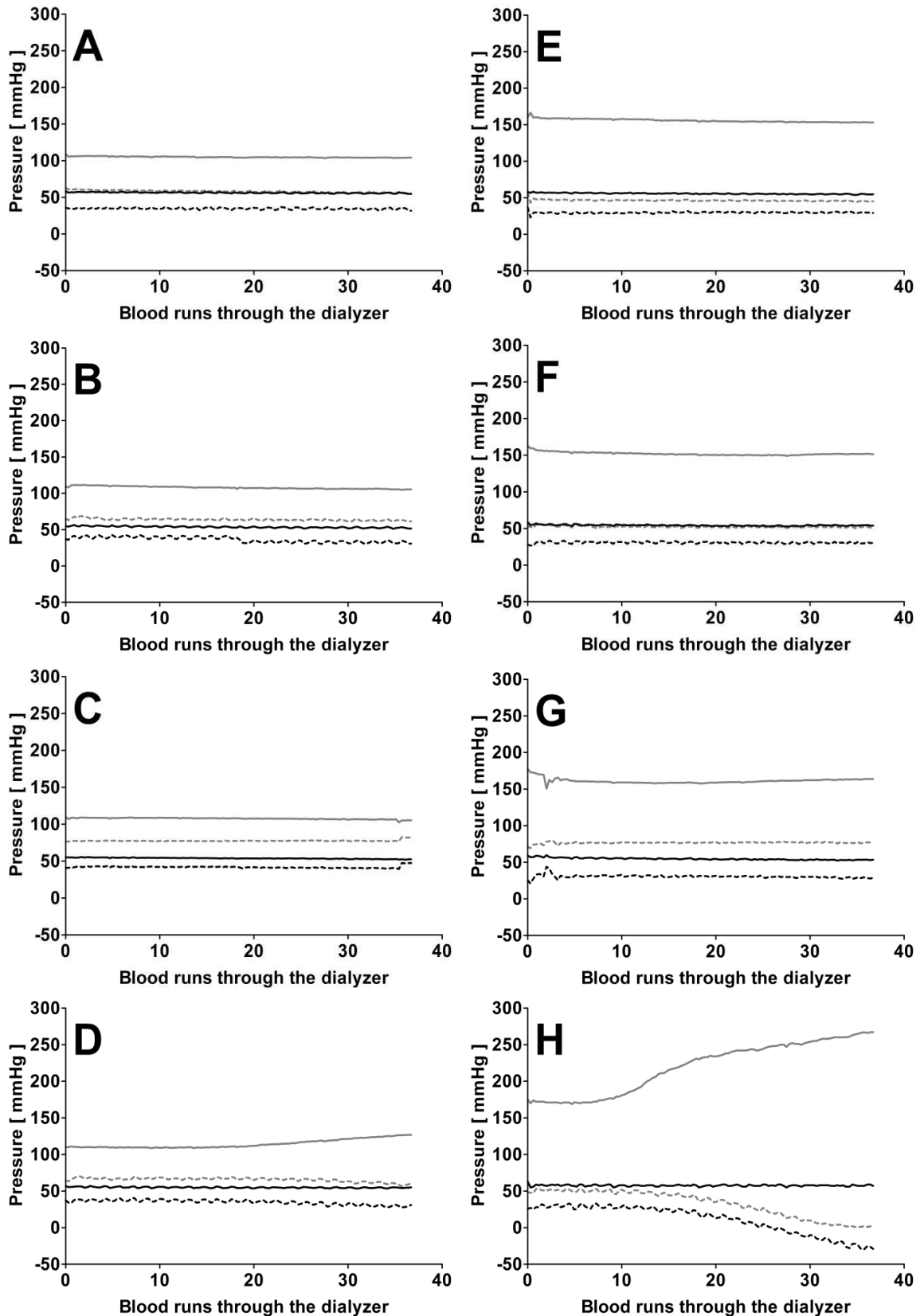
Fig. 64: Course of the online pressures during pre-dilution HDF at different [NaCl] and setups.
Results are mean (n = 3): standard pre-HDF with 0.15 (A), 0.75 (B), 1.00 (C), and 1.20 M (D) $[NaCl]_{SUB}$; SDial pre-HDF with 0.15 (E), 0.36 (F), 0.50 (G), and 0.75 M (H, n = 1) $[NaCl]_{blood}$. Pressures were measured on-line upstream the pre-dilution port (———), in the venous line (———), at the second dialyzer dialysate inlet (-----) and outlet (-----).

All pressures were constant during the experiments except for the SDial pre-HDF with 0.75 M [NaCl]$_{blood}$ (**Fig. 64**, H) and the standard pre-HDF with 1.20 M [NaCl]$_{SUB}$ (**Fig. 64**, D), in which the arterial (upstream the pre-dilution) pressure increased and dialysate pressure decreased.
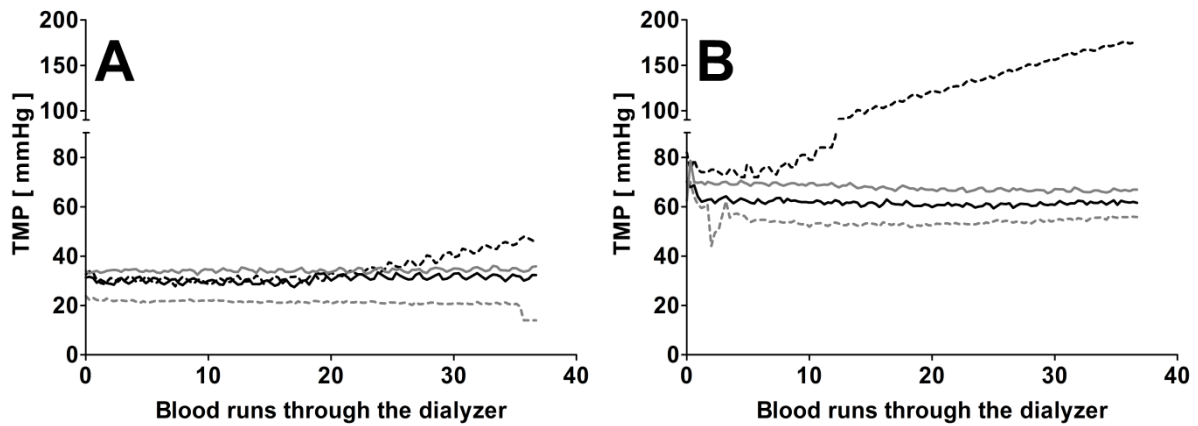
Fig. 65: Comparison of the TMP during pre-dilution HDF at different [NaCl] and setups.
Course of mean TMP (n = 3): A, standard pre-HDF with 0.15 (———), 0.75 (———), 1.00 (-----), and 1.20 M (▬▬▬▬) [NaCl]$_{SUB}$; B, SDial pre-HDF with 0.15 (———), 0.36 (———), 0.50 (-----), and 0.75 M (▬▬▬▬, n = 1) [NaCl]$_{blood}$. The TMP was lower ($P < 0.05$) in the standard pre-HDF group as compared to the serial dialyzers group.

Since the arterial pressure (upstream the pre-dilution port) was measured before the first dialyzer in the SDial pre-HDF group, the pressure was higher ($P < 0.05$) as compared to the standard pre-HDF group due to the pressure drop along the serial setup (first dialyzer: 50 mmHg, second dialyzer: 52 mmHg). During the dialysis session with the SDial setup, the pressure in between both dialyzers was not transduced. Therefore, as shown in **Fig. 65**, the TMP was higher ($P < 0.05$) in the SDial pre-HDF group. However, when considering only the second hemodialyzer of the SDial setup, the TMP was in the range 30 to 35 mmHg with both setups. [NaCl] did not have any effect on the TMP.

b. Serial dialyzers pre-dilution HDF *versus* serial dialyzers transmembrane pre-dilution HDF

In order to decrease the [NaCl] gradient between the buffered solution and blood using the serial dialyzers system (see also **Fig. 45**), the substituate line was connected to the external dialysate loop of the first dialyzer. The SDial-TM pre-HDF was compared to the SDial pre-HDF for 0.50 M [NaCl]$_{blood}$.

Temperature and pressures remained unchanged for both settings. [NaCl]$_{blood}$ and [NaCl]$_{VEN}$ were higher with the SDial-TM pre-HDF as compared to SDial pre-HDF: [NaCl]$_{blood}$, 535 ± 19 *versus* 474 ± 7 mM, $P < 0.01$; [NaCl]$_{VEN}$, 135 ± 4 *versus* 122 ± 4 mM, $P < 0.05$.
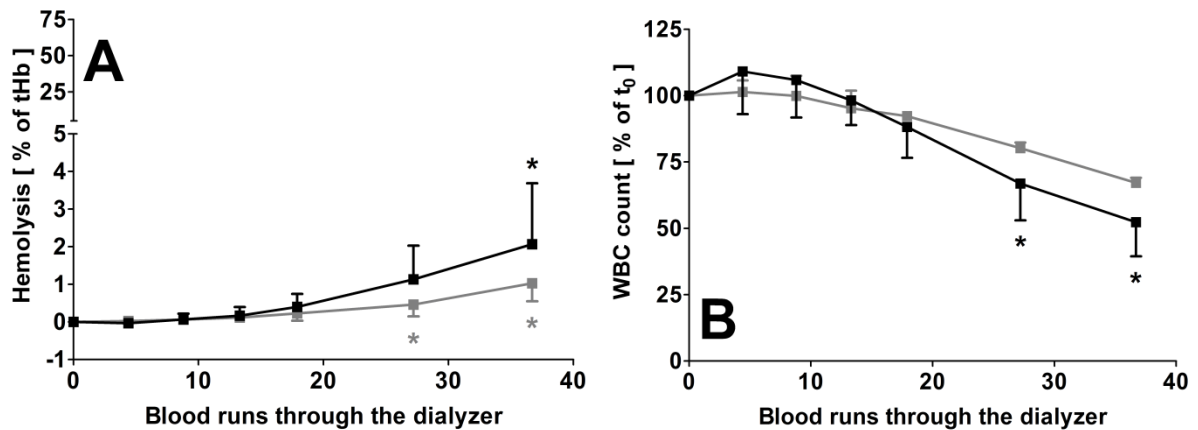
Fig. 66: Comparison of the pre-dilution mode on *ex vivo* hemocompatibility of increased ionic strength with the SDial setup.

A, hemolysis; B, WBC count. Results were obtained with the SDial pre-HDF (■) and the SDial-TM pre-HDF (■) both at 0.50 M [NaCl]$_{blood}$. Mean ± SD (n = 3); *, $P < 0.05$ *versus* t_0. Hemolysis increased at the end of the experiment for both settings, whereas the WBC count decreased only with the SDial pre-HDF.

At baseline, WBC, RBC, and PLT counts were similar ($P > 0.05$). As shown in **Fig. 66**, the hemolysis increased ($P < 0.05$) at the end of the treatment for both settings; the difference in hemolysis between both settings was not significant ($P = 0.34$) at the end of the experiment. Different to the SDial pre-HDF, the WBC count (**Fig. 66**, B) did not decrease during SDial-TM pre-HDF, although, the difference between both settings was not significant. RBC and PLT counts were steady during dialysis with both SDial pre-HDF and SDial-TM pre-HDF at 0.50 M [NaCl]$_{blood}$.
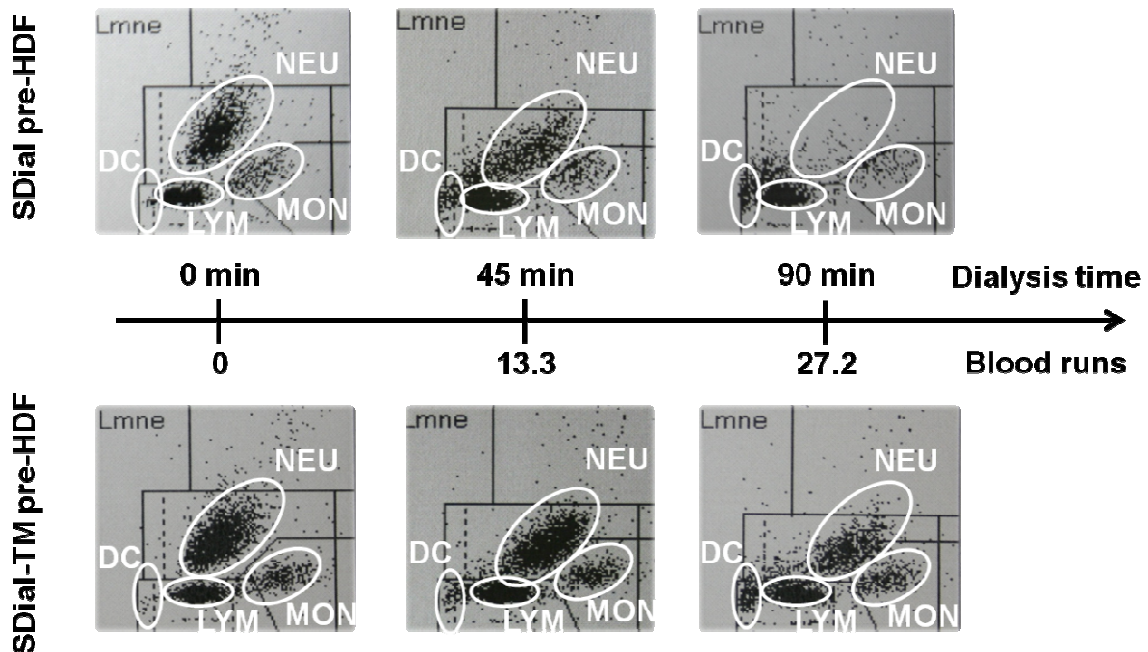
Fig. 67: Dot plots of the WBC subpopulations during different modes of pre-dilution HDF with the SDial setup.

Typical dot plots obtained at baseline, 45, and 90 min for both serial dialyzers setups at 0.50 M [NaCl]$_{blood}$: normal (top) and transmembrane (bottom) pre-dilution HDF. Four areas are highlighted: dead cells (DC, bottom left), lymphocytes (LYM, bottom middle), granulocytes (NEU, top), and monocytes (MON, bottom right).
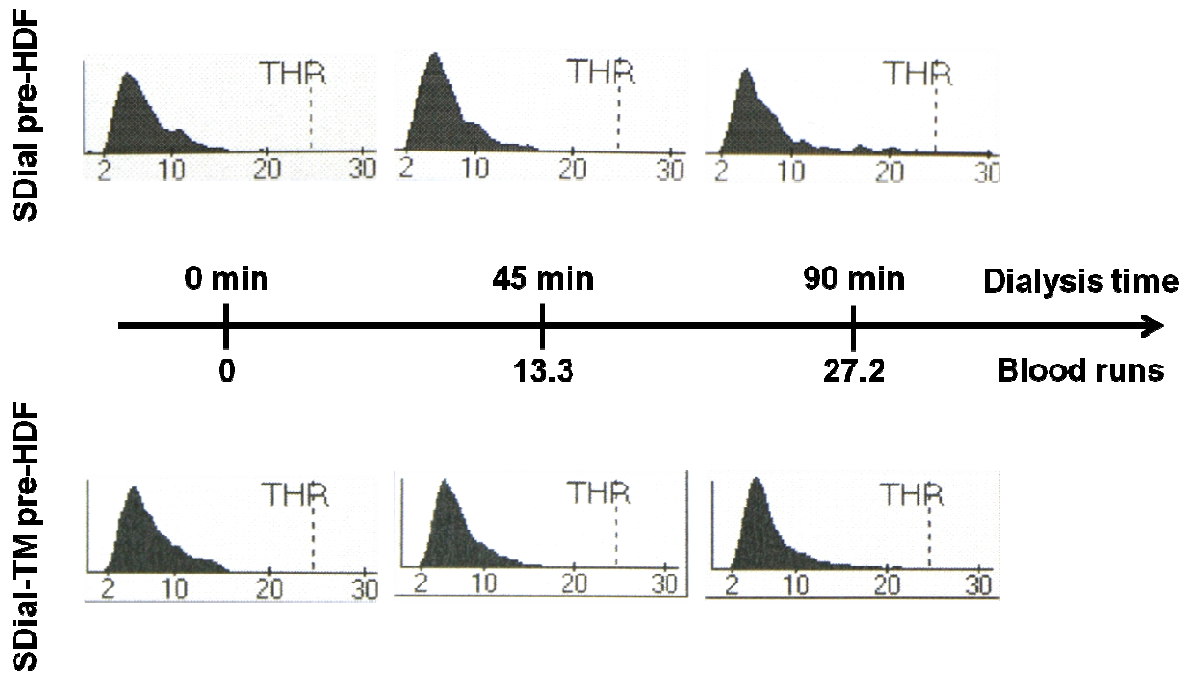
Fig. 68: Platelet volume histograms during different modes of pre-dilution HDF with the SDial setup.
Baseline, 45, and 90 min (0, 13.3, and 27.2 blood runs, respectively) samples are depicted. Normal (top) and transmembrane (bottom) pre-dilution HDF with the serial dialyzers setup at 0.50 M [NaCl]$_{blood}$.

The dot plots of the WBC (**Fig. 67**) demonstrated less loss of monocytes and granulocytes after 45 and 90 min treatment when using the SDial-TM pre-HDF. Even though the number of dead cells was still important, particles bigger than 15 fL were not observed (see **Fig. 68**).

IV.   *In vitro* toxin removal with NaCl dialysis

1) Mini-dialyzer model

a.   Effect of plasma proteins on the instantaneous clearance

The instantaneous clearance of IS was determined using the same type of mini-dialyzers and similar flow rates as for the experiments described below. Aqueous clearance was compared before and after coating of the membrane with plasma proteins; plasma clearance was compared to the aqueous clearance after membrane coating calculated from the free toxin fraction (**Eq. 12**).
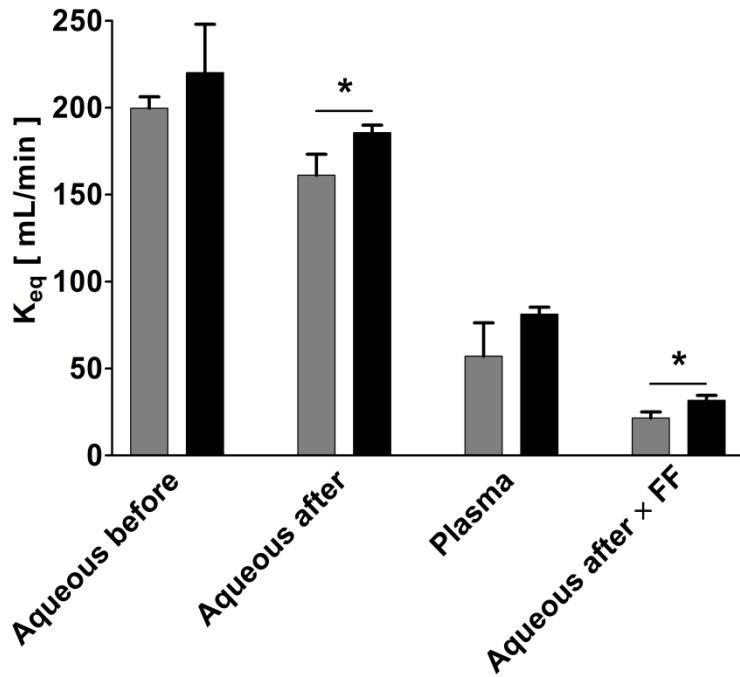
Fig. 69: Instantaneous equivalent clearance of IS in the mini-dialyzer setup.
The IS clearance was determined for $Q_{B\ eq}$ = 300 mL/min (▬) and $Q_{B\ eq}$ = 400 mL/min (▬) in aqueous solution before and after coating of the membrane with plasma proteins, in plasma and calculated from the toxin free fraction. Results are presented as mean ± SD (n = 3). Equivalence calculations referred to a membrane of 1.8 m² surface area. *, $P < 0.05$. Abbreviations: FF, free fraction; K_{eq}, equivalent instantaneous clearance.

The instantaneous clearance (**Fig. 69**) was higher ($P < 0.05$) for $Q_{B\ eq}$ = 400 mL/min compared with $Q_{B\ eq}$ = 300 mL/min. Coating of the membrane with plasma proteins decreased the aqueous IS clearance ($P < 0.05$). The plasma ($P < 0.001$) and the aqueous clearances calculated from the free toxin fraction in plasma ($P < 0.01$) were largely lower compared to the aqueous clearance.

b. **Comparison of HD, HDF, and HDF with NaCl using normal plasma**

In this experiment, the mean albumin concentration in plasma was 28.3 ± 3.7 g/L and the mean IS concentrations at the start of the dialysis were 95.0 ± 8.7 and 88.4 ± 9.6 µM for $Q_{B\ eq}$ = 300 mL/min and $Q_{B\ eq}$ = 400 mL/min, respectively.
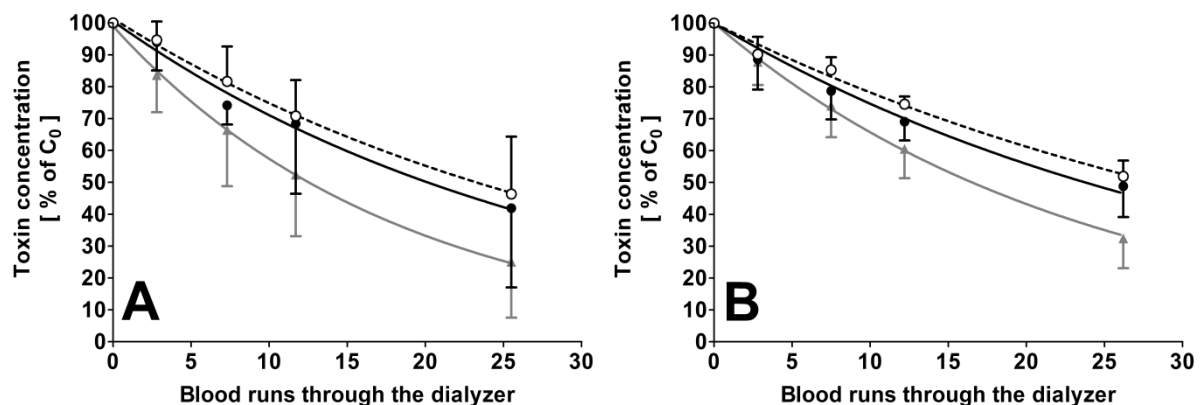
Fig. 70: *In vitro* removal of IS from normal human plasma using mini-dialyzers and different dialysis strategies.
Dialysis experiments were performed at $Q_{B\ eq}$ = 300 mL/min (A) and $Q_{B\ eq}$ = 400 mL/min (B) in HD (--O--), pre-dilution HDF with saline (—●—) and pre-dilution HDF with increased ionic strength (—▲—, infusion of 1.00 M NaCl solution). Results are presented as mean ± SD (n = 3).

As presented in **Fig. 70**, the removal rate γ of IS from plasma of healthy donors was not different between standard pre-HDF (i.e., physiological saline as substitution fluid; $\gamma = 3.7 \pm 2.1$ %/run and $\gamma = 2.9 \pm 0.4$ %/run for $Q_{B\ eq} = 300$ mL/min and $Q_{B\ eq} = 400$ mL/min, respectively) and HD ($\gamma = 3.1 \pm 1.5$ %/run and $\gamma = 2.5 \pm 0.4$ %/run for $Q_{B\ eq} = 300$ mL/min and $Q_{B\ eq} = 400$ mL/min, respectively). Compared to standard pre-HDF, the removal rate was higher using 1.00 M NaCl as substitution fluid particularly at lower Q_B ($\gamma = 6.1 \pm 2.9$ %/run and $\gamma = 4.3 \pm 1.3$ %/run for $Q_{B\ eq} = 300$ mL/min and $Q_{B\ eq} = 400$ mL/min, respectively; $P < 0.05$ and $P = 0.22$, respectively). This finding was also confirmed by the post dialysis IS concentration. For both Q_B, it was lower when using 1.00 M NaCl as substitution fluid compared to the other treatments ($P < 0.05$ and $P < 0.01$ for $Q_{B\ eq} = 300$ mL/min and $Q_{B\ eq} = 400$ mL/min, respectively).

c. <u>Removal rates in uremic and normal plasma</u>

The efficacy of dialysis with increased ionic strength was tested in uremic plasma. At the beginning of the experiments, the IS concentrations of normal and uremic plasma were similar being 98.3 ± 5.4 and 105.8 ± 13.6 µM, respectively. The pCS concentration in normal plasma was lower ($P < 0.05$) compared to uremic plasma (119.0 ± 5.4 *versus* 139.0 ± 6.4 µM, respectively). No difference was seen between the pre- and post-dialysis albumin concentrations: 38.9 ± 0.5 *versus* 34.2 ± 3.3 g/L in normal plasma and 35.1 ± 4.0 *versus* 35.3 ± 4.8 g/L in uremic plasma.
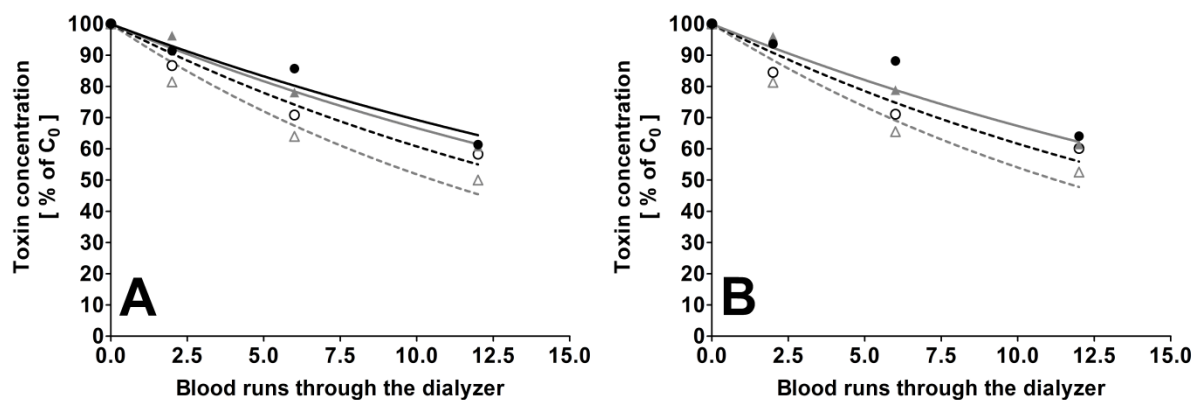
Fig. 71: *In vitro* removal of uremic toxins in normal and uremic human plasma using mini-dialyzers.
The experiment was performed at $Q_{B\ eq} = 300$ mL/min; removal of IS (A) and pCS (B) was determined in normal (●, ○) and uremic plasma (▲, △) at 0.15 (solid lines) and 0.36 M NaCl (dotted lines). Results are presented as means (n = 3).

When switching the substitution fluid from saline to 1.00 M NaCl solution (plasma [NaCl] = 0.36 M), the IS removal rate during HDF using mini-dialyzers did not significantly increase neither in plasma of healthy individuals (3.8 ± 1.9 *versus* 5.0 ± 0.4 %/run; $P = 0.36$) nor in plasma of ESRD patients (4.5 ± 3.1 *versus* 6.6 ± 1.3 %/run; $P = 0.20$). Additionally, at similar [NaCl]$_{SUB}$, the removal rate of IS was not different ($P > 0.05$) between plasma from healthy

and uremic individuals. No difference between physiological and increased ionic strength was found in the post-dialysis IS concentration in both normal and uremic plasma. Similar results were obtained for pCS: in normal plasma, $\gamma = 3.37 \pm 1.56$ %/run and $\gamma = 4.85 \pm 0.79$ %/run with infusion of saline and 1.00 M NaCl, respectively; in uremic plasma, $\gamma = 4.33 \pm 3.04$ %/run and $\gamma = 6.20 \pm 1.19$ %/run with infusion of saline and 1.00 M NaCl, respectively.
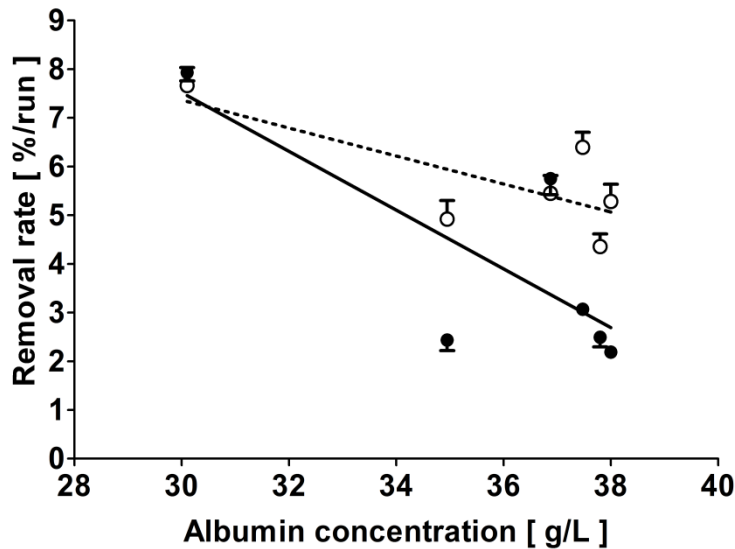
Fig. 72: Comparison of the removal rate of uremic toxins *versus* **the albumin concentration.**
The mean removal rate of IS and pCS is plotted *versus* the albumin concentration (mean pre-post dialysis) for plasma [NaCl] of 0.15 (●) and 0.36 M (○). Regression coefficients are: 0.15 M NaCl, $r^2 = 0.61$; 0.36 M NaCl, $r^2 = 0.52$.

In this experiment comparing the removal of IS and pCS between normal and uremic plasma, the toxin removal rate (**Fig. 72**) did not correlate with the albumin concentration ($r^2 = 0.61$, $P = 0.07$, and $r^2 = 0.55$, $P = 0.09$, for [NaCl] = 0.15 and 0.36 M, respectively).

d. <u>Complete removal of IS and *p*CS with HDF</u>

It can argued that protein bound molecules cannot be fully removed during dialysis because of the protein binding even after a very long treatment. In order to assess complete removal of IS and pCS from native uremic plasma, an experiment was performed using a mini-dialyzer in HDF modus with infusion of 1.00 M NaCl.
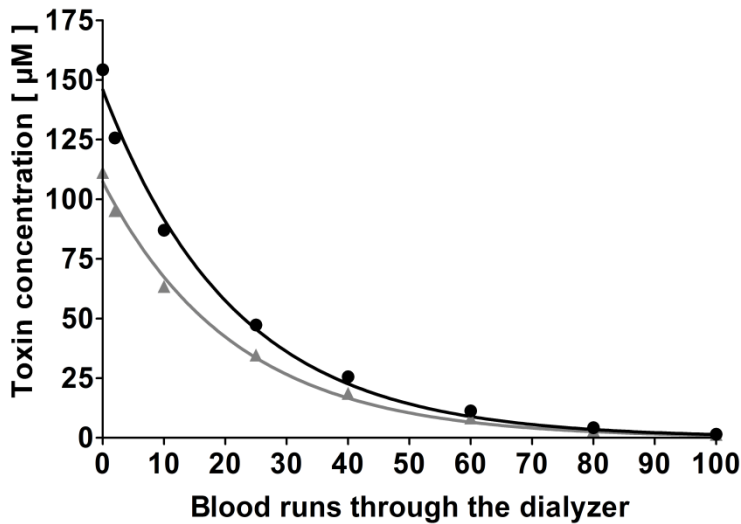
Fig. 73: *In vitro* removal of IS and *p*CS from uremic plasma. IS (—●—) and *p*CS (—▲—) concentrations during a pilot pre-dilution HDF experiment (n = 1) with infusion of 1.00 M NaCl are shown. Toxin concentrations decreased exponentially over time and reached 0 after 100 blood runs.

Both IS and *p*CS were removed completely from uremic plasma *in vitro* during extended dialysis (about 9 h, i.e., 100 blood runs through the dialyzer). The corresponding removal rates were 4.66 %/run for both toxins.

e. Single- *versus* serial-hemodialysis

In order to quantify the removal rate of IS when using two serial dialyzers, an experiment was performed comparing single and serial HD in plasma of healthy individuals.
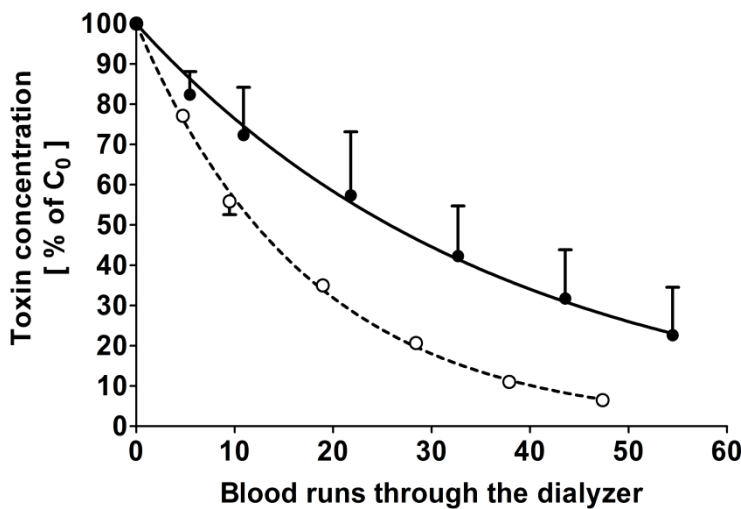
Fig. 74: *In vitro* removal of IS in normal human plasma using single or serial hemodialysis. Comparison between single HD (—●—) and serial HD (--○--), mean ± SD (n = 2).

In normal plasma, the removal rate of IS with serial HD (γ = 5.72 ± 0.21 %/run) was about twice the one of single HD (γ = 2.81 ± 1.09 %/run).

2) <u>Comparative toxin removal with the dialysis machine</u>

The *in vitro* removal of IS from normal human plasma during pre-dilution HDF with a dialysis machine preparing online substitution fluid was studied using different setups and different $[NaCl]_{blood}$: standard pre-HDF with 0.15 and 0.50 M $[NaCl]_{blood}$, SDial pre-HDF with 0.15 and 0.50 M $[NaCl]_{blood}$ or SDial pre-HDF with a charcoal adsorber and 0.15 M $[NaCl]_{blood}$.

The temperature during dialysis was similar for all treatments and in the range of 36.0 ± 0.7 to 36.5 ± 0.1 °C. Blood and venous [NaCl] were higher ($P < 0.001$) when using increased ionic strength HDF as compared to isotonic HDF (**Tab. 17**).

Setting	$[NaCl]_{blood}$ [mM]	$[NaCl]_{VEN}$ [mM]
Standard pre-HDF 0.15 M	126 ± 1	126 ± 1
Standard pre-HDF 0.50 M	477 ± 23 [*]	132 ± 2 [*]
SDial pre-HDF 0.15 M	126 ± 0	126 ± 0
SDial pre-HDF 0.15 M + charcoal	125 ± 1	126 ± 0
SDial pre-HDF 0.50 M	485 ± 8 [*]	131 ± 1 [*]

Tab. 17: [NaCl] during different dialysis treatments.
Concentrations are given in [mM] as mean ± SD (n = 3). Abbreviations: $[NaCl]_{blood}$, NaCl concentration in blood with increased ionic strength (standard pre-HDF: downstream the pre-dilution; SDial: second dialyzer blood inlet); $[NaCl]_{VEN}$, NaCl concentration in the venous line (blood downstream the second dialyzer). [*], $P < 0.001$ *versus* standard pre-HDF 0.15 M, SDial pre-HDF 0.15 M, and SDial pre-HDF 0.15 M + charcoal.

The IS concentration at the beginning of the dialysis experiments were similar for each setting being in the range of 65 to 74 µM. As presented in **Fig. 75**, the removal rate of IS normalized to the blood runs through the dialyzer was increased in both standard and SDial pre-HDF with increased $[NaCl]_{blood}$ ($P < 0.001$). Both standard and serial dialyzers setups yielded similar results. The presence of a charcoal adsorber within the closed dialysate loop of the first hemodialyzer did not increase the removal rate of IS.
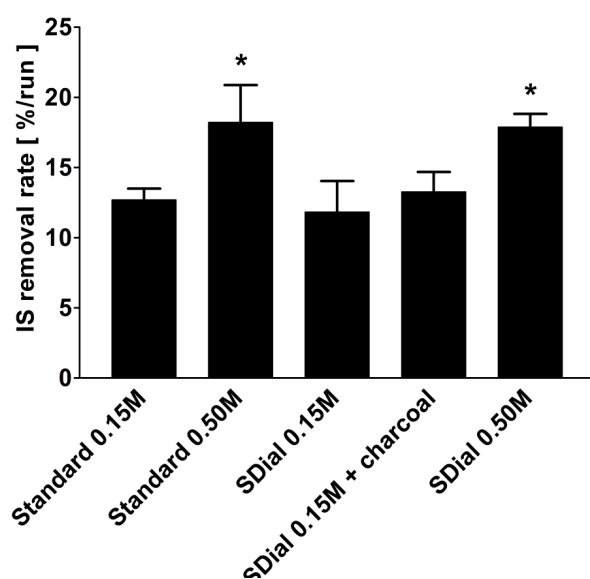
Fig. 75: *In vitro* removal rate of IS in normal human plasma on a dialysis machine.
Increasing the ionic strength significantly increased the IS removal rate. Different settings of pre-dilution HDF and $[NaCl]_{blood}$: standard pre-HDF with 0.15 or 0.50 M NaCl, SDial pre-HDF with 0.15 and 0.50 M NaCl, and SDial pre-HDF with charcoal adsorber and 0.15 M NaCl. Mean ± SD (n = 9); *, $P < 0.001$ *versus* standard 0.15 M NaCl, SDial 0.15 M, and SDial 0.15 M + charcoal. The removal rate is expressed in %/run.

V.   Animal model

1) Ovine RBC resistance to increased ionic strength

a.   Resistance under static conditions

Blood from 4 sheep was incubated at different ionic strengths as performed with human blood (see **Fig. 46**). As shown in **Fig. 76**, hemolysis increased with $[NaCl]_{blood} > 0.50$ M under static conditions in both human and ovine blood. Furthermore, hemolysis at 0.35, 0.60, and 0.75 M NaCl was higher ($P < 0.05$) in human blood as compared to ovine blood.
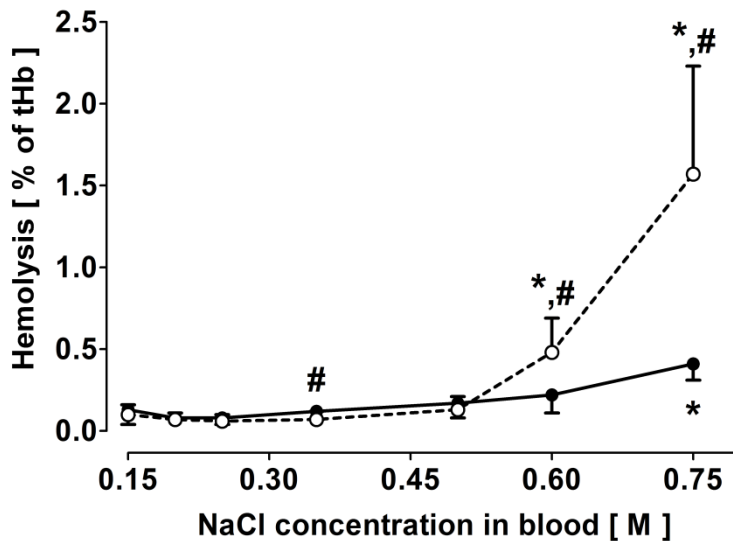
Fig. 76: Static *in vitro* resistance of human and ovine erythrocytes to increased [NaCl].
Results are mean ± SD from experiments in human (–O–, n = 21; same data as presented in **Fig. 46**) and sheep (–●–, n = 4) blood. *, $P < 0.001$ *versus* 0.15 M NaCl; #, $P < 0.05$ *versus* sheep.

b.   Resistance under dynamic conditions

Human and ovine RBC resistance to osmotic changes was also studied under dynamic conditions using a mini-dialyzer system with infusion of either 0.15 or 1.20 M NaCl solution. $[NaCl]_{VEN}$ resulting from infusion of saline was 134 ± 1 and 130 ± 5 mM in ovine and human blood, respectively, whereas infusion of 1.20 M NaCl led to 354 ± 10 and 503 ± 24 mM, respectively. Infusion of saline yielded $[NaCl]_{ART}$ of 141 ± 1 and 140 ± 0 mM in ovine and human blood, respectively, whereas infusion of 1.20 M NaCl resulted in 618 ± 12 and 687 ± 22 mM, respectively.

As presented in **Fig. 77**, hemolysis did not increase during dialysis with infusion of saline in both human and ovine blood. On the opposite, hemolysis occurred when infusing 1.20 M NaCl solution with a trend to being higher in ovine blood as compared to human blood (at 180 min 13.7 ± 2.0% and 10.7 ± 3.6%, respectively). However, the difference was not significant ($P = 0.41$, n = 2).
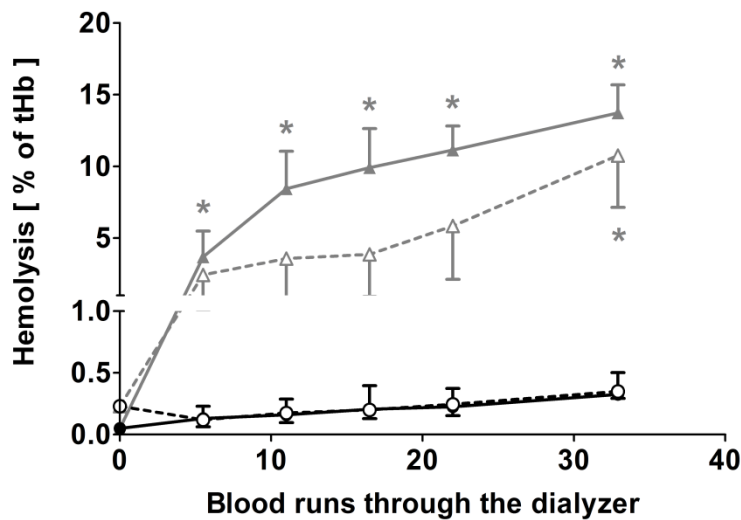
Fig. 77: *Ex vivo* hemolysis rate in human and ovine blood under dynamic conditions.
The hemolysis rate was studied during pre-dilution HDF with either infusion of saline (●—, --○--) or 1.20 M NaCl solution (▲—, --△--) in human (dotted line) and ovine (solid line) blood. Mean ± SD (n = 2); *, $P < 0.05$ *versus* t_0. Hemolysis in ovine blood was significantly increased after 5 blood runs.

2) *In vivo* dialysis experiments

The biocompatibility of increased ionic strength during modified HDF was studied during 2 hours on four female Merino sheep (mean weight 42.8 ± 3.0 kg, n = 4) using standard pre-HDF with 0.36 and 0.45 M [NaCl]$_{blood}$ (corresponding to [NaCl]$_{SUB}$ of 0.75 and 1.10 M, respectively) and SDial-TM pre-HDF with 0.36 and 0.60 M [NaCl]$_{blood}$.
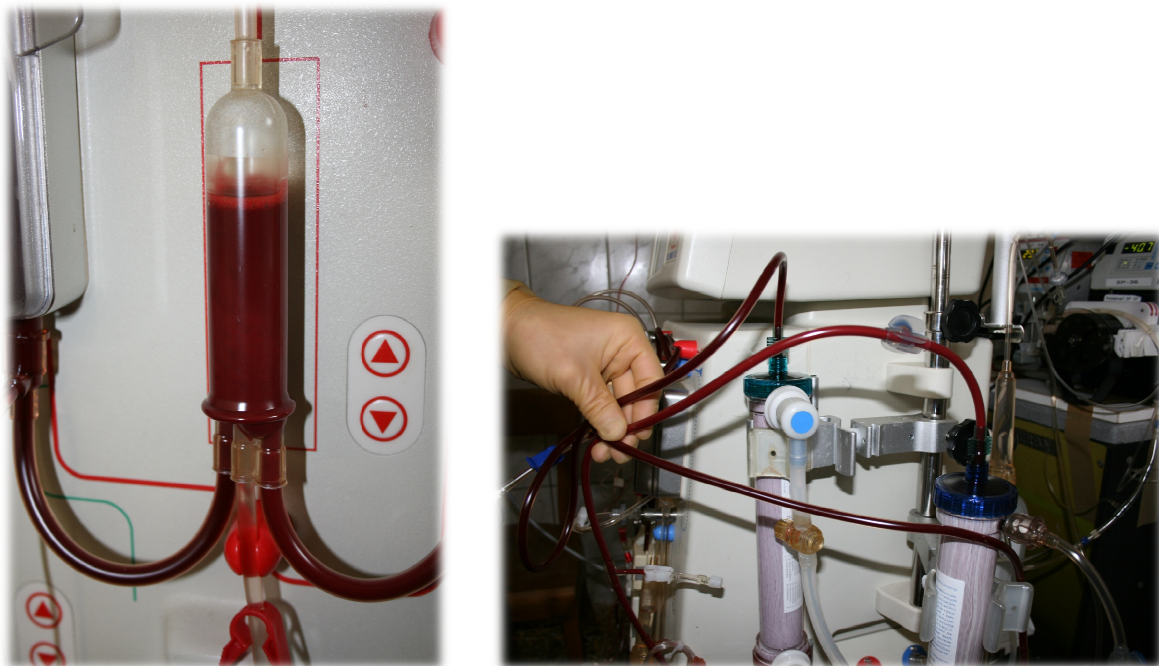
Fig. 78: Visual effects of increased ionic strength HDF in the extracorporeal circuit during the animal experiments.
Left: standard pre-HDF; arterial mixing chamber (pre-dilution position) of blood and modified substitution fluid; blood flew direction from left to right. Right: SDial setup (bottom, arterial line; middle, between dialyzers; top, venous line). Change of blood coloration from dark to light red after infusion of NaCl.

As presented in **Tab. 18**, arterial and venous pH, partial pressure of arterial pO_2 and pCO_2, venous K^+ concentration, and arterial and venous HCO_3^- concentration were constant during all dialysis treatments while increasing the ionic strength in blood. In all settings, arterial K^+ concentration decreased ($P < 0.01$) compared to baseline. Arterial Ca^{2+} concentration was constant over time. Venous Ca^{2+} concentration decreased ($P < 0.05$) and $[NaCl]_{blood}$ increased. [NaCl] was constant in arterial blood over the treatment for all settings (see **Tab. 19**). The $[NaCl]_{blood}$ downstream of the substitution fluid was in the expected range. For all settings, $[NaCl]_{VEN}$ increased ($P < 0.05$) together with the ionic strength of the substitution fluid. Increased ionic strength led to a change of the blood coloration into light red (arterial and venous line: dark red) (**Fig. 78**). Interestingly, downstream the pre-dilution (BM) the proportion of oxy- and deoxyhemoglobin (O_2Hb and HHb, respectively) significantly changed when increasing the ionic strength with the standard pre-HDF at 0.36 M $[NaCl]_{blood}$ (**Tab. 20**).

Setting		Standard pre-HDF 0.36 M [NaCl]blood (0.75 M [NaCl]SUB)				Standard pre-HDF 0.45 M [NaCl]blood (1.10 M [NaCl]SUB)				SDial-TM pre-HDF 0.36 M [NaCl]blood				SDial-TM pre-HDF 0.60 M [NaCl]blood			
Time [min]		0	30	60	120	0	30	60	120	0	30	60	120	0	30	60	120
pH	ART	7.46 ± 0.02	7.48 ± 0.02	7.48 ± 0.02	7.49 ± 0.02	7.47 ± 0.01	7.46 ± 0.05	7.49 ± 0.01	7.48 ± 0.01	7.45 ± 0.03	7.45 ± 0.02	7.46 ± 0.03	7.47 ± 0.03	7.46 ± 0.02	7.48 ± 0.02	7.49 ± 0.01	7.47 ± 0.02
	VEN	-	7.36 ± 0.03	7.34 [b] ± 0.03	7.35 ± 0.02	-	7.35 ± 0.03	7.35 ± 0.02	7.35 ± 0.02	-	7.35 ± 0.02	7.33 [b] ± 0.03	7.34 ± 0.02	-	7.37 ± 0.02	7.32 [b] ± 0.02	7.33 [b] ± 0.00
pO$_2$ [mmHg]	ART	54.0 ± 7.0	44.0 ± 2.5	44.1 ± 4.9	43.5 ± 4.6	47.9 ± 5.3	43.8 ± 13.0	42.7 ± 2.3	40.5 ± 7.5	65.2 ± 11.5	43.2 [a] ± 1.8	46.7 [a] ± 0.8	43.5 [a] ± 1.3	51.0 ± 8.2	43.2 ± 2.6	43.5 ± 8.5	43.2 ± 3.0
pCO$_2$ [mmHg]	ART	38.5 ± 3.5	39.1 ± 3.6	38.7 ± 3.3	38.6 ± 2.6	41.8 ± 0.9	45.4 ± 5.3	41.9 ± 1.8	42.5 ± 2.3	41.3 ± 4.4	41.5 ± 4.0	40.6 ± 3.9	41.9 ± 4.3	41.4 ± 2.2	41.5 ± 1.5	42.5 ± 2.6	42.7 ± 1.6
HCO$_3^-$ [mM]	ART	26.6 ± 2.6	28.5 ± 1.6	28.2 ± 1.5	28.7 [a] ± 1.3	29.5 ± 0.9	31.1 [a] ± 0.2	30.6 ± 0.7	30.4 ± 0.8	27.7 ± 2.3	28.1 ± 2.3	27.9 [§] ± 1.9	29.3 [a] ± 1.8	28.8 ± 0.8	30.6 [a] ± 1.4	31.2 [a] ± 1.5	30.5 [a] ± 0.7
	VEN	-	30.4 ± 0.8	31.0 ± 0.8	30.7 ± 0.6	-	31.0 ± 0.7	31.4 ± 0.3	31.3 ± 0.6	-	29.9 ± 0.9	30.5 ± 0.6	30.5 ± 0.6	-	31.2 ± 0.6	31.6 ± 0.3	31.6 ± 0.2
K$^+$ [mM]	ART	4.26 ± 0.41	3.62 [a] ± 0.32	3.58 [a] ± 0.26	3.64 [a] ± 0.22	4.24 ± 0.60	3.40 [a] ± 0.48	3.49 [a] ± 0.35	3.48 [a] ± 0.38	4.11 ± .033	3.45 [a] ± 0.10	3.53 [a] ± 0.21	3.40 [a] ± 0.10	4.20 ± 0.25	3.43 [a] ± 0.26	3.38 [a] ± 0.28	3.40 [a] ± 0.22
	VEN	-	2.01 ± 0.10	2.03 ± 0.08	2.3 ± 0.08	-	2.02 ± 0.03	2.02 ± 0.03	2.01 ± 0.03	-	2.06 ± 0.09	2.03 ± 0.07	2.02 ± 0.09	-	2.01 ± 0.04	2.00 ± 0.05	1.95 ± 0.12
Ca^{2+} [mM]	ART	1.21 ± 0.10	1.19 ± 0.09	1.19 ± 0.06	1.16 ± 0.06	1.13 ± 0.09	1.10 ± 0.04	1.09 ± 0.04	1.08 ± 0.04	1.20 ± 0.06	1.20 ± 0.06	1.20 ± 0.07	1.17 ± 0.08	1.14 ± 0.06	1.13 ± 0.07	1.11 ± 0.07	1.08 ± 0.08
	VEN	-	1.13 ± 0.05	1.09 [b] ± 0.04	1.07 [b] ± 0.03	-	1.11 ± 0.01	1.06 [b] ± 0.01	1.06 [b] ± 0.01	-	1.13 ± 0.06	1.09 [b] ± 0.04	1.08 [b] ± 0.04	-	1.13 ± 0.05	1.07 ± 0.02	1.04 [b] ± 0.01

Tab. 18: Blood gas analyses and electrolyte concentrations during modified HDF in the animal model.

The [NaCl] was increased after a 30 min baseline period. The presented parameters were constant when [NaCl] was increased. Abbreviations: pO$_2$, dioxygen partial pressure; pCO$_2$, carbon dioxide partial pressure. Results are mean ± SD (n = 4); [a], $P < 0.05$ *versus* 0 min; [b], $P < 0.05$ *versus* 30 min; [§], $P < 0.05$ *versus* SDial-TM pre-HDF 0.60 M NaCl.

Setting		Standard pre-HDF 0.36 M [NaCl]$_{blood}$ (0.75 M [NaCl]$_{SUB}$)				Standard pre-HDF 0.45 M [NaCl]$_{blood}$ (1.10 M [NaCl]$_{SUB}$)				SDial-TM pre-HDF 0.36 M [NaCl]$_{blood}$				SDial-TM pre-HDF 0.60 M [NaCl]$_{blood}$			
Time [min]		0	30	60	120	0	30	60	120	0	30	60	120	0	30	60	120
Na$^+$ [mM]	ART	143.6 ± 4.4	143.0 ± 3.8	143.2 ± 3.7	141.9 ± 4.4	143.5 ± 1.7	141.6 ± 1.8	142.6 ± 1.5	142.3 ± 1.6	144.0 ± 3.9	142.8 ± 3.7 [a]	142.4 ± 3.9 [a]	142.0 ± 4.1 [a]	145.3 ± 2.7	143.9 ± 3.0	145.9 ± 4.6	145.3 ± 4.9
	BM	-	138.8 ± 4.6	392.4 ± 15.1 [b]	383.4 ± 14.8 [b]	-	139.0 ± 1.3	501.8 [#] ± 6.0 [b]	498.7 [#] ± 17.6 [b]	-	138.6 ± 3.9	385.2 ± 14.0 [b]	387.9 ± 4.0 [b]	-	141.7 ± 3.1	647.1 [$] ± 15.8 [b]	649.9 [$] ± 11.8 [b]
	VEN	-	137.3 ± 3.4	141.1 ± 3.3 [b]	140.5 ± 3.1 [b]	-	138.5 ± 1.2	143.3 ± 1.2 [b]	143.1 ± 1.1 [b]	-	137.3 ± 3.2	140.9 ± 3.0 [b]	140.3 ± 3.3 [b]	-	139.3 ± 2.3	148.9 ± 6.3 [b]	146.7 ± 4.0 [b]
Cl$^-$ [mM]	ART	110.3 ± 3.1	109.6 ± 2.9	110.3 ± 2.6	110.0 ± 2.4	107.3 ± 1.1	106.7 ± 1.6	108.0 ± 0.6	108.6 ± 0.6	110.3 ± 1.4	110.2 ± 0.8	110.1 ± 0.7	109.2 ± 1.2	108.5 ± 1.3	109.3 ± 1.3	109.9 ± 1.6	110.1 ± 1.1
	BM	-	109.8 ± 2.5	348.1 ± 12.8 [b]	340.6 ± 13.3 [b]	-	107.7 ± 1.0	454.4 [#] ± 5.6 [b]	450.7 [#] ± 17.6 [b]	-	110.2 ± 1.0	342.4 ± 9.8 [b]	344.8 ± 3.9 [b]	-	109.4 ± 0.8	586.3 [$] ± 14.5 [b]	588.5 [$] ± 14.5 [b]
	VEN	-	104.5 ± 2.2	107.3 ± 2.2 [b]	107.5 ± 1.8 [b]	-	103.1 ± 0.6	107.7 ± 0.5 [b]	107.6 ± 0.6 [b]	-	104.7 ± 1.9 [b]	107.3 ± 2.0 [b]	107.1 ± 2.2 [b]	-	104.6 ± 1.7	111.9 ± 5.0 [b]	110.5 ± 2.5 [b]

Tab. 19: Sodium and chloride concentration during modified HDF in the animal model.

The [NaCl] was increased after a 30 min baseline period. Both Na$^+$ and Cl$^-$ concentrations were constant in arterial blood whereas they increased ($P < 0.05$) in venous blood when the ionic strength was increased in the blood stream; the venous Na$^+$ and Cl$^-$ concentrations did not differ significantly between the different treatments at 60 and 120 min dialysis. Abbreviations: ART, arterial line ; BM, between hemodialyzers (downstream the pre-dilution) ; VEN, venous line. Results are mean ± SD (n = 4); [a], $P < 0.05$ versus 0 min; [b], $P < 0.05$ versus 30 min; [$], $P < 0.001$ versus all other treatments; [#], $P < 0.001$ versus standard pre-HDF 0.36 M [NaCl]$_{blood}$ and SDial-TM pre-HDF 0.36 M [NaCl]$_{blood}$.

Setting		Standard pre-HDF 0.36 M [NaCl]$_{blood}$ (0.75 M [NaCl]$_{SUB}$)				Standard pre-HDF 0.45 M [NaCl]$_{blood}$ (1.10 M [NaCl]$_{SUB}$)				SDial-TM pre-HDF 0.36 M [NaCl]$_{blood}$				SDial-TM pre-HDF 0.60 M [NaCl]$_{blood}$			
Time [min]		0	30	60	120	0	30	60	120	0	30	60	120	0	30	60	120
O$_2$Hb [%]	ART	73.4 ± 8.6	58.7 ± 8.1	61.1 ± 10.2	63.8 ± 13.0	71.2 ± 1.8	63.3 ± 16.0	64.8 ± 6.1	59.7 ± 9.2	82.1 ± 10.3	57.0 ± 6.1 [a]	64.2 ± 6.4 [a]	60.4 ± 8.8 [a]	77.4 ± 8.4	63.4 ± 5.4	58.7 ± 4.8	65.6 ± 8.9
	BM	-	89.4 ± 4.2	63.5 ± 3.4 [b]	68.4 ± 9.5 [b]	-	83.2 ± 10.1	82.7 ± 3.8	72.0 ± 9.6	-	77.3 ± 10.2	81.7 ± 6.3	71.0 ± 6.9 [c]	-	83.5 ± 11.5	70.7 ± 6.6	78.4 ± 12.2
	VEN	-	73.9 ± 7.7	70.1 ± 10.6	71.2 ± 12.2	-	76.3 ± 12.7	78.9 ± 3.1	74.2 ± 5.9	-	78.5 ± 5.8	73.5 ± 4.6	71.6 ± 5.3	-	77.9 ± 6.6	71.6 ± 1.6	71.2 ± 3.1
COHb [%]	ART	1.8 ± 0.2	1.8 ± 0.1	1.7 ± 0.2	1.7 ± 0.2	1.7 ± 0.1	1.6 ± 0.2	1.7 ± 0.1	1.6 ± 0.2	1.3 ± 1.2	1.5 ± 0.1	1.8 ± 0.3	1.7 ± 0.3	1.7 ± 0.2	1.7 ± 0.1	1.6 ± 0.2	1.7 ± 0.2
	BM	-	2.1 ± 0.0	1.6 ± 0.0	1.7 ± 0.3	-	1.9 ± 0.1	1.7 ± 0.3	1.8 ± 0.1	-	2.0 ± 0.5	1.8 ± 0.3	1.8 ± 0.5	-	1.9 ± 0.1	1.6 ± 0.1 [b]	1.6 ± 0.1 [b]
	VEN	-	1.9 ± 0.1	1.8 ± 0.2	2.0 ± 0.1	-	1.9 ± 0.2	1.9 ± 0.1	1.8 ± 0.2	-	1.9 ± 0.3	1.9 ± 0.2	1.9 ± 0.3	-	1.8 ± 0.1	1.8 ± 0.1	1.7 ± 0.2
MetHb [%]	ART	0.9 ± 0.2	1.0 ± 0.0	1.0 ± 0.1	0.9 ± 0.2	0.8 ± 0.1	0.9 ± 0.1	0.9 ± 0.1	0.9 ± 0.2	0.7 ± 0.2	1.0 ± 0.1	0.9 ± 0.1	0.9 ± 0.1	0.8 ± 0.1	1.0 ± 0.0	1.0 ± 0.1	0.8 ± 0.2
	BM	-	0.4 ± 0.0	1.1 ± 0.0 [b]	1.0 ± 0.2 [b]	-	0.6 ± 0.1	0.8 ± 0.1 [b]	0.9 ± 0.1 [b]	-	0.7 ± 0.1	0.8 ± 0.1	0.9 ± 0.2	-	0.6 ± 0.2	1.0 ± 0.3	1.0 ± 0.1
	VEN	-	0.8 ± 0.1	0.9 ± 0.2	0.8 ± 0.1	-	0.8 ± 0.2	0.7 ± 0.1	0.8 ± 0.1	-	0.7 ± 0.2	0.8 ± 0.1	0.9 ± 0.1	-	0.8 ± 0.2	0.9 ± 0.1	0.8 ± 0.1
HHb [%]	ART	24.0 ± 8.6	41.9 ± 13.8	36.2 ± 10.3	33.6 ± 13.1	26.4 ± 1.8	34.3 ± 16.1	32.7 ± 6.1	37.8 ± 9.3	15.3 ± 10.3	40.4 ± 6.5 [a]	33.0 ± 6.6 [a]	37.0 ± 9.0 [a]	20.2 ± 8.3	34.0 ± 5.5	38.7 ± 5.0	31.9 ± 8.9
	BM	-	8.1 ± 4.2	33.8 ± 3.5 [b]	28.9 ± 9.5 [b]	-	14.4 ± 10.1	14.9 ± 3.8	25.3 ± 9.5	-	20.0 ± 10.5	15.7 ± 6.4	26.3 ± 7.1 [c]	-	14.0 ± 11.4	26.6 ± 6.5	19.1 ± 12.0
	VEN	-	23.3 ± 7.7	27.2 ± 10.6	26.0 ± 12.2	-	21.1 ± 12.7	18.6 ± 3.0	23.3 ± 5.8	-	18.9 ± 6.0	23.9 ± 4.7	25.6 ± 5.3	-	19.5 ± 6.5	25.6 ± 1.5	26.2 ± 3.2

Tab. 20: Hemoglobin states during modified HDF in the animal model.

The [NaCl] was increased after a 30 min baseline period. Infusion of NaCl during standard pre-HDF with 0.36 M [NaCl]$_{blood}$ decreased the amount of O$_2$Hb and increased the one of HHb downstream the pre-dilution (BM). Abbreviations: O$_2$Hb, oxyhemoglobin; COHb, carboxyhemoglobin; MetHb, methemoglobin; HHb, deoxyhemoglobin; ART, arterial line ; BM, between hemodialyzers (downstream the pre-dilution) ; VEN, venous line. Results are mean ± SD (n = 4); [a], $P < 0.05$ *versus* 0 min; [b], $P < 0.05$ *versus* 30 min; [c], $P < 0.05$ *versus* 60 min.

As shown in **Tab. 21**, the WBC count was constant over the dialysis time in all treatments except for SDial-TM pre-HDF at 0.36 M [NaCl]$_{blood}$. There it increased after 60 min of dialysis ($P < 0.05$). The differential cell counts did not reveal any change in the WBC subpopulations. For all settings, RBC and PLT counts, Hct, and tHb were decreased after 30 min as compared to the beginning of the dialysis session.

Setting	Time [min]	WBC [10³/mm³]	RBC [10⁶/mm³]	PLT [10³/mm³]	Hct [%]	tHb [g/dL]
Standard pre-HDF 0.36 M [NaCl]$_{blood}$ (0.75 M [NaCl]$_{SUB}$)	0	6.2 ± 0.6	9.4 ± 1.2	446 ± 28	27 ± 4	9.9 ± 1.4
	30	6.4 ± 0.7	8.6 [a] ± 0.7	358 [a] ± 44	25 [a] ± 3	9.0 [a] ± 0.7
	60	7.9 ± 2.0	8.4 [a] ± 0.7	334 [a] ± 52	24 [a] ± 2	8.9 [a] ± 0.8
	120	8.1 ± 1.8	8.4 [a] ± 0.7	338 [a] ± 50	25 [a] ± 3	8.8 [a] ± 0.7
Standard pre-HDF 0.45 M [NaCl]$_{blood}$ (1.10 M [NaCl]$_{SUB}$)	0	7.1 ± 1.7	9.8 ± 0.6	460 ± 82	27 ± 2	10.0 ± 1.0
	30	7.4 ± 1.3	8.9 [a] ± 0.4	407 ± 74	24 [a] ± 2	9.1 ± 0.4
	60	8.1 ± 2.4	8.7 [a] ± 0.5	386 [a,b] ± 69	25 [a] ± 2	8.9 [a] ± 0.8
	120	8.4 ± 2.3	8.7 [a] ± 0.7	336 [b] ± 43	24 [a] ± 2	9.0 ± 0.9
SDial-TM pre-HDF 0.36 M [NaCl]$_{blood}$	0	6.0 ± 0.9	9.4 ± 0.3	493 ± 72	26 ± 3	9.4 ± 0.5
	30	6.6 ± 0.9	8.8 ± 0.7	406 [a] ± 91	25 ± 2	8.8 ± 0.7
	60	7.7 [a] ± 1.4	8.8 ± 0.6	397 [a] ± 88	24 ± 3	8.9 ± 0.6
	120	8.0 [a,b] ± 1.7	8.6 [a] ± 0.6	361 [a] ± 76	24 ± 3	8.7 ± 0.6
SDial-TM pre-HDF 0.60 M [NaCl]$_{blood}$	0	7.3 ± 2.3	10.0 ± 1.1	481 ± 162	27 ± 4	10.1 ± 1.4
	30	6.8 ± 1.5	8.5 [a] ± 0.6	348 ± 115	23 [a] ± 2	8.6 [a] ± 1.0
	60	7.3 ± 1.9	8.5 [a] ± 0.8	342 [a,b] ± 136	24 [a] ± 3	8.6 [a] ± 1.4
	120	6.8 ± 2.5	8.7 [a] ± 1.0	311 [a,b] ± 113	24 [a] ± 3	8.7 [a] ± 1.3

Tab. 21: Cell count, hematocrit, and total hemoglobin during modified HDF in an animal model.
The [NaCl] was increased after a 30 min baseline period. No change of the leucocyte subpopulations was observed. Abbreviations: WBC, leucocytes; RBC, erythrocytes; PLT, platelets; Hct, hematocrit; tHb, total hemoglobin concentration. Results are mean ± SD (n = 4); [a], $P < 0.05$ *versus* 0 min; [b], $P < 0.05$ *versus* 30 min.

The heart rate decreased ($P < 0.01$) within the first 30 min of treatment in all settings (range: t = 0 min, 100 to 125 beats/min; t = 30 min, 70 to 90 beats/min) except for the SDial-TM pre-HDF with 0.60 M [NaCl]$_{blood}$. There, it was steady at about 100 beats/min. After the 90 min of increased ionic strength, the heart rate was constant for standard pre-HDF at 0.45 M [NaCl]$_{blood}$ and SDial-TM pre-HDF at 0.36 M [NaCl]$_{blood}$. It slightly decreased ($P < 0.05$, range 80 to 90 beats/min) during standard pre-HDF at 0.36 M [NaCl]$_{blood}$ and SDial-TM pre-HDF at 0.60 M [NaCl]$_{blood}$. On the opposite, the mean arterial pressure was constant at about 60 mmHg ($P > 0.05$) during the whole dialysis session at the different settings.

As presented in **Fig. 79**, hemolysis slightly increased ($P < 0.05$) during dialysis independently of the setup and the [NaCl]$_{blood}$. After 120 min of treatment, the hemolysis level was not different ($P > 0.05$) between each setting. Furthermore, the LDH concentration was constant during dialysis with increased ionic strength.
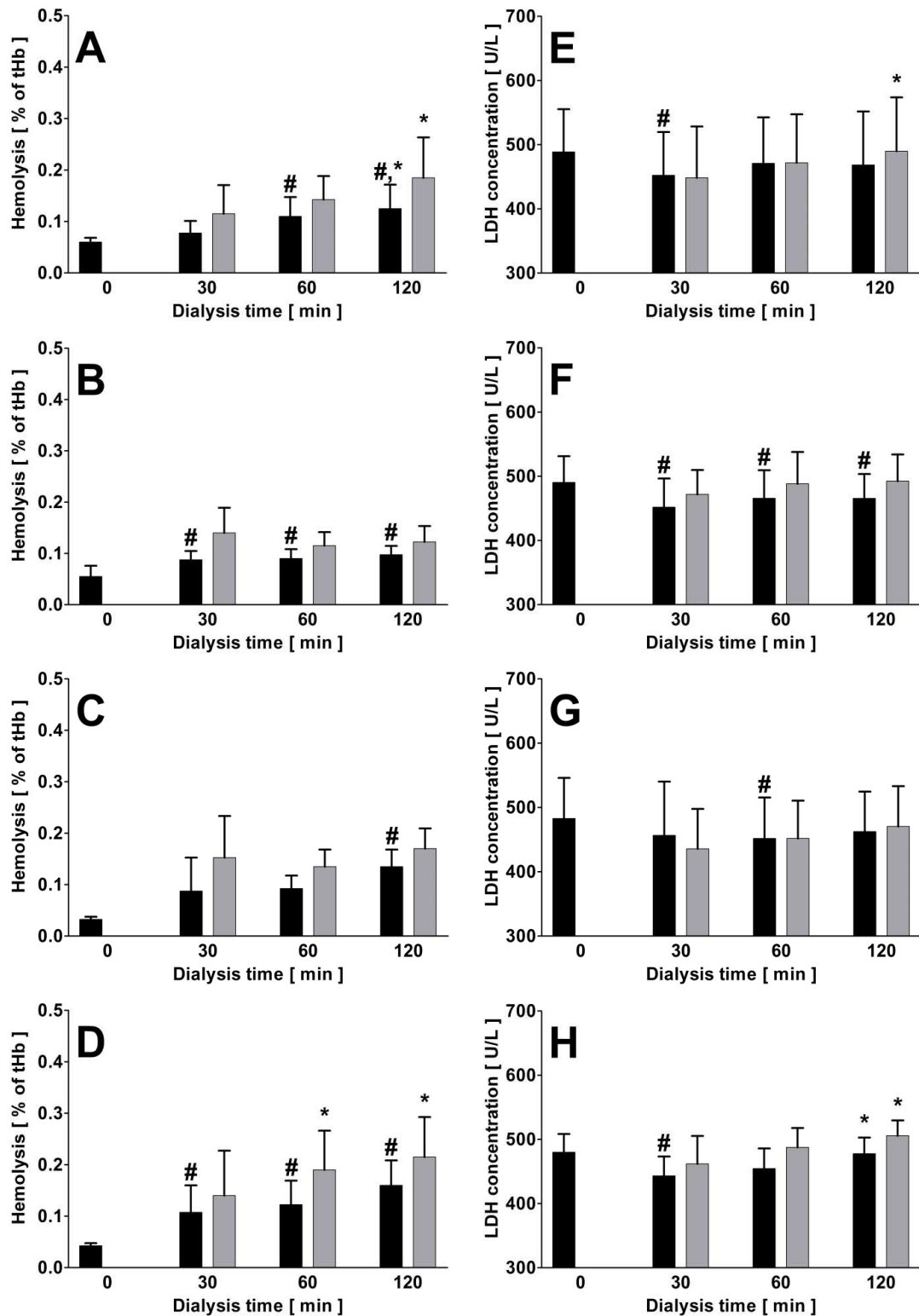
Fig. 79: Hemolysis and LDH concentration during modified HDF in an animal model.
Hemolysis (A-D) increased during standard pre-HDF at 0.36 M $[NaCl]_{blood}$ and SDial-TM pre-HDF at 0.60 M $[NaCl]_{blood}$. LDH concentration (E-H) was constant. During the first 30 min of treatment, physiologic saline was infused; the $[NaCl]_{blood}$ was increased during the following 90 min. Treatment modalities were: A and E, standard pre-HDF at 0.36 M $[NaCl]_{blood}$ (substitution fluid 0.75 M NaCl); B and F, SDial-TM pre-HDF at 0.36 M $[NaCl]_{blood}$; C and G, standard pre-HDF at 0.45 M $[NaCl]_{blood}$ (substitution fluid 1.10 M NaCl); and D and H, SDial-TM pre-HDF at 0.60 M $[NaCl]_{blood}$. Mean ± SD (n = 4); arterial (■) and venous samples (▨); #, $P < 0.05$ *versus* 0 min; *, $P < 0.05$ *versus* 30 min.

DISCUSSION

Uremic toxins are biological agents accumulating in renal failure which may produce biological responses deleterious to the human body (7). The uremic toxins have been classified and stratified into three groups according to MW and protein binding (8): 1, small solutes with no protein binding (< 500 Da) (e.g. urea, **Tab. 2**); 2, solutes with known or likely protein binding (e.g. IS and pCS, **Tab. 3**); 3, middle molecules ($\geq$ 500 Da) (e.g. β_2m, **Tab. 4**).

The protein-bound uremic solutes IS (**Fig. 1**) and pCS (**Fig. 3**) result from the metabolism of the amino acids tryptophan (21) and tyrosine (32), respectively. Both toxins accumulate in blood with progression of CKD (23; 36; 37) possibly due to reduced uptake by organic anion transporters in the kidney (24; 38). Moreover their deleterious effects on biological systems have been proven *in vitro* (29; 30; 43). Both IS and pCS are related to CKD progression (28) and to all-cause and cardiovascular mortality in HD patients (23; 37; 39; 40) contributing to the reduced survival probability of dialysis patients which is only 85.9%, 76.0%, and 50.3% after 1, 2, and 5 years, respectively (6). PAA largely accumulates in plasma of ESRD patients (about 3.4 mM) (10), and is suspected to play a role in bone disorder in CKD by affecting proliferation, differentiation, mineralization, and responsiveness to PTH of osteoclasts (48) and in immunodeficiency by inhibiting macrophage function (49).

The clearance of uremic toxins differs between the three toxin groups. Although urea is easily removed during HD, protein bound uremic toxins, such as IS and pCS, and middle molecules, such as β_2m, are only poorly removed (22; 33; 59; 60; 61). In spite of their small MW, IS and pCS with a protein binding of about 90% to 95% (22; 35) behave like larger molecules since their carrier protein albumin (77; 79) is unable to pass dialysis membranes and, therefore, is retained in blood. Only the free, unbound fraction is dialyzed (86). Therefore, current diffusive- and convective-based dialysis strategies (PD, HD, HF, and high-flux HDF) are not effective to remove such molecules (7).

The present thesis was motivated by the development of a hemodialysis method based on the transitory modification of the ionic strength in the extracorporeal blood stream to increase the removal of non-covalently protein bound uremic toxins.

I.   Reducing the protein binding of uremic toxins

> **Main findings:**
> - Together with plasma dilution and higher temperature, increasing the [NaCl] is effective to reduce the PBF of IS, *p*CS, and PAA in normal and uremic plasma.
> - The binding affinity of HSA for IS was in the same range as the one of plasma proteins.
> - The binding affinity for IS and *p*CS can be assessed by **Eq. 3** in uremic plasma, and depends linearly on the ionic strength, which can be modified by adding NaCl or other salts.

HSA is the most important carrier protein for hydrophobic compounds, such as drugs, fatty acids, hormones, and waste products (73; 74; 75; 76). Ligands that bind to site I (such as CMPF (77)) of HSA are dicarboxylic acids and/or bulky heterocyclic molecules with a negative charge within the molecule, whereas ligands that bind to site II (like IS and *p*CS (77; 79)) of HSA are aromatic carboxylic acids with a negatively charged acidic group at one end of the molecule that is separate from a hydrophobic center. The binding involves interactions with the amino acid residues (e.g. Trp214 for site I, Arg410 and Tyr411 for site II) in each binding pocket (72). Such intermolecular forces include dipole-dipole forces, hydrogen bonding, and London dispersion forces (73; 94). Moreover, the free and bound forms of such ligands are in a dynamic equilibrium (83). It is therefore possible to shift the equilibrium by modifying the electrochemical environment of the protein (i.e., modifying the ionic strength) and/or by changing the charge of the amino acid residues (i.e., modifying the pH). The choice of NaCl salt to increase the ionic strength in blood was motivated by: i), electrostatic interactions and/or Van der Waals forces are involved in the protein binding of IS and *p*CS (46; 95); ii), increasing its concentration to 0.30 M reduced the binding affinity of both *p*-cresol and *p*CS in HSA solution (96); iii), its concentration in blood is already high (about 120 mM); and iv), NaCl is inexpensive (about 16 €/kg (97)) and well approved for pharmaceutical application in human.

1) Validation of frozen plasma

The binding experiments with the uremic toxins IS, *p*CS, and PAA presented in the present thesis have been performed mostly in frozen human plasma. It is known from plasma fractionation that freezing of plasma alters the solubility of plasma proteins and leads to agglutination of, e.g. fibrinogen (98), thus changing the total protein concentration in the sample. Before using frozen plasma the aggregates were removed either by centrifugation or filtration. Therefore, it initially was verified if freezing of the plasma samples had an influence on both the PBF and the binding ability of uremic toxins in uremic and normal plasma (refer to "Effect of storage conditions").

In uremic plasma samples, the PBF of both IS and *p*CS was slightly higher (about 1.0%) after freezing. The reason for the decreased free toxin concentration after freezing (**Fig. 21**) may be the precipitation of other molecules, such as fatty acids, which are no longer bound to

albumin (74). Thus, less competitive reactions for the limited number of binding receptors occured after freezing leading to stronger toxin binding in uremic plasma. It is also possible that the small difference in both total (4 µM for both IS and pCS, thus representing an error of 4% and 2%, respectively) and free (1.4 and 1.9 µM for IS and pCS, respectively, thus representing an error of 21% and 26%, respectively) toxin concentrations may be due to pipetting.

Freezing of normal samples revealed that the K_D of proteins for IS was constant in plasma (K_D = 14.3 ± 5.3 and 14.7 ± 7.5 µM before and after freezing, respectively) as well as the albumin concentration. However, apart from the limitation that only very few experiments were performed (n = 2), the binding capacity of the plasma was reduced because B_m slightly decreased after freezing (from 614 ± 47 to 565 ± 33 µM).

Taken together, these experiments demonstrated that freezing of plasma did not significantly influence the binding ability of plasma proteins for protein bound uremic toxins, such as IS and pCS, allowing the use of this medium for further binding experiments.

2) NaCl decreases the protein binding of uremic toxins

a. Concept validation in pilot experiments

Pilot experiments (**Fig. 24** and **Fig. 25**) on the protein binding of IS, pCS, and PAA in normal human plasma were performed mainly by using a cocktail of toxins. Thus, it was possible to assess the influence of an increased toxin concentration (**Fig. 25**) and of the [NaCl] (**Fig. 24**) on the PBF of the toxins.

As predicted by **Eq. 3** and as shown in **Fig. 7**, increasing the toxin concentration ($[L_T]$) decreased the PBF of protein bound toxins (**Fig. 25**) since the ratio $[L_T]/B_m$ increased (73). Moreover, since many toxins were added together competitive reactions for the limited number of binding sites on HSA (99) and other proteins must be assumed especially at the highest concentrations (35; 100). Spiking plasma of HD patients with 100 µM of IS increased ($P < 0.001$) the free fraction of pCS from 6.7% (native uremic plasma) to 8.6%, whereas spiking plasma of HD patients with 166 µM of pCS increased ($P < 0.001$) the free fraction of IS from 9.3% (native uremic plasma) to 12.1% (35). This finding was confirmed by the work of Watanabe et al. who reported competitive reaction between IS and pCS in HSA solution by a Klotz analysis and a spiking experiment (85). The assumption that competition occurs between uremic toxins for the limited number of binding sites also explains the stronger decrease of the PBF of IS compared to pCS with increasing toxin concentration (**Fig. 25**) since the experiments involving pCS were performed only with the single toxin. Furthermore, to estimate the influence of increased [NaCl] on the PBF (**Fig. 24**), displacement experiments were performed with 100 µM of IS and pCS, and 200 µM of PAA with an [NaCl] of 0.15, 0.30, 0.50, and 1.00 M. Increasing the [NaCl] decreased the PBF of all protein bound toxins under investigation, i.e., IS, pCS, and PAA. Using **Eq. 3**, the possible effect of [NaCl] on K_D of plasma

proteins for IS and *p*CS was calculated (**Tab. 10**). The resulting values at 0.15 M NaCl (IS, about 48 µM; *p*CS, about 18 µM) were unexpectedly different compared to previous report, although, they were measured in HSA solution: IS, K_D = 0.6 to 1.1 µM (77; 79); *p*CS: K_D = 2.5 mM (96). Moreover, assuming B_m = 300 µM to assume K_D may not reflect the actual binding capacity of normal plasma. Therefore, it was interesting to elucidate this difference more accurately, i.e., in HSA solution and in normal human plasma by studying a single toxin.

b. <u>Binding of IS to HSA</u>

In order to demonstrate the influence of increased ionic strength on the binding affinity of HSA for IS, fatty acid free HSA was used. This material was preferred to albumin solution which contains stabilizers interfering with ligand binding (101). Briefly, 65 µM HSA was incubated for 30 min at room temperature with PBS pH 7.4 in the presence of IS (concentration ranging from 2.5 to 25 µM) and at different ionic strengths (0.15, 0.30, 0.50, and 0.75 M NaCl). The PBF was determined by ultrafiltration. The experiments demonstrated that K_D of albumin for IS positively correlated with the [NaCl] (K_D = 8.7 ± 0.6 and 40.8 ± 10.8 µM at 0.15 and 0.75 M NaCl, respectively; **Fig. 26**, A), i.e., increasing the [NaCl] decreases the binding affinity. This result is in agreement with previous findings which demonstrated that increasing the ionic strength to 0.30 M NaCl decreased the binding affinity of HSA for both *p*-cresol and *p*CS (96), which are protein bound toxins like IS. Furthermore, the same was shown for the binding of naproxen to bovine serum albumin (102), a drug known to bind to Sudlow's site II (101). The Scatchard plot (**Fig. 26**, B) demonstrated a single high-affinity binding site for IS on HSA, more exactly Sudlow's site II as already documented by Sakai et al. (77). Since IS and *p*CS share the same binding site (35; 85) and have nearly the same binding strength in plasma (22; 33; 35), it can be concluded that the effect of increased ionic strength on the binding of IS and *p*CS is similar.

The binding experiments of the present study were performed in 4.25 g/L HSA solution which is not representative for the physiologically much higher concentration in plasma (about 38 g/L) (37; 72). However, this difference should not have influenced the affinity of the binding sites. Sakai et al. reported that the binding affinity of HSA for dansylsarcosine, a marker ligand of HSA site II, was similar when using 40 or 200 µM HSA (77). The determined K_D value of HSA for IS at physiologic [NaCl] and room temperature are in the range of reported data in the literature: K_D ranges from about 1.0 µM (77; 79) to 10 µM (85). The experimental conditions may largely influence the results. Watanabe et al., who reported K_D = 10 µM, had incubated the protein with IS in PBS pH 7.4 at room temperature and used ultrafiltration (85), thus, similarly to our method. Although Sakai et al. performed their study at room temperature, they used 67 mM phosphate buffer (that did not contain Cl⁻ ions) and equilibrium dialysis (77; 79). The lower ionic strength in the solution may explain why Sakai et al. found a higher binding affinity (K_D = 0.6 and 1.1 µM) as compared to Watanabe et al. (85). Ultrafiltration was used because equilibrium dialysis is time consuming (103). Since fatty acid free HSA (≥99% purity) was used and IS binds to a single high-affinity binding site

(77; 85), it can be considered that the number of binding sites is equal to the HSA concentration. Thus, in order to calculate more accurately K_D, B_m was estimated to be equal to the HSA concentration (65 µM).

c. Binding of IS, pCS, and PAA in normal human plasma

Binding experiments in normal human plasma showed that both IS and pCS were bound specifically to one single binding site in normal human plasma as shown on the corresponding Scatchard plots (**Fig. 29**). This binding site has been identified by several authors as Sudlow's site II of albumin in plasma (35; 77; 79). At low concentrations (< 500 µM), PAA also was bound to a single, but likely different high affinity binding site (**Fig. 82**). When increasing the ionic strength in plasma by addition of NaCl, the results show a positive correlation of K_D of these uremic toxins with the [NaCl] (**Fig. 28**, A): IS, K_D = 71.2 × [NaCl] + 5.1; pCS, K_D = 82.4 × [NaCl] + 1.9; and PAA, K_D = 1007 × [NaCl] + 55.3. The binding affinity of plasma proteins for both IS and pCS is similar (0.15 M NaCl, K_D = 13.2 ± 3.7 and 16.3 ± 9.0 µM for IS and pCS, respectively; 0.50 M NaCl, K_D = 43.9 ± 13.2 and 44.6 ± 16.0 µM for IS and pCS, respectively), whereas the PAA binding affinity is about tenfold lower (K_D = 284 ± 74 and 459 ± 307 µM at 0.15 and 0.50 M NaCl, respectively). The reduction of the binding affinity with higher [NaCl], i.e., increased ionic strength, may be attributed to a modification of the electrostatic charges within the binding pocket of albumin (94) and/or a modification of the protein conformation (104), particularly, because no decrease of B_m was observed in the studied [NaCl] range. Thus, increased [NaCl] also positively correlated with the ratio K_D/B_m (**Fig. 28**, B: IS, K_D/B_m = 0.20 × [NaCl] + 0.03; pCS, K_D/B_m = 0.18 × [NaCl] + 0.02; and PAA, K_D/B_m = 3.19 × [NaCl] - 0.03) which corresponds to a decrease of the PBF (**Eq. 3**). In contrast, the PAA binding strength was not strong, which is in accordance with other reports confirming low protein binding (about 30%) (46). Therefore, this toxin can be easily removed by standard hemodialysis (105). Consequently, it was decided to not further study PAA since it did not fulfill the criteria of an ideal protein bound solute.

Similarly to the experiments performed in HSA solution, those using human plasma also had been performed at room temperature and pH 7.4 as well as by applying ultrafiltration, which is closer to clinical dialysis. The measured K_D for IS was slightly higher in human plasma than in HSA solution. This may be best explained by the presence of a variety of potential competing ligands in normal plasma, e.g. fatty acids, which may alter the binding properties of albumin by occupying the binding site (81) and/or inducing conformational changes of the protein (106). A methodological artifact can be excluded because comparative PBF of IS were obtained with both ultrafiltration and equilibrium dialysis (see "Temperature"). Together with protein adsorption onto the semi-permeable dialysis membrane (107), ultrafiltration of plasma water leads to an increase of the protein concentration in the retentate and, thus, a shift in the equilibrium. This phenomenon is well known from clinical hemodialysis, especially during post-dilution HDF (52). Previously reported binding affinities of HSA for both p-cresol and pCS (96) were largely lower (K_D = 2.0 ± 0.1 and 2.5 ± 0.2 mM,

respectively) compared to those observed in the present experiments in human plasma, thus, being not consistent with the reported high protein binding (33; 35) and similar behavior of IS during HD (64). The high variability of K_D observed in the present experiments using human plasma (**Fig. 28**, A) reflects the interindividual difference in the ability of plasma from different donors to bind toxins. As shown by Scatchard plot (**Fig. 29**), it is mainly determined by the albumin concentration. The albumin concentrations in the plasma samples used for the IS experiments considerably varied between 161 and 257 µM. Differences in the plasma content of present competing ligands may play an additional role, even though, toxins were incubated at low concentration (toxin-albumin ratio ≤ 1) and isolated to avoid extensive competitive reactions.

d. Comparison of the PBF in normal and uremic plasma

Synthetic toxins were added to normal human plasma but this method is regarded to not being sufficiently adequate to conclude on the effectiveness of increased ionic strength in uremic plasma (8). Therefore, the influence of increased [NaCl] also was demonstrated in plasma of ESRD patients on maintenance hemodialysis. Since plasma dilution influences the PBF (**Fig. 31**), the same plasma dilution was used to compare the PBF between normal and uremic plasma. Increasing the [NaCl] from physiological (0.15 M) to 0.75 M effectively decreased the PBF (**Fig. 30**) of IS and *p*CS in both normal (IS, from 93 ± 3% to 83 ± 4%; *p*CS, from 94 ± 2% to 89 ± 3% (at 0.50 M NaCl)) and uremic plasma (IS, from 89 ± 3% to 81 ± 3%; *p*CS, from 91 ± 2% to 84 ± 2%) but the PBF in uremic plasma was lower. This difference may be due to competition of the multiple uremic toxins for the same albumin binding site in ESRD patients (8; 35) while in human plasma from healthy donors, uremic toxins are not present (8). Supporting this argument, the mean native IS and *p*CS concentrations in uremic plasma were 69.4 ± 35.5 and 90.2 ± 27.9 µM, respectively.

Since only the free toxin fraction is removed during HD (86; 105), the present results implicated that adding NaCl to plasma would enhance the clearance of the protein bound uremic toxins. The blood clearance of protein bound toxins can be estimated by "*clearance = Q_B × free toxin fraction*" (73). Thus, an increase of the free IS fraction in uremic plasma from 11% to 19% (at 0.15 and 0.75 M NaCl, respectively) resulting from increased [NaCl] will approximately double its clearance (i.e., for Q_B = 300 mL/min, IS blood clearance should increase from ≈ 33 mL/min to ≈ 57 mL/min). To develop a modified dialysis method based on increased ionic strength in order to prove this assumption was a rational next step.

e. Estimation of K_D in uremic plasma

The binding affinity of uremic plasma proteins for both IS and *p*CS was determined. This problem could have been approached by isolating and purifying some plasma proteins known to be involved in ligand binding (e.g., albumin and α_1-acid glycoprotein) from uremic plasma (72). However, such an approach is time consuming and not representative for the

plasma milieu. In the present study, the protein binding was directly assessed in uremic plasma (**Fig. 83**). To note, performing direct binding studies in native uremic plasma is very difficult to interpret because competition occurs between the multiple protein bound uremic toxins present in plasma and any newly added ligand (46; 77; 79; 80). Alternatively, the free and bound toxin concentrations in plasma of a large number of uremic patients could be assessed and the binding constants determined from these data. Drawback of this approach is the array of required samples and the interindividual variability interfering with accurate calculations.

In a first set, the influence of HD on the binding ability of plasma proteins was shown. Both IS and pCS behaved similarly during dialysis (**Fig. 23**). This finding is in accordance with Meijers et al. who settled that these compounds are interchangeable marker molecules to monitor protein bound uremic retention solutes during dialysis (35). In the present investigation on a cohort of hemodialysis patients (n = 49), the K_D and B_m pre- and post-dialysis were estimated (**Fig. 22**). Both K_D and B_m decreased over the dialysis treatment (IS, pre-dialysis, K_D = 5.3 ± 1.7 µM and B_m = 217 ± 36 µM; post-dialysis, K_D = 3.5 ± 1.5 µM and B_m = 151 ± 37 µM). Nishio et al. reported that the free fatty acid concentration is largely increased post dialysis treatment which reduces the binding capacity of albumin (more exactly the binding capacity of its Sudlow's site II) (82). Thus, the accumulation of free fatty acids may explain that B_m decreased between pre- and post-treatment (**Fig. 22**). The decrease of K_D can be explained by the fall of the osmolarity, thus, of the ionic strength (**Fig. 28**), during hemodialysis (108; 109).

In a second set, the influence of a higher ionic strength on the binding constants of IS and pCS was studied. Firstly, it was verified if **Eq. 3** is suited in normal plasma to allow an accurate prediction of the experimental PBF of IS from the binding constants independently of the plasma dilution (**Tab. 11** and **Tab. 12**). At low toxin concentrations, the PBF is known to directly correlate with the binding affinity K_D and the number of binding sites B_m and, thus, with the protein concentration (83). Advantageously reflected by **Eq. 3**, the binding affinity can be assessed in uremic plasma when knowing the PBF, the toxin and the receptor protein concentrations which all can be determined experimentally. Since albumin was not measured in the plasma samples, a mean albumin concentration of 570 µM (38 g/L), which is in accordance with previous studies in dialysis patients (35; 37; 39), and also that B_m = [HSA] were taken as assumptions for the calculations. Applying **Eq. 3** yields that increasing the [NaCl] in uremic plasma from 0.15 to 0.75 M NaCl enhances K_D for IS from 27.3 ± 8.6 to 55.9 ± 15.3 µM and for pCS from 20.1 ± 5.3 to 39.7 ± 9.4 µM. This estimated binding affinity reflects the apparent affinity of uremic plasma for both IS and pCS and is similar to the one found in normal plasma (**Fig. 28**).

f. Cumulative effect of plasma dilution

Two to tenfold dilution of plasma also showed to be effective to decrease the PBF of IS (**Fig. 31**) which is explained by a decrease of B_m (**Fig. 31**, B). This effect was additive to increasing K_D by an increase of ionic strength through elevating the [NaCl] (**Fig. 31**, A). Both effects complement one another and lead to an increase in the ratio K_D/B_m and, *a fortiori,* to a reduction of the PBF (**Eq. 3**). Clinical and experimental observations support this phenomenon. Low serum albumin concentrations in uremic patients were found to correlate with a higher free fraction of *p*CS (41). The same authors confirmed this finding by testing different bovine serum albumin concentrations *in vitro* (41), thereby, supporting the data of the present study which demonstrated that plasma dilution did not influence K_D. Thus, it is important to take the protein concentration or plasma dilution into consideration when comparing the PBF from different experiments or clinical studies.

g. Cumulative effect of the temperature

Increasing the temperature from room (25 °C) to body temperature (37 °C) also decreased the PBF of IS in normal human plasma from 91 ± 2% to 85 ± 2%, respectively. Confirming Bergé-Lefranc et al. who reported that enhancing the temperature reduced the affinity (i.e., increased K_D) of HSA for both *p*-cresol and *p*CS without changing of the protein structure in this temperature range (96), this finding is in accordance with the Van't Hoff equation (**Eq. 17**). Since toxin unbinding from a protein is an endothermic reaction ($\Delta H^o > 0$), i.e., it absorbs energy (110), and with $T_2 > T_1$, **Eq. 17** gives $K_2 > K_1$ (111). Consequently (**Eq. 3**), performing experiments at room temperature must have overestimated the PBF and the binding affinity of IS, *p*CS, and PAA in human plasma compared to body temperature. Therefore, the influence of increased ionic strength during clinical dialysis, which usually is performed at body temperature, should even be greater compared to the results from the present experiments.

$$\ln\left(\frac{K_2}{K_1}\right) = \frac{\Delta H^o}{R} \times \left(\frac{1}{T_1} - \frac{1}{T_2}\right)$$

Eq. 17: Van't Hoff equation (111).
Where K_1 and K_2 are the equilibrium constants at the temperatures T_1 and T_2, respectively; ΔH^o is the standard enthalpy change for the process; and R is the gas constant with R = 8.31 J/K.

h. Influence of ions and pH

Not only NaCl but also KCl was able to reduce the PBF of IS in uremic plasma (**Fig. 34**). The effect of both salts was similar for comparable ionic strength. Moreover, mixing both salts had the same effect as a single salt at the same concentration. Thus, only an increased ionic strength affects the protein binding. Since the albumin conformation depends on pH (74), some blood purification methods (112; 113; 114) are based on pH shift, such as the heparin-

induced extracorporeal lipoprotein precipitation (HELP), which primarily is not designated for the treatment of renal failure (39; 40). Lowering the pH to 5.4 (112) reduced the PBF of native IS (**Fig. 34**). Collins et al. described a method to improve the clearance of e.g. protein bound solutes by modifying the pH (7.8 < pH < 11) in blood upstream the hemodialyzer. In this invention, the pH in blood is restored after exposition to standard dialysate (7.0 < pH < 7.8) (114). However, physiologic pH in blood is very narrow (pH between 7.35 and 7.45). Thus, shifting of the pH directly in blood (114) may induce bioincompatibility, which may explain that no data on this topic has ever been published so far. In the present work, adding NaCl together with reducing pH has the same effect like adding NaCl only. Both effects are not cumulative in the concentration range studied (**Fig. 34**).

II.   Modification of pre-dilution HDF for increased ionic strength

Main findings:
• Ionic strength is effectively increased in the blood line by a simple modification of the standard pre-dilution HDF setup.
• Some parameters such as K_0A of the hemodialyzer and Q_B have to be carefully adjusted to avoid retention of the NaCl excess in the blood stream.
• Mini-dialyzer setups revealed that increased ionic strength during dialysis in plasma effectively enhances the removal rate of protein bound uremic toxins.
• *Ex vivo* HDF with increased ionic strength up to 0.75 M $[NaCl]_{SUB}$ showed acceptable hemocompatibility (no hemolysis, no decrease of the WBC count, no activation of the complement or coagulation systems) to be transferred to the animal model.

Modification of standard pre-dilution HDF (as drawn in **Fig. 8** and **Fig. 9**) appeared to be the dialysis method which most simply allowed the application of increased ionic strength. The substitution fluid permits the addition of highly concentrated NaCl solution, which in turn injects the NaCl into the blood stream. It is necessary to increase the ionic strength upstream the hemodialyzer, i.e., doing pre-dilution, in order to eliminate untied protein bound toxins but also to remove the excess NaCl and restore blood osmolarity to a physiological level by the downstream dialysis before the blood is flowing back to the patient. Similarly to the clearance concept of the human kidney, the solute transport characteristics of a hemodialyzer may be expressed as clearance. Clearance represents the volume of fluid (e.g. blood or plasma) cleansed from a given substance per unit of time by the device (91).

1) **Pilot experimentation of increased ionic strength during standard pre-dilution HDF**

Pilot experiments were performed in aqueous solution on a dialysis machine to assess the feasibility of increasing ionic strength using standard high-flux hemodialyzers (1.8 m²). For NaCl infusion, a 5.00 M (292.2 g/L) solution was used because it approaches the maximal solubility of NaCl in ultrapure water (358 g/L at 20 °C) (97).

Since measurement of ion concentration by ion specific electrodes is time consuming, it was decided to measure instantaneously the conductivity in aqueous solution to estimate the ionic strength. The conductivity of a solution is directly proportional to the ion concentration (**Eq. 8**) and its respective molar conductivity. Since H_3O^+ and HO^- ions have the highest molar conductivity (34.95 and 19.86 mS.m²/mol, respectively) compared to Na^+ and Cl^- (5.01 and 7.63 mS.m²/mol, respectively), a pH shift may largely influence the conductivity. Measuring the conductivity during dialysis was possible because the dialysate composition is constant during dialysis and buffered at pH of about 7.4. Therefore, the standard curve of the conductivity *versus* the [NaCl] was generated (**Fig. 35**). Surprisingly, in the range of 0.10 to 5.00 M NaCl, the curve was not linear which is not in accordance with the calculation of conductivity according to Kohlrausch's law (**Eq. 8**). It could be explained by a saturation of the electrode for concentrations greater than 1.00 M. However, the conductivity was nearly linear in the most interesting range between 10 and 50 mS/cm and it was possible to perform a linear regression between [NaCl] and conductivity in the range of 10 – 35 mS/cm (**Eq. 15**). This information allowed a sufficiently accurate estimate of the [NaCl] from the conductivity in this range.

Since saline has a physiological [NaCl] (0.15 M), its infusion at different flow rates (Q_{NaCl}) did not change the conductivity in the system (**Fig. 36**). Infusion of 5.00 M NaCl solution to the substituate increased the conductivity, i.e., [NaCl] in blood entering the dialyzer (**Fig. 38** and **Fig. 39**). Furthermore, a constant NaCl infusion increased the ionic strength to equilibrium (**Fig. 37**). After modifying the external pump (**Fig. 9**) to synchronously injecting NaCl solution and removing dialysate, higher infusion flow rates Q_{NaCl} were possible. The previous setup was limited by the ultrafiltration flow rate Q_{UF} (usually 0 < Q_{UF} < 40 mL/min) since no excess fluid volume added to the blood reservoir. The modification allowed avoiding this problem. Q_{NaCl} further was only limited by the substitution flow rate Q_{inf} (usually 0 < Q_{inf} < 160 mL/min in pre-dilution HDF).

Depending on the blood flow rate Q_B, the NaCl excess was not entirely removed from the blood stream (**Fig. 40**). This observation was predictable by simple models of the clearance from blood (**Fig. 42** and **Eq. 18**) taking into account the K_0A of urea (MW = 60 Da, i.e., similar to Na^+ and Cl^-: 23 and 35 Da, respectively), Q_B, and Q_D. Actually the clearance increases with Q_B, however, the increase is not proportional since the efficiency of diffusion decreases as blood flow increases (5). The [NaCl] in the blood entering the dialyzer depends only on the dilution factors (= flow rates) of NaCl solution and substituate and of substituate and blood.

K_0A has the greatest influence on the removal of NaCl (**Fig. 43**) (5). Thus, high-flux filters (with high K_0A) were preferred to low-flux filters (rather low K_0A) for the application of increased ionic strength during HDF because an adequate NaCl balance is mandatory in maintenance dialysis patients lacking the renal control of homeostasis (115; 116). Increasing Q_D, as already exposed (5), has only a minor effect on small solute removal (**Fig. 40** and **Fig. 43**). Furthermore, a low Q_B ($\leq$ 300 mL/min) is mandatory to remove the excess NaCl in order to avoid the retention of NaCl in the blood leaving the dialyzer which is reinfused into the patient.

2) <u>Toxin removal increased with higher ionic strength</u>

Mini-dialyzers (membrane surface area reduced to about 250 cm²) with similar high-flux membranes like standard dialyzers were used to perform preliminary studies on the removal of uremic toxins. Major advantage of such a miniaturized setup is the small filling volume (dialyzer + tubing $\approx$ 30 mL) allowing the use of plasma from reduced blood donation (60 mL) of ESRD patients. Since the flow rates had to be adjusted to the membrane surface area, the number of plasma/blood runs through the mini-dialyzer was determined (**Eq. 7**) to compare directly to normal setups. It corresponds to the number of times blood passes through the hemodialyzer. A clinical reference can be established for a standard dialysis duration of 4 h, a Q_B = 300 mL/min, and a normal patient with about 5.0 L blood. In this respect, blood is pumped about 15 times during hemodialysis.

Mini-dialyzers may differ from larger hemodialyzers in term of clearance. Therefore, initially, an experiment was designed to assess the clearance of IS in different milieus, namely in aqueous solution before and after coating with plasma protein and in human plasma (**Fig. 69**). Aqueous clearance of IS was reduced (between 15% and 20%) after coating of the membrane with plasma proteins. The protein (albumin, fibrin/fibrinogen) coating effect has been described to occur immediately after exposure to blood or plasma because of the hydrophobicity of the membrane material (11). Although albumin coating decreases solute clearances (11), it improves the hemocompatibility, e.g. by reducing thrombocyte adhesion (13). Similarly to standard hemodialyzers (117), increasing Q_B increased the clearance of the mini-dialyzers (**Fig. 69**) but not proportionally (as expected from **Eq. 18**). Therefore, interpreting the results with respect to the blood runs was preferred. The plasma clearance of IS was largely lower compared to the aqueous clearance because newly added IS must have bound to plasma proteins and only the free toxin fraction could be removed (86; 105). However, the plasma clearance was higher than the aqueous clearance relative to the free toxin fraction (calculated by **Eq. 12**; **Fig. 69**). It must be considered that removal of IS change the binding equilibrium (83) so that bound toxin is released and then removed from plasma (86; 105).

In a consecutive pilot *in vitro* experiment (**Fig. 73**), both IS and *p*CS were demonstrated to be completely removed from native uremic undiluted plasma at the same rate. This was the

case when long time dialysis (about 9 h) was applied. An [NaCl] in plasma increased to about 0.32 M was used to accelerate the removal and shorten the experiment duration.

Mini-dialyzer experiments also revealed that increasing the ionic strength in the substitute to 1.00 M NaCl (0.36 M NaCl in plasma) effectively increased the removal rate of IS in normal plasma (**Fig. 70**) (plus 65% and 48% for $Q_{B\ eq}$ = 300 and 400 mL/min, respectively). However, compared to HD, plasma dilution as obtained by HDF did not increase the removal rate of IS. Since the uremic toxin is diluted to the same proportion as it is released (118) both effects oppose themselves without changing the free mass of toxin (**Eq. 3**). The results also confirm that IS is mainly removed by diffusion as demonstrated by recent studies (63; 64).

Another set of experiments comparing uremic and normal plasma and normal HDF with increased ionic strength HDF was done (**Fig. 71**). Increasing the [NaCl] increased the removal rate of both IS and *p*CS but the statistical power of the trial (n = 3) was too low to reach significance (*P* = 0.36 and *P* = 0.20 in normal and uremic plasma, respectively). However, the results rather confirmed than refuted the observation that IS and *p*CS behave similarly in normal and uremic plasma. Although low serum albumin concentration correlates with a higher free fraction of *p*CS (41), thus potentially with higher clearance (105), the removal rate of IS and *p*CS in human plasma did not significantly (*P* = 0.07 and *P* = 0.09 for [NaCl] = 0.15 and 0.36 M) correlate with albumin concentration (**Fig. 72**).

3) *Ex vivo* hemocompatibility of increased ionic strength

The hemocompatibility was assessed in freshly donated heparinized blood from healthy volunteers according to ISO 8637:2010.

a. Single contact experiments

In order to illustrate the experimental results of hemolysis and cell count obtained during modified pre-dilution HDF, preliminary experiments were carried out by single contact of blood with hypertonic solutions (i.e., with increased [NaCl]). Other parameters assessing hemocompatibility (i.e., activation of the complement and coagulation systems) are only relevant under conditions closed to clinical application (i.e., longer lasting dialysis experiments as discussed below).

Exposition of blood to increased ionic strength (**Fig. 46**) led to hemolysis when [NaCl]$_{blood}$ > 0.50 M, which is in accordance with published results reporting a critical level of osmotic stress of 1.4 Osm (119; 120; 121). Green et al. also reported a hemolysis level of about 2% in 1.00 M NaCl solution (120). The transformation of the cell morphology towards hemolysis corresponded to the increasing osmolarity (**Fig. 48**) (122; 123). In hypertonic solution, cells lose water through osmosis resulting in significant cell shrinking and appearance of the cytoskeleton (122). This is called crenation (124) and RBCs can be observed in form of echinocytes (122; 125) already at 0.25 M NaCl (124). If the milieu is excessively hypertonic, the cell membrane can no longer support the water loss and disrupts.

Interestingly, the resistance of RBC to osmotic changes correlates with the RBC count and tHb (**Fig. 47**). Only few publications are available on this relationship, particularly investigating hypotonic media (126; 127; 128). Reddy et al. did not find in tuberculosis patients any correlation between tHb or RBC count and osmotic fragility (126). Similarly, in human female subjects, the erythrocyte membrane resistance to hypotonic lysis was correlated neither with RBC count nor with the cell volume (127). On the opposite, Karai et al. found a close relationship between RBC osmotic fragility and both cell volume and tHb in workers from lead industry, whereas in healthy controls they found a close relationship between RBC osmotic fragility and both cell volume and RBC count (128). These data may not reflect the RBC resistance to hypertonic solution as studied here (**Fig. 46**, **Fig. 47**, and **Fig. 48**) since the water flux is in the opposite direction in hypo- and hypertonic media (124) and the osmotic fragility test is performed by exposing RBC to hypotonic solutions (0% to 0.9% NaCl) (129). An explanation for the apparently higher RBC resistance in hypertonic media for higher RBC counts (**Fig. 47**) could be that the higher the number of cells, the lower the volume loss (i.e., the lower the crenation) in order to equilibrate the osmolarity on both sides of the cell membrane. Since the hypertonic milieu is diluted when the cells loose water, the osmolarity decreases, especially in the present *in vitro* conditions. This effect will be of interest when selecting a study population suited for the clinical application of modified pre-dilution HDF. Together with low hemoglobin levels in uremic patients (11.9 ± 1.3 (67) *versus* 15.5 ± 2 g/dL in the normal population (130)), the erythrocyte osmotic fragility of both diabetic and uremic (on maintenance HD) patients is higher than in healthy humans (131; 132; 133; 134) because of the decreased deformability of the cells (135; 136). Therefore the erythrocytes of uremic patients may be more susceptible to lysis during modified pre-dilution HDF compared to those of healthy people.

A difference was seen between blood dilution and dialysis with NaCl solutions (**Fig. 46**). Hemolysis was worse in the latter case. This phenomenon could be attributable to the shear stress induced by the passage through the capillaries (internal diameter 215 μm) of the dialyzer (137). RBC deformability decreases with both hypo- and hypertonicity (138), which plays a significant role in spontaneous hemolysis (137) and cell life span (139; 140). Furthermore, the incubation time at increased ionic strength could have also added to the observed difference since blood samples were incubated for 1 h under dilution *versus* 4 h for single pass dialysis.

The hemolysis increased exponentially with the [NaCl] starting at about 0.50 M with both single pass dialysis and blood dilution (**Fig. 46**). The most fragile population of RBC would be the first to be damaged by the sudden exposure to hypertonic media (137). Although osmotic resistance is used to differentiate old and young RBC because the young human erythrocytes are more resistant to hemolysis in hypotonic media compared to older cells (141; 142), cellular aging does not produce a gradual increase in osmotic fragility (143). It decreases the RBC volume (142) which is correlated with a higher resistance to a hyperosmotic milieu since small RBCs are more resistant compared to larger ones (121).

The WBC morphology also changed in a similar manner with increased ionic strength (**Fig. 50**), i.e., the cellular size decreased with higher tonicity because of osmosis (124). In principal, the phenomenon of cellular shrinking is reversible (140; 144) for both RBC and WBC (**Fig. 49** and **Fig. 50**) as long as lysis does not occur. Interestingly, WBC seem to be more resistant to osmotic changes compared to RBC (134; 145; 146). The median osmotic fragility in hypotonic NaCl solution was about 0.25% and 0.39% NaCl for normal lymphocytes (145) and erythrocytes (134), respectively.

From these single contact experiments it was concluded that blood cells may support up to 0.50 M NaCl without sustained damages. Because of the higher susceptibility to osmotic changes of the RBC of patients on maintenance hemodialysis and diabetic patients (131; 132; 133; 134), it would have been an interesting issue to perform similar experiments (**Fig. 46**, **Fig. 47**) on the blood of ESRD patients on maintenance hemodialysis.

b. Experiments on a dialysis machine and under dynamic conditions

A first set of experiments comparing the effect of increased ionic strength ($[NaCl]_{SUB}$ = 1.00 M and $[NaCl]_{blood}$ = 0.50 M) on the blood volumes between 500 and 1500 mL revealed a strong impact of the blood volume on the hemolysis (**Fig. 51**, A) and WBC count (**Fig. 52**, A and **Fig. 53**). It best is explained by the number of stimulations inflicted upon the blood cells. Compared to 500 mL blood, blood cells in a larger blood volume (1500 mL) encounter three times less often osmotic changes from increased [NaCl] and mechanical stress through the blood pump of the circuit. Therefore, **Eq. 7** was used to determine the number of blood runs τ, corresponding to the number of stimulations, to set the experimental results into perspective. When plotting the degree of hemolysis *versus* τ (**Fig. 51**, B), no difference between 500 and 1500 mL blood could be identified. This finding was of great importance for the interpretation of the *in vitro* results before transferring it into the clinical application. Since 15 τ are commonly obtained during clinical hemodialysis of a 70 kg patient with approximately 5 L of blood (see above), a hemolysis < 1% *in vitro* after 30 τ, representing twice the standard dialysis duration, is by far on the safe side even after taking into account an additional security margin because the hemolysis increased exponentially with the mechanical stresses (**Fig. 51** and **Fig. 55**). An Acceptable level of hemolysis for medical devices is not defined in standards, such as ISO 10993-4:2002 (147) but a reference value of 1% hemolysis is used to assess biocompatibility of blood storage materials (137). Moreover, free plasma Hb concentrations of 0.3 to 2.1 g/dL (i.e., corresponding to about 2% to 17% hemolysis, respectively) were associated with the manifestation of symptomatic illness of hemodialysis patients during acute hemolysis (148).

The observed increase of the TMP when using 500 mL blood (**Fig. 54**, A) may be due to membrane clotting because of damaged cell particles. Damaged RBCs during treatment with

increased ionic strength will release Hb and cellular organelles (124; 148). The membrane pores are obstructed by the cell particles and the membrane surface area is decreased (11). Since the Q_{UF} is constant, the TMP increases.

Subsequently, the hemocompatibility of increased ionic strength was determined during standard pre-dilution HDF at different [NaCl]$_{blood}$ (0.15, 0.36, and 0.50 M). After pilot experiments (**Fig. 55**) had revealed that the [NaCl]$_{SUB}$ plays a role in hemolysis, two different [NaCl]$_{SUB}$, 0.75 and 1.00 M, were compared to obtain a 0.36 M [NaCl]$_{blood}$. The experiments were designed with a Q_B of 150 mL/min applicable to the planned sheep animal model of dialysis (149) and Q_{inf} representative for the clinical application (60) (Q_{inf} was 75 and 50 mL/min at [NaCl]$_{SUB}$ of 0.75 and 1.00 M, respectively, to reach 0.36 M [NaCl]$_{blood}$). The treatment duration of 120 min was calculated from the blood volume in order to pump blood more than 30 times to reach the acceptance criteria for hemolysis. Blood Hct and TP were adjusted according to ISO 8637:2010.

As a main requirement, the [NaCl]$_{VEN}$ (**Tab. 16**) should not be higher than the control (0.15 M) in all experiments performed in standard pre-dilution HDF as a measure for a complete removal of the NaCl excess by the downstream HD (**Eq. 18**). The experiments further confirmed that the osmotic shock, as defined by the difference between [NaCl]$_{SUB}$ (0.75 and 1.00 M) and [NaCl]$_{blood}$ (0.36 M), plays the major role for the RBC damage (**Fig. 60**, A) because the hemolysis was significantly more intense with 1.00 M NaCl substituate compared with 0.75 M, although, the obtained [NaCl]$_{blood}$ was identical. Furthermore, the hemolysis correlated with [NaCl]$_{SUB}$. Since hemolysis after 30 τ was below 1% (see above) only for the 0.75 M NaCl substituate, it was concluded that this setting represents the maximum [NaCl]$_{SUB}$ which achieves *ex vivo* results being acceptable to be transferred into the animal model.

Although, post-dialysis hemolysis was high using 1.20 M NaCl substitution fluid (17.6 ± 7.2%, $P < 0.05$), the RBC count did not decrease (range 3.45 ± 0.51 to 4.19 ± 0.65 ×10^6 cells /mm^3 at the beginning of the dialysis experiments). This observation can be explained as follows. When cell membranes disrupted in hypertonic solution, free Hb was released into the plasma. Due to hydrophobic interactions, the cell membranes merged few instants later resulting in damaged RBCs of nearly the same size as normal (124) not differentiated by the automated cell counter (measurement by impedance). Thus, RBC damage should be assessed by measuring the Hb release.

The WBC count was constant over time when increasing the [NaCl]$_{SUB}$ up to 1.00 M (**Fig. 61**, A) and did not differ from physiologic ionic strength. Furthermore, the course of the WBC count was similar to that observed in patients during hemodialysis with biocompatible membranes (150). Confirming the experiments performed with single contact of blood with hypertonic NaCl solutions (see above), the WBC (**Fig. 61**, A) seemed to be more resistant to the osmotic shock compared to RBC (**Fig. 60**, A) since no difference was observed in the WBC count between 0.75 and 1.00 M [NaCl]$_{SUB}$ (**Fig. 61**, A; 92.4 ± 7.7% *versus* 89.4 ± 6.5% after

120 min dialysis with 0.75 and 1.00 M [NaCl]$_{SUB}$, respectively). However, they finally decreased with 1.20 M [NaCl]$_{SUB}$ (57.7 ± 6.5% after 120 min dialysis; $P < 0.05$). This finding was consistent with the dot plots (**Fig. 62**, A) and the platelet volume histograms (**Fig. 63**, A). Dead cells or cell fragments appeared only with 1.20 M NaCl substituate. Dot plots (**Fig. 62**) and platelet volume histograms (**Fig. 63**) were performed after a dialysis duration of 0, 13.3, and 27.2 τ corresponding to baseline (0 τ), near to full-time clinical dialysis (15 τ), and defined performance criteria (30 τ), respectively.

In order to assess the activation of the coagulation and complement system by increased ionic strength, the course of TAT (MW = 96 kDa (151)) and C5a concentrations, respectively, were measured at the different [NaCl]. These parameters are recommended by European guidelines to assess the biocompatibility of medical devices in contact with blood (147) because thrombin and C5a are activated downstream the coagulation and complement cascades, respectively, and are independent of the activation pathways (152; 153). No activation of the coagulation system was observed (the TAT concentration remained in the range of 6 to 32 µg/L during the dialysis experiments without any influence of the [NaCl]). Krieter et al. reported TAT concentrations between 2 to 6 µg/L *in vitro* for biocompatible dialysis membranes (150). Since C5a concentrations were below the detection limit after 15 min treatment, this 11 kDa protein must have been removed by high-flux hemodialysis as shown in previous studies (154). The Cuprophan® membrane, which is classified as bioincompatible membrane (155), induces activation of complement with rising of the C5a concentration of up to 49 mg/L (154). This is by far higher compared to biocompatible polyethersulfone membranes (C5a concentration in the range of 1 to 3 mg/L) (150). Taken together increased ionic strength applied in the defined range during pre-dilution HDF demonstrated adequate biocompatibility.

III. <u>Iterated application of increased ionic strength by serial dialyzers HD / HDF</u>

Main findings:
- Better hemocompatibility of increased ionic strength dialysis is obtained with the SDial setup.
- Transmembrane pre-dilution further improves hemocompatibility by decreasing the [NaCl] gradient at the porous membrane.
- Inadequate flow rates (i.e., $Q_{ex} << Q_B$) may increase the concentration gradient leading to deteriorated hemocompatibility.
- Both standard pre-HDF and SDial pre-HDF are efficient to increase protein bound uremic toxin removal.

To reduce the detrimental effects of osmotic shock, the infusion of the substitution fluid was split to several sites of the circuit (see **Fig. 14**) during a pilot experiment of standard pre-dilution HDF. This setting did not reduce hemolysis compared to single site infusion (**Fig. 55**).

Alternatively, blood can be dialyzed against a solution with the targeted ionic strength to reduce the osmotic shock. Therefore, the SDial setup was developed as an iteration step (**Fig. 10**). In the first cartridge, blood was dialyzed against a solution with elevated [NaCl] to increase the concentration in blood. Then, blood passed through a second serial cartridge (high-flux hemodialyzer) in which the NaCl excess and toxins were removed.

The validation of this setting was performed in different steps: control of the ionic strength in aqueous solution, *ex vivo* hemocompatibility, and toxin removal efficacy.

1) <u>Control of the NaCl concentration in aqueous solution</u>

Since the final $[NaCl]_{blood}$ with the SDial setup did not depend directly on the different flow rates but also on the semi-permeable membrane properties (11) (i.e., K_0A), pilot experiments using aqueous solutions were designed.

First experiments showed that the ionic strength was stable over time at different flow rates (**Fig. 41**). Moreover, the second cartridge effectively removed the NaCl excess ($[NaCl]_{VEN}$ was about 137 mM). However, there was still a difference in the [NaCl] between the blood (BM) and the dialysate compartment (IN) ($[NaCl]_{IN}$ / $[NaCl]_{BM} = 1.45 \pm 0.05$, 1.38 ± 0.10, and 1.36 ± 0.05 for $Q_{ex} = 200$, 225, and 250 mL/min, respectively) indicating that Na^+ and Cl^- ions did not diffuse completely from the dialysate into the blood stream. The difference was reduced by increasing the dialysate flow rate of the external closed loop Q_{ex}. Using recursion calculation, the [NaCl] at the different sites of the setup was simulated (see **Fig. 87** and **Fig. 44**) in order to explain the difference between the $[NaCl]_{BM}$ and $[NaCl]_{IN}$, and to assess the stability of the ionic strength over time. The experimental results were well approached by the simulation of the $[NaCl]_{BM}$, $[NaCl]_{IN}$, and $[NaCl]_{VEN}$ with relative errors of $2.1 \pm 2.1\%$, $11.5 \pm 2.0\%$, and $1.5 \pm 0.7\%$, respectively, whereas $[NaCl]_{OUT}$ was underestimated (relative error of $26.6 \pm 5.8\%$).

In a consecutive iteration, the concentration gradient, i.e., the osmotic shock, was further reduced by performing transmembrane pre-dilution HDF (**Fig. 11**). Adding convection to diffusion increases the mass transfer of NaCl (156) from the dialysate closed loop into the blood stream resulting in lower concentration gradients between both sides of the semi-permeable membrane (**Fig. 45**) as compared to SDial pre-HDF.

2) <u>*Ex vivo* hemocompatibility in dynamic conditions</u>

Several pre-dilution HDF experiments with human blood comparing the SDial setup with normal and transmembrane substitution were performed. The same flow rates (Q_B, Q_D, Q_{inf}) and hemodialyzers as with the standard pre-HDF setting were taken in order to allow a direct comparison of the results.

Different $[NaCl]_{blood}$ were studied: 0.15 M in order to validate the influence of the second serial cartridge on the hemocompatibility, 0.36 and 0.50 M in order to compare the performance of the SDial system to standard pre-HDF of the same $[NaCl]_{blood}$, and 0.75 M in order to verify the maximal admissible [NaCl] in blood.

Firstly, adding a second cartridge to the setup did not induce hemolysis *ex vivo* (**Fig. 60**, B). Secondly, hemolysis did not occur below a $[NaCl]_{blood}$ of 0.50 M. At this concentration, hemolysis was largely lower compared to standard pre-HDF at 1.20 M $[NaCl]_{SUB}$ which corresponded to the same $[NaCl]_{blood}$. Therefore, the iteration of the experimental setup in form of a second serial dialyzer for infusion of NaCl effectively reduced the osmotic shock as indicated by improved hemocompatibility at the highest ionic strength. Thirdly, a concentration of 0.75 M NaCl in the blood stream also was tested but, since RBCs were severely damaged (71.7% hemolysis post treatment), only a single experiment was performed. Although the osmotic shock was reduced with the SDial setup, cells, which were not damaged after a single contact (**Fig. 46**), hemolyzed after repeated osmotic stimulations as shown by the increasing hemolysis during dialysis treatment (**Fig. 60**).

Compared to the standard pre-HDF at the same $[NaCl]_{blood}$ (0.50 M), survival of WBCs (**Fig. 61**, **Fig. 62**, and **Fig. 63**) was not improved with the SDial pre-HDF as indicated by an equally decreasing WBC count. Therefore, WBCs seem to be particularly sensitive to the $[NaCl]_{blood}$ independently of the osmotic shock (in the range of the concentrations studied). Similarly to standard pre-HDF, no activation of the coagulation system (TAT) was seen with SDial pre-HDF.

Although the $[NaCl]_{blood}$ was higher (535 ± 19 mM *versus* 474 ± 7 mM, *P* < 0.01), performing SDial pre-HDF using transmembrane substitution to 0.50 M $[NaCl]_{blood}$ further reduced hemolysis (**Fig. 66**, A) compared to SDial pre-HDF. Furthermore, no significant decrease of the WBC count was measured (**Fig. 66**, B). This result was confirmed by the dot plots (**Fig. 67**) and platelet volume histograms (**Fig. 68**) demonstrating fewer destroyed cells when using transmembrane substitution. This was in contrast to the finding mentioned above leading to the conclusion that WBCs are even very sensitive to the osmotic shock and SDial pre-HDF using transmembrane substitution represents a particularly gentle method of infusing NaCl at high concentrations.

The TMP increased only for the standard pre-HDF with 1.20 M $[NaCl]_{SUB}$ and for the SDial pre-HDF 0.75 M $[NaCl]_{blood}$ (**Fig. 65**) conforming fouling of the dialysis membrane surface with the cell fragments as indicated above (see "Experiments on a dialysis machine and under dynamic conditions") (52).

In order to assess the protective effect of the first cartridge of the SDial setup against the concentration gradient, a pilot experiment in HD modus (Q_{inf} = 0 mL/min) at 0.50 M $[NaCl]_{blood}$ was designed. Two concentration gradients (0.55 and 1.10 M NaCl on the dialysate side; see **Fig. 80**) were compared and a single blood pool was taken allowing a better comparison of the biological parameters in only a single experiment. Hemolysis was higher with the higher [NaCl] gradient (i.e., 1.10 M NaCl; **Fig. 56**) reaching 4.0% *versus* 0.2% with 0.55 M NaCl on the dialysate side. Therefore, the porous membrane represents no direct physical protection for the blood cells against the hypertonic dialysate. The formation of a highly hypertonic aqueous layer in the blood stream next to the porous membrane inducing an important osmotic stress onto the RBC may explain the stronger hemolysis

obtained with the more concentrated dialysate. The WBC count increased at the beginning of the experiment until 30 min, most probably because of insufficient mixing of the blood at baseline. Subsequently, it slightly faster decreased with 1.10 M [NaCl] in the dialysate (**Fig. 57**) confirming the hypothesis of sensitivity of these cells to the concentration gradient.
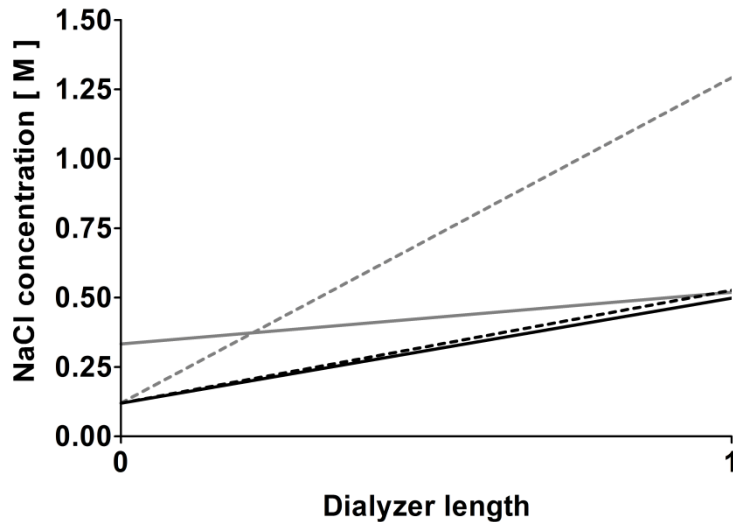
Fig. 80: Modeling of the [NaCl] gradient along the semi-permeable membrane in the first cartridge of the SDial setup. The [NaCl] was assessed by simulation of HD with the SDial setup on the blood (——, - - - -) and dialysate side (——, - - - -) for different flow rates: Q_{ex} = 300 mL/min (solid line) and Q_{ex} = 50 mL/min (dotted line). The dialyzer length corresponds to the blood inlet (0) and outlet (1). The concentration gradient is minimized by maximizing Q_{ex}.

In the second part of the continued experiment, blood was further dialyzed without infusion of 5.00 M NaCl solution, thus, $[NaCl]_{blood}$ was restored to physiologic conditions. The decrease of the $[NaCl]_{blood}$ from about 0.50 to 0.15 M led to no further damage of blood cells (**Fig. 56**, **Fig. 57**, and **Fig. 58**). Thus, it can be concluded that NaCl dialysis is safe since, after stopping the osmotic challenge, blood cells are no more sensitive to mechanical stresses.

Interestingly, although HD was performed (Q_{inf} = Q_{UF} = 0 mL/min), when switching from 0.50 M to 0.15 M $[NaCl]_{blood}$, the TMP in the first cartridge increased about 20 to 25 mmHg which is in the range of the oncotic pressure (91). Thus, at high [NaCl] on the dialysate side, water is osmotically driven into this compartment (TMP < 0 mmHg), a process well-known in peritoneal dialysis where the tonicity is obtained by altering the dextrose concentration (5), whereas under physiological conditions, the protein concentration drags water into the blood (TMP > 0 mmHg) (124).

3) <u>Toxin removal efficacy</u>

After having demonstrated adequate hemocompatibility of the SDial setup, the protein bound toxin removal was assessed. A pilot experiment was designed with mini-dialyzers to compare the removal of IS from normal human normal plasma between single dialyzer HD and serial dialyzers HD (**Fig. 17**). Since IS was removed much more efficiently with serial HD using independent dialysate loops compared with standard single dialyzer HD (**Fig. 74**; 5.72 ± 0.21 %/run *versus* 2.81 ± 1.09 %/run), it was tried to further exploit the first hemodialyzer of the SDial setup. Additionally to its function as NaCl diffuser, the first cartridge was set up to also remove uremic toxins like the second hemodialyzer. Different setups to implement the

additional hemodialyzer for this function are presented in **Tab. 22** illustrating respective advantages and drawbacks. The SDial setup with charcoal adsorber was implemented because this setup requires a single dialysis machine, the volume of dialysate is not increased, the volume of NaCl solution is minimized, and it allows an adjustment of the dialysate temperature in the first cartridge. Since activated charcoal is known to adsorb hydrophobic compounds, such as fatty acids (157), protein bound uremic toxins (110; 158), and also β_2m (158; 159), it was decided to add a charcoal adsorber. The adsorber consisted of a reservoir filled with activated carbon which was integrated into the dialysate loop to remove IS diffusing into the dialysate (**Fig. 18**). Activated charcoal-based adsorbers are used in specific clinical situations since decades. The MARS (160; 161; 162) and the Prometheus (163) systems are typical, elaborated representatives, which are applied for the treatment of liver failure.

The removal of IS from normal human plasma was studied on a dialysis machine. The setup was built in order to switch from one setting to the other but the plasma volume was different between standard pre-HDF and SDial pre-HDF because of the additional volume of the second cartridge. The removal rate γ of IS was calculated based on the blood runs (**Eq. 13**). Therefore, the results were independent from the plasma volume. The same high-flux dialyzers (1.7 m²) deriving from the same batch as the hemocompatibility experiments were used to avoid variations in the membrane permeability (91).

Based on removal models (86; 105) and the binding experiments performed in normal human plasma at different ionic strength (**Fig. 30**) , the removal rate of IS should be doubled when increasing the ionic strength from 0.15 to 0.50 M NaCl in undiluted normal plasma to increase the free IS fraction from about 3% to 7% (**Eq. 3** and **Fig. 28**). Nevertheless, γ of IS increased only about 43% and 52% for both the standard pre-HDF and the SDial pre-HDF, respectively (**Fig. 75**). A likely explanation for the difference between the theoretical approach (**Eq. 3**) and the experimental results could be the removal of NaCl within the hemodialyzer which leads to a progressively decreasing concentration along the cartridge with the consequence of a proportionally reduced free toxin fraction.

Adding the charcoal adsorber into the closed dialysate loop not significantly increased γ of IS of about 13%. The adsorber was tailored with sufficiently activated charcoal (2 g) to bind the diffused toxin. Based on a pilot experiment in aqueous solution, which estimated the adsorption capacity of charcoal for IS to be about 17 μmol/g, γ of IS with the activated charcoal adsorber was expected to be doubled. This estimation by far was not reached, most probably, because the dialysate perfusion through the self made charcoal adsorber was insufficient. Therefore, the experiment should be repeated with a commercially available adsorber to verify the results of the setting. It was not possible to perform this experiment in the laboratory because of the expensiveness of such devices.

Set-up	Dual dialyzers with dialysate lines connected in parallel (164)	Dual dialyzers with dialysate lines connected in series (164)	Collins' set-up (114)	Serial dialyzers with charcoal adsorber
Description				
Advantages	• Both dialyzers independent allowing increased dialysis doses. • HD, pre- and post-HDF feasible. • Adjustment of the dialysate temperature possible.	• Normal dialysate volume. • Low volume of NaCl solution. • HD, pre- and post-HDF feasible.	• Normal dialysate volume. • HD, pre- and post-HDF feasible.	• Normal dialysate volume. • Low volume of NaCl solution. • HD, pre- and post-HDF feasible. • Adjustment of the dialysate temperature possible.
Drawbacks	• Requires high volume of dialysate. • Requires a 2nd dialysis monitor. • Requires high volume of NaCl solution.	• Q_D split to the dialyzers resulting in lower clearance.	• Requires peristaltic pump between both dialyzers on the dialysate line to control flow rates and avoid shunt-flow. • Recirculation of toxins removed in the 2nd cartridge possible. • Requires high volume of NaCl solution.	• Requires peristaltic pump to circulate dialysate in the 1st cartridge. • Requires adsorber to remove toxins diffused into the closed loop.

Tab. 22: Variations of serial dialyzers HD with increased ionic strength.
Advantages and drawbacks are given.

IV. Transfer of increased ionic strength HDF to the animal model

> **Main findings:**
> - The animal model demonstrated the adequate hemocompatibility of increased ionic strength during HDF.

1) Validation of the animal model

Sheep models, which are accepted in the ISO 10993-4, have been used to study the influence of hemodialysis membranes on living biological systems in the past (92; 149; 165). Since the behavior of blood cells during increased ionic strength HDF and, to a lesser extent, the activation of coagulation were the main focus, pilot experiments comparing human and ovine RBC at different ionic strengths under static and dynamic conditions were performed.

Under static conditions, ovine RBCs were significantly more resistant to high [NaCl] compared to human RBC (**Fig. 76**), more precisely, the hemolysis level was 0.2 ± 0.1% in ovine blood *versus* 0.5 ± 0.2% ($P < 0.05$) in human blood. This finding, supported by previous studies reporting a higher osmotic resistance of sheep RBC compared to human RBC in both hypotonic (166) and hypertonic media (121), may be explained as follows. As mentioned above, the osmotic resistance of erythrocytes increases as cell volume decreases (121). Moreover, sheep RBC are smaller than human's (121; 167) (mean cell volume: 29.0 ± 0.41 fL *versus* 89.2 ± 0.59 fL) which correlates with an improved cell deformability (168). The higher osmotic resistance of sheep RBC might also be explained by this specie's evolution. Sheep belong to the bovidea family like caprids and antelopes. These animals originate from dry geographical regions (169). Therefore, their metabolism is adapted to overcome periods without water (170). When retaining mineral salts during insufficient fluid supply, their blood cells must be adapted to support high osmolarity, i.e., ovine RBCs are more resistant to osmotic changes.

However, under dynamic conditions using a mini-dialyzer apparatus (**Fig. 77**), hemolysis was similar between human and ovine blood when exposed to the same [NaCl] as well as the minor hemolysis induced by the blood pump. Therefore, the choice of sheep for the dialysis model of increased ionic strength HDF was justified.

2) Feasibility of increased ionic strength HDF

A low-flux filter was chosen for the first serial cartridge of the SDial setup to avoid as much as possible backfiltration as an interfering factor (171). The second dialyzer consisted in a high-flux membrane with high K_0A in order to remove as much as possible the NaCl excess (**Fig. 43**). Initially, the [NaCl] of the two tested settings, i.e., standard pre-HDF (0.75 M $[NaCl]_{SUB}$) and SDial-TM pre-HDF (0.15 M $[NaCl]_{SUB}$), was set at 0.36 M $[NaCl]_{blood}$ because adverse effects were never previously seen at this concentration *ex vivo* (**Fig. 60** to **Fig. 63**).

The [NaCl]$_{blood}$ was increased after an initial 30 min baseline period to wait for fluid equilibration in the setup and to generate baseline data to refer to without running an additional, the animal affecting experiment. After 30 min, cell counts, Hct, and tHb in the arterial sample were slightly decreased (**Tab. 21**; $P < 0.05$) as compared to 0 min because of the mixing of blood with the prerinsing fluid in the extracorporeal circuit. Ion concentrations (K$^+$, range 3.40 – 3.62 mM *versus* 4.11 – 4.26 mM; HCO$_3^-$, range 28.1 – 31.1 mM *versus* 26.6 – 29.5 mM; Na$^+$, range 141.6 – 143.9 mM *versus* 143.5 – 145.3 mM) and the pO$_2$ (range 43.2 – 44.0 mmHg *versus* 47.9 – 65.2 mmHg) were slightly decreased ($P < 0.05$) at baseline indicating an equilibration of the blood electrolytes with the dialysate. The stress relaxation of the animals after catheter placing for blood access and treatment starting was illustrated by the decrease of the heart rate within the first 30 min (0 min, range 100 – 120 beats/min; 30 min, range 70 – 90 beats/min).

Increasing the ionic strength after 30 min dialysis increased the [NaCl]$_{BM}$ (**Tab. 19**; range 362.0 – 370.2 mM) to the expected concentration (0.36 M). It also slightly increased the [NaCl]$_{VEN}$ (range 123.7 – 124.2 mM *versus* 121.0 mM at baseline, $P < 0.05$) indicating an incomplete removal of the NaCl excess. Both hemolysis (0.2 ± 0.1% after 120 min *versus* 0.1 ± 0.1% at baseline, $P < 0.05$) and LDH concentration (490 ± 84 U/L after 120 min *versus* 449 ± 80 U/L at baseline, $P < 0.05$) as an additional clinical marker of hemolysis slightly increased only during the standard pre-HDF with 0.36 M [NaCl]$_{blood}$ (**Fig. 79**). It is however possible that the cell damages result partially from the mechanical stress induced by the extracorporeal setup itself, which was identical during all treatments (blood pump, passage through the hemodialyzer, catheter as blood access) (172; 173; 174; 175). Thus, this very low, but still acceptable hemolysis, most probably, was due to the increased ionic strength. Moreover, no clinical symptoms of bioincompatibility (hypoxia, collapse, increase of the heart rate, tachypnea, etc. (149; 165)) were seen.

After the results were acceptable with 0.36 M [NaCl]$_{blood}$, in a next step, the ionic strength was increased to the presumed maximal admissible *ex vivo* level in order to produce minor hemolysis. The settings were standard pre-HDF at 0.45 M [NaCl]$_{blood}$ (1.10 M [NaCl]$_{SUB}$) and SDial-TM pre-HDF at 0.60 M [NaCl]$_{blood}$ (0.15 M [NaCl]$_{SUB}$). The higher [NaCl] for the SDial-TM pre-HDF was chosen because *ex vivo* results were favorably (see above) with this setup compared to the standard pre-HDF (**Fig. 60** and **Fig. 66**). As compared to 0.36 M [NaCl]$_{blood}$ tested, the PLT count slightly decreased with increased ionic strength (120 min, range 311 – 336 ×10^3/mm^3; baseline, range 348 – 407 ×10^3/mm^3) with both SDial-TM pre-HDF at 0.60 M [NaCl]$_{blood}$ and standard pre-HDF at 0.45 M [NaCl]$_{blood}$. No adverse event was seen in the animal. Blood pressure and heart rate were always constant when increasing the [NaCl]$_{blood}$. Increasing the ionic strength after 30 min dialysis increased the [NaCl]$_{BM}$ (**Tab. 19**; standard pre-HDF, about 475 mM; SDial-TM pre-HDF, about 618 mM) to the expected concentration (0.45 and 0.60 M, respectively). Again, the NaCl excess was not entirely removed ([NaCl]$_{VEN}$ range 125.4 – 130.4 mM *versus* 121.0 mM at baseline, $P < 0.05$). Both hemolysis (0.2 ± 0.1% after 120 min *versus* 0.1 ± 0.1% at baseline, $P < 0.05$) and LDH concentration (506 ± 24 U/L after 120 min *versus* 462 ± 44 U/L at baseline, $P < 0.05$) slightly increased only during the

SDial-TM pre-HDF with 0.60 M $[NaCl]_{blood}$ (**Fig. 79**) pointing again at the increased ionic strength as the likely reason.

Since animal weighted about 43 kg in average, their blood volume can be estimated to be about 2.5 L (176). Hence, their blood had passed about five times through the hemodialyzer (**Eq. 7**). The preliminary *ex vivo* experiments were performed to reach 30 τ in order to design a safe dialysis strategy for the clinical application. It was not possible to dialyze the animals comparably long (30 τ would correspond to about 8 h treatment at Q_B = 150 mL/min, **Eq. 7**) but it provided an idea of an adequate biocompatibility even if a typical normal four hour dialysis session in a maintenance dialysis patient (about 15 τ, see above) is not fully reflected.

NaCl slightly accumulated in the venous line for all settings because of the increased ionic strength (**Tab. 19**; Na^+, range 140.3 – 146.7 mM after 120 min *versus* 137.3 – 139.3 mM at baseline; Cl^-, range 107.1 – 110.5 mM after 120 min *versus* 103.1 – 104.7 mM at baseline). Although the $[NaCl]_{VEN}$ after 60 and 120 min did not significantly (*P* > 0.05) differ between the different settings (possibly because of the small population (i.e., n = 4)), the accumulation of NaCl seemed to be proportional with the $[NaCl]_{blood}$ (**Tab. 19**). Retention of NaCl must be carefully monitored during a clinical application since its homeostasis in uremic patients is crucial (1). Overload of NaCl may lead to hypertension, increased cardiovascular risk, and ultimately to death (115; 116; 177). However, all animals were healthy including a normal renal function allowing the correction of any electrolyte disturbance.

Increasing the ionic strength in blood changed the coloration of the blood into light red (**Fig. 78**). This phenomenon may be explained by the difference of the absorption spectra between O_2Hb and HHb (178) and the decreased amount of O_2Hb (**Tab. 20**; range 77.3% – 89.4% at baseline, range 63.5% – 82.7% at 60 min dialysis) to the benefit of HHb (range 8.1% – 20.0% at baseline, range 14.9% – 33.8% at 60 min dialysis). Increasing the intracellular Cl^- concentration may induce the dissociation of oxygen bound to Hb (O_2Hb dissociates to HHb) (179). HHb in turn would bind HCO_3^- ions, thus, reducing its plasma concentration (180) as observed in the experiment (range 29.4 – 31.5 mM at baseline *versus* range 19.9 – 24.7 at 60 min dialysis). Since carbon monoxide poisoning changes the coloration of the blood into light red too (181; 182), the observed coloration change (**Fig. 78**) arose this question. However, in the present experiments, COHb and MetHb levels were not changed because of increased ionic strength (**Tab. 20**). Moreover the modification of O_2Hb to HHb because of higher $[NaCl]_{blood}$ was reversible. After removal of the excess of NaCl, normal levels of both O_2Hb and HHb were recovered, and no difference was seen between the arterial (O_2Hb; range 57.0% – 63.4% at baseline *versus* range 58.7% – 64.8% at 60 min dialysis; HHb accordingly; range 34.0% – 41.9% *versus* range 32.7% – 38.7%) and venous (O_2Hb; range 73.9% – 78.5% at baseline *versus* range 70.1% – 78.9% at 60 min dialysis; HHb accordingly; range 18.9% –

23.3% *versus* range 18.6% – 27.2%) samples. Therefore, the modification of the Hb induced by increased ionic strength has no impact on the clinical application of modified pre-HDF.

A single alarming event was observed during SDial-TM pre-HDF. Previously uneventfully treated with standard pre-HDF, the TMP of the second hemodialyzer increased immediately after beginning of the dialysis experiment before increasing the $[NaCl]_{blood}$. After restitution of the blood from the extracorporeal circuit, it became obvious that the hemodialyzer membrane was clotted as already indicated by accumulation of NaCl in the venous line ($[NaCl] = 170$ mM). The reason for this event remained unclear because it occurred despite correctly administered anticoagulation. From the long lasting experience with the sheep dialysis model, it was already known that this species seems to possess a more active coagulation compared to human patients (personal communication of unpublished data). Nevertheless, this incident underlines a potential hazard of ionic strength HDF which requires a fully patent dialyzer not only for toxin elimination but also for restoration of the NaCl balance.

CONCLUSION

The present thesis demonstrated that increasing the ionic strength by increasing the [NaCl] in human blood was effective to increase the removal of the protein bound uremic toxins IS and pCS by decreasing their binding affinity in both normal and uremic plasma. This method was applicable during modified pre-dilution HDF with adequate hemocompatibility. The hemocompatibility was further improved by developing a serial dialyzers setup which has the major advantage to allow HD, pre-dilution HDF, and post-dilution HDF. The SDial setup was designed with a closed dialysate loop at the first cartridge to use the same dialysate flow rate as for standard treatments and minimize the required volume of NaCl solution. This setup may be further developed to fully exploit the first hemodialyzer, which potentially could double the normal dialysis dose by adding commercially available adsorbers (183). Furthermore, in order to dissociate the protein binding, the temperature in the first cartridge may be increased. This must be done with caution to avoid protein denaturation and hemolysis. According to the literature, a maximum of 47 °C may be tolerated (52; 184). The second cartridge will be used to restore the blood temperature to the desired level.

After the feasibility of the method was demonstrated in an animal model, its clinically safe applicability and efficacy has to be proven on the short and the long term by demonstrating increased protein bound uremic toxin clearance and, ideally, improved patient outcome. Even if the clearance of protein bound toxins is improved, the equilibrium between the different compartments of the body, which is proportional to the distribution volume of the toxin, will impact on the total elimination and finally on clinical outcomes (1; 185). For long term studies, a partnership with dialysis machine manufacturers must be developed in order to modify current hemodialysis machines for a safe use in the patient (186). Particularly crucial aspects are the control of the flow rates (Q_{ex}) to avoid excessive concentration gradients at the first cartridge and the prevention of the accumulation of NaCl. In the experimental setting, two separate hemodialyzers were applied to perform SDial dialysis. Such an arrangement could be integrated in a single device similarly to the Nephros OLpūr™ MD hemodiafilter (187) or the Bellco HFR Aequilibrium dialyzer.

Increasing the Q_B to comply with clinical practice (Q_B up to 500 mL/min) correlates with decreased clearance of NaCl. Concentrations higher than physiologic may flow back to the patients. In order to avoid this problem, an alternative would be to reduce the ionic strength in the dialysate similarly to the description of Collins et al. for pH shift (114). The handling of the [NaCl] is of great importance in clinical practice because hypernatremia is related to hypertension and morbidity in uremic patients (115; 116; 188; 189). Since at the end of dialysis the extracorporeal circuit is rinsed with saline to return the blood to the patient (91), the infusion of NaCl has to be stopped before completion of the treatment. Clinical application requires also the use of sterile and non-pyrogenic NaCl solution which has to be manufactured according to pharmacopoiea.

Together with ameliorations of the technology, the patient recruitment should be done carefully. Patients with low Hb concentration may be at greater risk for hemolysis when $[NaCl]_{blood}$ is increased. Moreover, during the first clinical trial, the influence of increased ionic strength hemodialysis on the *in vivo* RBC life span (134) and RBC fragility (134) has to be determined.

The present work focused on CKD but protein bound substances also play a role in other diseases. Modified ionic strength HDF may be applicable in liver insufficiency or in the treatment of intoxications with protein bound drugs. Furthermore, this dialysis strategy may be coupled with other methods. Flow rates and larger dialyzers may be adjusted to selectively increase the clearance of protein bound uremic toxins (190). The dialysis frequency and duration with and without NaCl infusion may be adapted to increase toxin removal and improve biocompatibility (191). Moreover, the closed dialysate loop of the SDial setup may be filled with an albumin solution and adsorbents similarly to the MARS system (162). In such a manner, the clearance of protein bound toxins would be increased in the first cartridge while NaCl diffuses into the blood stream. The functional efficacy would be restored in the adsorbers.

APPENDIX

I. Additional theoretical aspects

A complete demonstration of the ligand-receptor theory (84) for a single high-affinity binding site on the protein surface is proposed as follows.

Abbreviations:
- *[R]*   free receptor concentration
- *[L]*   free ligand concentration
- *[RL]*   complex ligand-receptor concentration
- *[L_T]*   total ligand concentration (*[L_T] = [RL] + [L]*)

The maximal binding capacity B_m (84) is given by

$$B_m = [R] + [RL]$$

The binding affinity will be described through the dissociation constant K_D of the equilibrium (84)
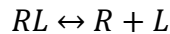
$$RL \leftrightarrow R + L$$

with:

$$K_D = \frac{[R].[L]}{[RL]}$$

Since *[R] = B_m − [RL]*, then

$$K_D = \frac{(B_m - [RL]).[L]}{[RL]}$$

The equation can be solved for *[RL]*:

$$[RL] = \frac{B_m.[L]}{K_D + [L]}$$

This equation is for proteins presenting a single type of **high affinity binding site**. When *[L] = K_D*, 50% of the receptors are bound to ligands. It is proposed here to define the protein bound fraction *PBF* as a function of K_D and B_m as follows:

$$PBF = \frac{[RL]}{[L] + [RL]} = \frac{[RL]}{[L_T]}$$

For that purpose, *[RL]* has to be expressed depending on *[L_T]*:

$$[RL] = \frac{B_m.[L]}{K_D + [L]} = \frac{B_m.([L_T] - [RL])}{K_D + ([L_T] - [RL])}$$

$$[RL] = \frac{B_m.[L_T] - B_m.[RL]}{K_D + [L_T] - [RL]}$$

It leads to

$$[RL].K_D + [RL].[L_T] - [RL]^2 = B_m.[L_T] - B_m.[RL]$$

$$[RL].K_D + [RL].[L_T] - [RL]^2 - B_m.[L_T] + B_m.[RL] = 0$$

$$[RL].(K_D + [L_T] + B_m) - [RL]^2 - B_m.[L_T] = 0$$

This equation is of the type $a.x^2 + b.x + c = 0$ and to solve it, its differential Δ has to be calculated with:

$$\begin{cases} a = -1 \\ b = K_D + [L_T] + B_m \\ c = -B_m.[L_T] \end{cases}$$

$$\Delta = b^2 - 4.a.c = (K_D + B_m + [L_T])^2 - 4 \times (-1) \times (-B_m.[L_T])$$

$$\Delta = K_D{}^2 + B_m{}^2 + [L_T]^2 + 2.K_D.B_m + 2.K_D.[L_T] + 2.B_m.[L_T] - 4.B_m.[L_T]$$

$$\Delta = K_D{}^2 + B_m{}^2 + [L_T]^2 + 2.K_D.B_m + 2.K_D.[L_T] - 2.B_m.[L_T]$$

$\Delta > 0$ if $[L_T] = 0$, or if $[L_T] << K_D$, or if $[L_T] << B_m$, or if $[L_T] >> K_D$, or if $[L_T] >> B_m$.

It means that the equation $a.x^2 + b.x + c = 0$ admits two solutions:

$$\begin{cases} x_1 = \frac{-b - \sqrt{\Delta}}{2a} \\ x_2 = \frac{-b + \sqrt{\Delta}}{2a} \end{cases}$$

Since $x_1 < 0$, this solution is not physically possible, thus only x_2 remains:

$$[RL] = \frac{-(K_D + B_m + [L_T]) + \sqrt{\Delta}}{2 \times (-1)}$$

$$[RL] = \frac{(K_D + B_m + [L_T]) - \sqrt{\Delta}}{2}$$

$$[RL] = \frac{K_D + B_m + [L_T] - \sqrt{(K_D + B_m + [L_T])^2 - 4.B_m.[L_T]}}{2}$$

So the PBF becomes:

$$PBF = \frac{[RL]}{[L_T]} = \frac{K_D + B_m + [L_T] - \sqrt{(K_D + B_m + [L_T])^2 - 4.B_m.[L_T]}}{2.[L_T]}$$

The ratio toxin concentration / binding capacity α can be introduced here:

$$\alpha = \frac{[L_T]}{B_m} \Leftrightarrow [L_T] = \alpha.B_m$$

Then, the PBF becomes

$$PBF = \frac{K_D + (\alpha + 1).B_m - \sqrt{(K_D + (\alpha + 1).B_m)^2 - 4.\alpha.B_m^2}}{2.\alpha.B_m}$$

$$PBF = \frac{K_D + (\alpha + 1).B_m}{2.\alpha.B_m} - \frac{\sqrt{(K_D + (\alpha + 1).B_m)^2 - 4.\alpha.B_m^2}}{2.\alpha.B_m}$$

$$PBF = \frac{\left(\frac{K_D}{B_m} + \alpha + 1\right).B_m}{2.\alpha.B_m} - \sqrt{\frac{(K_D + (\alpha + 1).B_m)^2 - 4.\alpha.B_m^2}{4.\alpha^2.B_m^2}}$$

$$PBF = \frac{\left(\frac{K_D}{B_m} + \alpha + 1\right).B_m}{2.\alpha.B_m} - \sqrt{\frac{\left(\left(\frac{K_D}{B_m} + \alpha + 1\right).B_m\right)^2 - 4.\alpha.B_m^2}{4.\alpha^2.B_m^2}}$$

$$PBF = \frac{\left(\frac{K_D}{B_m} + \alpha + 1\right).B_m}{2.\alpha.B_m} - \sqrt{\frac{\left(\frac{K_D}{B_m} + \alpha + 1\right)^2.B_m^2 - 4.\alpha.B_m^2}{4.\alpha^2.B_m^2}}$$

B_m can be eliminated as follows:

$$PBF = \frac{\frac{K_D}{B_m} + \alpha + 1}{2.\alpha} - \sqrt{\frac{\left(\frac{K_D}{B_m} + \alpha + 1\right)^2 - 4.\alpha}{4.\alpha^2}}$$

Finally, the PBF may be described by:

$$PBF = \frac{\frac{K_D}{B_m} + \alpha + 1 - \sqrt{\left(\frac{K_D}{B_m} + \alpha + 1\right)^2 - 4.\alpha}}{2.\alpha}$$

With $\alpha = [L_T] / B_m$.

II. Interest of calculating the blood runs through the dialyzer

The concentration reduction of toxin from blood or plasma corresponds to a first-order process (11). It is possible to present results on a time t dependant axis or a blood run τ dependant axis, with

$$\tau = t.\frac{Q_B}{V_B}$$

Where Q_B is the blood flow rate [mL/min], and V_B the blood volume [mL]; τ is dimensionless.

The concentration is given by (83):

$$\begin{cases} C = C_0.e^{-\beta.t} \\ C = C_0.e^{-\gamma.\tau} \end{cases}$$

With β and γ the corresponding slopes. What is the relationship between β and γ? Since

$$C = C_0.e^{-\beta.t} = C_0.e^{-\gamma.\tau}$$

Removing C_0,

$$e^{-\beta.t} = e^{-\gamma.\tau}$$

Finally,

$$\beta.t = \gamma.\tau$$

It is known that (83):

$$\beta = \frac{K_B}{V_B}$$

With K_B, the blood clearance of the solute [mL/min]. According to the definition of τ and β,

$$\beta.t = \gamma.t.\frac{Q_B}{V_B} \Leftrightarrow \beta = \gamma.\frac{Q_B}{V_B} \Leftrightarrow \frac{K_B}{V_B} = \gamma.\frac{Q_B}{V_B}$$

leading to

$$\gamma = \frac{K_B}{Q_B}$$

Yet, it is known that K_B corresponds to the blood flow rate Q_B times the apparent free fraction FF_{app} of the toxin:

$$\gamma = \frac{K_B}{Q_B} = \frac{FF_{app}.Q_B}{Q_B} = FF_{app}$$

To conclude:

$$\begin{cases} C = C_0 . e^{-\frac{K_B}{V_B}.t} \\ C = C_0 . e^{-FF_{app}.\tau} \end{cases}$$

Note: further refinement is to describe the apparent free fraction FF_{app} of the toxin, which corresponds to the actual fraction removed, from the free toxin fraction FF (depending only on the binding constants K_D and B_m and the toxin concentration) and the filter permeability π (taking into account the diffusion and convection capacity of the dialyzer and restoration of the equilibrium).

$$\gamma = FF_{app} = FF.\pi$$

III.   Determination of the binding constants K_D and B_m

1) Of healthy plasma for PAA

The binding affinity of normal human plasma for PAA was assessed at different ionic strengths. Different plasma dilutions (final volume 4 mL) were used: 0.15 M NaCl was tested with 3.48 mL plasma; 0.40, 0.50, and 0.65 M NaCl was tested with 3.08 mL plasma.
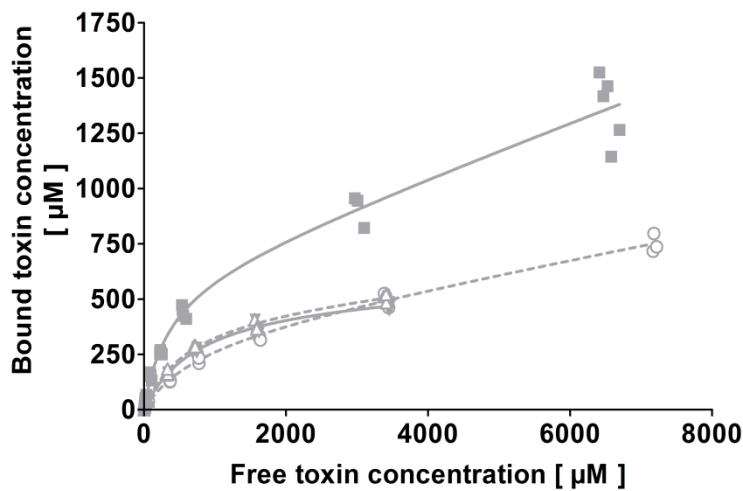
Fig. 81: Binding of PAA in normal human plasma at different ionic strengths.
Binding experiments were performed in citrate plasma from the same donor in triplicate (n = 3) at room temperature, pH 7.4, and with 0.15 (■), 0.40 (△), 0.50 (▼), and 0.65 M (○) NaCl. The plasma dilution factor was 1.15 for 0.15 M NaCl and otherwise 1.30.
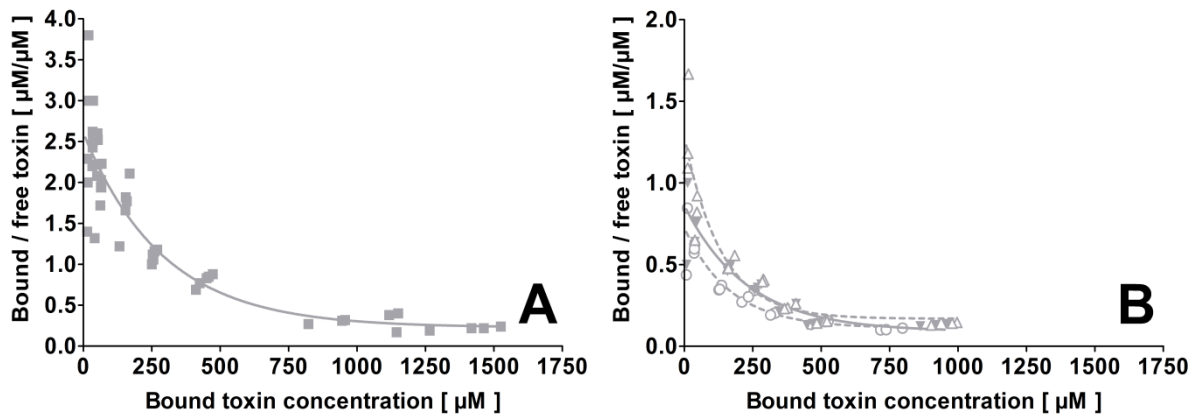
Fig. 82: Scatchard plot deriving from the binding studies on PAA in normal human plasma.
The Scatchard plot is shown for: A, 0.15 M NaCl (■); B, 0.40 (△), 0.50 (▼), and 0.65 M (○) NaCl. Plasma dilution factor was 1.15 (A) and 1.30 (B). These curves indicate two types of binding sites: the first one of high affinity and the second one of low affinity corresponding to the specific and nonspecific binding, respectively.

2) <u>Of uremic plasma for IS and *p*CS</u>

The binding constants of uremic plasma for IS and *p*CS (native concentrations) were assessed at different ionic strengths in a population of 15 ESRD patients. As shown below, the population was still too small to obtain relevant values for K_D and B_m.
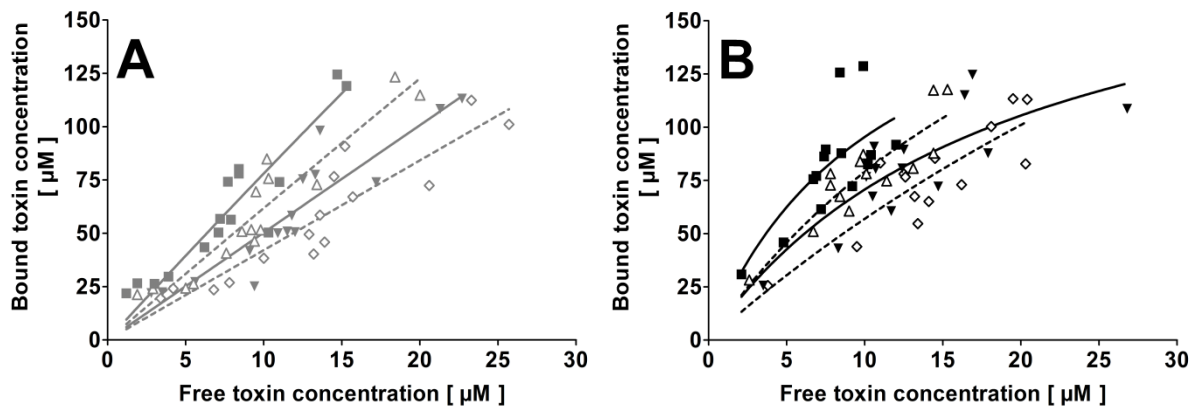
Fig. 83: Binding of IS and *p*CS in uremic plasma at different ionic strengths.
Binding experiments were performed in half-diluted human plasma from 15 different ESRD patients (n = 15) with IS (A) and *p*CS (B) at room temperature, pH 7.4, and with 0.15 (■), 0.30 (△), 0.50 (▼), and 0.75 M (○) NaCl. Binding constants were: for IS, K_D = 406, 1186, 136219, and 58750 µM; B_m = 3247, 7390, 686137, and 247429 µM; for *p*CS, K_D = 11.2, 26.8, 19.3, and 68.1 µM; B_m = 202, 291, 207, and 445 µM, at 0.15, 0.30, 0.50, and 0.75 M NaCl, respectively.

3) Effect of dilution on the binding ability of plasma for IS

The effect of plasma dilution (plasma 1:2- and 1:10-diluted) on the binding constant K_D and B_m for IS was studied at 0.15 and 0.50 M NaCl at room temperature and pH 7.4. The binding curves presented below (**Fig. 84**) were obtained in citrate plasma from three single donors (n = 3).
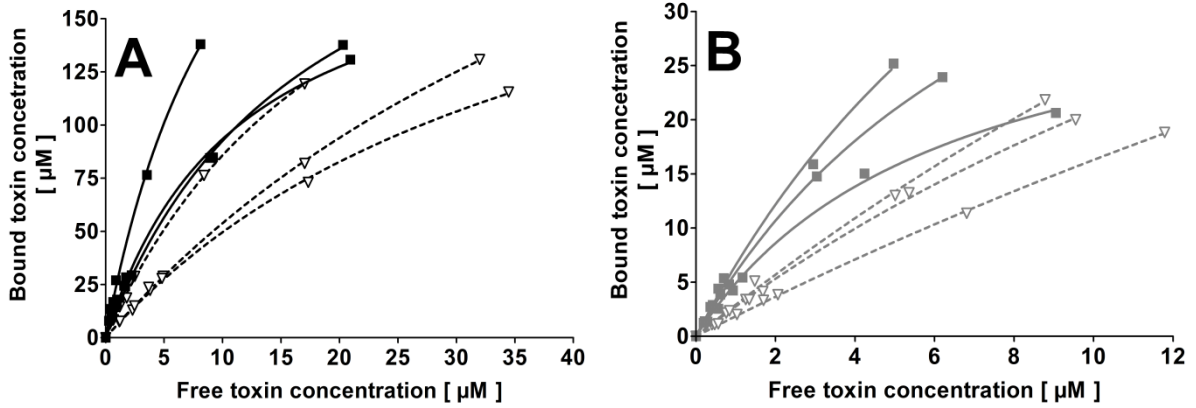
Fig. 84: Binding of IS in normal human plasma at different plasma dilutions and ionic strengths.
Binding experiments were performed in human plasma from 3 single donors (n = 3) at 0.15 (—■—, —■—) and 0.50 M NaCl (--▽--, --▽--). Plasma was 1:2- (A) and 1:10-diluted (B). Data were interpolated by non linear regression using **Eq. 2**; each curve represents one single donor.

IV.   Simulation of increased ionic strength in aqueous solution on a dialysis machine

1) Definitions and notations

V_B, blood volume [mL]; $C_{NaCl\ blood}$, NaCl concentration in blood [M]; $C_{NaCl\ dialysate}$, NaCl concentration in the dialysate [M]; Δt, time interval [min]; Q_B, blood flow rate [mL/min]; Q_D, dialysate flow rate [mL/min]; $Q_{D\ in}$, dialysate flow rate entering the hemodialyzer [mL/min]; $Q_{D\ out}$, dialysate flow rate exiting the hemodialyzer [mL/min]; Q_{ex}, dialysate flow rate in the closed loop (serial dialyzers setup only); Q_{NaCl}, infusion flow rate (default: a 5.00 M NaCl solution) [mL/min]; Q_{inf}, substituate flow rate [mL/min]; Q_{UF}, ultrafiltration flow rate [mL/min]; K, instantaneous whole blood clearance [mL/min]; and K_0A, the mass transfer coefficient over the area [mL/min]. $C_{NaCl\ blood}$ and $C_{NaCl\ dialysate}$ are set to 0.12 M NaCl.

$$K = Q_B \cdot \left[\frac{e^{K_0 A \cdot \left(\frac{Q_D - Q_B}{Q_D \cdot Q_B} \right)} - 1}{e^{K_0 A \cdot \left(\frac{Q_D - Q_B}{Q_D \cdot Q_B} \right)} - \frac{Q_B}{Q_D}} \right]$$

Eq. 18: Instantaneous blood clearance calculated from the K_0A(11)**.**
Where K is the clearance [mL/min], Q_B the blood flow rate [mL/min], Q_D the dialysate flow rate [mL/min], and K_0A the mass transfer coefficient over the area of urea [mL/min].

2) Algorithm

a. Standard pre-dilution HDF with the Bellco dialysis machine

i. Working hypotheses

With the dialysis apparatus Bellco Formula 2000 (see **Fig. 8**), Q_{inf} and Q_{UF} are both removed from the dialysate line according to $Q_{D\ in} = Q_D - Q_{inf} - Q_{UF}$. V_B is supposed to be constant during dialysis (whether restored *in vitro* by an external pump or *in vivo* through fluid equilibrium within the body). Within the hemodialyzer, NaCl removal occurs firstly by convection and secondly by diffusion. Therefore, the concentrations on both the blood and dialysate side are modified after convection to take into account the mass transfer and counter-current flows.

Fig. 85: Model of NaCl mass balance during standard pre-dilution HDF with the Bellco dialysis machine.
The following spots are highlighted: A, patient; B, blood line; C, substituate line; D, dialyzer blood inlet; E, NaCl removal within the dialyzer (occurring by convection and diffusion); F, dialyzer blood outlet.

$$Q_F = Q_{inf} + Q_{UF}$$

$$Q_{B\ app} = Q_B - Q_{UF}$$

$$Q_{D\ in} = Q_D - Q_F$$

$$K = Q_{B\ app}.\left[\frac{e^{K_0 A.\left(\frac{Q_{D\ in} - Q_{B\ app}}{Q_{D\ in}.Q_{B\ app}}\right)} - 1}{e^{K_0 A.\left(\frac{Q_{D\ in} - Q_{B\ app}}{Q_{D\ in}.Q_{B\ app}}\right)} - \frac{Q_{B\ app}}{Q_{D\ in}}}\right].\Delta t$$

A - Patient (see Fig. 85):

$$C_{NaCl\ patient}^{t=0} = C_{NaCl\ blood} \Rightarrow n_{NaCl\ patient}^{t=0} = C_{NaCl\ patient}^{t=0}.V_B$$

$$n_{NaCl\ patient}^{t} = n_{NaCl\ patient}^{t-1} - n_{NaCl\ blood\ line}^{t-1} + n_{NaCl\ ven}^{t-1} \Rightarrow C_{NaCl\ patient}^{t} = \frac{n_{NaCl\ patient}^{t}}{V_B}$$

B - Blood line before access of the substituate line (see Fig. 85) :

$$C_{NaCl\ blood\ line}^{t} = C_{NaCl\ patient}^{t} \Rightarrow n_{NaCl\ blood\ line}^{t} = C_{NaCl\ blood\ line}^{t}.Q_B.\Delta t$$

C - Substituate line (see Fig. 85):

$$n_{NaCl\ inf}^{t} = C_{NaCl\ dialysate}.Q_{inf}.\Delta t + 5.Q_{NaCl}.\Delta t \Rightarrow C_{NaCl\ inf}^{t} = \frac{n_{NaCl\ inf}^{t}}{(Q_{inf} + Q_{NaCl}).\Delta t}$$

D - Dialyzer blood inlet (see Fig. 85):

$$n_{NaCl\ art}^{t} = n_{NaCl\ inf}^{t} + n_{NaCl\ blood\ line}^{t} \Rightarrow C_{NaCl\ art}^{t} = \frac{n_{NaCl\ art}^{t}}{(Q_B + Q_{inf} + Q_{NaCl}).\Delta t}$$

E - NaCl removal within the dialyzer (see Fig. 85):

$$n_{NaCl\ convection}^{t} = (Q_F + Q_{NaCl}).C_{NaCl\ art}^{t}.\Delta t$$

$$\Rightarrow \begin{cases} C'^{t}_{NaCl\ art} = \dfrac{n_{NaCl\ art}^{t} - n_{NaCl\ convecection}^{t}}{(Q_B - Q_{UF}).\Delta t} \\[4mm] C'_{NaCl\ dialysate} = \dfrac{C_{NaCl\ dialysate}.Q_{D\ in}.\Delta t + n_{NaCl\ convecection}^{t}}{Q_D.\Delta t} \end{cases}$$

$$n_{NaCl\ diffusion}^{t} = K.\left(\frac{2.C_{NaCl\ art}^{t} + C'^{t}_{NaCl\ art}}{3} - \frac{2.C_{NaCl\ dialysate} + C'_{NaCl\ dialysate}}{3}\right).\Delta t$$

F - Dialyzer blood outlet (see Fig. 85):

$$n_{NaCl\ ven}^{t} = n_{NaCl\ art}^{t} - n_{NaCl\ convecection}^{t} - n_{NaCl\ diffusion}^{t} + C_{NaCl\ blood}.Q_{UF}.\Delta t$$

$$C_{NaCl\ ven}^{t} = \frac{n_{NaCl\ ven}^{t}}{Q_B.\Delta t}$$

b. Standard pre-dilution HDF with the Nikkiso dialysis machine

i. Working hypotheses

With the dialysis apparatus Nikkiso DBB-03 (see **Fig. 9**), Q_{inf} and Q_{UF} are independent from the dialysate line according to $Q_{D\ in} = Q_D$ and $Q_{D\ out} = Q_D + Q_{inf} + Q_{UF}$. V_B is supposed to be constant during dialysis (whether restored *in vitro* by an external pump or *in vivo* through fluid equilibrium within the body). Substitute is withdrawn at the same flow rate (Q_{NaCl}) as 5.00 M NaCl solution is injected. NaCl removal occurs firstly by convection and secondly by diffusion. Therefore, the concentrations on both the blood and dialysate side are modified after convection to take into account the mass transfer and counter-current flows.
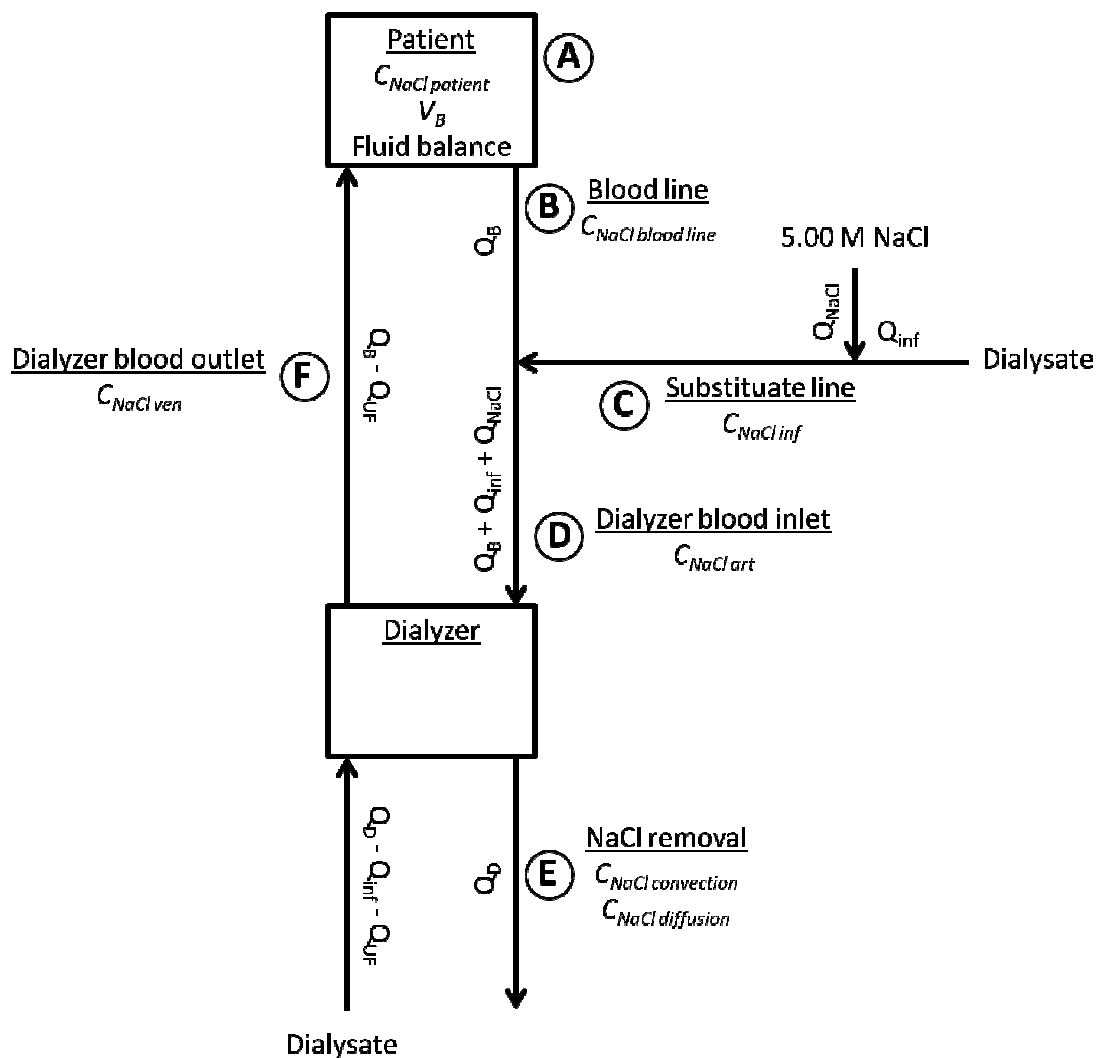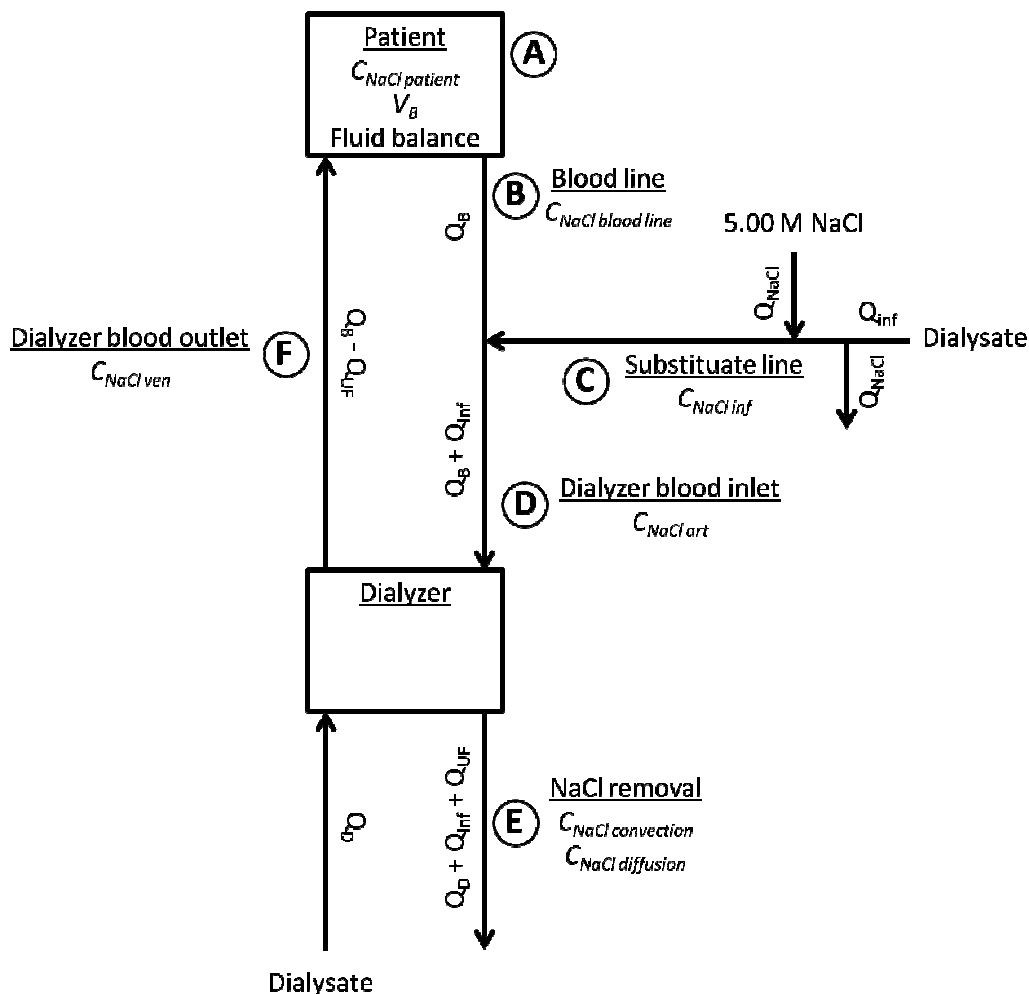

Fig. 86: Model of NaCl mass balance during standard pre-dilution HDF with the Nikkiso dialysis machine.
The following spots are highlighted: A, patient; B, blood line; C, substituate line; D, dialyzer blood inlet; E, NaCl removal within the dialyzer (occurring by convection and diffusion); F, dialyzer blood outlet.

ii. Equations

$$Q_F = Q_{inf} + Q_{UF}$$
$$Q_{B\,app} = Q_B - Q_{UF}$$
$$K = Q_{B\,app}.\left[\frac{e^{K_0A.\left(\frac{Q_D-Q_{B\,app}}{Q_D.Q_{B\,app\,2}}\right)}-1}{e^{K_0A.\left(\frac{Q_D-Q_{B\,app}}{Q_D.Q_{B\,app}}\right)}-\frac{Q_{B\,app}}{Q_D}}\right].\Delta t$$

A - Patient (see Fig. 86):

$$C^{t=0}_{NaCl\,patient} = C_{NaCl\,blood} \Rightarrow n^{t=0}_{NaCl\,patient} = C^{t=0}_{NaCl\,patient}.V_B$$

$$n^t_{NaCl\,patient} = n^{t-1}_{NaCl\,patient} - n^{t-1}_{NaCl\,blood\,line} + n^{t-1}_{NaCl\,ven} \Rightarrow C^t_{NaCl\,patient} = \frac{n^t_{NaCl\,patient}}{V_B}$$

B - Blood line before substituate line (see Fig. 86):

$$C^t_{NaCl} = C^t_{NaCl\,patient} \Rightarrow n^t_{NaCl} = C^t_{NaCl}.Q_B.\Delta t$$

C - Substituate line (see Fig. 86):

$$n^t_{NaCl\,inf} = C_{NaCl\,dialysate}.Q_{inf}.\Delta t + \left(5 - C_{NaCl\,dialysate}\right).Q_{NaCl}.\Delta t$$
$$C^t_{NaCl\,inf} = \frac{n^t_{NaCl\,inf}}{Q_{inf}.\Delta t}$$

D - Dialyzer blood inlet (see Fig. 86):

$$n^t_{NaCl\,art} = n^t_{NaCl\,inf} + n^t_{NaCl} \Rightarrow C^t_{NaCl\,art} = \frac{n^t_{NaCl\,art}}{(Q_B + Q_{inf}).\Delta t}$$

E - NaCl removal within the dialyzer (see Fig. 86):

$$n^t_{NaCl\,convection}$$
$$= Q_F.C^t_{NaCl\,art}.\Delta t \Rightarrow \begin{cases} C'^t_{NaCl\,art} = \frac{n^t_{NaCl\,art} - n^t_{NaCl\,convection}}{(Q_B - Q_{UF}).\Delta t} \\ C'^t_{NaCl\,dialysate} = \frac{C_{NaCl\,dialysate}.Q_D.\Delta t + n^t_{NaCl\,convection}}{(Q_D + Q_F).\Delta t} \end{cases}$$
$$n^t_{NaCl\,diffusion} = K.\left(\frac{2.C^t_{NaCl\,art} + C'^t_{NaCl\,art}}{3} - \frac{2.C_{NaCl\,dialysate} + C'^t_{NaCl\,dialysate}}{3}\right).\Delta t$$

F - Dialyzer blood outlet (see Fig. 86):

$$n^t_{NaCl\,ven} = n^t_{NaCl\,art} - n^t_{NaCl\,convection} - n^t_{NaCl\,diffusion} + C_{NaCl\,blood}.Q_{UF}.\Delta t$$
$$C^t_{NaCl\,ven} = \frac{n^t_{NaCl\,ven}}{Q_B.\Delta t}$$

c. Serial dialyzers setup in pre-dilution HDF

i. Working hypotheses

Additionally to the hypotheses described above (see "Standard pre-dilution HDF with the Nikkiso dialysis machine"), it is supposed that no convection happens within the first hemodialyzer (NaCl transfer through the semi-permeable membrane is purely diffusive). Number "1" and "2" refer to the first and second dialyzer, respectively (see **Fig. 10**).

Fig. 87: Model of NaCl mass balance during SDial pre-dilution HDF with the Nikkiso dialysis machine.
The following spots are highlighted: A, patient; B, blood line; C, substitute line; D, 1st dialyzer blood inlet; E, 1st dialyzer dialysate inlet; F, NaCl transfer within the 1st dialyzer (occurring only by diffusion); G, 1st dialyzer dialysate outlet; H, between dialyzers; I, NaCl removal within the 2nd dialyzer (occurring by convection and diffusion); J, 2nd dialyzer blood outlet.

$$Q_F = Q_{inf} + Q_{UF}$$

$$\begin{cases} Q_{B\ app\ 1} = Q_B + Q_{inf} \\ Q_{B\ app\ 2} = Q_B - Q_{UF} \end{cases}$$

$$\begin{cases} K_1 = Q_{B\ app\ 1} \cdot \left[\dfrac{e^{K_0 A. \left(\frac{Q_{ex} - Q_{B\ app\ 1}}{Q_{ex} \cdot Q_{B\ app\ 1}} \right)} - 1}{e^{K_0 A. \left(\frac{Q_{ex} - Q_{B\ app\ 1}}{Q_{ex} \cdot Q_{B\ app\ 1}} \right)} - \dfrac{Q_{B\ app\ 1}}{Q_{ex}}} \right] . \Delta t \\[30pt] K_2 = Q_{B\ app\ 2} \cdot \left[\dfrac{e^{K_0 A. \left(\frac{Q_D - Q_{B\ app\ 2}}{Q_D \cdot Q_{B\ app\ 2}} \right)} - 1}{e^{K_0 A. \left(\frac{Q_D - Q_{B\ app\ 2}}{Q_D \cdot Q_{B\ app\ 2}} \right)} - \dfrac{Q_{B\ app\ 2}}{Q_D}} \right] . \Delta t \end{cases}$$

A - Patient (see Fig. 87):

$$C_{NaCl\ patient}^{t=0} = C_{NaCl\ blood} \Rightarrow n_{NaCl\ patient}^{t=0} = C_{NaCl\ patient}^{t=0} \cdot V_B$$

$$n_{NaCl\ patient}^{t} = n_{NaCl\ patient}^{t-1} - n_{NaCl\ blood\ line}^{t-1} + n_{NaCl\ ven}^{t-1} \Rightarrow C_{NaCl\ patient}^{t} = \frac{n_{NaCl\ patient}^{t}}{V_B}$$

B - Blood line before substituate line (see Fig. 87):

$$C_{NaCl\ blood\ line}^{t} = C_{NaCl\ patient}^{t} \Rightarrow n_{NaCl\ blood\ line}^{t} = C_{NaCl\ blood\ line}^{t} \cdot Q_B . \Delta t$$

C - Substituate line (see Fig. 87):

$$n_{NaCl\ inf}^{t} = C_{NaCl\ dialysate} \cdot Q_{inf} . \Delta t \Rightarrow C_{NaCl\ inf}^{t} = \frac{n_{NaCl\ inf}^{t}}{Q_{inf} . \Delta t}$$

D - 1st dialyzer blood inlet (see Fig. 87):

$$n_{NaCl\ art\ 1}^{t} = n_{NaCl\ inf}^{t} + n_{NaCl\ blood\ line}^{t} \Rightarrow C_{NaCl\ art\ 1}^{t} = \frac{n_{NaCl\ art\ 1}^{t}}{(Q_B + Q_{inf}) . \Delta t}$$

E - 1st dialyzer dialysate inlet (see Fig. 87):

$$n_{NaCl\ IN\ 1}^{t=0} = C_{NaCl\ dialysate} \cdot Q_{ex} . \Delta t + (5 - C_{NaCl\ dialysate}) \cdot Q_{NaCl} . \Delta t$$

$$n_{NaCl\ IN\ 1}^{t} = C_{NaCl\ OUT\ 1}^{t-1} \cdot Q_{ex} . \Delta t + (5 - C_{NaCl\ OUT\ 1}^{t-1}) \cdot Q_{NaCl} . \Delta t \Rightarrow C_{NaCl\ IN\ 1}^{t} = \frac{n_{NaCl\ IN\ 1}^{t}}{Q_{ex} . \Delta t}$$

F - NaCl transfer through the porous membrane of the 1st dialyzer (see Fig. 87):

$$n_{NaCl\ convection\ 1}^{t} = 0$$

$$n_{NaCl\ diffusion\ 1}^{t} = K_1 \cdot (C_{NaCl\ art\ 1}^{t} - C_{NaCl\ IN\ 1}^{t}) . \Delta t$$

G - 1st dialyzer dialysate outlet (see Fig. 87):

$$n_{NaCl\ OUT\ 1}^{t} = n_{NaCl\ IN\ 1}^{t} + n_{NaCl\ convection\ 1}^{t} + n_{NaCl\ diffusion\ 1}^{t} \Rightarrow C_{NaCl\ OUT\ 1}^{t} = \frac{n_{NaCl\ OUT\ 1}^{t}}{Q_{ex}.\Delta t}$$

H - 1st dialyzer blood outlet / 2nd dialyzer blood inlet (see Fig. 87):

$$n_{NaCl\ A/V}^{t} = n_{NaCl\ art}^{t} - n_{NaCl\ convection\ 1}^{t} - n_{NaCl\ diffusion\ 1}^{t} \Rightarrow C_{NaCl\ A/V}^{t} = \frac{n_{NaCl\ A/V}^{t}}{(Q_B + Q_{inf}).\Delta t}$$

I - NaCl removal within the 2nd dialyzer (see Fig. 87):

$$n_{NaCl\ convection\ 2}^{t}$$

$$= C_{NaCl\ A/V}^{t}.Q_F.\Delta t \Rightarrow \begin{cases} C'_{NaCl\ A/V}^{t} = \dfrac{n_{NaCl\ A/V}^{t} - n_{NaCl\ convection\ 2}^{t}}{(Q_B - Q_{UF}).\Delta t} \\[4mm] C'_{NaCl\ IN\ 2}^{t} = \dfrac{C_{NaCl\ dialysate}.Q_D.\Delta t + n_{NaCl\ convection\ 2}^{t}}{(Q_D + Q_F).\Delta t} \end{cases}$$

$$n_{NaCl\ diffusion\ 2}^{t} = K_2.\left(\frac{2.C_{NaCl\ A/V}^{t} + C'_{NaCl\ A/V}^{t}}{3} - \frac{2.C_{NaCl\ dialysate} + C'_{NaCl\ IN\ 2}^{t}}{3} \right).\Delta t$$

J - 2nd dialyzer blood outlet (see Fig. 87):

$$n_{NaCl\ ven}^{t} = n_{NaCl\ A/V}^{t} - n_{NaCl\ convection\ 2}^{t} - n_{NaCl\ diffusion\ 2}^{t} + C_{NaCl\ blood}.Q_{UF}.\Delta t$$

$$C_{NaCl\ ven}^{t} = \frac{n_{NaCl\ ven}^{t}}{Q_B.\Delta t}$$

d. **Serial dialyzers setup with transmembrane pre-dilution HDF**

i. Working hypotheses

See above ("Standard pre-dilution HDF with the Nikkiso dialysis machine"). Number "1" and "2" refer to the first and second dialyzer, respectively. The setup is represented in **Fig. 11**.
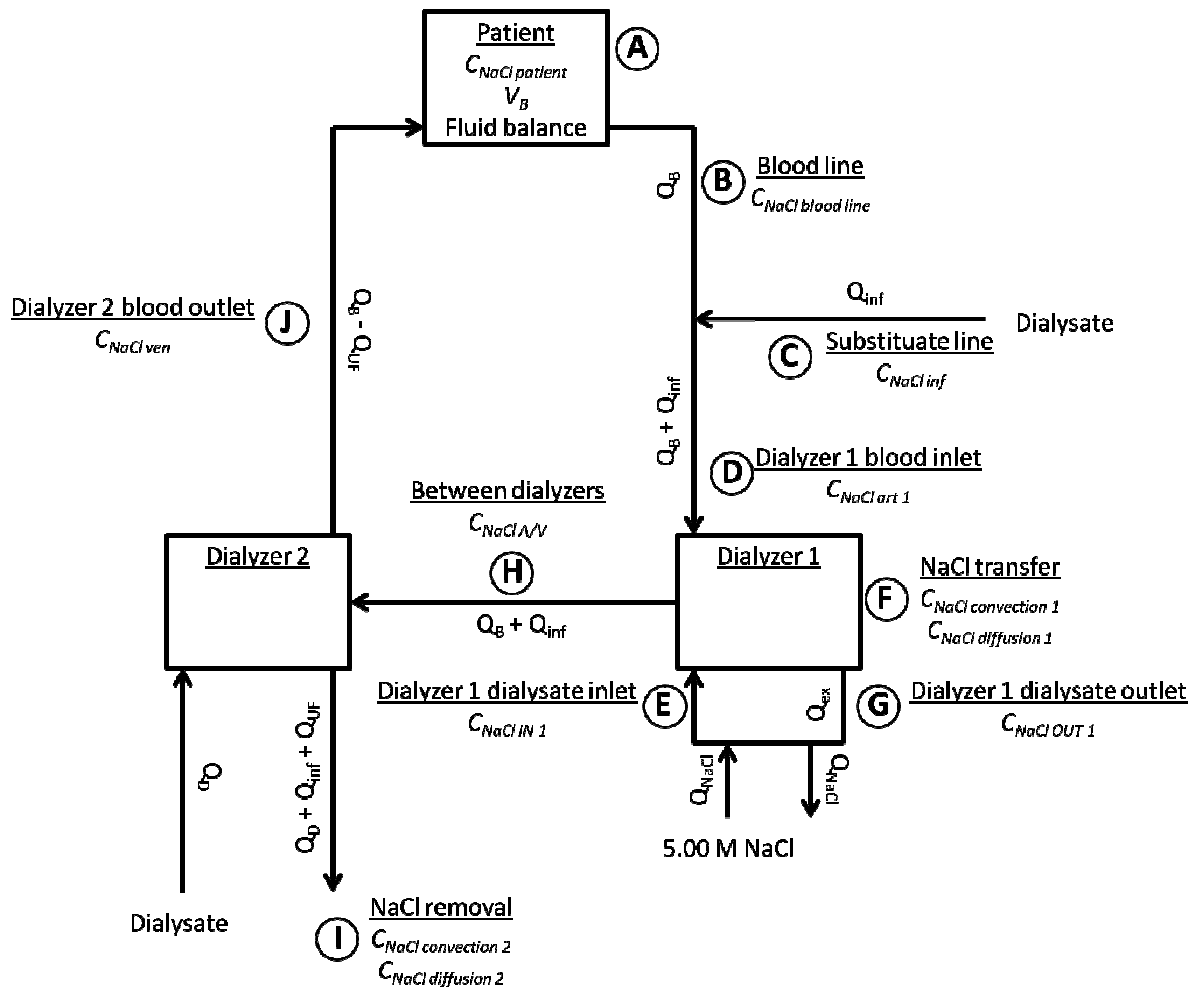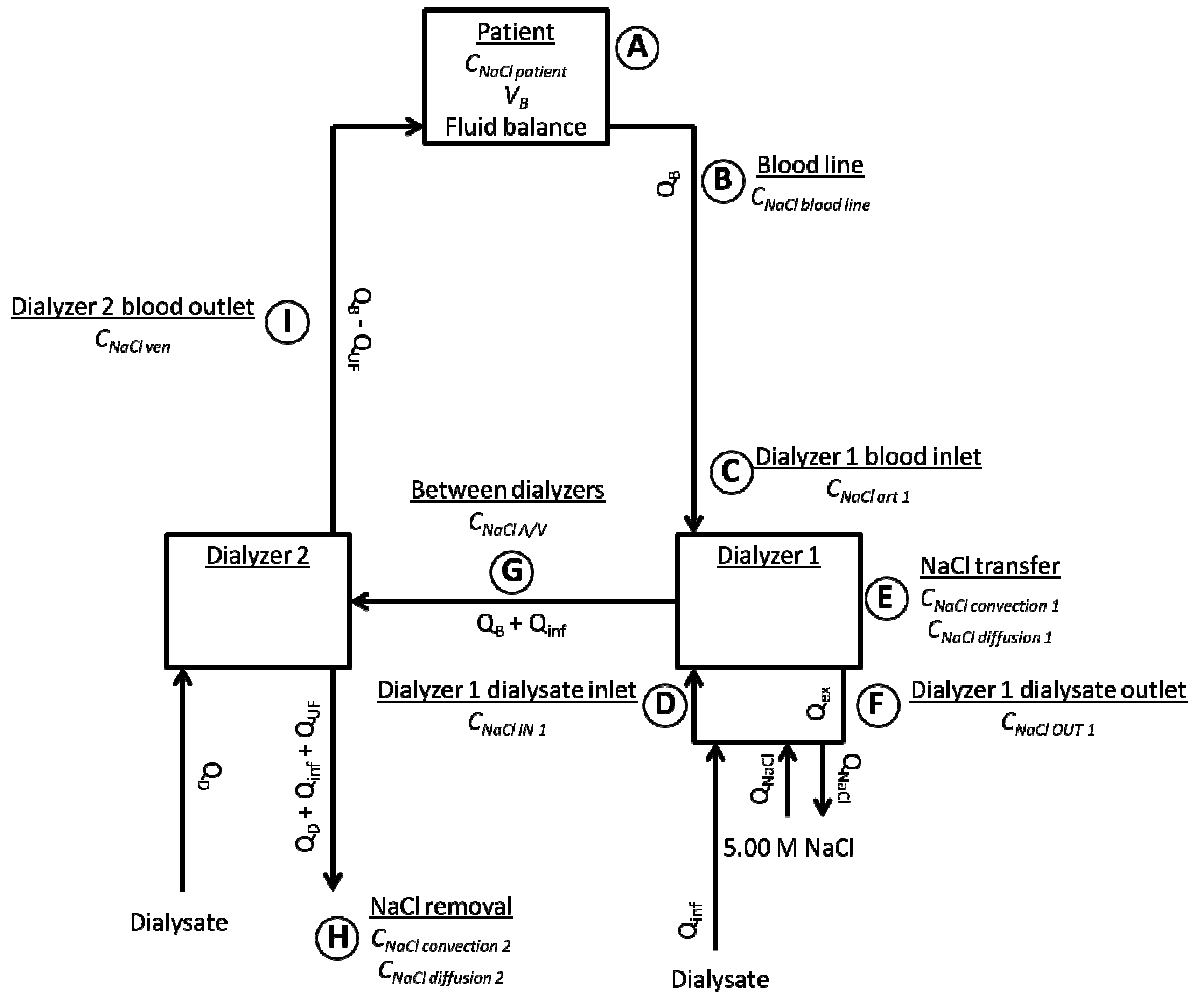
Fig. 88: Model of NaCl mass balance during SDial with transmembrane pre-dilution HDF with the Nikkiso dialysis machine.

The following spots are highlighted: A, patient; B, blood line; C, 1st dialyzer blood inlet; D, 1st dialyzer dialysate inlet; E, NaCl transfer within the 1st dialyzer (occurring by convection and diffusion); F, 1st dialyzer dialysate outlet; G, between dialyzers; H, NaCl removal within the 2nd dialyzer (occurring by convection and diffusion); I, 2nd dialyzer blood outlet.

   ii. <u>Equations</u>

$$Q_F = Q_{inf} + Q_{UF}$$

$$\begin{cases} Q_{B\,app\,1} = Q_B + Q_{inf} \\ Q_{B\,app\,2} = Q_B - Q_{UF} \end{cases}$$

$$\begin{cases} K_1 = Q_{B\,app\,1} \cdot \left[\dfrac{e^{K_0 A \cdot \left(\frac{Q_{ex} - Q_{B\,app\,1}}{Q_{ex} \cdot Q_{B\,app\,1}} \right)} - 1}{e^{K_0 A \cdot \left(\frac{Q_{ex} - Q_{B\,app\,1}}{Q_{ex} \cdot Q_{B\,app\,1}} \right)} - \dfrac{Q_{B\,app\,1}}{Q_{ex}}} \right] \\[4em] K_2 = Q_{B\,app\,2} \cdot \left[\dfrac{e^{K_0 A \cdot \left(\frac{Q_D - Q_{B\,app\,2}}{Q_D \cdot Q_{B\,app\,2}} \right)} - 1}{e^{K_0 A \cdot \left(\frac{Q_D - Q_{B\,app\,2}}{Q_D \cdot Q_{B\,app\,2}} \right)} - \dfrac{Q_{B\,app\,2}}{Q_D}} \right] \end{cases}$$

A - Patient (see Fig. 88):

$$C_{NaCl\ patient}^{t=0} = C_{NaCl\ blood} \Rightarrow n_{NaCl\ patient}^{t=0} = C_{NaCl\ patient}^{t=0}.V_B$$

$$n_{NaCl\ patient}^{t} = n_{NaCl\ patient}^{t-1} - n_{NaCl\ blood\ line}^{t-1} + n_{NaCl\ ven}^{t-1} \Rightarrow C_{NaCl\ patient}^{t} = \frac{n_{NaCl\ patient}^{t}}{V_B}$$

B - Blood line before substituate line (see Fig. 88):

$$C_{NaCl\ blood\ line}^{t} = C_{NaCl\ patient}^{t} \Rightarrow n_{NaCl\ blood\ line}^{t} = C_{NaCl\ blood\ line}^{t}.Q_B.\Delta t$$

C - 1st dialyzer blood inlet (see Fig. 88):

$$n_{NaCl\ art\ 1}^{t} = n_{NaCl\ blood\ line}^{t} \Rightarrow C_{NaCl\ art\ 1}^{t} = \frac{n_{NaCl\ art\ 1}^{t}}{Q_B.\Delta t}$$

D - 1st dialyzer dialysate inlet (see Fig. 88):

$$\begin{cases} n_{NaCl\ IN\ 1}^{t=0} = C_{NaCl\ dialysate}.Q_{ex}.\Delta t + \left(5 - C_{NaCl\ dialysate}\right).Q_{NaCl}.\Delta t + C_{NaCl\ dialysate}.Q_{inf}.\Delta t \\ n_{NaCl\ IN\ 1}^{t} = n_{NaCl\ OUT\ 1}^{t-1} + (5 - C_{NaCl\ OUT\ 1}^{t-1}).Q_{NaCl}.\Delta t + C_{NaCl\ dialysate}.Q_{inf}.\Delta t \end{cases}$$

$$\Rightarrow C_{NaCl\ IN\ 1}^{t} = \frac{n_{NaCl\ IN\ 1}^{t}}{(Q_{inf} + Q_{ex}).\Delta t}$$

E - NaCl transfer through the porous membrane of the 1st dialyzer (see Fig. 88):

$$n_{NaCl\ convection\ 1}^{t} = C_{NaCl\ IN\ 1}^{t}.Q_{inf}.\Delta t \Rightarrow \begin{cases} C'_{NaCl\ art\ 1}^{t} = \dfrac{n_{NaCl\ art\ 1}^{t} + n_{NaCl\ convection\ 1}^{t}}{(Q_B + Q_{inf}).\Delta t} \\ C'_{NaCl\ IN\ 1}^{t} = \dfrac{n_{NaCl\ IN\ 1}^{t} - n_{NaCl\ convection\ 1}^{t}}{Q_{ex}.\Delta t} \end{cases}$$

$$n_{NaCl\ diffusion\ 1}^{t} = K_1.\left(\frac{2.C_{NaCl\ art\ 1}^{t} + C'_{NaCl\ art\ 1}^{t}}{3} - \frac{2.C_{NaCl\ IN\ 1}^{t} + C'_{NaCl\ IN\ 1}^{t}}{3}\right).\Delta t$$

F - 1st dialyzer dialysate outlet (see Fig. 88):

$$n_{NaCl\ OUT\ 1}^{t} = n_{NaCl\ IN\ 1}^{t} - n_{NaCl\ convection\ 1}^{t} + n_{NaCl\ diffusion\ 1}^{t} \Rightarrow C_{NaCl\ OUT\ 1}^{t} = \frac{n_{NaCl\ OUT\ 1}^{t}}{Q_{ex}.\Delta t}$$

G - 1st dialyzer blood outlet / 2nd dialyzer blood inlet (see Fig. 88):

$$n_{NaCl\ A/V}^{t} = n_{NaCl\ art\ 1}^{t} + n_{NaCl\ convection\ 1}^{t} - n_{NaCl\ diffusion\ 1}^{t} \Rightarrow C_{NaCl\ A/V}^{t}$$

$$= \frac{n_{NaCl\ A/V}^{t}}{(Q_B + Q_{inf}).\Delta t}$$

H - NaCl removal within 2nd dialyzer (see Fig. 88):

$$n_{NaCl\ convection\ 2}^{t}$$

$$= C_{NaCl\ A/V}^{t} \cdot Q_F \cdot \Delta t \Rightarrow \begin{cases} C'^{t}_{NaCl\ A/V} = \dfrac{n_{NaCl\ A/V}^{t} - n_{NaCl\ convection\ 2}^{t}}{(Q_B - Q_{UF}) \cdot \Delta t} \\ \\ C'^{t}_{NaCl\ IN\ 2} = \dfrac{C_{NaCl\ dialysate} \cdot Q_D \cdot \Delta t + n_{NaCl\ convection\ 2}^{t}}{(Q_D + Q_F) \cdot \Delta t} \end{cases}$$

$$n_{NaCl\ diffusion\ 2}^{t} = K_2 \cdot \left(\frac{2 \cdot C_{NaCl\ A/V}^{t} + C'^{t}_{NaCl\ A/V}}{3} - \frac{2 \cdot C_{NaCl\ dialysate} + C'^{t}_{NaCl\ IN\ 2}}{3} \right) \cdot \Delta t$$

I - 2nd dialyzer blood outlet (see Fig. 88):

$$n_{NaCl\ ven}^{t} = n_{NaCl\ A/V}^{t} - n_{NaCl\ convection\ 2}^{t} - n_{NaCl\ diffusion\ 2}^{t} + C_{NaCl\ blood} \cdot Q_{UF} \cdot \Delta t$$

REFERENCES

1. **Vanholder RC, De Smet R, and Lameire NH.** Uremic toxicity. [book authors] WH Hörl, et al. *Replacement of renal function by dialysis.* Fifth revised edition. Dordrecht, The Netherlands : Kluwer Academic Publishers, 2004, pp. 15-55.

2. **National Kidney Foundation.** *NKF KDOQI Guidelines.* 2002. http://www.kidney.org/professionals/kdoqi/guidelines_ckd/p4_class_g1.htm.

3. *Chronic kidney disease and progression.* **Choi MJ and Fried LF.** 2011, Nephrology self assessment program, Vol. 10, No. 5, pp. 429-436.

4. CKD stages. *The renal association.* [Online] [Citation : 01/04/2013.] http://www.renal.org.

5. **Levy J, Morgan J, and Brown E.** *Oxford handbook of dialysis.* New York : Oxford university press, 2001. ISBN 0-19-2631608.

6. **Vanholder R, et al.** *ERA-EDTA Registry.* Annual report 2010. ISBN 978-90-817480-1-8.

7. *Uremic toxicity: present state of the art.* **Vanholder R, et al.** 2001, Vol. 24, No. 10, pp. 695-725.

8. *Review on uremic toxins: classification, concentration, and interindividual variability.* **Vanholder R, et al.** 2003, Kidney International, Vol. 63, pp. 1934-1943.

9. *What is new in uremic toxicity?* **Vanholder R, Van Laecke S, and Glorieux G.** 2008, Pediatr Nephrol, Vol. 23, pp. 1211-1221.

10. *Normal and pathologic concentrations of uremic toxins.* **Duranton F, et al.** 2012, J Am Soc Nephrol, Vol. 23, pp. 1258-1270.

11. **Depner T and Garred L.** Solute transport mechanisms in dialysis. [book authors] WH Hörl, et al. *Replacement of renal function by dialysis.* Fifth revised edition. Dordrecht, The Netherlands : Kluwer Academic Publishers, 2004, pp. 73-93.

12. *Protein-bound uremic solutes: the forgotten toxins.* **Vanholder R, De Smet R, and Lameire N.** Suppl. 78, 2001, Kidney International, Vol. 59, pp. 266-270.

13. **Schmaldienst S and Hörl WH.** The biology of hemodialysis. [book authors] WH Hörl, et al. *Replacement of renal function by dialysis.* Fifth revised edition. Dordrecht, The Netherlands : Kluwer Academic Publishers, 2004, pp. 157-179.

14. *The middle-molecule hypothesis 30 years after: lost and rediscovered in the universe of uremic toxicity?* **Vanholder R, Van Laecke S, and Glorieux G.** 2008, JNephrol, Vol. 21, pp. 146-160.

15. *Beta-2 microglobulin in renal disease.* **Miyata T, et al.** 1998, J Am Soc Nephrol, Vol. 9, No. 9, pp. 1723-1735.

16. *Beta2-microglobulin and amyloidosis.* **Drüeke TB.** 2000, Nephrol Dial Transplant, Vol. 15, Suppl. 1, pp. 17-24.

17. *Plasma beta-2 microglobulin is associated with cardiovascular disease in uremic patients.* **Liabeuf S, et al.** 2012, Kidney International, Vol. 82, No. 12, pp. 1297-1303.

18. *Serum beta2-microglobulin level is a significant predictor of mortality in maintenance haemodialysis patients.* **Okuno S, et al.** 2009, Nephrol Dial Transplant, Vol. 24, No. 2, pp. 571-577.

19. *The impact of ß2-microglobulin clearance on the risk factors of cardiovascular disease in hemodialysis patients.* **Kuragano T, et al.** 2010, ASAIO Journal, Vol. 56, pp. 326-332.

20. *Association of heart valve calcification with malnutrition-inflammation complex syndrome, beta-microglobulin, and carotid intima media thickness in patients on hemodialysis.* **Ikee R, et al.** 2008, Ther Apher Dial, Vol. 12, No. 6, pp. 464-468.

21. *Uremic toxicity of indoxyl sulfate.* **Niwa T.** 2010, Nagoya J Med Sci, Vol. 72, pp. 1-11.

22. *Effect of the super-flux cellulose triacetate dialyser membrane on the removal of non-protein-bound and protein-bound ureamic solutes.* **De Smet R, et al.** 2007, Nephrol Dial Transplant, Vol. 22, pp. 2006-2012.

23. *Serum indoxyl sulfate is associated with vascular disease and mortality in chronic kidney disease patients.* **Barreto FC, et al.** 2009, Clin J Am Soc Nephrol, Vol. 4, pp. 1551-1558.

24. *Role of organic anion transporters in the tubular transport of indoxyl sulfate and the induction of its nephrotoxicity.* **Enomoto A, et al.** 2002, J Am Soc Nephrol, Vol. 13, pp. 1711-1720.

25. *Indoxyl sulfate, a circulating uremic toxin, stimulates the progression of glomerular sclerosis.* **Niwa T and Ise M.** 1994, J Lab Clin Med, Vol. 124, No. 1, pp. 96-104.

26. *Indoxyl sulphate inhibits osteoclast differentiation and function.* **Mozar A, et al.** 2012, Nephrol Dial Transplant, Vol. 27, pp. 2176-2181.

27. *Indoxyl sulfate induces skeletal resistance to parathyroid hormone in cultured osteoblastic cells.* **Nii-Kono T, et al.** 2007, Kidney International, Vol. 71, No. 8, pp. 738-743.

28. *p-cresyl sulphate and indoxyl sulphate predict progression of chronic kidney disease.* **Wu IW, et al.** 2011, Nephrol Dial Transplant, Vol. 26, No. 3, pp. 938-947.

29. *Indoxyl sulphate promotes aortic calcification with expression of osteoblast-specific proteins in hypertensive rats.* **Adijiang A, et al.** 2008, Nephrol Dial Transplant, Vol. 23, pp. 1892-1901.

30. *The uremic solutes p-cresol and indoxyl sulfate inhibit endothelial proliferation and wound repair.* **Dou L, et al.** 2004, Kidney international, Vol. 65, pp. 442-451.

31. *The uremic solute indoxyl sulfate induces oxidative stress in endothelial cells.* **Dou L, et al.** 2007, Journal of Thrombosis and Haemostasis, Vol. 5, pp. 1302-1308.

32. *Uremic solutes from colon microbes.* **Meyer TW and Hostetter TH.** 2012, Kidney International, Vol. 81, pp. 949-954.

33. *Removal of p-cresol sulfate by hemodialysis.* **Martinez AW, et al.** 2005, J Am Soc Nephrol, Vol. 16, pp. 3430-3436.

34. *Gas chromatographic-mass spectrometric analysis for measurement of p-cresol and its conjugated metabolites in uremic and normal serum.* **De Loor H, et al.** 2005, Clinical Chemistry, Vol. 51, No. 8, pp. 1535-1538.

35. *p-cresyl sulfate and indoxyl sulfate in hemodialysis patients.* **Meijers BKI, et al.** 2009, Clin J Am Soc Nephrol, Vol. 4, pp. 1932-1939.

36. *Comparative kinetics of the uremic toxin p-cresol versus creatinine in rats with and without renal failure.* **Lesaffer G, et al.** 2003, Kidney International, Vol. 64, pp. 1365-1373.

37. *Free p-cresylsulphate is a predictor of mortality in patients at different stages of chronic kidney disease.* **Liabeuf S, et al.** 2010, Nephrol Dial Transplant, Vol. 25, pp. 1183-1191.

38. *Organic anion transporters play an important role in the uptake of p-cresyl suflfate, a uremic toxin, in the kidney.* **Miyamoto Y, et al.** 2011, Nephrol Dial Transplant, Vol. 26, No. 8, pp. 2498-2502.

39. *Free p-cresol is associated with cardiovascular disease in hemodialysis patients.* **Meijers BKI, et al.** 2008, Kidney International, Vol. 73, pp. 1174-1180.

40. *Serum free p-cresyl sulfate levels predict cardiovascular and all-cause mortality in elderly hemodialysis patients - a prospective cohort study.* **Wu IW, et al.** 2012, Nephrol Dial Transplant, Vol. 27, pp. 1169-1175.

41. *Toxicity of free p-cresol: a prospective and cross-sectional analysis.* **De Smet R, et al.** 2003, Vol. 49, No. 3, pp. 470-478.

42. *P-cresol, a uremic toxin, decreases endothelial cell response to inflammatory cytokines.* **Dou L, et al.** 2002, Kidney international, Vol. 62, pp. 1999-2009.

43. *P-cresylsulphate, the main in vivo metabolite of p-cresol, activates leucocyte free radical production.* **Schepers E, et al.** 2007, Nephrol Dial Transplant, Vol. 22, pp. 592-596.

44. *The uremic retention solute p-cresyl sulfate and markers of endothelial damage.* **Meijers BKI, et al.** 2009, American Journal of Kidney Diseases, Vol. 54, No. 5, pp. 891-901.

45. *p-cresol, but not p-cresylsulphate, disrupts endothelial progenitor cell function in vitro.* **Zhu JZ, et al.** 2012, Nephrol Dial Transplant, Vol. 27, No. 12, pp. 4323-4330.

46. *Protein-bound toxins - Update 2009.* **Jourde-Chiche N, et al.** 2009, Seminars in dialysis, Vol. 22, No. 4, pp. 334-339.

47. *Increased plasma phenylacetic acid in patients with end-stage renal failure inhibits iNOS expression.* **Jankowski J, et al.** 2003, J Clin Invest, Vol. 112, pp. 256-264.

48. *The uraemic toxin phenylacetic acid inhibits osteoblastic proliferation and differentiation: an implication for the pathogenesis of low turnover bone in chronic renal failure.* **Yano S, et al.** 2007, Nephrol Dial Transplant, Vol. 22, No. 11, pp. 3160-3165.

49. *The uraemic toxin phenylacetic acid impairs macrophage function.* **Schmidt S, et al.** 2008, Nephrol Dial Transplant, Vol. 23, No. 11, pp. 3485-3493.

50. **Leypoldt JK and Ronco C.** Optimization of high-flux, hollow-fiber artificial kidneys. [book authors] WH Hörl, et al. *Replacement of renal function by dialysis.* Fifth revised edition. Dordrecht, The Netherlands : Kluwer Academic Publishers, 2004, pp. 95-113.

51. **Krediet RT.** Peritoneal anatomy and physiology during peritoneal dialysis. [book authors] WH Hörl, et al. *Replacement of renal function by dialysis.* Fifth revised edition. Dordrecht, The Netherlands : Kluwer Academic Publishers, 2004, pp. 115-155.

52. **Polaschegg HD and Levin NW.** Hemodialysis machines and monitors. [book authors] WH Hörl, et al. *Replacement of renal function by dialysis.* Fifth revised edition. Dordrecht, The Netherlands : Kluwer Academic Publishers, 2004, pp. 325-449.

53. **Krieter DH and Wanner C.** Membranes for dialysis and hemofiltration. [book authors] A Jörres, C Ronco et JA Kellum. *Management of acute kidney problems.* Heidelberg : Springer Verlag, 2010, p. 491.

54. *Blood material interactions at the surfaces of membranes in medical applications.* **Deppisch R, et al.** 1998, Separation and Purification Technology, Vol. 14, pp. 241-254.

55. *High permeability of dialysis membranes: what is the limit of albumin loss?* **Krieter DH and Canaud B.** 2003, Nephrol Dial Transplant, Vol. 18, pp. 651-654.

56. **National Kidney Foundation.** *NKF KDOQI Guidelines.* 2006. http://www.kidney.org/professionals/kdoqi/guideline_upHD_PD_VA/hd_rec4.htm.

57. **Locatelli F, Di Filippo S, and Manzoni C.** Hemodialysis fluid composition. [book authors] WH Hörl, et al. *Replacement of renal function by dialysis.* Fifth revised edition. Dordrecht, The Netherlands : Kluwer Academic Publishers, 2004, pp. 585-596.

58. *The effect of high-flux hemodialysis on hemoglobin concentrations in patients with CKD: results of the MINOXIS study.* **Schneider A, et al.** 2012, Clin J Am Soc Nephrol, Vol. 7, pp. 52-59.

59. *On-line haemodiafiltration versus low-flux haemodialysis. A prospective randomized study.* **Wizemann V, et al.** 2000, Nephrol Dial Transplant, Vol. 15, Suppl. 1, pp. 43-48.

60. *Effective removal of protein-bound uraemic solutes by different convective strategies: a prospective trial.* **Meert N, et al.** 2009, Nephrol Dial Transplant, Vol. 24, pp. 562-570.

61. *Intradialytic removal of protein-bound uraemic toxins: role of solute characteristics and of dialyser membrane.* **Lesaffer G, et al.** 2000, Nephron Dial Transplant, Vol. 15, pp. 50-57.

62. *Superior dialytic clearance of b2-microglobulin and p-cresol by high-flux hemodialysis as compared to peritoneal dialysis.* **Evenepoel P, Bammens B, and Vanrenterghem Y.** 2006, Kidney International, Vol. 70, pp. 794-799.

63. *Removal of the protein-bound solute p-cresol by convective transport: a randomized crossover study.* **Bammens B, et al.** 2004, American Journal of Kidney Diseases, Vol. 44, No. 2, pp. 278-285.

64. *Protein-bound uraemic toxin removal in haemodialysis and post-dilution haemofiltration.* **Krieter DH, et al.** 2010, Nephrol Dial Transplant, Vol. 25, pp. 212-218.

65. *Prospective evaluation of the change of predialysis protein-bound uremic solute concentration with postdilution online hemodiafiltration.* **Meert N, et al.** 2010, Artificial Organs, Vol. 34, No. 7, pp. 580-585.

66. *On-line haemodiafiltration. Remarkable removal of beta2-microglobulin. Long-term clinical observations.* **Lornoy W, et al.** 2000, Nephrol Dial Transplant, Vol. 15, Suppl. 1, pp. 49-54.

67. *Effect of online hemodiafiltration on all-cause mortality and cardiovascular outcomes.* **Grootman MPC, et al.** 2012, J Am Soc Nephrol, Vol. 23, pp. 1087-1096.

68. *High-efficiency postdilution online hemodiafiltration reduces all-cause mortality in hemodialysis patients.* **Maduell F, et al.** 2013, J Am Soc Nephrol, Vol. 24, No. 3, pp. 487-497.

69. *Mortality and cardiovascular events in online haemodiafiltration (OL-HDF) compared with high-flux dialysis: results from the Turkish OL-HDF Study.* **Ok E, et al.** 2013, Nephrol Dial Transplant, Vol. 28, pp. 192-202.

70. *beta(2)-microglobulin kinetics in nocturnal haemodialysis.* **Raj DS, et al.** 2000, Nephrol Dial Transplant, Vol. 15, No. 1, pp. 58-64.

71. **National Institutes of Health.** *USRDS annual data report.* 2012.

72. *A molecular functional study on the interactions of drugs with plasma proteins.* **Otagiri M.** 2005, Drug Metab Pharmacokinet, Vol. 20, No. 5, pp. 309-323.

73. *A review of albumin binding in CKD.* **Meijers BKI, et al.** 2008, American Journal of Kidney Diseases, Vol. 51, No. 5, pp. 839-850.

74. *Albumin as fatty acid transporter.* **van der Vusse GJ.** 2009, Drug Metab Pharmacokinet, Vol. 24, No. 4, pp. 300-307.

75. *Binding of bromosulphthalein to serum albumins.* **Deutschmann G, Gratzl M, and Ullrich V.** 1974, Biochimica et Biophysica Acta, Vol. 371, pp. 470-481.

76. *Binding of the general anesthetics propofol and halothane to human serum albumin.* **Bhattacharya AA, Curry S, and Franks NP.** 2000, The Journal of Biological Chemistry, Vol. 275, No. 49, pp. 38731-38738.

77. *Characterization of binding site of uremic toxins on human serum albumin.* **Sakai T, Takadate A, and Otagiri M.** 1995, Biol Pharm Bull, Vol. 18, No. 12, pp. 1755-1761.

78. *The characterization of two specific drug binding sites on human serum albumin.* **Sudlow G, Birkett DJ, and Wade DN.** 1975, Molecular Pharmacology, Vol. 11, pp. 824-832.

79. *Interaction mechanism between IS, a typical uremic toxin bound to site II, and ligands bound to site I of human serum albumin.* **Sakai T, et al.** 2001, Pharmaceutical Research, Vol. 18, No. 4, pp. 520-524.

80. *Effects of uremic toxins and fatty acids on serum protein binding of furosemide: possible mechanism of the binding defect in uremia.* **Takamura N, Maruyama T, and Otagiri M.** 1997, Clinical Chemistry, Vol. 43, No. 12, pp. 2274-2280.

81. *Albumin-binding capacity (ABiC) is reduced in patients with chronic kidney disease along with an accumulation of protein-bound uraemic toxins.* **Klammt S, et al.** 2012, Nephrol Dial Transplant, Vol. 27, pp. 2377-2383.

82. *Influences of haemodialysis on the binding sites of human serum albumin: possibility of an efficacious administration plan using binding inhibition.* **Nishio T, et al.** 2008, Nephrol Dial Transplant, Vol. 23, pp. 2304-2310.

83. **Schwinn DA and Schafer SL.** Basic principles of pharmacology related to anesthesia. [book authors] RD Miller. *Anesthesia.* Fifth Edition. s.l. : Churchill Livingstone, 2000, pp. 15-48.

84. *Analyzing Data with GraphPad Prism.* **Motulsky H.** 1999, pp. 244-249.

85. *Interaction between two sulfate-conjugated uremic toxins, p-cresyl sulfate and indoxyl sulfate, during binding with human serum albumin.* **Watanabe H, et al.** 2012, Drug Metab Dispos, Vol. 40, No. 7, pp. 1423-1428.

86. *Increasing dialysate flow and dialyzer mass transfer area coefficient to increase the clearance of protein-bound solutes.* **Meyer TW, et al.** 2004, J Am Soc Nephrol, Vol. 15, pp. 1927-1935.

87. **Etzell JE and Corash LM.** Laboratory hematology: methods for the analysis of blood. [book authors] RI Handin, SE Lux et TP Stossel. *Blood: principle and practice of hematology.* Philadelphia : Lippincott Williams & Wilkins, 2003, pp. 15-58.

88. *Rapid method for the estimation of plasma haemoglobin levels.* **Cripps, CM.** 1968, J Clin Pathol, Vol. 21, No. 1, pp. 110-112.

89. *Conductance of electrolytes.* 05/01/2013. http://www.chem.boun.edu.tr/webpages/courses/chem356/EXP6procedure.pdf.

90. *Reverse mid-dilution: new way to remove small and middle molecules as well as phosphate with high intrafilter convective clearance.* **Santoro A, et al.** 2007, Nephrol Dial Transplant, Vol. 22, pp. 2000-2005.

91. **Hoenich NA, Ghezzi PM, and Ronco C.** Thrombogenesis and anticoagulation in patients undergoing chronic hemodialysis. [book authors] WH Hörl, et al. *Replacement of renal function by dialysis.* Fifth revised edition. Dordrecht, The Netherlands : Kluwer Academic Publishers, 2004, pp. 273-299.

92. *Anaphylactoid reactions during hemodialysis in sheep are ACE inhibitor dose-dependent and mediated by bradykinin.* **Krieter DH, et al.** 1998, Kidney International, Vol. 53, pp. 1026–1035.

93. **NIPRO.** *PUREFLUX, Purema hollow fiber dialyzer .* Nipro Corporation. 2009. Directions for use. I-PUR-CE-12-0606.

94. **Thompson S and Staley J.** *Chemical bonding.* Colorado State University. 2013. p. 23, Learning module.

95. *Extraction of protein bound ligands from azotemic sera: comparison of 12 deproteinization methods.* **Vanholder R, et al.** 1992, Kidney International, Vol. 41, pp. 1707-1712.

96. *Binding of p-cresylsulfate and p-cresol to human serum albumin studied by microcrocalorimetry.* **Bergé-Lefranc D, et al.** 2010, J Phys Chem B, Vol. 114, pp. 1661-1665.

97. **Merck KGaA.** *106404 Sodium chloride.* Darmstadt, Germany, 2013. Product data sheet.

98. **Poullin P and Legrand D.** Médicaments dérivés du plasma. [book authors] G Sébahoun. *Hématologie clinique et biologique.* Seconde édition. s.l. : Wolter Kluwer France, 2005, p. 515.

99. *Lessons from the crystallographic analysis of small molecule binding to human serum albumin.* **Curry S.** 2009, Drug Metab Pharmacokinet, Vol. 24, No. 4, pp. 342-357.

100. *Serum uremic toxins from patients with chronic renal failure displace the binding of L-tryptophan to human serum albumin.* **Mingrone G, et al.** 1997, Clin Chem Acta, Vol. 260, No. 1, pp. 27-34.

101. *Pharmaceutical-grade albumin: impaired drug-binding capaciy in vitro.* **Olsen H, et al.** 2004, BMC Clinical Pharmacology, Vol. 4, pp. 1-9.

102. *Binding of naproxen and amitriptyline to bovine serum albumin: biophysical aspects.* **Banerjee T, Singh SK, and Kishore N.** 2006, J Phys Chem B, Vol. 110, No. 47, pp. 24147-24156.

103. *Updates on contemporary protein binding techniques.* **Chuang VTG, Maruyama T, and Otagiri M.** 2009, Drug Metab Pharmacokinet, Vol. 24, No. 4, pp. 358-364.

104. *Practical aspects of the ligand-binding and enzymatic properties of human serum albumin.* **Kragh-Hansen U, Chuang VTG, and Otagiri M.** 2002, Biol Pharm Bull, Vol. 25, No. 6, pp. 695-704.

105. *Increasing the clearance of protein-bound solutes by addition of a sorbent to the dialysate.* **Meyer TW, et al.** 2007, J Am Soc Nephrol, Vol. 18, pp. 868-874.

106. *Probing conformational changes of human serum albumin due to unsaturated fatty acid binding by chemical cross-linking and mass spectrometry.* **Huang BX, Dass C, and Kim HY.** 2005, Biochem J, Vol. 387, pp. 695-702.

107. *Proteomic analysis of protein adsorption capacity of different haemodialysis membranes.* **Urbani A, et al.** 2012, Mol Biosyst, Vol. 8, No. 4, pp. 1029-1039.

108. *The importance of osmolality fall and ultrafiltration rate on hemodialysis side effects. Influence of intravenous mannitol.* **Rosa AA, et al.** 1981, Nephron, Vol. 27, No. 3, pp. 134-141.

109. *Osmolality changes during hemodialysis. Natural history, clinical correlations, and influence of dialysate glucose and intravenous mannitol.* **Rodrigo F, et al.** 1977, Ann Intern Med, Vol. 86, No. 5, pp. 554-561.

110. *Extraction of uraemic toxins with activated carbon restores the functional properties of albumin.* **Sarnatskaya VV, et al.** 2003, Nephron Physiol, Vol. 95, pp. 10-18.

111. **McQuarrie C, McQuarrie DA, and Rock PA.** *Chimie Générale.* Bruxelles : De Boeck, 2000. p. 1174. ISBN 2-8041-3703-1.

112. *New approaches to the removal of protein-bound toxins from blood plasma of uremic patients.* **Sarnatskaya VV, et al.** 2007, Artif Cells Blood Substit Immobil Biotechnol, Vol. 35, No. 3, pp. 287-308.

113. *Six years of treatment with the HELP system of a patient with familial hypercholesterolemia.* **Nascimento MM, et al.** 2002, Brazilian Journal of Medical and Biological Research, Vol. 35, pp. 775-782.

114. **Collins GR, Summerton J, and Spence E.** *Ionic enhanced dialysis / diafiltration system. EP 1 809 410* Europe, 09/22/2005.

115. *Salt - A potential "uremic toxin".* **Ritz E, et al.** 2006, Blood Purif, Vol. 24, pp. 63-66.

116. *Significance of hypo- and hypernatremia in chronic kidney disease.* **Kovesdy CP.** 2012, Nephrol Dial Transplant, Vol. 27, pp. 891-898.

117. **Gambro.** *Polyflux H.* 2008. HCEN2489_5.

118. **Hendersen LW.** Biophysics of ultrafiltration and hemofiltration. [book authors] C Jacobs, et al. *Replacement of renal function by dialysis.* 4th edition. s.l. : Kluwer Academic Publishers, 1996, pp. 114-145.

119. *Thermal shock hemolysis in human red cells. I. The effects of temperature, time, and osmotic stress.* **Takahashi T and Williams RJ.** 1983, Cryobiology, Vol. 20, No. 5, pp. 507-520.

120. *Cold-induced hemolysis in a hypertonic milieu.* **Green FA and Jung CY.** 1977, J Membr Biol, Vol. 33, pp. 249-262.

121. *Resistance of mammalian red blood cells of different size to hypertonic milieu.* **Betticher DC and Geiser J.** 1989, Comp Biochem Physiol A Comp Physiol, Vol. 93, No. 2, pp. 429-432.

122. **Kim Y, Kim K, and Park Y.** Measurement techniques for red blood cell deformability: recent advances. [book authors] TE Moschandreou. *Blood cell - An overview of studies in hematology.* Rijeka : InTech, 2012, pp. 167-194.

123. *Biological membranes as bilayer couples.* **Sheetz MP, Painter RG, and Singer SJ.** 1976, The Journal of Cell Biology, Vol. 70, pp. 193-203.

124. **Das D.** *Biochemistry.* s.l. : Bimal Kumar Dhur of Academic Publishers, 1978. p. 634. ISBN 81-87504-82-X.

125. **Dörner K.** *Klinische Chemie und Hämatologie.* 4. Auflage. Stuttgart : Georg Thieme Verlag, 2001. p. 308. ISBN 3-13-129714-X.

126. *A study on osmotic fragility of erythrocytes of tuberculosis patient's blood.* **Reddy NM, Lingam SC, and Ahmad A.** 2012, CIBTech Journal of microbiology, Vol. 1, pp. 48-56.

127. *Influence of age on the stability of human erythrocyte membranes.* **Penha-Silva N, et al.** 2007, Mech Ageing Dev, Vol. 128, pp. 444-449.

128. *Relationships between osmotic fragility of red blood cells and various hematologic data in workers exposed to lead.* **Karai I, Fukumoto K, and Horiguchi S.** 1982, Int Arch Environ Health, Vol. 50, No. 1, pp. 17-23.

129. **Means RT and Glader B.** Anemia: general considerations. [book authors] JP Greer, et al. *Wintrobe's clinical hematology.* 12th ed. Philadelphia : Wolters Kluwer, 2008, Vol. 1, pp. 779-809.

130. **National Kidney Foundation.** *NKF KDOQI Guidelines.* 2000. http://www.kidney.org/professionals/kdoqi/guidelines_updates/doqiupan_i.html.

131. *Haemodialyser biocompatibility and erythrocyte structure and function.* **Martos MR, et al.** 1997, Clin Chim Acta, Vol. 265, No. 2, pp. 235-246.

132. *Erythrocyte fragility increases with level of glycosylated haemoglobin in type 2 diabetic patients.* **Kung CM, Tseng ZL, and Wang HL.** 2009, Clin Hemorheol Microcirc, Vol. 43, No. 4, pp. 345-351.

133. *Altered red and white bloob cell rheology in type II diabetes.* **Ernst E and Matrai A.** 1986, Diabetes, Vol. 35, No. 12, pp. 1412-1415.

134. *Red blood cell osmotic fragility in chronically hemodialyzed patients.* **Wu SG, et al.** 1988, Nephron, Vol. 78, No. 1, pp. 28-32.

135. *Osmotic fragility of erythrocytes, cell deformability and secondary hyperparathyroidism in uremic patients on maintenance hemodialysis.* **Docci D, et al.** 1985, Clin Nephrol, Vol. 23, No. 2, pp. 68-73.

136. *Impaired deformability of erythrocytes and neutrophils in children with newly diagnosed insulin-dependent diabetes mellitus.* **Linderkamp O, et al.** 1999, Diabetologia, Vol. 42, No. 7, pp. 865-869.

137. *Red blood cell hemolysis during processing.* **Sowemimo-Coker SO.** 2002, Transfusion medicine reviews, Vol. 16, No. 1, pp. 46-60.

138. *Analysis of factors regulating erythrocyte deformability.* **Mohandas N, Clark MR, Jacobs MS, and Shohet SB.** 1980, J Clin Invest, Vol. 66, pp. 563-573.

139. *The influence of membrane skeleton on red cell deformability, membrane material properties, and shape.* **Mohandas N, Chasis JA, and Shohet SB.** 1983, Semin Hematol, Vol. 20, No. 3, pp. 225-242.

140. *Membrane structure and its relation to haemodialysis.* **Weed RI.** 1975, Clin Haematol, Vol. 4, No. 1, pp. 3-28.

141. *Relationship between the age of human erythrocytes and their osmotic resistance: a basis for separating young and old erythrocytes.* **Marks PA and Johnson AB.** 1958, J Clin Invest, Vol. 37, No. 11, pp. 1542-1549.

142. **Glader B.** Destruction of erythrocytes. [book authors] JP Greer, et al. *Wintrobe's clinical hematology.* 12th ed. Philadelphia : Wolters Kluwer, 2008, Vol. 1, pp. 156-169.

143. *The relationship between the osmotic fragility of human erythrocytes and cell age.* **Rifkind JM, Araki K, and Hadley EC.** 1983, Arch Biochem Biophys, Vol. 222, No. 2, pp. 582-589.

144. *Control of the erythrocyte membrane shape: recovery from the effect of crenating agents.* **Alhanaty E and Sheetz MP.** 1981, The journal of cell biology, Vol. 91, pp. 884-888.

145. *The relative osmotic resistance of chronic lymphocytic leukemia lymphocytes.* **Westring DW and Brittin SB.** 1967, Blood, Vol. 30, No. 5, pp. 674-679.

146. *The fragility of normal and leukemic lymphocytes of AKR mice: a study of cell injury by physical agents.* **Reif AE and Allen JM.** 1966, Cancer Res, Vol. 26, pp. 131-136.

147. **International Organization for Standardization.** *Selection of tests for interactions with blood.* 2002. ISO 10993-4:2002.

148. *Hemodialysis intravascular hemolysis and kinked blood lines.* **Gault MH, et al.** 1992, Nephron, Vol. 62, No. 3, pp. 267-271.

149. *Anaphylactoid reactions during haemodialysis in sheep are associated with bradykinin release.* **Krieter DH, et al.** 1995, Nephrol Dial Transplant, Vol. 10, No. 4, pp. 509-513.

150. *Effects of a polyelectrolyte additive on the selective dialysis membrane permeability for low-molecular-weight proteins.* **Krieter DH, et al.** 2007, Nephrol Dial Transplant, Vol. 22, pp. 491-499.

151. **Enzyme Research Laboratories.** *Matched-pair antibidy set for ELISA of human thrombin-antithrombin complex.* ELISA data sheet. OPI0262, rev 1.

152. *Clinical use of topical thrombin as a surgical haemostat.* **Lew WK and Weaver FA.** 2008, Biologics: Targets & Therapy, Vol. 2, No. 4, pp. 593-599.

153. *Complement activation as a mediator of antiphospholipid antibody induced pregnancy loss and thrombosis.* **Salmon JE, Girardi G, and Holers VM.** 2002, Ann Rheum Dis, Vol. 61, Suppl. II, pp. ii46-ii50.

154. *Effect of permeability on indices of haemodialysis membrane biocompatibility.* **Masaki T, et al.** 1999, Nephrol Dial Transplant, Vol. 14, pp. 1176-1181.

155. *Effect of biocompatibility of hemodialysis membranes on mortality in acute renal failure: a meta-analysis.* **Jaber BL, et al.** 2002, Clin Nephrol, Vol. 57, No. 4, pp. 274-282.

156. **Hoenich NA, Woffindin C, and Ronco C.** Haemodialysers and associated devices. [book authors] C Jacobs, et al. *Replacement of renal function by dialysis.* 4th ed. s.l. : Kluwer Academic Publishers, 1996, pp. 188-230.

157. *Removal of fatty acids from serum albumin by charcoal treatment.* **Chen RF.** 1967, The Journal of Biological Chemistry, Vol. 242, No. 2, pp. 173-181.

158. *Clearance of p-cresol sulfate and b-2-microglobulin from dialysate by commercially available sorbent technology.* **Kruse A, et al.** 2011, ASAIO Journal, Vol. 57, pp. 219-224.

159. *First clinical experience with an adjunctive hemoperfusion device designed specifically to remove b2-microglobulin in hemodialysis.* **Ronco C, et al.** 2001, Blood Purif, Vol. 19, pp. 260-263.

160. *Molecular adsorbent recirculating system (MARS).* **Tan HK.** 2004, Ann Acad Med Singapore, Vol. 33, pp. 329-335.

161. *Improvement of hepatorenal syndrome with extracorporeal albumin dialysis MARS: results of a prospective, randomized, controlled clinical trial.* **Mitzner SR, et al.** 2000, Liver transplantation, Vol. 6, No. 3, pp. 277-286.

162. *Extracorporeal detoxification using the molecular adsorbent recirculating system for critically ill patients with liver failure.* **Mitzner SR, et al.** 2001, J Am Soc Nephrol, Vol. 12, Suppl. 17, pp. S75-S82.

163. *Removal of asymmetric dimethylarginine during artificial liver support using fractionated plasma separation and adsorption.* **Rifai K, et al.** 2010, Scand J Gatroenterol, Vol. 45, No. 9, pp. 1110-1115.

164. *A comparison of dual dialyzers in parallel and series to improve urea clearance in large hemodialysis patients.* **Fritz BA, et al.** 2003, American Journal of Kidney Diseases, Vol. 41, No. 5, pp. 1008-1015.

165. *Biocompatibility of hemodialysis membranes: evaluation in an ovine model.* **Burhop KE, et al.** 1993, J Lab Clin Med, Vol. 121, No. 2, pp. 276-293.

166. *Different resistance of mammalian red blood cells to hemolysis by bile salts.* **Salvioli G, et al.** 1993, Lipids, Vol. 28, No. 11, pp. 999-1003.

167. *Hair sheep blood, citrated or defibrinated, fulfills all requirements of blood agar diagnostic microbiology laboratory tests.* **Yeh E, et al.** 2009, PLoS ONE, Vol. 4, No. 7, pp. 1-8.

168. *Deformability of red blood cells from different species studied by resistive pulse shape analysis technique.* **Baskurt OK.** 1996, Biorheology, Vol. 33, No. 2, pp. 169-179.

169. **BBC.** Cattle family. *NATURE Wildlife.* [Online] [Citation : 05/02/2013.] http://www.bbc.co.uk/nature/life/Bovid.

170. *The water metabolism of a small East African antelope: the dik-dik.* **Maloiy GMO.** 1973, Proc R Soc Lond B, Vol. 184, pp. 167-178.

171. *High-flux dialyzers, backfiltration, and dialysis fluid quality.* **Schiffl H.** 2011, Semin Dial, Vol. 24, No. 1, pp. 1-4.

172. *Hemolytic reactions mechanically induced by kinked hemodialysis lines.* **Sweet SJ, et al.** 1996, Am J Kidney Dis, Vol. 27, No. 2, pp. 262-266.

173. *In vitro characterization of the occurrence of hemolysis during extracorporeal blood circulation using a mini hemodialyzer.* **Yang MC and Lin CC.** 2000, ASAIO J, Vol. 46, No. 3, pp. 293-297.

174. *Mechanical haemolysis related to the use of tandem dialyzers.* **Kazmi A, Canada R, and Wall BM.** 2008, NDT Plus, Vol. 2, pp. 89-91.

175. *In vitro evaluation of hemolysis and sublethal blood trauma in a novel subcutaneous vascular access system for hemodialysis.* **Kameneva MV, et al.** 2002, ASAIO Journal, Vol. 48, pp. 34-38.

176. **Gaudio KM.** A compendium of drugs used for laboratory animal anesthesia, analgesia, tranquilization and restraint. [Online] [Citation : 01/20/2013.] Drexel University. http://www.drexelmed.edu/documents/ULAR. IACUC_drugs.

177. *The ultimate salt war? Uraemic toxins are all that count in dialysis patients.* **Vanholder R.** 2012, Nephrol Dial Transplant, Vol. 27, pp. 62-66.

178. *Absorption spectra of human fetal and adult oxyhemoglobin, de-oxyhemoglobin, carboxyhemoglobin, and methemoglobin.* **Zijistra WG, Buursma A, and Meeuvsen-van der Roest WP.** 1991, Clin Chem, Vol. 37, No. 9, pp. 1633-1638.

179. *Mutual effects of protons, NaCl, and oxygen on the dimer-tetramer assembly of human hemoglobin.* **Chu AH and Ackers GK.** 1981, J Biol Chem, Vol. 256, No. 3, pp. 1199-1981.

180. *Analysis of bicarbonate binding to crocodilian hemoglobin.* **Bauer C, et al.** 1981, J Biol Chem, Vol. 256, No. 16, pp. 8429-8435.

181. *Pulse oximetry in severe carbon monoxide poisoning.* **Hampson HB.** 1998, Chest, Vol. 114, No. 4, pp. 1036-1041.

182. **Health Protection Unit.** *Carbon monoxide poisoning.* 2011.

183. *Removal of the uremic retention solute p-cresol using fractioned plasma separation and adsorption.* **Meijers BK, et al.** 2008, Artificial organs, Vol. 32, No. 3, pp. 214-219.

184. *Damage to erythrocytes from long-term heat stress.* **Utoh J and Harasaki H.** 1992, Vol. 82, pp. 9-11.

185. *The pharmacokinetics of the interstitial space in humans.* **Levitt DG.** 2003, BMC Clinical Pharmacology, Vol. 3, pp. 1-29.

186. *Acute haemolysis due to concentrated dialysis fluid.* **Mulligan I, et al.** 1982, British Medical Journal, Vol. 284, pp. 1151-1152.

187. *Mid-dilution on-line haemodiafiltration in a standard dialyser configuration.* **Krieter DH, et al.** 2005, Nephrol Dial Transplant, Vol. 20, pp. 155-160.

188. *Dialysate sodium, serum sodium and mortality in maintenance hemodialysis.* **McCausland FR, Brunelli SM, and Waikar SS.** 2012, Nephrol Dial Transplant, Vol. 27, pp. 1613-1618.

189. *The challenge of hyponatremia.* **Adrogué HJ and Madias NE.** 2012, J Am Soc Nephrol, Vol. 23, pp. 1140-1148.

190. *Selectively increasing in the clearance of protein-bound uremic solutes.* **Sirich TL, et al.** 2012, Nephrol Dial Transplant, Vol. 27, pp. 1574-1579.

191. *Impact of increasing haemodialysis frequency versus haemodialysis duration on removal of urea and guanidino compounds a kinetic analysis.* **Eloot S, et al.** 2009, Nephrol Dial Transplant, Vol. 24, pp. 2225-2232.

PUBLICATIONS

<u>Thesis-related publications in preparation</u>

E Devine, DH Krieter, HD Lemke. Binding affinity and capacity for the uremic toxin indoxyl sulfate in normal and uremic plasma.

E Devine, HD Lemke, B Flocon, M Raine, DH Krieter. Modification of ionic strength for improved removal of protein bound uremic toxins during hemodiafiltration.

<u>Poster presentations at meetings</u>

E Devine, DH Krieter, HD Lemke; 2013. Increase of plasma ionic strength for improved removal of protein bound uremic toxins. 50th ERA-EDTA congress, Istanbul, Turkey.

<u>Further publications in preparation</u>

E Devine, DH Krieter, HD Lemke. *In vitro* clearance of bortezomib, thalidomide and dexamethasone with HCO membranes.

CURRICULUM VITAE

Eric DEVINE

Am Saint-Pierre Platz 14

D-63839 Kleinwallstadt

Germany

Phone: +49 (0)6022 70 79 840

Handy: +33 (0)6 71 02 08 02

E-mail: devineer@gmail.com

Date of birth: June 10th, 1986 in Créteil (FRANCE)

Nationality: French

PROFESSIONAL EXPERIENCES:

05/2010 – 01/2013 Research engineer within the **eXcorLab GmbH** (Obernburg, GERMANY). Design of test protocols (bio- and hemocompatibility, cytotoxicity, primary cell cultures, animal studies, simulations), results analysis, and research project management (innovative dialysis strategy; orthopedic implants with antimicrobial properties). Team management and interns supervision.

10/2009 – 03/2010 R&D design manager within **Tornier SAS** (Montbonnot, FRANCE). Feasibility study (state of the art, competition) of a cruciate retaining total knee arthroplasty.

INTERNSHIPS:

02/2009 – 07/2009 R&D internship graduation within **Tornier SAS** (Montbonnot, FRANCE). CE marking file for a polyethylene inlay of total hip replacement; technical and industrial feasibility study of a cementless acetabular implant with highly crosslinked polyethylene bearing.

09/2007 – 02/2008 Internship by **eXcorLab GmbH** (Obernburg, GERMANY). Carrying out of experiments on dialysis machines, topic: removal of protein bound uremic toxins by hemodiafiltration.

02/2005 Training as worker by **Vinci Technologies** (Nanterre, FRANCE). R&D activities (study on a capillary viscometer 1000 bars) and pressure tests on equipments.

EDUCATION AND QUALIFICATIONS:

Since 04/2011   PhD student of the **Julius-Maximilians University of Würzburg**, deanery of Biology (Würzburg, GERMANY).

03/2006 – 07/2006   ERASMUS semester in the **Fachhochschule Furtwangen**, field Medical Engineering (Villingen-Schwenningen, GERMANY).

09/2004 – 09/2009   Engineer degree of the **University of Technology of Compiègne** (Compiègne, FRANCE), field Biological Engineering – Biomechanic and Biomaterials.

SKILLS:

Languages   English   fluent
    French   native speaker
    German   fluent
    Japanese   basic knowledge

Sofwares   Pack office
    CAD (ProEngineer, Solidworks)
    Programming (C, Pascal, VBA)
    Data analysis (GraphPad, Minitab)